TECHNISCHE UNIVERSITÄT WIEN

PhD thesis

Dissertation

Tin-based long wavelength photoinitiators for dental composites

ausgeführt zum Zwecke der Erlangung
des akademischen Grades eines Doktors der technischen Wissenschaften

unter der Leitung von
Univ. Prof. Dipl.-Ing. Dr. techn. Robert Liska

Institut für Angewandte Synthesechemie

IAS
Institute of Applied Synthetic Chemistry

eingereicht an der Technischen Universität Wien
Fakultät für Technische Chemie

von
Dipl.-Ing. Moritz Mitterbauer, BSc
01025848
Spitalgasse 1/37, 1090 Wien

Danksagung

Zuallererst möchte ich mich bei Univ. Prof. Dr. Robert Liska dafür bedanken, dass er mir ermöglicht hat, meine Dissertation in der Forschungsgruppe „Polymer Chemistry and Technology“ am Institut für Angewandte Synthesechemie durchzuführen. Vielen Dank Robert, für die interessante Themenstellung, deine fachliche Expertise zu jeder Zeit und auch die netten Stunden abseits des Arbeitsalltags. Ich bin sehr stolz, Teil deiner Arbeitsgruppe, die du mit unglaublichem Engagement aufgebaut hast, gewesen sein zu dürfen. Du hast es geschafft, einerseits wissenschaftliche Exzellenz zu liefern und andererseits eine unfassbar nette und angenehme Arbeitsatmosphäre zu bieten, was sicherlich in dieser Form einzigartig ist.

Großer Dank gebührt auch Prof. Dr. Norbert Moszner und seinen Kollegen von Ivoclar Vivadent. Prof. Moszner hat mich nicht nur einmal mit seinem enormen Fachwissen beeindruckt und damit ebenfalls einen wesentlichen Beitrag zum Erfolg dieser Arbeit beigesteuert.

Außerdem möchte ich mich hier explizit bei Dr. Patrick Knaack bedanken, der meine Dissertation mitbetreut hat und stets die richtigen Ratschläge für mich parat hatte. Deine herausragende fachliche Kompetenz aber auch deine ruhige und besonnene Art machen dich zu einem unverzichtbaren Teil der Forschungsgruppe, sowohl für mich als auch für den Rest des Teams.

Selbstverständlich möchte ich mich bei all den Kollegen, die mich während meiner Dissertation begleitet haben, bedanken. Danke für das tolle Arbeitsklima, den fundierten fachlichen Input und die Hilfsbereitschaft. Ich habe die Zeit mit euch im Labor sehr genossen und werde die vergangenen Jahre sicherlich lange in Erinnerung behalten. Ganz besonders möchte ich mich an dieser Stelle bei Markus, Paul, György und Chris bedanken, mit denen ich besonders viel Zeit verbracht habe und viele sehr unterhaltsame Erlebnisse teile. Danke euch

für die großartige Unterstützung! Dieser Dank geht auch an meine Kollegen Christoph und Daniel, die mich vor allem in der finalen Phase meiner Arbeit enorm unterstützt haben. Ich freue mich wirklich sehr, dass wir die nächsten Schritte unserer beruflichen Laufbahn gemeinsam gehen können.

Nicht zuletzt möchte ich mich auch bei meinen Bachelorstudenten Gerry, Laurenz, Aktan und Carola bedanken, die mit ihrem Fleiß einen äußerst wertvollen Beitrag zu meiner Dissertation geleistet haben und mit ihren Arbeiten außerdem die Grundlagen für meine Publikationen beisteuern konnten.

Besonders möchte ich mich außerdem bei meinen Eltern Brigitta und Hans, sowie meiner Schwester Nora bedanken. Danke, dass ihr immer an mich geglaubt habt und vielen Dank für die große Unterstützung, ohne die ein Studium wie dieses nicht möglich gewesen wäre.

Zu guter Letzt danke ich dir, Lisa, für die Kraft und die Liebe, die du mir jeden Tag aufs Neue schenkst. Danke, dass du immer für mich da bist! Du hast aus mir den Menschen gemacht, der ich heute bin und ich bin so unglaublich froh, dich an meiner Seite zu haben.

Danke!

Abstract

The evolution of photopolymerization towards advanced applications like dental curing or lithography-based ceramic manufacturing was mainly facilitated due to the development of highly reactive acylgermane-initiators, such as Ivocerin®, operating in the visible light range with wavelengths up to 490 nm. Nevertheless, a working Type I system, which allows cleavage upon light exposure with wavelengths above 500 nm and in addition to that shows sufficient photobleaching is not existing as of yet. Such a system would provide significant advantages regarding reachable penetration depths of the light into the material, though. Within this work, the synthesis and characterization of such new long wavelength photoinitiators was envisaged. To achieve a bathochromic shift of the nπ* absorption band, a heteroatom can be introduced next to the benzoyl chromophore (e.g. acylphosphine oxides, acylsilanes, acylgermanes), which is why the underexplored compound class of the acylstannanes was targeted due to its potential of solving the issues described above.

In order to prepare different derivatives of mono-, bis- and tetrakisacylstannanes, numerous synthetic pathways were evaluated resulting in the successful isolation of various compounds. The assumption of a red-shifted absorption band (compared to acylgermanes) due to the tin atom could be confirmed to be true for the acylstannanes, as shown by UV/Vis spectroscopy. The newly synthesized compounds were then further characterized regarding their photochemical properties. Especially tetrakis(2,4,6-trimethylbenzoyl)stannane (**26**) showed an outstanding performance, if compared to current state-of-the-art photoinitiators in terms of long-wavelength absorption, reactivity towards (meth)acrylic double bonds, photobleaching as well as cytocompatibility. Additionally, it could be impressively demonstrated, that this compound is able to cleave upon green light irradiation (522 nm), enabling much higher curing depths in filled systems. Additionally, the compound class of the acylstannanones was targeted for the first time within this work. Although a practicable synthetic route for such a compound has yet to be developed, valuable knowledge could be gathered in various experiments, though.

Kurzfassung

Die Entwicklung der Photopolymerisation hin zu Hightech-Anwendungen wie der Härtung von Kunststoffplomben oder der lithografiebasierten Keramikherstellung wurde hauptsächlich durch die Entwicklung hochreaktiver Acylgerman-Initiatoren wie Ivocerin® ermöglicht, da diese hohe Reaktivität im sichtbaren Bereich des Lichts (bis 490 nm) aufweisen. Ein Typ I System, das eine Spaltung bei Belichtung mit Wellenlängen über 500 nm erlaubt und darüber hinaus ausreichend schnelles Photobleaching zeigt, ist jedoch bisher nicht bekannt. Ein solches System würde erhebliche Vorteile hinsichtlich erreichbarer Eindringtiefen des Lichts in das Material bieten. In dieser Arbeit wurde die Synthese und Charakterisierung solcher Photoinitiatoren ins Auge gefasst. Um eine bathochrome Verschiebung der nπ*-Absorptionsbande zu erreichen, kann neben dem Benzoylchromophor ein Heteroatom eingeführt werden (Acylphosphinoxide, Acylgermane), weshalb auf die wenig untersuchte Verbindungsklasse der Acylstannane abgezielt wurde. Zur Herstellung verschiedener Derivate von Mono-, Bis- und Tetrakisacylstannanen wurden zahlreiche Syntheserouten untersucht, die zur erfolgreichen Isolierung verschiedener Verbindungen führten. Die Annahme einer bathochrom verschobenen Absorptionsbande (im Vergleich zu Acylgermanen) aufgrund des Zinnatoms konnte für die Acylstannane bestätigt werden. Die neu synthetisierten Verbindungen wurden außerdem hinsichtlich ihrer photochemischen Eigenschaften charakterisiert. Insbesondere Tetrakis(2,4,6-trimethylbenzoyl)stannan (**26**) zeigte im Vergleich zu den derzeitigen Photoinitiatoren herausragende Eigenschaften, vor allem hinsichtlich der Reaktivität gegenüber (meth)acrylischen Doppelbindungen, des Photobleachings sowie in Bezug auf seine Zytokompatibilität. Es konnte eindrucksvoll gezeigt werden, dass diese Verbindung bei Bestrahlung mit grünem Licht (522 nm) spalten kann, was in gefüllten Systemen deutlich höhere Durchhärtetiefen ermöglicht. Zusätzlich wurde im Rahmen dieser Arbeit erstmals die Verbindungsklasse der Acylstannanone untersucht und in verschiedensten Experimenten wertvolle Erkenntnisse gewonnen, die sicherlich als Basis für zukünftige Arbeiten dienen könnten.

Contents

Introduction

For decades, amalgam was the material of choice for dental fillings. Being a metal alloy, dental amalgam consists of mercury to a degree of around 50% as well as other metals like tin, silver and copper.[1, 2] It allows very user-friendly processing, hardens quickly, has a low market price and provides high stability. For those reasons, it seemed to be the ideal solution for the filling of dental cavities. However, the use of amalgam comes with huge disadvantages as well. Recent technological progress in terms of the available analytical methods brought proof to the release of highly neurotoxic mercury to the body from amalgam fillings. Furthermore, its metallic color does not match the natural white of the teeth at all and is therefore undesired regarding esthetic considerations (Figure 1). With modern composite fillings the mentioned problems can be largely circumvented, resulting in the patients preference of those fillings compared to amalgam ones.

Figure 1: Composite filling compared to amalgam[3]

To understand the functionality of dental composites and more importantly to be able to influence the properties, which have to be achieved for those systems, one has to be familiar with the basic structure of a human tooth (Figure 2).

Dental enamel is a biogenic material[4] consisting of inorganic crystalline hydroxyl apatite and organic collagen fibers, gluing the crystals (diameters of 40 nm) together. This specific structure is responsible for the outstanding mechanical properties provided by enamel and

are certainly demanded considering the teeth's role in food intake, however it shows relatively low stability towards acidic conditions. Dentin[4] is a bone-like material and it is basically comprised of the same components as enamel, however the hydroxyl apatite content is significantly lower. Moreover, the material is crossed by tubules of 5 µm in diameter, which are filled with dentinal fluid.

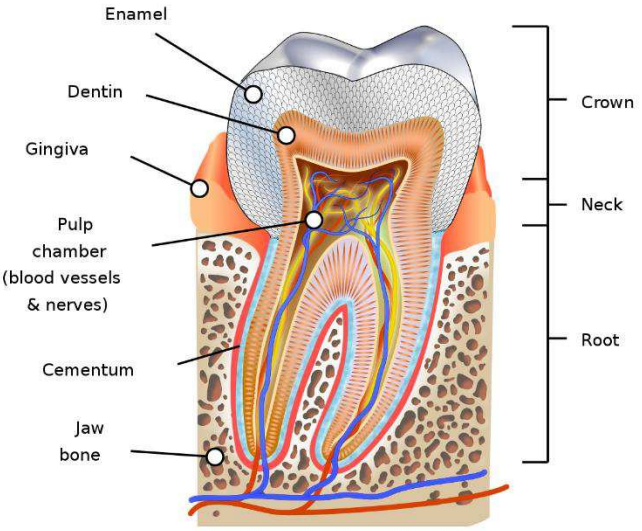

Figure 2: Basic structure of a human tooth[5]

To mimic the properties of those biomaterials when applying a dental filling, the artificial filling material has to meet numerous technical requirements. Aside from that, factors like easy handling as well as costs should not be disregarded as well. A suitable material for dental filling exhibits the following properties:[4]

- Outstanding mechanical properties in terms of hardness and toughness
- Plasticity at room temperature
- Hardening within minutes
- High stability in acidic environments
- Low abrasion
- Full covering of the cavity to prevent bacteria invasion
- Appealing color (no color difference between filling and natural tooth)

- High biocompatibility

Research within this field led to the development of several different material classes for dental fillings, all approaching those requirements in order to fully substitute amalgam. Being one of those classes, ormoceres are organically modified ceramics, which is also where the name is derived from.[4] Similar to silicones, the matrix is prepared via hydrolysis and condensation of silanes. The spatially branched Si-O-Si network contains one organic group per silicon atom, which is, in the case of dental ormoceres, a methacrylate moiety. It can therefore be polymerized readily, resulting in materials with low shrinkage, high abrasion resistance and high biocompatibility due to the low solubility of residual monomer.

Another inexpensive alternative to amalgam is glass ionomer cements.[4] Starting from an aqueous solution of organic acids (mostly polyacrylic acid) and a fluoride-containing aluminosilicate, the ionic network is formed, incorporating the glass particles as well as apatite crystals from the adjacent tooth substance. The aluminosilicate releases fluoride ions, which embed into the natural tooth and therefore caries resistance is increased. Although glass ionomer cements show significant advantages like easy processing and low price, they also reveal drawbacks for example in terms of material strength. To circumvent the sensitivity of glass ionomer cements towards ever-present humidity, a radically polymerizible monomer can be added to the cement formulation to accomplish hardening on demand via photopolymerization and therefore facilitate processing even more. However, although using these polymer-modified glass ionomer cements, poor strength and low abrasion resistance of the material is still problematic.

Dental compomeres[4] are very similar to glass ionomer cements, except for the fact, that they do not contain any water. The hardening reaction is induced solely via diffusion of salivary juice from the oral cavity into the formulation resulting in a higher toughness of the final polymer. Compomeres are very similar to dental composites, however they show higher shrinkage and lower abrasion resistance. Due to the slow hardening mechanism via acid-base reaction, a bonding agent for proper adhesion to the natural tooth material is required.

Dental composites[4] are materials mainly comprised of an organic polymer matrix (dimethacrylates)as well as inorganic filler particles (aluminosilicates, quartz). Usually, hardening of those formulations is triggered via light-induced radical polymerization (photopolymerization). Typical principal monomers (Scheme 1) are difunctional resins like urethane dimethacrylate (UDMA), decanediol dimethacrylate (D_3MA) and bisphenol A diglycidylmethacrylate (bis-GMA). After the initiation, compounds like these form a three-dimensional polymer network. By choosing the exact composition of the matrix components, properties like the viscosity and the reactivity are adjusted as well as the mechanical properties and shrinkage in the final material can be defined.

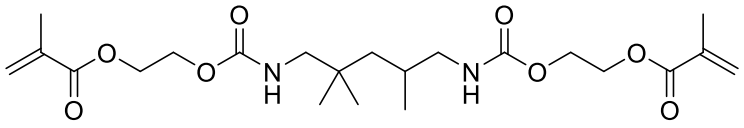

UDMA

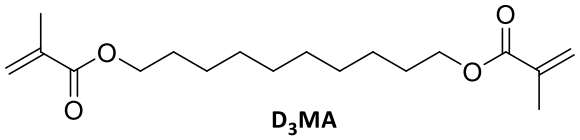

D_3MA

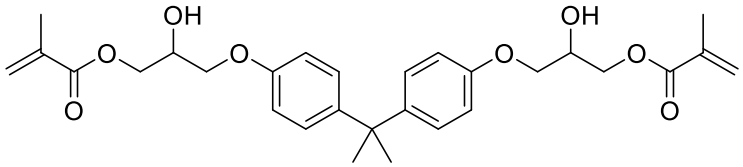

bis-GMA

Scheme 1: Common resins used in dental composites

To ensure proper bonding of the restorative materials to the dental tissues, specific bonding systems[6] have to be used. In the first step, the dentist usually applies an etchant (phosphoric, nitric or maleic acid-based) to decalcify the uppermost 10-15 µm of the intertubular and the peritubular dentin. By doing so, the smear layer is also removed and the dentinal tubules open up. Afterwards, a primer substance can be applied, penetrating the collagen network and increasing the decalcified dentin surface energy. Primer compounds like 4-methacryloxyethyl trimellitic acid (Scheme 2) provide on one hand a hydrophilic moiety with

high affinity towards the dentin surface and on the other hand a methacrylate moiety with a high chemical affinity towards the resin.

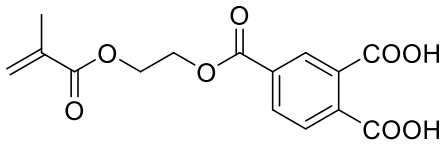

Scheme 2: 4-Methacryloxyethyl trimellitic acid[6] used as primer

In order to reduce the number of components and therefore the number of required working steps advanced bonding systems with so-called self-etching primers[6, 7] were developed. Instead of applying the etchant and the primer components one after another, compounds like the one shown below (Scheme 3) are used to fulfil both requirements in one single component.

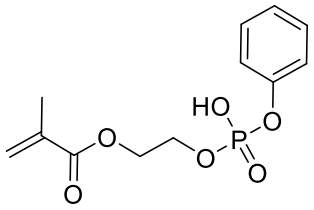

Scheme 3: 2-(Methacryloxy)ethyl phenyl hydrogen phosphate[6] used as self-etching primer

After taking care of proper bonding to the dental tissues, the actual photopolymerizible composite formulation[6] can be applied. Besides principal monomers with relatively high molecular weight, it usually contains lower molecular weight diluent monomers like triethylen glycol dimethacrylate (TEGDMA) to regulate viscosity. Additionally, those mixtures contain inorganic fillers such as aluminosilicates and quartz as well as photoactive compounds (photoinitiator) and polymerization inhibitors to prevent early curing. The photoinitiator (PI) is the UV-VIS active component and is therefore a key component in dental composites. The choice of photoinitiator is essential for the whole system, because it has an influence on the achievable curing times and determines the usable type of light source to start the polymerization.

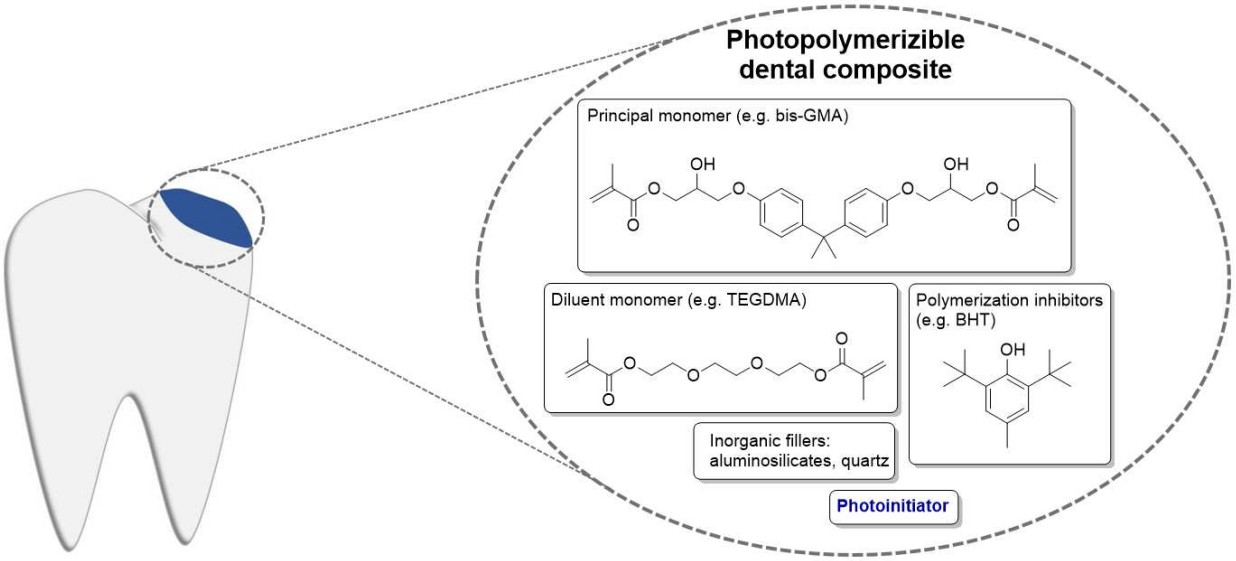

Figure 3: Constituents of modern dental composites

To achieve sufficient curing depths in such highly filled systems, very reactive photoinitiators, which show absorption at rather high wavelengths in the visible range are of great interest. The longer the wavelength of the light used for the curing of these systems, the higher curing depths can be achieved (Figure 4) due to higher penetration depths of the light into the material.

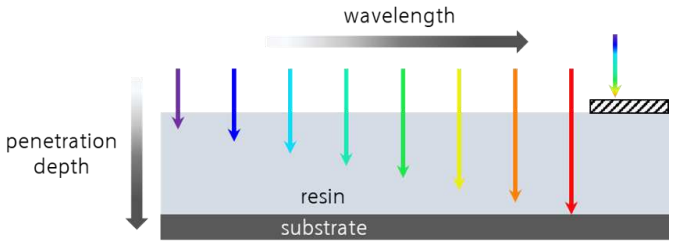

Figure 4: Schematic illustration of the wavelength-dependency of the penetration depth of light into the resin

The penetration of light follows the Lambert-Beer law as given below, where P_z is the power of light (usually in mW cm^{-2}) at a certain depth z below the surface, P_0 is the power at the surface and D_p is the depth at which the penetrating light intensity falls to 1/e of the surface intensity.[8]

$$P_z = P_0 e^{-z/D_p}$$

For practical reasons the power terms are converted into energy terms and z becomes the curing depth C_d, as long as long as the needed amount of light is present, resulting in the formula below.

$$C_d = D_P \ln\left(\frac{E_0}{E_c}\right)$$

C_d is the depth of the cured resin, E_0 is the energy of light on the surface and E_c is the "critical" energy needed for the initiation of polymerization.[9]

Photosensitive molecules (e.g. photoinitiators) are able to convert the energy of electromagnetic waves into chemical energy by transferring it to their electronic structure.[10] For that process to occur, the energy of the light either has to be absorbed directly by the photoinitiator molecule or it has to be transferred to it by a so-called photosensitizer. The latter usually happens via triplet-triplet transfer. To be able to absorb the light, a photoinitiator has to display certain structural elements, in other words it has to have specific functional groups in its molecular structure to be able to do so. These functional groups are called chromophores. Depending on the exact functionalities, transitions to an excited state can be triggered upon irradiation of different wavelengths. Most commonly, chromophores are conjugated π-systems containing moieties like the carbonyl group. However, structural elements like C-C double bonds, thionyl- or diazenyl-groups appear quite often as well (Table 1).

Table 1: Chromophores and absorption maxima of the relevant electronic transitions

	Absorption maxima	
Chromophore	**λ_{max} [nm] ππ***	**λ_{max} [nm] nπ***
C=C	170	
C=O	166	280
C=N	190	300
N=N		350
C=S		500

Regarding molecular energy states,[11] absorption of light, facilitated by chromophoric groups, leads to an excitation of the photoinitiator molecule from its ground state to the excited singlet state S^1 (Scheme 4). From there, it can either release the absorbed energy via fluorescence and drop back to the ground state or it can be transferred to an excited triplet state T^1 via intersystem crossing (ISC). From the T^1 state, radical (or cation) formation is a possibility together with phosphorescence, radiation-free deactivation and bimolecular quenching processes (e.g. caused by oxygen).

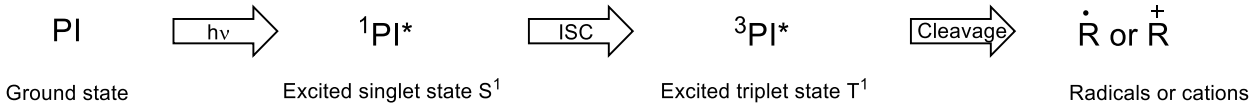

Scheme 4: Excitation, intersystem crossing and formation of radicals or cations[11]

Additionally, the relevant processes are summarized in a Jablonski diagram (Figure 5).[12] Due to the much longer lifespan of the triplet state T^1 ($1x10^{-6}$ s) compared to the singlet state S^1 ($<1x10^{-8}$ s), radical formation is highly favored to occur from the triplet state, despite the various competition processes.

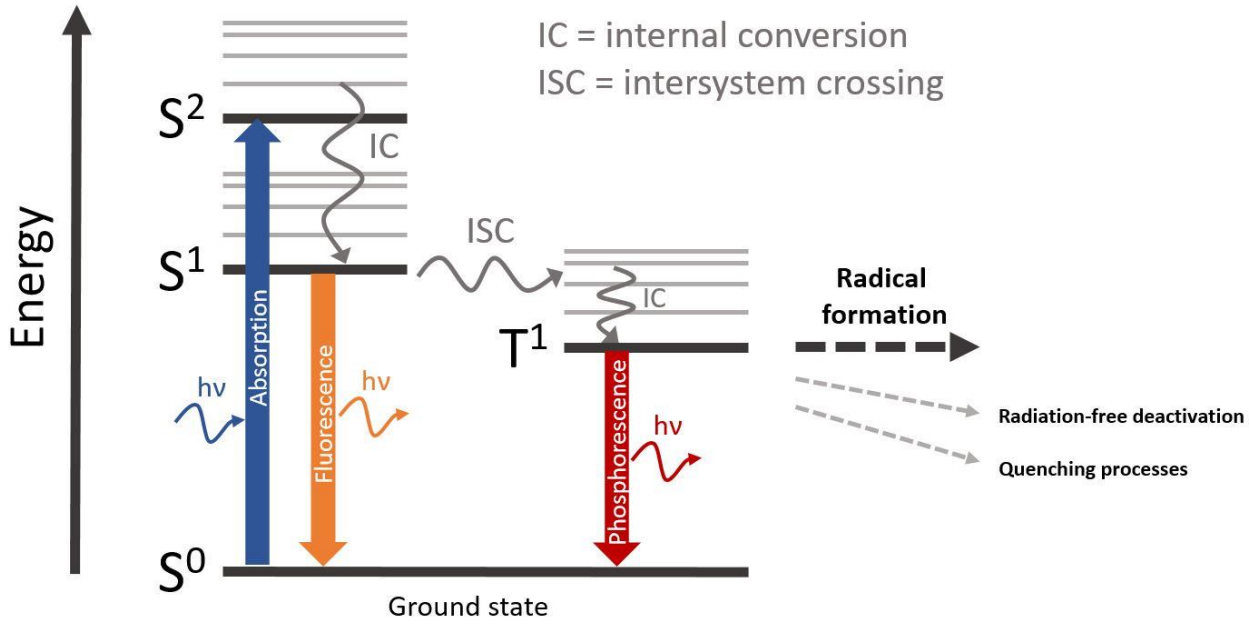

Figure 5: Jablonski diagram[12]

Generally, there are two main types of photoinitiators, depending on what particular mechanism leads to radical formation.[10] Type I photoinitiators or so-called cleavable photoinitiators, the initiating compound undergoes a transition to its excited state first and then forms radicals in a unimolecular fragmentation reaction (Scheme 5). Usually, Type I photoinitiators feature very high efficiency and are mostly beneficial in UV applications, rather than in visible light curing

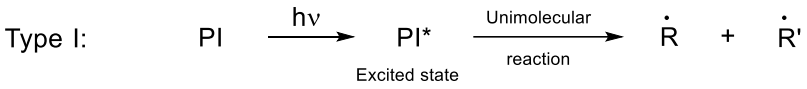

Scheme 5: Radical formation in Type I photoinitiators

Type II systems on the other hand, form radicals in a bimolecular reaction mechanism.[10] The photosensitive compound undergoes a transition to the excited state upon irradiation and then reacts with a coinitiator in a bimolecular reaction in order to form radicals (Scheme 6). These systems are very versatile and often used for visible light curing, however they suffer from lower efficiency compared to Type I systems, due to the bimolecular mechanism.

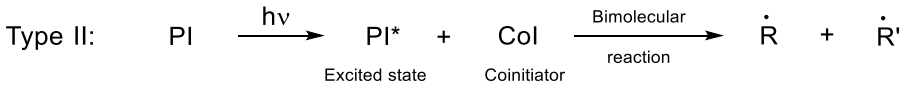

Scheme 6: Radical formation in Type II photoinitiators

As mentioned above, Type II photoinitiating systems consist of two components, the actual photosensitive compound as well as a coinitiator, reaction in a bimolecular fashion to form radicals. For these type of systems, two main reaction pathways lead to radical formation: hydrogen abstraction and photoinduced electron transfer.[10] Regarding the first of those two types, diaryl ketones like benzophenone are able to abstract a hydrogen atom from a suitable donor compound (Scheme 7). As shown below, isopropanol can act as such. Prior to that, irradiation with light of a suitable wavelength leads to the excitation of an electron from the oxygen n orbital to the delocalized π* orbital in benzophenone. This results in a partial positive charge δ+ on the oxygen atom, which can then interact with the electron-rich C-H bond in isopropanol and, in further consequence, a hydrogen atom is abstracted giving two radicals. For this process to occur, the energy of the triplet state has to exceed the bond dissociation energy of the C-H bond. The reactivity of the formed radicals towards double bonds is not equal though. Naturally, the highly conjugated ketyl radicals appear to be rather inactive compared to the radicals formed by the hydrogen-donating component (in this case isopropanol).

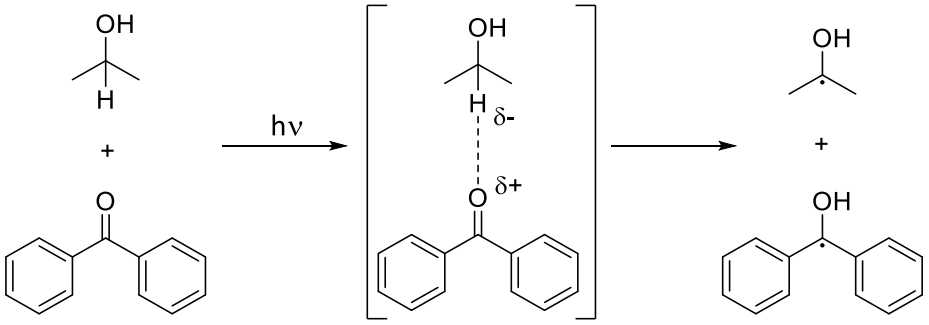

Scheme 7: Photoinduced H-abstraction in benzophenone/isopropanol Type II system

Type II systems involving a photoinduced electron transfer are more frequently used in industry, mainly because of their versatility, especially in terms of the applicable irradiation

wavelengths. Especially in visible light induced polymerization, systems like diketone/amine,[13] dye/coinitiator[14] or metal complexes (e.g. titanocene[15]) reveal great advantages over other systems. A system widely used in dental applications is the camphorquinone/dimethylaminobenzoic acid (CQ/DMAB) system[6] (Scheme 8). Camphorquinone contains a visible light chromophore and is excited to its excited singlet state upon irradiation. From this state, an electron can be transferred to the amine coinitiator. This step is highly dependent on the redox potential of the donor/acceptor pair. The process is followed by a proton transfer, leading to a highly reactive amine-radical, which can then initiate radical polymerization as well as another rather inactive radical originating from camphorquinone. The absorption maximum of camphorquinone lies at 468 nm showing a low extinction coefficient due to the symmetry-forbidden nπ* transition.

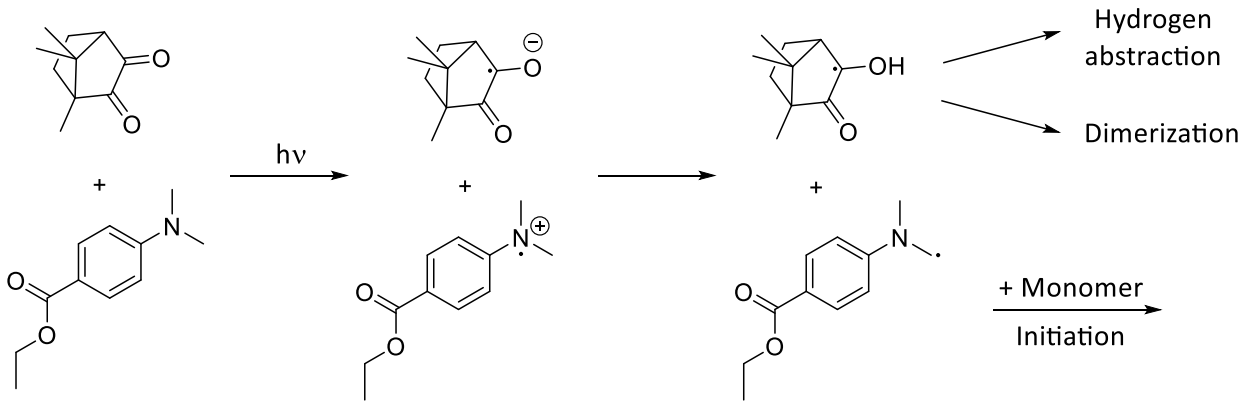

Scheme 8: Photoinduced electron transfer followed by proton transfer and radical formation in CQ/DMAB Type II system

Generally, Type II systems like CQ/DMAB are strongly affected by the surrounding environment, which can be problematic in aqueous media. Overall reactivity of Type II systems is lower, compared to Type I photoinitiators, due to their bimolecular nature.

As mentioned, Type I photoinitiators form radicals in a fragmentation reaction. Being aromatic carbonyl compounds, most of the Type I photoinitiators cleave adjacent to the carbonyl moiety, forming a highly reactive benzoyl radical and another radical depending on

the substituents in α-position R, R' and R''. This reaction is therefore known as α-cleavage (Scheme 9). . If the photoinitiator contains a visible light chromophore, this chromophore can be cleaved during the fragmentation reaction leading to a loss of the long wavelength absorption (so-called photobleaching), which is desired, especially in dental applications.

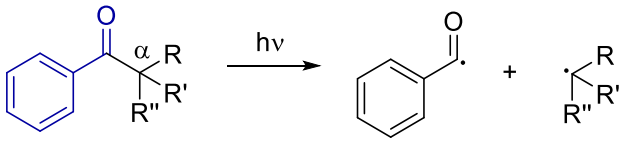

Scheme 9: Photoinduced α-cleavage of classical Type I photoinitiators such as arylketones (containing the benzoyl chromophore)

The molecule is able to absorb the radiation energy (due to the benzoyl chromophore) and can undergo a transition to its excited state. As described above, intersystem crossing can cause a transition from the singlet to the triplet state, from where α-cleavage and radical formation occurs. ISC happens particularly rapidly and efficiently in aromatic ketones, due to the small singlet-triplet energy difference.[10]

Regarding arylketones, two main factors determine the rate of the α-cleavage from the lowest triplet state: The configuration of the excited state (ππ* or nπ*) and the type of substituent at the α-position.[10] Figure 6 shows the possible electronic transitions for the carbonyl group in aryl ketones. The reactivity of triplet state in nπ* configuration shows much higher reactivity towards α-cleavage compared to the ππ* configuration. Therefore, a change in the molecular structure, which leads to a configuration change from nπ* to ππ* often results in a considerable loss of reactivity.[10] The energy of the reactive excited state needs to be higher than the bond dissociation energy of the C-C bond to make efficient α-cleavage possible.

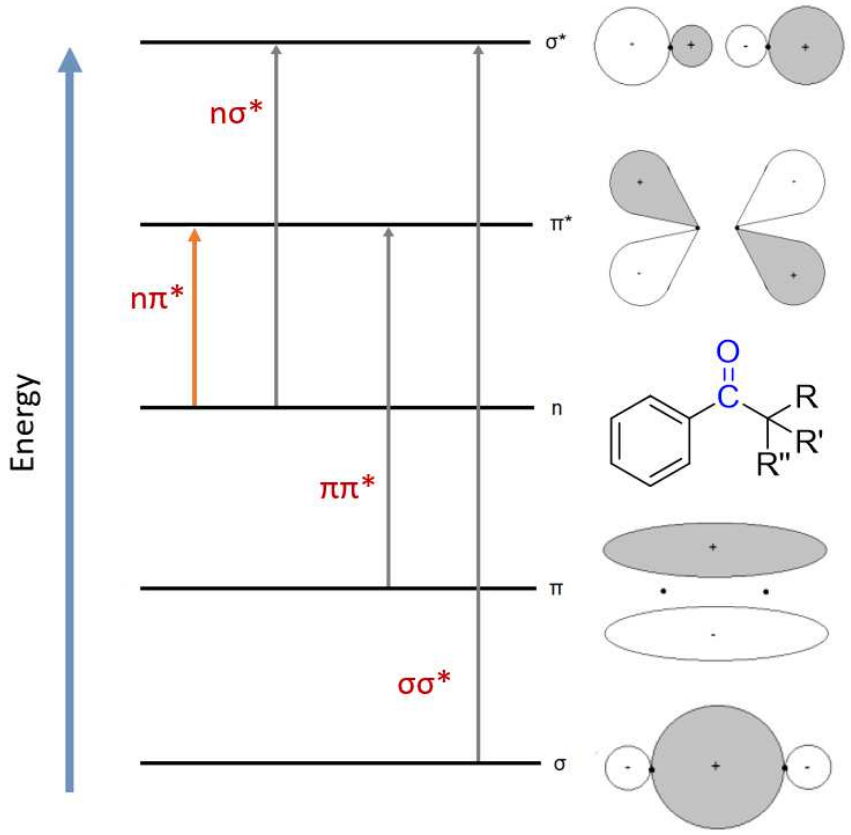

Figure 6: Possible electronic transitions for the carbonyl group

Beyond that, the substituents at the α-position strongly affect the rate of the α-cleavage in a way, that substituents, which stabilize a positive charge on the α-carbon increase the rate of cleavage significantly. For this reason many Type I photoinitiators possess heterosubstituents like hydroxyl, ether, amine or possible aryl moieties (Scheme 10). For those compounds the potential occurrence of competing processes like phosphorescence and radiation-free deactivation can usually be ignored.

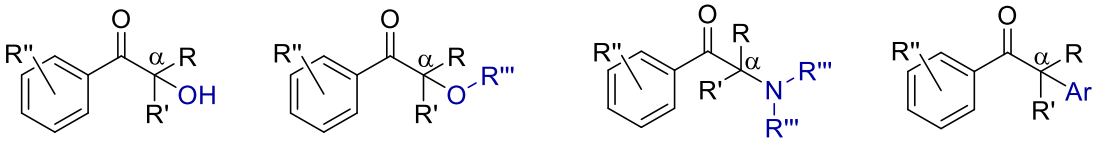

Scheme 10: Arylalkyl ketones with different substituents in α-position

Another way to influence the cleavage reaction of Type I photoinitiators is the introduction of heteroatoms directly at the α-position next to the benzoyl chromophore. In this case, the d-orbitals of the heteroatom can overlap with the π orbitals of the carbonyl group[16] leading to an increase in energy of the π and to a decrease of the energy of the π* orbital as shown in Figure 7. Since the energy of the n orbital remains unchanged, the energy difference between n and π* is decreased, meaning that the wavelength needed to cause the nπ* transition is increased. This is the reason, why heteroatom-containing Type I photoinitiators usually cleave upon irradiation with light of longer wavelengths, if compared to arylketones.

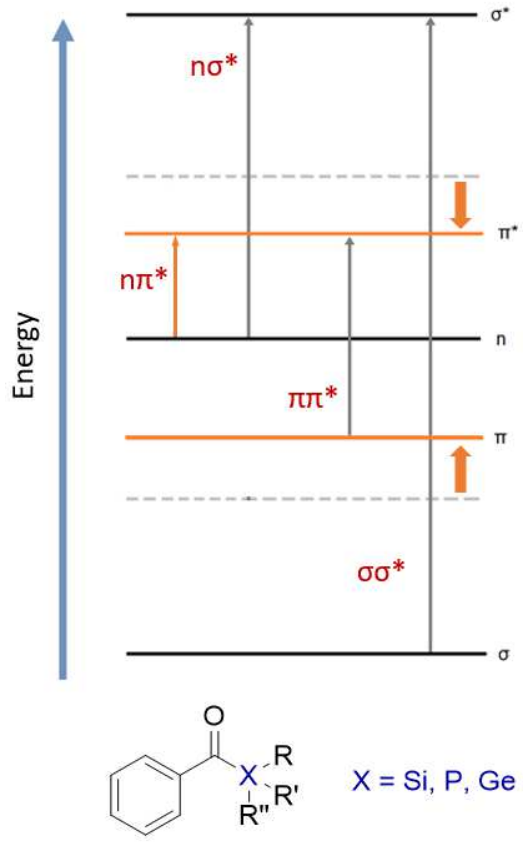

Figure 7: Bathochromic shift of the nπ transition due to the introduction of heteroatoms next to the carbonyl group in Type I photoinitiators*

Due to this bathochromic shift in absorption, compound classes like acylphosphine oxides,[17-19] acylsilanes,[20] and acylgermanes[21, 22] are of high interest for visible light radical polymerization. Since the effect of the bathochromic shift increases from acylsilanes to

acylgermanes, another interesting heteroatom-containing class of Type I photoinitiators could be the acylstannanes, especially for applications requiring irradiation with light of longer wavelengths (e.g. highly filled systems)

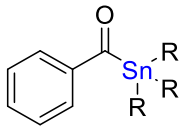

Scheme 11: Acylstannanes as potential new class of Type I photoinitiators

Objective

The goal of this work is the development of a novel Type I photoinitiator leading to improvements of the current state of the art in dental composites. To achieve this, the following criteria have to be met for the newly synthesized compounds: Photocleavage upon irradiation with light of wavelengths above 450 nm, high reactivity towards (meth)acrylates, sufficient solubility in the monomer mixture, fast photobleaching, cytocompatibility, high stability in the monomer mixture and low production costs.

To approach this, the compound class of the acylstannanes (Scheme 12) was chosen to be the main target within this work. The potential bathochromic shift, caused by an overlap of the π and π* orbitals of the carbonyl group with the empty d orbitals of the tin atom lets us expect the nπ*- transition in acylstannanes to occur above 450 nm.

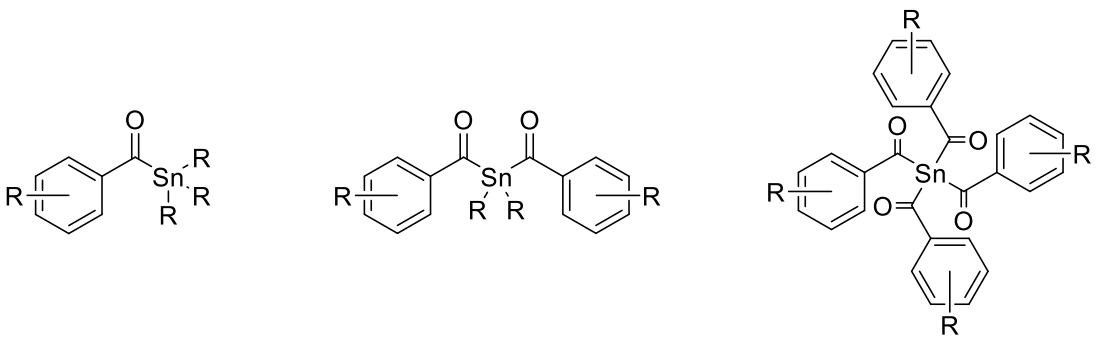

Scheme 12: Mono-, bis- and tetrakisacylstannanes

Besides the studies concerning mono-, bis- and tetrakisacylstannanes, another path should be taken for the unheard-of compound class of acylstannanones (Scheme 13). In contrast to acylstannanes, these compounds contain an oxygen-atom, which is directly bound to the tin atom. This is expected to influence the absorption properties as well as the potential cleavage process and the initiation itself.

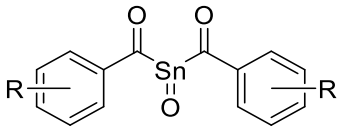

Scheme 13: Acylstannanones

The newly synthesized compounds can then be tested regarding their photochemical properties. UV-Vis spectra will be acquired to investigate the absorption properties. The reactivity towards double bonds can be investigated using photo-DSC. Additionally, the stability, the cytocompatibility as well as experiments to evaluate the achievable curing depths will be carried out.

State of the art

Towards visible light Type I photoinitiators

As mentioned already, Type I photoinitiators contain cleavable structures and form radicals in a unimolecular reaction upon irradiation (typically UV light). These compounds show various advantages (especially in terms of reactivity) compared to Type II systems and are therefore widely used in industry e.g. in printing inks or coatings. Recently, their field of application was further extended by more sophisticated techniques like dental curing[23, 24] or lithography-based ceramic manufacturing.[25] This development was strongly facilitated, due to numerous scientific investigations and excellent research within this field over the last decades. Every single application reveals its own demands and limitations, therefore choosing a suitable compound for the specific application is not an easy task. Especially the usable wavelength of irradiation determines which kind of initiating system can be used in each and every case. If photopolymerization is the applied technique for the curing of dental fillings, only visible light can be used to start the polymerization, because UV light would harm the mouth cavity.

Typical examples for Type I initiators, which are active in the UV region are α-hydroxy alkylphenones such as 2-hydroxy-1-(3-(hydroxymethyl)phenyl)-2-methylpropan-1-one (APi-180, Figure 8). The absorption maximum of the nπ* transition band lies at 330 nm[26] for this compound. As shown in Figure 8, the absorption band does not overlap with the emission range of commercial light sources, used for dental fillings. Dental LEDs usually cover a wavelength range from 430 to 490 nm, which means, that APi-180 cannot be used in visible light-initiated dental curing. However, α-hydroxy alkylphenones reveal their benefits (low price, high reactivity) in areas, where UV curing is possible (coatings, inks etc.).

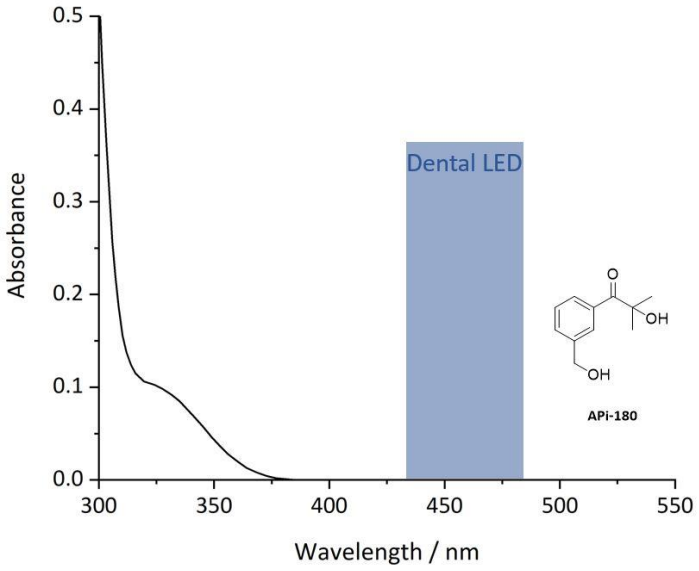

Figure 8: nπ transition band of an α-hydroxy alkyl phenome (APi-180) and emission range of dental LED*

Another class of typical Type I photoinitiators is represented by the bisacylphosphine oxides such as (phenylphosphoryl)bis(mesitylmethanone) or Irgacure 819 (Figure 9).

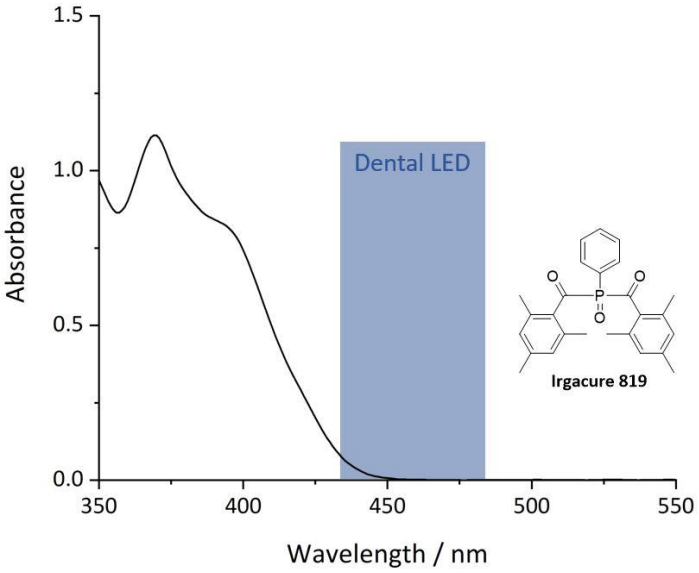

Figure 9: nπ transition band of a bisacylphosphine oxide such as Irgacure 819 and emission range of dental LED*

The absorption maximum of the nπ* transition band of Irgacure 819 is located at 368 nm[27] tailing out to approximately 450 nm. As shown in Figure 9, the absorption band reaches into

the emission range of dental LEDs, however the overlap is rather small. The shift to higher wavelengths most likely originates from the phosphorus atom next to the benzoyl chromophore. It can be explained by a conjugation between the phosphinoyl group and the carbonyl carbon atom.[17] In another theory, the bathochromic shift is explained by an overlap of the π*-orbital of the carbonyl carbon with the empty d-orbital of the phosphorus atom.[16] Commercially used acylphosphine oxide initiators contain methyl-substituted benzoyl chromophore(s) to increase their stability against aqueous hydrolysis,[10] although the 2,4,6-trimethylbenzoyl radical generally shows lower reactivity compared to the unsubstituted analogues.[10] Like classical carbon-based Type I initiators, acylphosphine oxides form reactive radicals upon irradiation via α-cleavage (Scheme 14). In terms of reactivity of the involved radical species, the phosphinoyl radicals show higher addition rate towards double bonds by a factor 2-3, when compared to the 2,4,6-trimethylbenzoyl radical.[10]

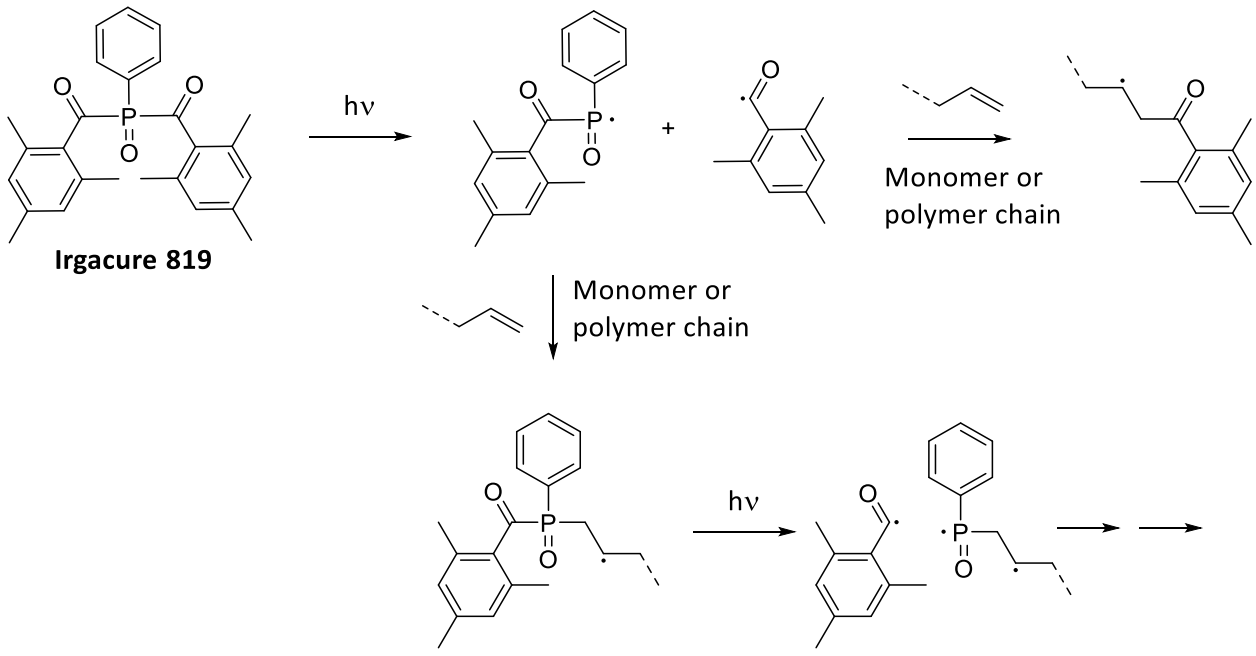

Scheme 14: Photoinduced radical formation in BAPO and initiation of polymerization

Mentioning heteroatom-containing Type I photoinitiators, acylsilanes are another interesting class of compounds, however their industrial relevance is rather low compared to the systems mentioned above. The reason for that is on one hand their rather low stability against

aqueous hydrolysis and on the other hand a phenomenon called “Brook rearrangement”.[28] It describes a photoinduced reversible rearrangement leading to the formation of a siloxycarbene (Scheme 15). This rearrangement competes with the α-cleavage reaction and if it is preferred, photoinitiation efficiency is dramatically lowered due to the formation of non-reactive siloxycarbene. Whether the desired α-cleavage is the dominating reaction is determined by the structure of the acylsilane as well as the surrounding conditions. The absorption maxima of acylsilanes typically lie at around 400 nm.[29]

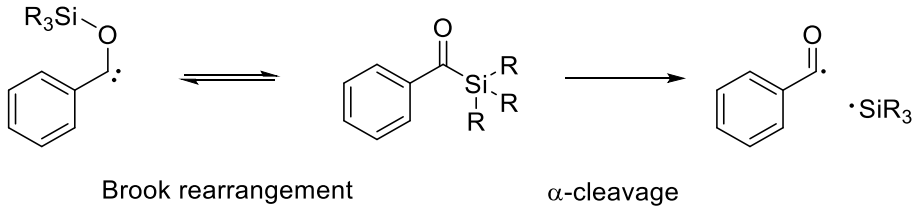

Scheme 15: Competition between photoinduced α-cleavage and Brook rearrangement[28] of acylsilanes

Very recently, tetrafunctional acylsilanes were investigated in terms of their suitability as photoinitiators in visible light curing.[20] Tetrakis(2,4,6-trimethylbenzoyl)silane has a absorption maximum at 382 nm, however its nπ* absorption band tails out at approximately 470 nm. As for the acylphosphine oxides, the bathochromic shift probably originates from an overlap of the π*-orbital of the carbonyl carbon with the empty d-orbital of the silicon atom. The shoulder in the absorption band can most likely be explained by the restricted rotational freedom and a twisting of the sterically demanding mesitoyl moieties in the structure of the tetraacylsilane resulting in a change of orbital set-up.[20] The overlap with the dental LED emission range is much higher compared to the acylphosphine oxides, however in terms of reactivity as well as photobleaching behavior, acylsilanes show significant disadvantages.[27]

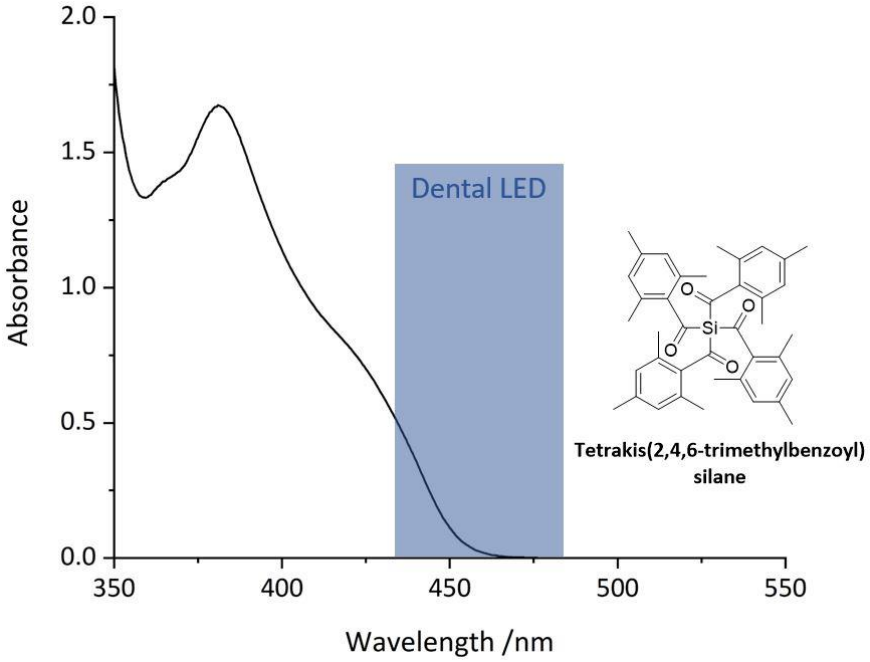

Figure 10: nπ transition band of tetrakis(2,4,6-trimethylbenzoyl)silane and emission range of dental LED*

A benefit of those tetrafunctional acylsilane compounds could further be their capability to cleave four times potentially, while maintaining the visible light chromophore Si-(Mes-C=O)$_x$ intact until the cleavage of the last acyl moiety (Scheme 16).

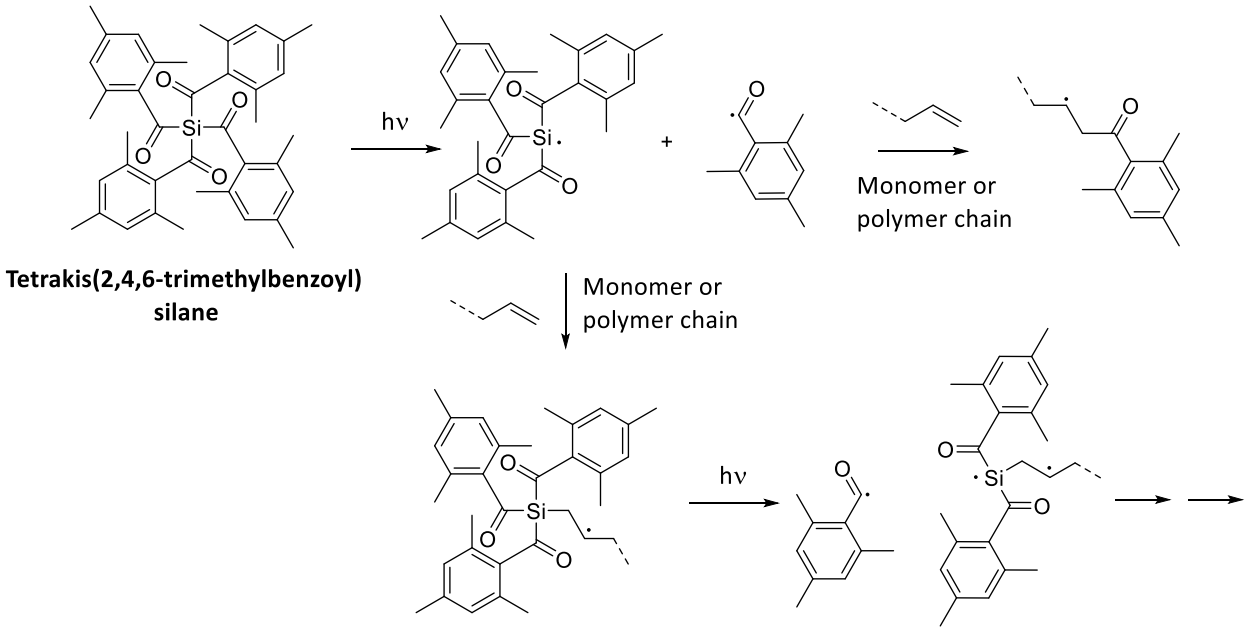

Scheme 16: Photoinduced radical formation in tetrakis(2,4,6-trimethylbenzoyl)silane and initiation of polymerization

A milestone regarding research on visible light photoinitiators was definitely created with the discovery of acylgermane initiators.[21, 23, 29, 30] Bisacylgermanes such as the commercially used product Ivocerin® (Ivoclar Vivadent), which has its nπ* absorption maximum at 408 nm have proven to be highly suitable for dental applications. With the germanium atom next to the benzoyl chromophore, an even further bathochromic shift compared to the phosphorus- and silicon-based compounds can be achieved due to the overlap of the π*-orbital of the carbonyl carbon with the d-orbitals of the germanium atom. As shown in Figure 11, the relevant absorption band reaches quite far into the visible light region and therefore into the emission range of the dental LED.

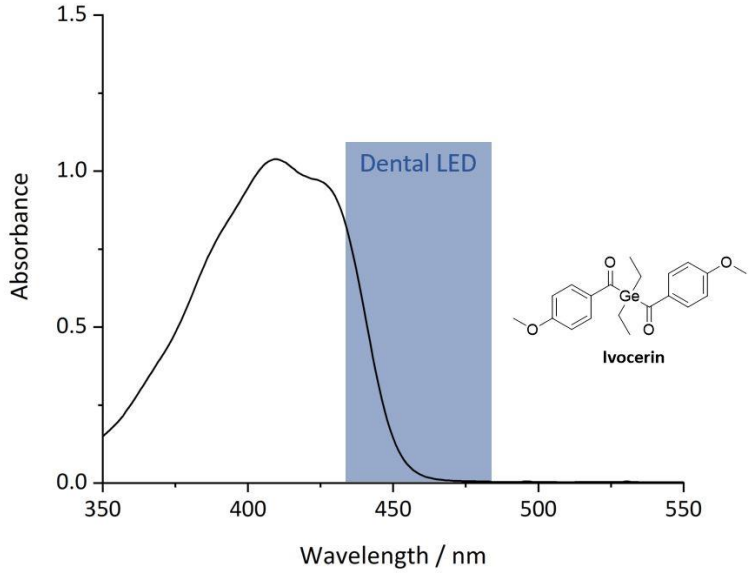

Figure 11: nπ transition band of bis(4-methoxybenzoyl)diethylgermane (Ivocerin) and emission range of dental LED*

Light-induced α-cleavage reaction leads to the formation of highly reactive germyl-radicals (Scheme 17). Generally, the rate constant for the addition reaction towards (meth)acrylate is three orders of magnitude higher than the respective value for benzoyl radicals.[15] On top of that, acylgermanes show very fast photobleaching as well as rather high stability against aqueous hydrolysis and high thermal stability. Acylgermanes reveal drawbacks mainly in terms of their very expensive production, making them usable only for special applications with low production volumes like dental curing. Usually, very small amounts of photoinitiator (0.05 – 1wt%) are required for most applications though.

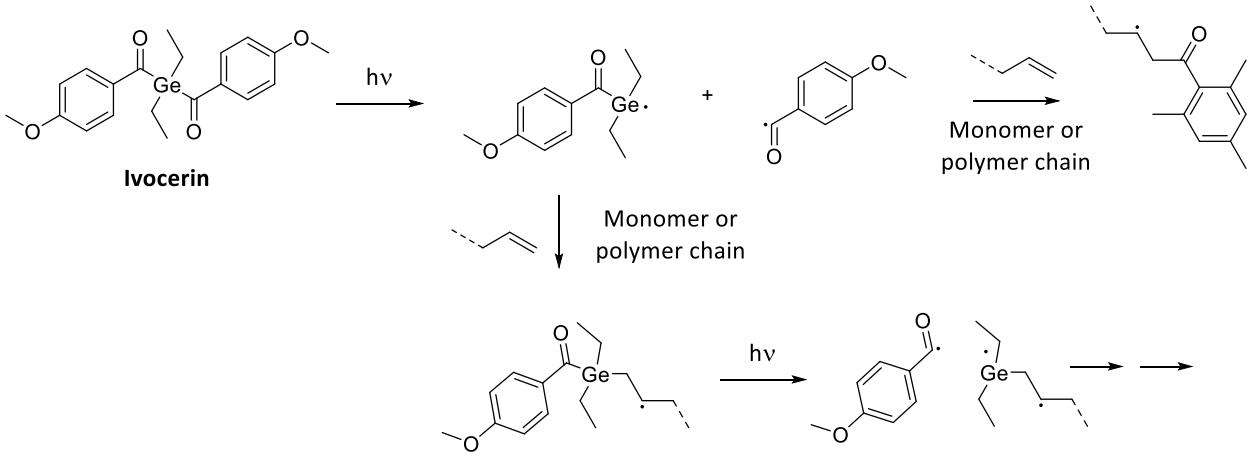

Scheme 17: Photoinduced radical formation in Ivocerin and initiation of polymerization

As mentioned already, introducing heteroatoms directly next to the benzoyl chromophore can lead to a significant bathochromic shift of the nπ* transition band. The overlap of the respective d orbitals of the heteroatoms (Si, P, Ge) with the π* orbital of the carbonyl group leads to an increase in energy of the π and to a decrease of the energy of the π* orbital. Since the energy of the n orbital remains unchanged, the energy difference between n and π* is decreased, meaning that the wavelength needed to cause that transition is increased (Figure 12).

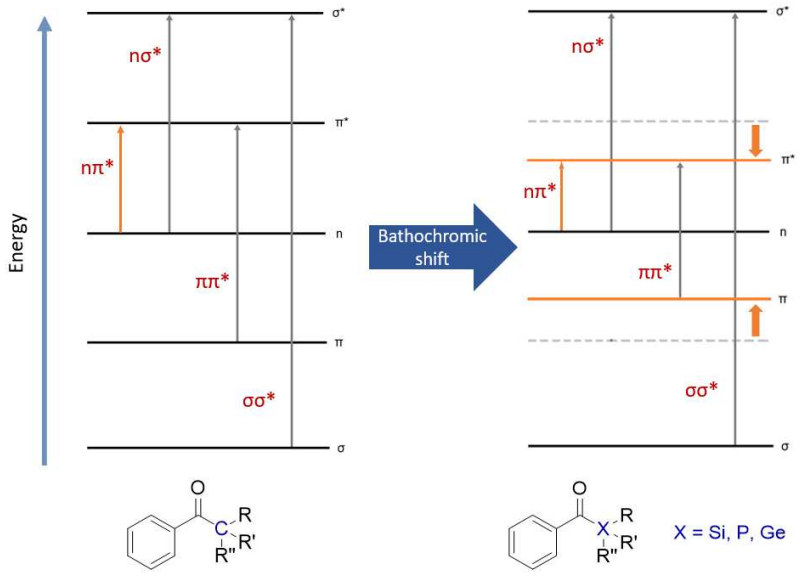

Figure 12: Bathochromic shift, caused by the introduction of heteroatoms next to the benzoyl chromophore

When it comes to the synthesis of Sn-containing photocleavable compounds, the logical approach is to assume, that the concept of acylsilanes and acylgermanes can also be applied to the respective stannanes. Since there was a bathochromic shift reported going from silicon to germanium, a further bathochromic shift is expected to occur by introducing tin instead of germanium (Figure 12). This was also investigated by Peddle[31] in the late sixties.

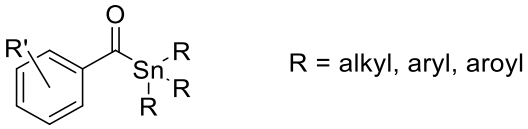

Scheme 18: Acylstannanes

The amount of published work for the synthesis of acylstannanes (Scheme 18) is quite limited. However, a small number of synthesis paths has been tested successfully in the past. Most of this synthetic routes involve a nucleophilic attack of an organostannylmetal derivative at an unsaturated carbon atom.[32] In most cases, the metal is lithium (Scheme 19). Starting from stannylhalides, -hydrides or distannanes, the stannyllithium species can be formed using elemental lithium,[33] lithium diisopropylamide (LDA)[34] or butyllithium.[35] The intermediate can then be reacted with various compounds bearing electrophilic carbon atoms such as acid halides,[31] esters,[36] thioesters[36] or aldehydes[37, 38] to form acylstannanes.

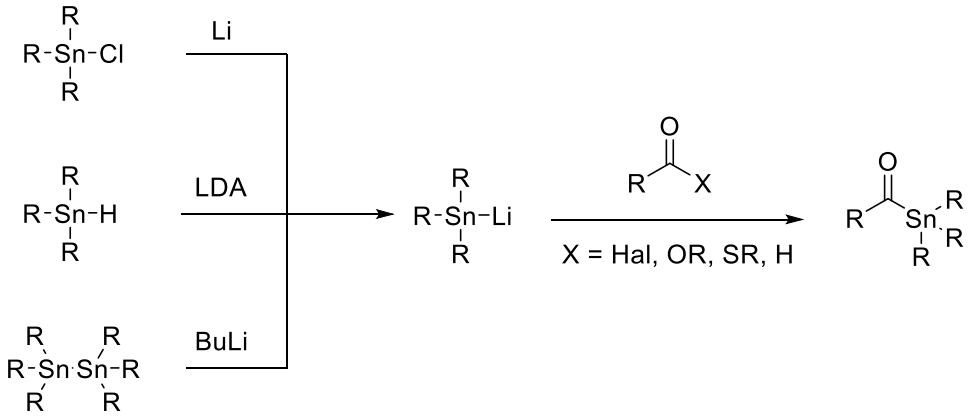

Scheme 19: Synthesis routes for acylstannanes via stannyllithium species

Similar synthetic approaches involving organostannyl lithium derivatives lead to the synthesis of triarylstannanecarbodithioate esters, which has been reported by Kunze et al.[39, 40] The lithium species can react with carbon disulfide in an addition reaction to form intermediate lithium carbodithioate salts, which can then be further converted to the final products.

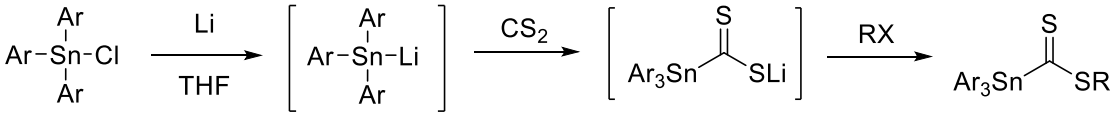

Scheme 20: Synthesis of stannanecarbodithioate esters[39, 40]

Quintard et al.[41] and Kosugi et al.[42] showed, that acylstannanes can also be synthesized using the corresponding stannyl Grignard-type reagents instead of the lithium derivatives by reacting those with an excess of aldehyde.

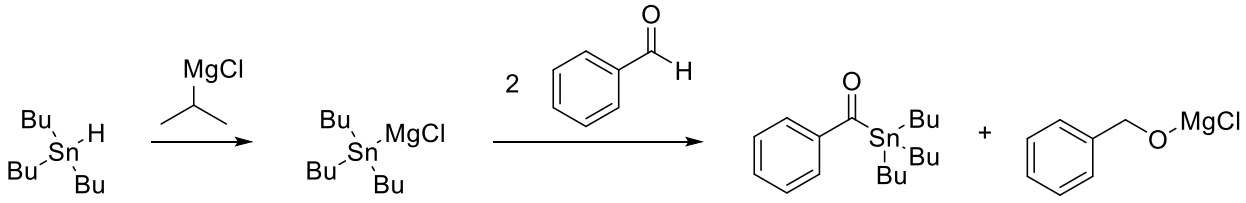

Scheme 21: Synthesis of benzoyltributylstannane via grignard reaction[41, 42]

Another approach towards similar stannyl compounds involves diazo compounds. Wheeler[43] showed, that compounds like phenyl(trimethylstannyl)diazomethane can be synthesized using phenyldiazomethane and an aminostannan.

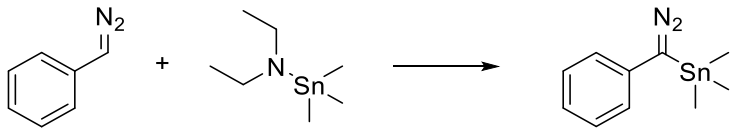

Scheme 22: Synthesis of phenyl(trimethylstannyl)diazomethane[43]

General section

1 Monoacylstannanes

Regarding monoacylstannanes, four different target compounds were selected (compounds **1**-**4**, Scheme 23). This selection of compounds was picked based on the assumption, that both the substituents on the aromatic benzoyl chromophore as well as the substituents directly bonded to the tin atom have an influence on the absorption properties as well as the hydrolytic stability of the stannanes. Furthermore, the reactants needed in order to synthesize these compounds are cheap and commercially available.

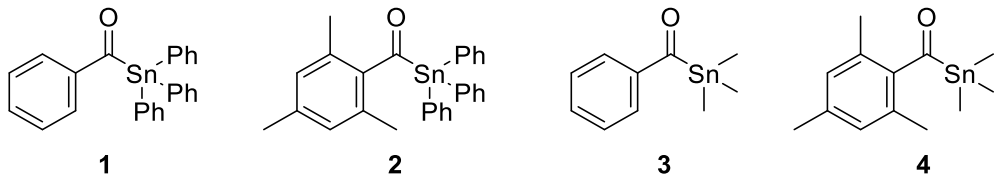

*Scheme 23: Selection of monoacylstannane target compounds **1-4***

As far as a successful isolation of those compounds **1**-**4** can be achieved, information about the influence of different substituents on the aromatic ring as well as on the tin atom with regard to stability, absorption properties and photoreactivity can be gathered. The strategies in order to do so are described in the following sections.

1.1 Synthesis

For the synthesis of the monoacylstannanes, two different pathways were envisaged (Scheme 24).

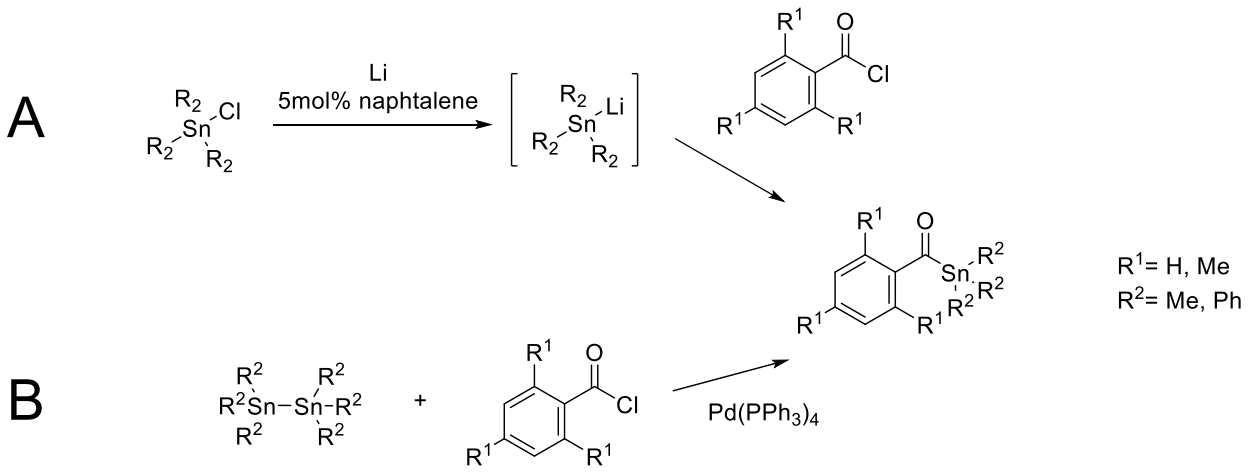

Scheme 24: Two different pathways towards monoacylstannanes

The first route (subsequently named pathway A) is based on the synthesis path described by Peddle[31] in 1968. An intermediate stannyl lithium species is reacted with acid chloride to obtain the acylstannane. For route A, this synthesis was combined with a method described by Wang et al.[44] to facilitate the formation of the stannyl lithium intermediate using naphthalene as a catalyst (Scheme 25).

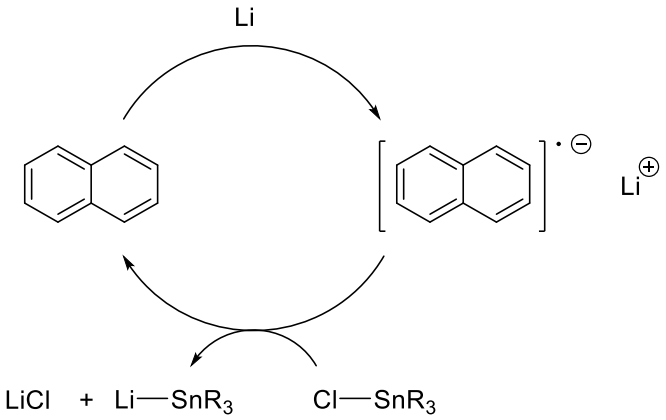

Scheme 25: Proposed catalytic cycle for naphtalene as a catalyst[44]

To avoid the use of hard to handle and highly toxic chlorotrimethylstannane and basically to have an alternative route ready to synthesize monoacylstannanes with various substituents, a second route (pathway B) was envisaged, based on the route described by Mitchell and

Kwetkat[45] in 1990 (Scheme 26). Herein, hexaorganodistannanes are used in a Palladium catalyzed step together with acid chlorides to prepare acylstannanes.

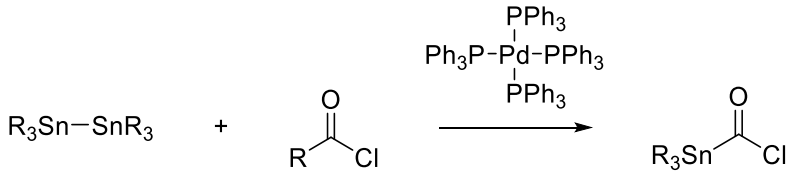

Scheme 26: Pd(0) catalyst for the synthesis of monoacylstannanes described by Mitchell and Kwetkat[45]

Since both pathways involved moisture-sensitive compounds and many of those being light-sensitive in addition to that, all reactions, which demand certain measures concerning these issues were carried out in an orange light lab to exclude light with wavelengths below 520 nm and Schlenk techniques were used to secure complete exclusion of oxygen and moisture.

1.1.1 Stannyl lithium route (Pathway A)

1.1.1.1 Synthesis of benzoyltriphenylstannane (1)

To synthesize benzoyltriphenylstannane (**1**), the well-known method of Peddle[31] should be applied, however the method was further adapted using a more up to date route, described by Wang et al..[44] Initially, the stannyl lithium species should be formed by reacting chlorotriphenylstannane with elemental lithium using naphthalene as a catalyst in dry THF. The intermediate should afterwards be reacted with benzoyl chloride to form the desired product.

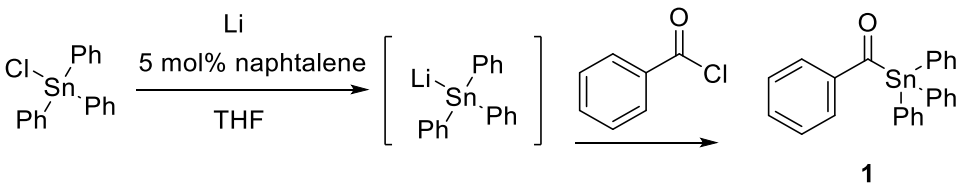

*Scheme 27: Synthesis of benzoyltriphenylstannane (**1**) using pathway A*

For the synthesis of benzoyltriphenylstannane (**1**), 3 eq. of fine cut lithium foil were stirred in dry THF in the presence of 0.05 eq. naphthalene to form the naphtyl lithium species. Stirring led to a color change of the suspension to dark green. During the addition of a solution of 1 eq. chlorotriphenylstannane, the color of the mixture changed back to colorless. Afterwards, the mixture was reacted with 1.06 eq. of benzoyl chloride. After a solvent change and filtration under inert conditions, the product could be obtained as intensively yellow powder (63%) in high purity. The structure of the compound was confirmed using NMR spectroscopy and GC-MS.

Although the chosen synthesis route for benzoyltriphenylstannane (**1**) led to quite satisfying results in the first attempt already, the route appeared to be trickier than expected, especially for larger scale batches. Without any notable changes in conditions, the purity of the product achieved varied significantly after several syntheses. Especially in the case of synthesis attempts of more than 2 g, the crude product obtained was not crystalline and pure, but sticky, viscous and to a considerable extent contaminated. The synthesis seemed to be relatively sensitive in terms of parameters such as reaction vessel, stirring speed, dropping speed etc. For that reason, a suitable purification method for larger batches should have been developed.

Using ^{1}H and ^{119}Sn-NMR spectroscopy, small amounts of unreacted chlorotriphenylstannane, benzoyl chloride and naphthalene could be identified as the impurities appearing in larger batches. Having purification with precipitation in mind, the crude mixture was carefully dissolved in various solvents (acetonitrile, dichloromethane, diethylether, toluene, acetone, ethyl acetate, methanol, n-pentane) and then reprecipitated by concentrating the solutions. Another approach was the addition of water to precipitate the product from a solution in organic solvents. However, none of these experiments led to satisfying results. The product and the impurities showed very similar solving behavior, which is why another method needed to be found. In the case of using water for precipitation, the product as well as chlorotriphenylstannane and benzoyl chloride probably hydrolyzed, making it even harder so achieve a pure compound. This also became important, when a classical aqueous workup was

tested for benzoyltriphenylstannane (**1**), which did not lead to an improvement in terms of purity as well. Another idea was the use of a chromatographic method. Columns filled with silica gel as well as aluminum oxide were tested for the purification of benzoyltriphenylstannane (**1**), however no pure product could be achieved after that as well. Apparently, the target compound is not stable enough to survive a chromatographic approach. Since no suitable purification method could be found for larger batches of benzoyltriphenylstannane (**1**), the only chance was to find the optimal reaction conditions, the get a fairly pure product in the first place, directly after synthesis.

For that reason, numerous synthesis experiments with varying reaction conditions were carried out to find the optimal ones. In general, the reaction can be split into 3 steps: formation of the naphthyllithium species, formation of the reactive stannyllithium species, and formation of the product **1**. For each of these steps, several studies were conducted to find the ideal reaction conditions. The findings from these studies leading to an improvement of the synthesis are summarized below:

- Formation of naphthyllithium species: 20 min in an ultrasonic bath (20°C) for breakup of the passive layer on the Li surface + 30 min intensive stirring at RT (dark coloration)
- Formation of stannyllithium species: Addition of chlorotriphenylstannane at RT over a period of 20 min + stirring at RT for 4 h
- Formation of benzoyltriphenylstannane (**1**): Addition of benzoyl chloride over 20min at -78°C + and stirring at RT for 17h

Following this exact protocol, benzoyltriphenylstannane (**1**) in high purity could be prepared consistently and the applicability of this synthesis path for larger batches could be improved. The updated working procedure, varied according to the optimization studies can be found in the experimental section of this thesis.

1.1.1.2 Synthesis of mesitoyltriphenylstannane (2)

To synthesize another monoacylstannane, mesitoyltriphenylstannane (**2**) was chosen as target structure. The o-methyl groups on the aromatic ring structure should in theory provide steric hindrance to the carbonyl group and therefore potentially lead to a higher stability against aqueous hydrolysis. For the synthesis of mesitoyltriphenylstannane (**2**), the optimized protocol, developed for the synthesis of benzoyltriphenylstannane (**1**), was applied.

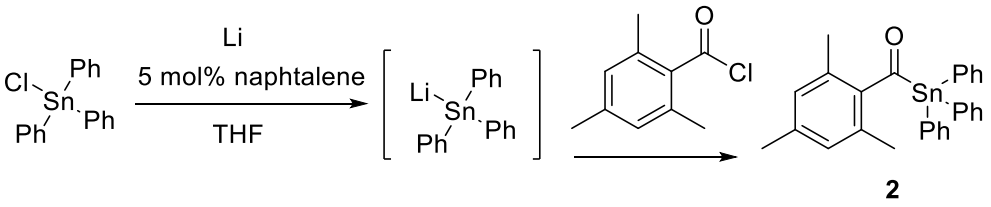

*Scheme 28: Synthesis of mesitoyltriphenylstannane (**2**) using pathway A*

For the synthesis of mesitoyltriphenylstannane (**2**), 3 eq. of fine cut lithium foil were stirred in dry THF in the presence of 0.05 eq. naphthalene to form the naphtyl lithium species. Stirring led to a color change of the suspension to dark green. During the addition of a solution of 1 eq. chlorotriphenylstannane, the color of the mixture changed back to colorless. Afterwards, the mixture was reacted with 1.06 eq. of mesitoyl chloride. After a solvent change and filtration under inert conditions, the crude product could be obtained as intensively yellow sticky substance (68%). The structure of the compound was confirmed using NMR spectroscopy.

Since mesitoytriphenylstannane (**2**) should be more stable against aqueous hydrolysis than benzoyltriphenylstannane (**1**) due to the sterical hindrance at the carbonyl group, an aqueous workup involving liquid-liquid extraction (diethyl ether / water) was envisaged to obtain the pure compound. After drying the organic layers over sodium sulfate and evaporation of the solvent, ^{1}H-NMR confirmed the success of this approach. However one organic impurity could not be removed. The remaining impurity could then be confirmed as mesitil (Scheme 29).

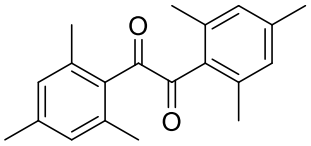

Scheme 29: Mesitil

Apparently, mesitoyltriphenylstannane (**2**) shows higher stability in aqueous media, but in turn seems to form radicals unintentionally in solution without any light triggering, which made any further purification impossible. This assumption is supported by the obvious formation of mesitil in solution (radical formation followed by recombination). The purity of the crude product, achieved after the aqueous workup was estimated to be approximately 80%. For this crude product, photochemical characterization was carried out using UV-VIS spectroscopy and photo-DSC.

1.1.2 Hexaorganodistannane route (Pathway B)

1.1.2.1 Synthesis of benzoyltrimethylstannane (3)

To synthesize benzoyltrimethylstannane (**3**), a method based on the route described by Mitchell and Kwetkat[45] should be applied. Starting from a hexaorganodistannane, a palladium catalyst tetrakis(triphenylphosphine)palladium should be used to prepare monoacylstannanes in a reaction with acid chlorides.

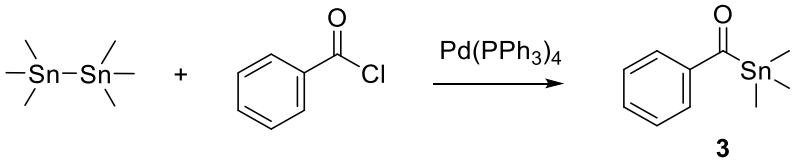

3

*Scheme 30: Synthesis of benzoyltrimethylstannane (**3**) using pathway B*

For the synthesis of benzoyltrimethylstannane (**3**), 1 eq. of hexamethyldistannane was reacted with 1 eq. of benzoyl chloride in the presence of 0.05 eq. of palladium catalyst (yellow

solid) by heating the reaction mixture to reflux. On the next day, a dark brown solution was obtained. Probably the decomposition of catalyst led to the formation of palladium nanoparticles.[46] According to ^{119}Sn-NMR, only one tin species, benzoyltrimethylstannane (**3**, -85.6 ppm) was present in the solution. Surprisingly, no trimethylstannyl chloride signal could be detected. It was assumed, that this side product evaporated during the reaction due to its high volatility. After removing the solvent in vacuo, a GC-MS measurement confirmed the slightly impure product, which showed a mol peak at 270 m/z. Subsequently, a successful polymerization attempt of the crude product in a 1:1 mixture of UDMA and D_3MA supported this assumption. For purification, the brown oily liquid was taken up in dry diethyl ether. Attempts to remove the supposed palladium nanoparticles by filtration (0.2 µm Teflon syringe filter) and centrifugation both failed. However, filtration using an aluminum oxide flash column (150 mesh) lead to successful separation of the Pd nanoparticles. The yellow/orange oil (83%) was confirmed to be the desired product using GC-MS, ^{119}Sn- and ^{1}H-NMR, still showing small impurities. The compound was stored under argon in the fridge (7°C) under complete exclusion of light. Further purification attempts (Kugelrohr distillation, column chromatography) did not lead to satisfying results, due to the low stability of benzoyltrimethylstannane (**3**).

Generally, benzoyltrimethylstannane (**3**) seemed to show quite low thermal stability. Increasing amounts of disintegration products like benzil (Scheme 31) and another compounds containing the PPh_3 moiety could be detected via HPLC, TLC and NMR a few days after the synthesis already.

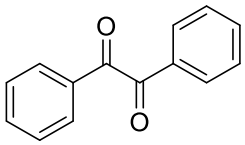

Scheme 31: Benzil

It was assumed, that the purity of the product could possibly be increased by applying shorter reaction times (and therefore reducing disintegration of the Pd catalyst). For that reason, the

reaction was carried out again with extensive reaction control. Using the same reaction conditions as described above, in this attempt, HPLC samples were taken every 30 min. However, interrupting the reaction after 4 h of reaction time did not lead to an improvement in the end.

After storing benzoyltrimethylstannane (**3**) for 3 weeks in the fridge under argon and protected from light the compound had decomposed completely. After realizing this, freshly prepared benzoyltrimethylstannane (**3**) was stored in the freezer at -18 °C to increase the achievable storage time. Photochemical characterization was carried out using UV-VIS spectroscopy as well as photo-DSC.

1.1.2.2 Synthesis of mesitoyltrimethylstannane (4)

Since benzoyltrimethylstannane (**3**) showed very low stability concerning thermal as well as hydrolytic degradation, the corresponding mesitoyl derivative (**4**, Scheme 32) should be synthesized as well. By providing steric hindrance to the carbonyl group, the o-methyl groups should at least increase the hydrolytic stability of the acylstannane.

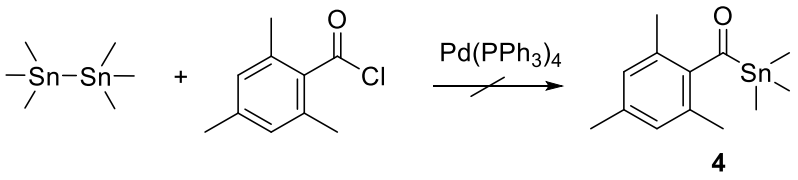

*Scheme 32: Synthesis of mesitoyltrimethylstannane (**4**) using pathway B*

For the synthesis of mesitoyltrimethylstannane (**4**), 1 eq. of hexamethyldistannane was weighed into a dry Schlenk tube within a Glove box. The Schlenk tube was then transferred to a Schlenk line and 1 eq. of mesitoyl chloride was added as well as 0.05 eq. of palladium catalyst (yellow solid) and dry THF. The clear yellow solution was then heated to reflux and stirred for 17 h. Completion was checked via HPLC and ^{119}Sn-NMR indicating that the

reactants were still present in the mixture and no product was formed yet. Therefore, the reaction was resumed for 3 more days. The brown mixture was then worked up in similarly to the work up used for benzoyltrimethylstannane (**3**), involving an aluminum oxide flash column (150 mesh). After evaporation of the solvent a polymerization attempt of the crude product in a 1:1 mixture of UDMA and D_3MA yielded a clear polymer with very low rigidity. However, no product signal could be obtained via GC-MS and also HPLC measurements were inconclusive, suggesting very low purity. This was also supported by TLC experiments, indicating very low stability.

Since the introduction of o-methyl groups to the benzoyl moiety did not lead to an increase in stability, but rather led to a much lower yield, no further synthesis attempts were conducted, concerning mesitoyltrimethylstannane (**4**).

1.1.2.3 Synthesis of benzoyltriphenylstannane (1)

Furthermore, pathway B should also be tested for the synthesis of benzoyltriphenylstannane (**1**), although this compound could be isolated already using the stannyl lithium route (pathway A). In order to do so, the reactant hexamethyldistannane was replaced by hexaphenyldistannane, which should react in a similar fashion with acid chlorides as in the syntheses described above.

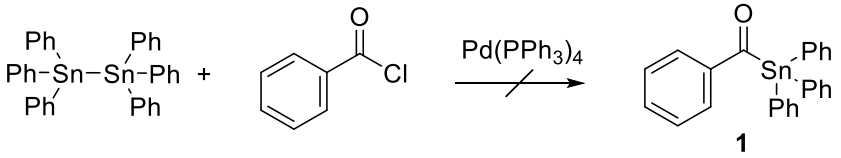

*Scheme 33: Alternative synthesis of benzoyltriphenylstannane (**1**) using pathway B*

For the synthesis of benzoyltriphenylstannane (**1**), 1 eq. of hexaphenyldistannane was weighed into a dry Schlenk tube within a Glove box. The Schlenk tube was then transferred

to a Schlenk line and 1 eq. of benzoyl chloride was added as well as 0.05 eq. of palladium catalyst (yellow solid) and dry THF. The solution was then heated to reflux and stirred overnight. A ^{119}Sn-NMR spectrum on the next day showed mainly signals from the reactants, which is why the mixture was refluxed for 5 more days. After that time, another ^{119}Sn-NMR spectrum was measured directly from the dark brown reaction mixture, showing signals coming from tetraphenylstannane (-128 ppm), small amounts of hexaphenyldistannane (-141 ppm) as well as another signal at -106 ppm (probably a tin-adduct with the catalyst). Benzoyltriphenylstannane (**1**, signal at -220 ppm) could not be observed. Nonetheless, the reaction mixture was worked up starting with a filtration over aluminum oxide. The filtrate was diluted with THF and water was added. The phases were separated and the aqueous phase was extracted 3 times with diethyl ether. After drying of the combined organic layers using sodium sulfate, filtration and evaporation of the solvent, a colorless, viscous substance was obtained, which did not initiate polymerization of a 1:1 mixture of UDMA:D_3MA in a first polymerization attempt.

It can be assumed, that the distannane route (pathway B) did not work for the triphenyl derivative, due to the much bulkier steric conditions. Apparently, the palladium catalyst did not have the desired effect on the conversion of hexaphenyldistannane, in contrast to the previously applied hexamethyl compound. Mitchell and Kwetkat[45] described this phenomenon already for the analogue butyl compound. This issue could potentially be circumvented by using another catalyst. Since pathway A led to the successful isolation of benzoyltriphenylstannane (**1**) already, this approach was not pursued further within this work.

1.2 Characterization

To investigate the potential of the synthesized monoacylstannanes as photoinitiators in visible light free radical polymerization, benzoyltriphenylstannane (**1**), mesitoyltriphenylstannane (**2**) benzoyltrimethylstannane (**3**), and mesitoyltrimethylstannane (**4**) were compared to the corresponding germanium compound benzoyltrimethylgermane[47] K37 (Scheme 34) in numerous experiments.

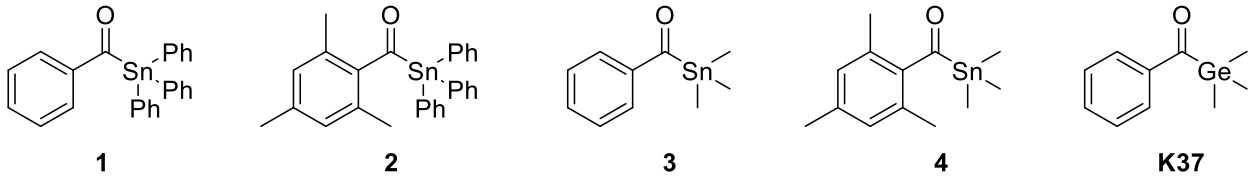

*Scheme 34: Synthesized monoacylstannanes **1**-**4** and germanium reference photoinitiator K37*

It is important to mention, that only the compound benzoyltriphenylstannane (**1**) was available in high purity. The other monoacylstannanes **2** and **3** were used as obtained from the syntheses (chapter 1.1), since either the reaction did not proceed as expected or no suitable purification protocol could be developed yet. The purity of the compounds was estimated to be > 75% for mesitoyltriphenylstannane (**2**) and > 80% for benzoyltrimethylstannane (**3**) using NMR spectroscopy. Nevertheless, it was very interesting to investigate the influence of the substitution pattern on the aromatic ring as well on the tin atom on the absorption properties, which is why these crude mixtures were examined using UV/Vis spectroscopy (chapter 1.2.1) and photo-DSC (chapter 1.2.2).

1.2.1 UV/Vis spectroscopy

To investigate the absorption behavior of the prepared monoacylstannane compounds **1**-**3** and to determine the position of the absorption maxima of the nπ* transition band, UV/Vis

spectra (c = 1 × 10^{-3} mol L^{-1} in acetonitrile) were acquired and the obtained results were compared with those of benzoyltrimethylgermane K37 (Figure 13).

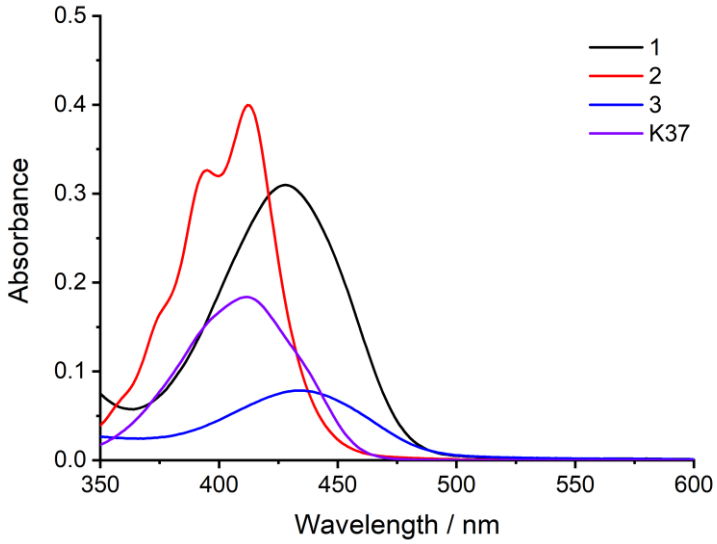

*Figure 13: UV/Vis spectra for the monoacylstannanes (**1**-**3**) in comparison to benzoyltrimethylgermane (K37)*

Regarding the obtained spectra, it has to be noted that the measured compounds were available in different purities (chapter 1.2). After the examination of the position of the absorption maxima, interesting trends can be observed. Whereas the maxima of the benzoyl derivatives are located in the range around 430 nm (benzoyltriphenylstannane (**1**): 433 nm benzoyltrimethylstannane (**3**): 430 nm), the maximum of the mesitoyl derivative appears at much shorter wavelengths (mesitoyltriphenylstannane (**2**): 413 nm). One of the reasons for this could be the different steric situation due to the mesitoyl residues (such as changes in the angles between the bonding axes), but on the other hand, this phenomenon could also occur due to the different electron distribution caused by the methyl groups. The +I effect of the methyl groups in the mesitoyl chromophore would in this case be responsible for a shift of the absorption maximum of about 20 nm. In this context, the question arises as to whether this phenomenon leads to maxima shifted to even longer wavelengths, such as by the introduction of strongly electron-withdrawing substituents (e.g., nitro or cyano groups). This could possibly result in monoacylstannanes with absorption maxima around 450 nm.

1.2.2 Photo-DSC

In order to investigate the reactivity of the synthesized compounds in methacrylates, photo-DSC measurements of the monoacylstannanes **1**-**3** and a comparison measurement with benzoyltrimethylgermane (K37) were carried out. The used monomer was a mixture of urethanedimethacrylate (UDMA) and decanedioldiacrylate (D_3MA) in a ratio of 1:1. A formulation containing 0.5wt% of the acylgermane was prepared first and then equimolar solutions of the monoacylstannanes **1**-**3** were prepared. The curing of the samples was carried out using a LED with an emission maximum at 460 nm. The light intensity was adjusted to be 1 W cm^{-2} directly after the lens of the LED.

Photo-DSC can be used to determine the double bond conversion (DBC [%]), the time until heat flow maximum is reached (t_{max} [s]), the time until 95 percent of total heat flow is reached (t_{95} [s]) as well as the total heat of polymerization, which is related to the peak area. Additionally, the rate of polymerization R_p can be calculated. These values provide quite good information on photoreactivity of the analyzed compounds.[27]

The double bond conversion can be calculated as shown below:

$$DBC\ [\%] = \frac{\Delta H}{\Delta H_T} \cdot 100$$

ΔH…peak area [kJ mol^{-1}]

ΔH_T…theoretical polymerization heat of the monomer [kJ mol^{-1}]

ΔH_T (UDMA/D_3MA)[48] = 115 kJ mol^{-1}

The rate of polymerization can be determined using:

$$R_p\ [mol\ L^{-1}\ s^{-1}] = \frac{h \cdot \rho_{monomer}}{\Delta H_T}$$

h…peak height [mW mg^{-1}]

$\rho_{monomer}$...density of the monomer

$\rho_{UDMA/D3MA}$[48] = 1030 mg mL^{-1}

The figures below (Figure 14, Figure 15) show the achieved results for the synthesized monoacylstannanes **1**-**3**.

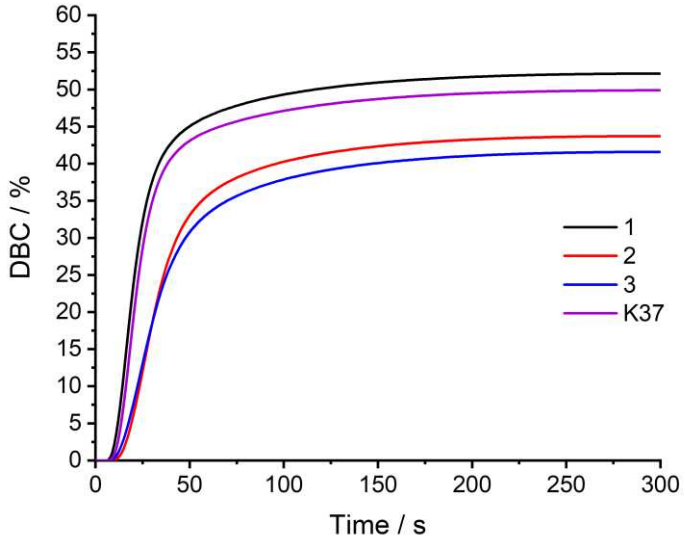

*Figure 14: Conversion curves obtained using different monoacylstannanes (**1**-**3**) as well as K37*

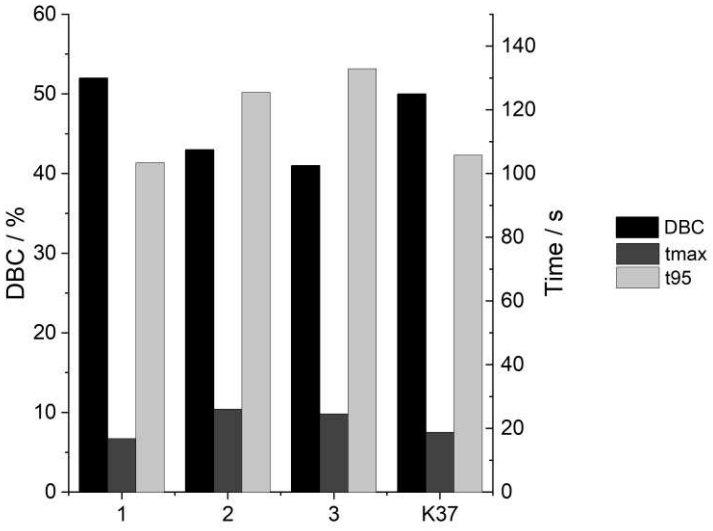

Figure 15: Obtained values for DBC, t_{max} and t_{95}

As with the absorption spectra, it has to be considered that the measured compounds were of different purity. Consequently, only approximate trends can be read from the data obtained. As can be seen from the figures (Figure 14, Figure 15), benzoyltriphenylstannane (**1**) shows very high reactivity in methacrylates. The relevant parameters calculated from the exothermic peaks (DBC, t_{max}, t_{95}) exhibited promising values for this compound. The double-bond conversion at the end of the polymerization was about 53% for benzoyltriphenylstannane (**1**) and 50% for benzoyltrimethylgermane (K37). The time to reach the heat flux maximum (t_{max}) was about 17 s for benzoyltriphenylstannane (**1**) and 19 s for the germane K37. The time to reach 95% of the final conversion (t_{95}) was for benzoyltriphenylstannane (**1**) 103 s, for benzoyltrimethylgermane (**3**) 106 s. Both benzoyltrimethylstannane (**3**) and mesitoyltriphenylstannane (**2**) showed slightly lower reactivities, however this may be due to the lower degree of purity of those compounds.

1.2.3 Stability in aqueous media

All monomers used in dental formulations contain a certain amount of water. Therefore, it is of importance to study the stability of the synthesized monoacylstannanes **1**-**3** in aqueous media (Scheme 35).

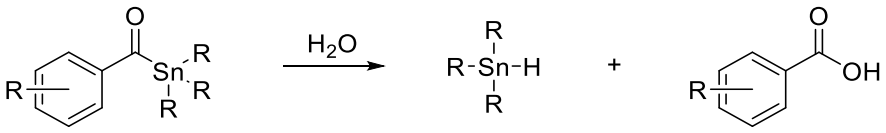

Scheme 35: Potential aqueous hydrolysis of monoacylstannanes

Solutions of benzoyltriphenylstannane (**1**), mesitoyltriphenylstannane (**2**), benzoyltrimethylstannane (**3**) and benzoyltrimethylgermane (K37) were prepared in a 9:1 mixture of acetonitrile and water ($c = 1 \times 10^{-5}$ mol L^{-1}). Afterwards, HPLC measurements with UV/Vis detection were carried out after 0, 4, 7 and 11 days. In between, the samples were stored at room temperature under light exclusion. The obtained peak areas where referred

to the peak area measured directly after dissolving. The obtained values are given in the figure below (Figure 16).

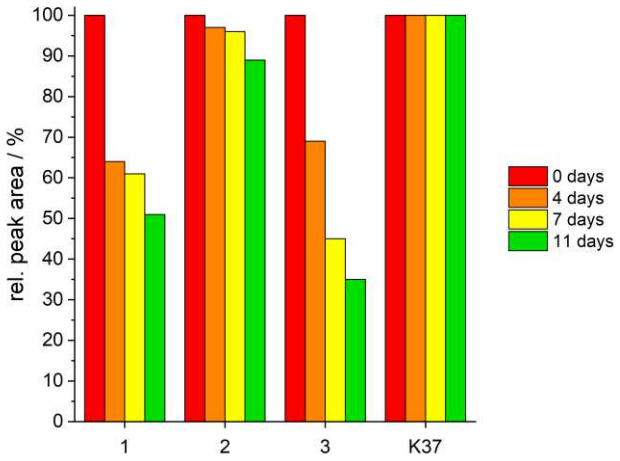

*Figure 16: Evaluation of the stability of the monoacylstannanes (**1**-**3**) and K37 in aqueous media*

It is quite obvious that benzoyltrimethylgermane (K37) did not decompose at all over the investigated time period. As already observed during the synthesis, benzoyltriphenylstannane (**1**) and benzoyltrimethylstannane (**3**) showed rather low stability in aqueous solution. After 4 days only ≈ 70% of the initial initiator concentration was achieved for those two compounds. This value sunk to ≈ 60% and ≈ 45% after a week and after 11 days the peak area had descreased to≈ 50% and ≈ 35%. On the contrary, mesitoyltriphenylstannane (**2**) showed increased stability in aqueous media. After 4 days on 97% of the initial amount was still present. Even after 11 days 89% of the initial peak area could be achieved. These findings confirm the assumption, that the methyl groups in the mesitoyl chromophore provide steric hindrance to the carbonyl group, thus preventing fast hydrolytic degradation.

1.2.4 Steady state photolysis

For many photopolymerization applications in the visible region of light, it is important that the resulting material does not show any coloration after the polymerization process. This is especially true for dental materials. The photocleavage of the Sn-CO bonds is expected to cause rapid photobleaching for acylstannanes (as well as for acylgermanes). To investigate this behavior, steady-state photolysis experiments were carried out for benzoyltriphenylstannane (**1**) and benzoyltrimethylgermane (K37) for comparison. Since the other monoacylstannanes **2**-**4** were not available in high purity, the photobleaching behavior of these compounds was not the target of this study.

For this purpose, solutions of $c_0 = 5 \times 10^{-4}$ mol L^{-1} of each photoinitiator in acetonitrile were transferred into a two-necked photoreactor. The solutions were degassed using argon for 20 minutes and then irradiated from below using a dental LED (Bluephase C 8, 430-490 nm). For irradiation, the mode "High Power" was selected, which corresponds to an intensity of 800 mW cm^{-2}. Within the flask directly behind the flask wall an "effective" intensity of 300 mW cm^{-2} was measured. The distance between dental LED and photoreactor was 4 mm. After starting the irradiation, samples were taken at regular intervals (0 min, 0.5 min, 1.5 min, 3 min, 6 min, 10 min, 15 min) and UV/Vis spectra were recorded subsequently. The maximum absorbance for both photoinitiators decreased with increasing irradiation time, as shown in the figure below (Figure 17).

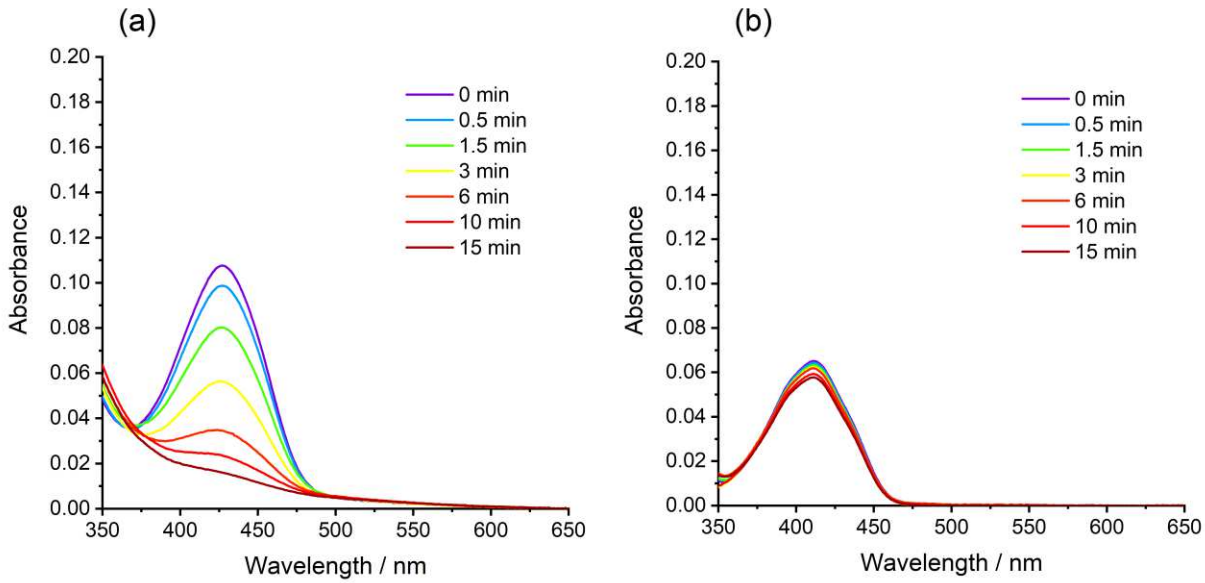

*Figure 17: Steady state photolysis experiments of (a) benzoyltriphenylstannane (**1**) and (b) benzoyltrimethylgermane (K37) in acetonitrile under argon*

After 15 minutes, the absorption band of the nπ * transition of benzoyltriphenylstannane (**1**) had fallen to a minimum, which means that no chromophore absorbing in the visible light range was present after 15 minutes of irradiation (complete photobleaching). For benzoyltrimethylgermane (K37), photobleaching occured much slower. After 15 minutes, the absorbance decreased only slightly, meaning the sample solution was still intensively yellow in color. The significantly faster photobleaching of benzoyltriphenylstannane (**1**) can probably be explained by the greater overlap of the absorption band with the emission band of the dental LED.

1.3 Recap

In order to synthesize monoacylstannanes **1**-**4** (Scheme 36) as potential visible light photoinitiators, two different synthetic pathways were tested (stannyl lithium route and hexaorganodistannane route). The stannyl lithium route (pathway A, chapter 1.1.1) led to the successful preparation of benzoyltriphenylstannane (**1**), for which a suitable purification protocol could be developed. For mesitoyltriphenylstannane (**2**), a lower product yield was obtained using pathway A and the compound was not isolated in high purity. Using pathway B (hexaorganodistannane route, chapter 1.1.2), the trimethyl derivatives benzoyltrimethylstannane (**3**) and mesitoyltrimethylstannane (**4**) could be prepared, however these compounds showed rather low stability and were therefore not isolated in high purity. Furthermore, pathway B was tested for the synthesis of benzoyltriphenylstannane (**1**), unsuccessfully though.

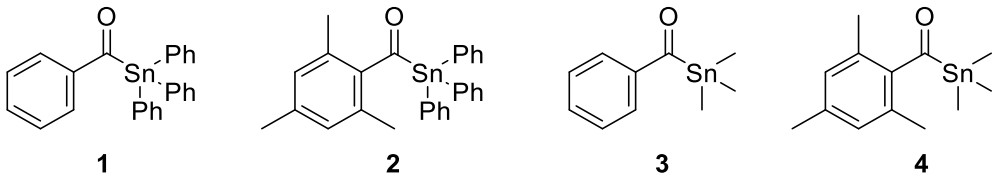

*Scheme 36: Targeted monoacylstannanes **1**-**4***

The synthesized monoacylstannanes **1**-**3** were then characterized regarding their photochemical properties. The nπ* absorption band of the benzoylstannanes **1** and **3** was clearly red-shifted compared to the germanium reference (chapter 1.2.1) and particularly benzoyltriphenylstannane (**1**) showed very high initiation activity in methacrylates (chapter 1.2.2). Investigations regarding the stability of the monoacylstannanes in aqueous media showed, that the introduction of a bulkier mesitoyl group instead of the benzoyl chromophore leads to increased stabilities (chapter 1.2.3). Additionally, steady state photolysis experiments in solution were carried out to evaluate the photobleaching behavior of benzoyltriphenylstannane (**1**) in comparison to a monoacylgermane, in which the acylstannane **1** showed extraordinarily fast photobleaching (chapter 1.2.4).

In summary, the compound benzoyltriphenylstannane (**1**) was found to be superior to similar germanium compounds in many ways. Benefits like the easy and rather cheap synthesis as well as the red-shifted absorbance, the high reactivity and the very fast photobleaching make benzoyltriphenylstannane (**1**) a potential alternative in applications like the curing of dental fillings. Solely in terms of hydrolytic stability, improvements could be necessary to realize its usage in dental composites.

2 Bisacylstannanes

Since bisacylgermanium compounds like Ivocerin® (Scheme 37) are applied in dental composites already, the corresponding difunctional stannane compounds are of high interest and should therefore be approached with high priority.

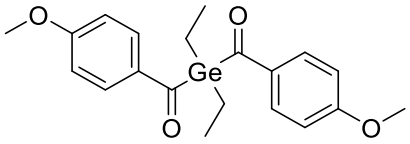

Ivocerin®

Scheme 37: Industrially applied bisacylgermane photoinitiator Ivocerin® (Ivoclar Vivadent)

Regarding bisacylstannanes, the three compounds below were chosen as target compounds (Scheme 38). This selection of compounds was picked based on the assumption, that both the substituents on the aromatic benzoyl chromophores as well as the substituents directly bonded to the tin atom have an influence on the absorption properties as well as the hydrolytic stability of the bisacylstannanes. Furthermore, the reactants needed in order to synthesize these compounds are cheap and commercially available.

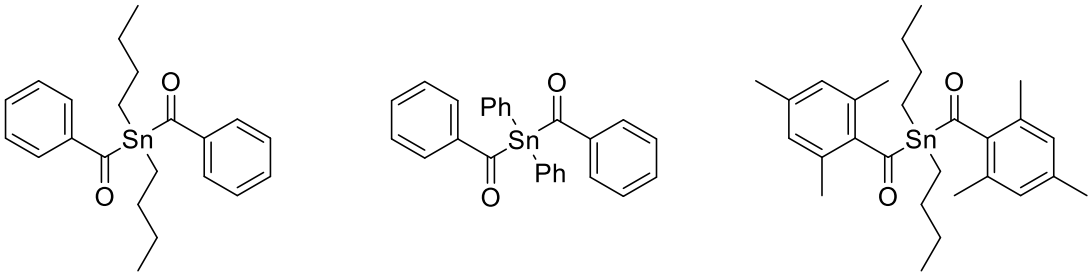

5 **6** **7**

*Scheme 38: Selection of bisacylstannane target compounds **5-7***

As far as a successful isolation of those compounds can be achieved, information about the influence of different substituents on the aromatic ring as well as directly on the tin atom with regard to stability, absorption properties and photoreactivity should be gathered.

2.1 Synthesis

For the synthesis of the bisacylstannanes, numerous potential synthetic routes (A-E) were envisaged (Scheme 39).

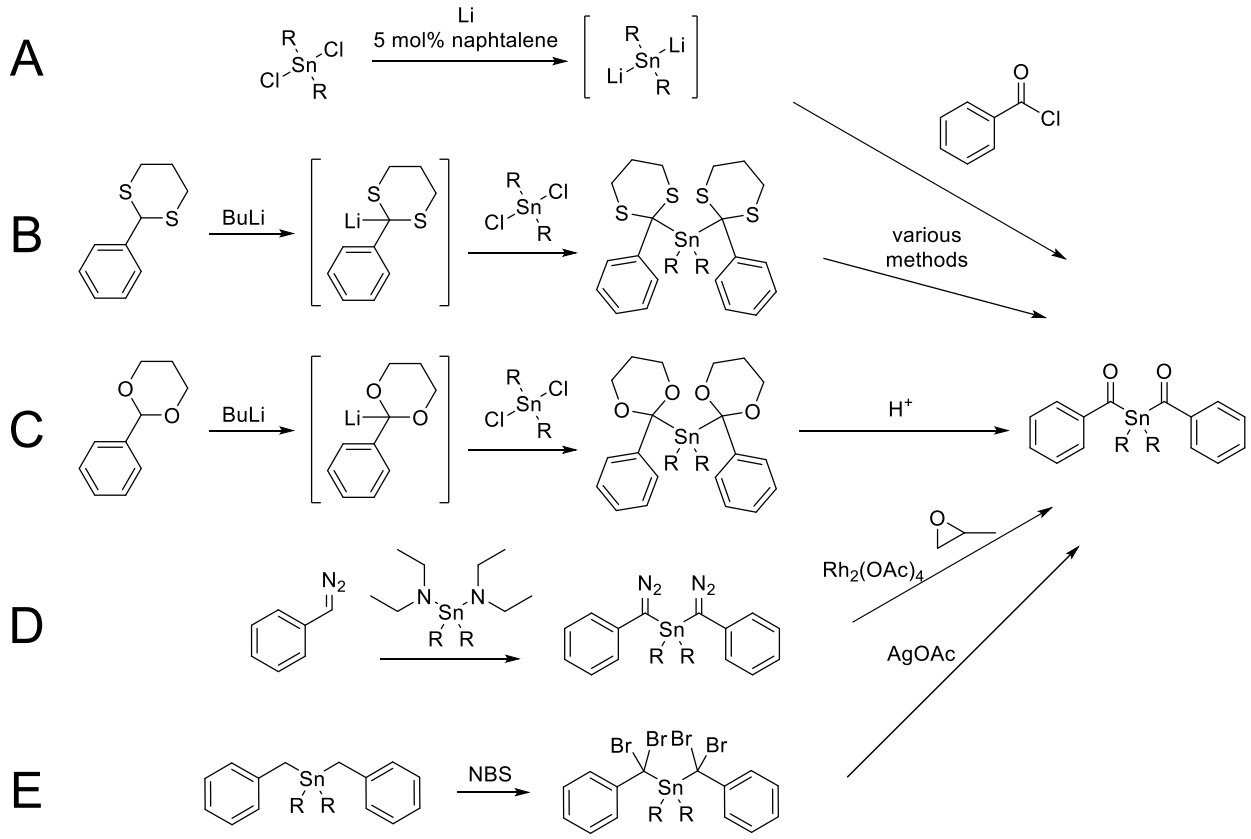

Scheme 39: Five different pathways towards the synthesis of bisacylstannanes

The first route (pathway A, Scheme 39) is based on the route, described by Peddle,[31] which was already successfully tested for the monoacylstannanes. Herein, an intermediately formed stannyl lithium species is reacted with an acid chloride to give monoacylstannanes. The stannyl lithium formation should be further modified using naphthalene as a catalyst as described by Wang et al..[44] In order to synthesize the desired bisacylstannanes, the method needs to be adapted even more by using the corresponding dichlorides.

Pathway B is based on the widely known Corey-Seebach reaction (Scheme 39).[49] This method could be successfully modified to synthesize bisacylgermanes[50] and is at this time the method of choice for those compounds. The acyl moiety undergoes an "Umpolung" after dithiane formation and lithiation, before being reacted with a diorganodichlorostannane. In the final step, the dithiane groups are cleaved off and the carbonyl functionalities are introduced. This should in theory lead to the desired bisacylstannanes.

A third potential route (pathway C, Scheme 39) is a route, quite similar to pathway B. Herein, instead of dithianes, dioxanes are used to achieve an "Umpolung" of the acyl moiety. The idea, which is supported by a publication of Kruithof et al.[51] is, that dioxane protection groups are much more labile compared to their sulfur analogues and could therefore potentially be cleaved off significantly easier. However, Kruithof et al. describe this method for the synthesis of silyl, germyl and stannyl alk-1-ynyl ketones.

Pathway D is based on a route (Scheme 39), which has been successfully applied in the synthesis of silyl- and germylglyoxylates[52] quite recently. It involves a diazo species, which could potentially be reacted with electrophilic stannyl moieties[43] to form the desired bisacylstannanes.

Another pathway potentially leading towards a successful isolation of bisacylstannanes could be a route described by Brook and Peddle[53] (pathway E, Scheme 39) for the corresponding acylsilanes. A suitable tetraorganostannane could be prepared in the first step, which could then be entirely brominated. In a final step, the carbonyl functionalities could afterwards be introduced by reacting it with silver acetate.

Since all pathways involved moisture-sensitive compounds and many of those being light-sensitive in addition to that, all reactions, which demand certain measures concerning these issues were carried out in an orange light lab to exclude light with wavelengths below 520 nm and Schlenk techniques were used to secure complete exclusion of oxygen and moisture.

2.1.1 Stannyl dilithium route (Pathway A)

2.1.1.1 Synthesis of bisbenzoyldiphenylstannane (6)

To synthesize the first bisacylstannane compound bisbenzoyldiphenylstannane (**6**), the known method of Peddle[31] to synthesize monoacylstannanes (chapter 1.1.1) should be tested for the difunctional derivatives. The method was further adapted using a route, described by Wang et al..[44] Initially, the stannyl dilithium species should be formed by reacting diphenyldichlorostannane with an excess of elemental lithium using naphthalene as a catalyst in dry THF. The intermediate should afterwards be reacted with benzoyl chloride to form the target compound **6**.

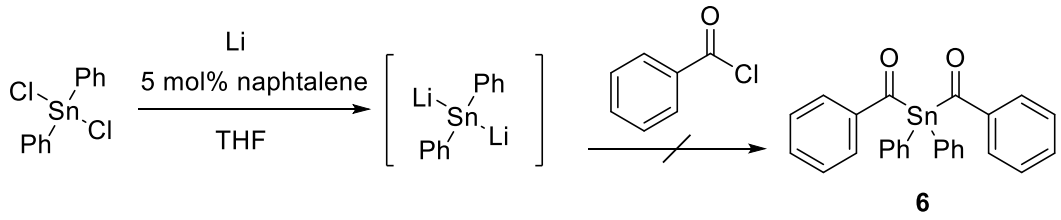

*Scheme 40: Synthesis of bisbenzoyldiphenylstannane (**6**) via pathway A*

For the synthesis of bisbenzoyldiphenylstannane (**6**), 1 eq. of dichlorodiphenylstannane and 6 eq. of fine cut lithium foil were weighed into separate Schlenk tubes inside a glove box and dry THF was added to each of the reaction vessels. The Schlenk tubes were connected to a Schlenk line and 0.05 eq. of naphthalene were added to the lithium suspension as a catalyst leading to a color change to dark green. The solution of dichlorodiphenylstannane was then added to the lithium suspension at RT over 5 min via syringe and septum. During stirring at RT for 3 h, a clearly visible black precipitate formed. In the meantime, another Schlenk tube was prepared containing a solution of 2.1 eq. of benzoyl chloride in dry THF. Both mixtures were then cooled to -78°C and the stannyl lithium solution was then added to the acid chloride solution at that temperature over 10 min. After complete addition, the cooling bath was removed and the reaction mixture was allowed to reach RT under complete light exclusion. After 2 h the solvent was evaporated directly using the Schlenk line and a cooling trap. The residue was then taken up in dry n-pentane and filtrated under inert conditions. A

dark solid was partially separated in this step. Interestingly, this solid formed a yellow solution when dissolved in acetone. The filter cake was washed with dry n-pentane and the solvent was then removed from the filtrate giving a yellow, sticky residue.

A GC-MS measurement of the product mixture was performed, however the target compound could not be confirmed. Instead, large amounts of unreacted benzoyl chloride could be detected. Therefore, the synthesis was repeated except that, after adding to the benzoyl chloride solution, the reaction mixture was stirred overnight this time. Even after this adaptation, GC-MS gave the same results: a mixture of at least 8 different substances, none of these could be identified as the target compound. In addition, HPLC was carried out, again confirming the presence of a multicomponent product mixture. One of these compounds (probably the target compound dibenzoyldiphenylstannane (**6**) showed absorption up to 500 nm, however it accounted for only about 5% of the complicated mixture. Furthermore, another synthesis attempt with subsequent aqueous work-up (Et_2O and water) was carried out, which did not lead to satisfying results either.

It is very likely that during the synthesis of bisbenzoyldiphenylstannane (**6**), oligo- and polystannane compounds were formed (Scheme 41). This phenomenon was already observed previously in the case of the corresponding germanium derivatives. This might also be an explanation for the odd dissolution behavior of the black solid, obtained as a side product.

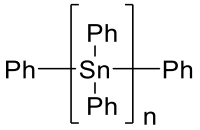

Scheme 41: Proposed formation of undesired polystannane compounds

2.1.1.2 Synthesis of bisbenzoyldibutylstannane (5)

Although the above described route did not lead to a successful isolation of a first bisacylstannane compound, it should be applied in a similar fashion for another derivative, namely the dibutyl compound. The substituents on the tin atom in diorganodichlorostannanes might have a huge influence on the reactivity of those compounds, which is why the route based on the method described by Peddle[31] and Wang et al.[44] should be tested for a potential synthesis of bisbenzoyldibutylstannane (**5**). The structure of this compound shows an even higher similarity to the structure of Ivocerin® and could therefore be accessible more easily.

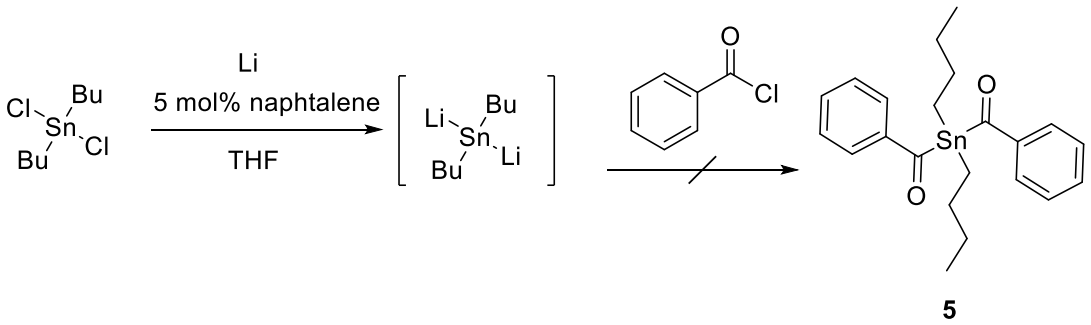

*Scheme 42: Synthesis of bisbenzoyldibutylstannane (**5**) via pathway A*

For the synthesis of bisbenzoyldibutylstannane (**5**), 1 eq. of dichlorodibutylstannane and 6 eq. of fine cut lithium foil were weighed into separate Schlenk tubes inside a glove box and dry THF was added to each of the reaction vessels. The Schlenk tubes were connected to a Schlenk line and 0.05 eq. of naphthalene were added to the lithium suspension as a catalyst leading to a color change to dark green. The solution of dichlorodibutylstannane was then added to the lithium suspension at RT over 5 min via syringe and septum. During stirring at RT for 3 h, a clearly visible black precipitate formed. In the meantime, another Schlenk tube was prepared containing a solution of 2.1 eq. of benzoyl chloride in dry THF. Both mixtures were then cooled to -78°C and the stannyl lithium solution was then added to the acid chloride solution at that temperature over 10 min. After complete addition, the cooling bath was removed and the reaction mixture was allowed to reach RT overnight under complete

light exclusion. The solvent was evaporated directly using the Schlenk line and a cooling trap. The residue was then taken up in dry n-pentane and filtrated under inert conditions. The filter cake was washed with dry n-pentane and the solvent was then removed from the filtrate giving a yellow, sticky residue.

As in the case of the synthesis of dibenzoyldiphenylstannane (**6**) already, this residue contained a mixture of several substances. Again, the target compound could not be confirmed via GC-MS, but large amounts of tetrabutylstannane and hexabutyldistannane could be detected (Scheme 43).

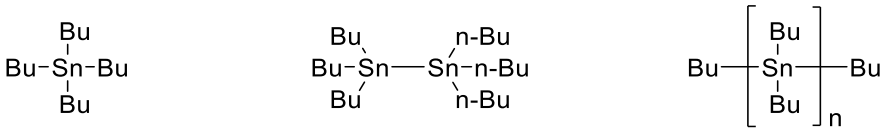

Scheme 43: Tetrabutylstannane, hexabutyldistannane and polystannane as probable components of the product mixture

The HPLC analysis additionally confirmed this presumption. Again a compound could be detected, which showed absorption up to 500 nm (possibly the target compound). An attempt to separate this compound from the rest of the mixture via precipitation was carried out. For this purpose, a portion of the crude product was dissolved in acetonitrile and then water was slowly added dropwise. Although a small amount of precipitate formed while doing so, no purifying effect could be achieved. In addition, attempts to wash out the impurities by addition of water were carried out. A small part of the crude product was dissolved in n-pentane and then added to water. Thin layer chromatography was carried out both before and after the extraction step, which showed that this experiment did not lead to success either. Seven spots in total could be detected on the TLC, probably coming from the corresponding oligo- and polystannanes. Nevertheless, a purification attempt using a silica gel column (PE 2:1 DCM) was carried out, with which, the desired target compound could not be isolated as well. The residue obtained after the separation column did no longer show a yellow coloration, which is why it can be assumed that the compound had decomposed on the column or in the previous steps.

In summary, pathway A did not lead to the successful isolation of a bisacylstannane compound. Neither bisbenzoyldiphenylstannane (**6**) nor bisbenzoyldibutylstannane (**5**) could be prepared using this method. The evaluation of the other proposed synthetic pathways (B-E) is described in the following chapters.

2.1.2 Dithiane route (Pathway B)

2.1.2.1 Synthesis of dibutyldi(2-phenyl-1,3-dithian-2-yl)stannane (8)

The Dithiane route (pathway B) is based on the widely known Corey-Seebach reaction (Scheme 39).[49] This method could be successfully modified for the synthesis of bisacylgermanes.[50] The acyl moiety undergoes an "Umpolung" after dithiane formation and lithiation, before being reacted with a diorganodichlorostannane. In the final step, the dithiane groups should be cleaved off and the carbonyl functionalities are introduced using a variety of different methods. The dithiane route should be tested for the synthesis of bisbenzoyldibutylstannane (**5**) due to its structural similarity to compounds like Ivocerin® (Scheme 37). In order to achieve this compound, the dithiane-protected compound dibutyldi(2-phenyl-1,3-dithian-2-yl)stannane (**8**) needed to be synthesized initially.

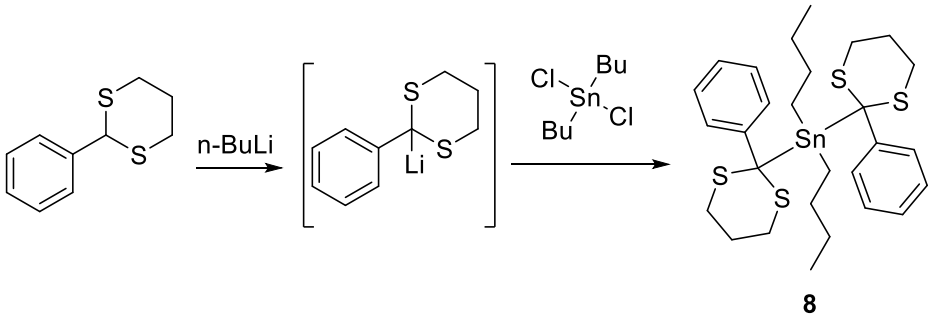

8

*Scheme 44: Synthesis of dibutyldi(2-phenyl-1,3-dithian-2-yl)stannane (**8**)*

For the synthesis of dibutyldi(2-phenyl-1,3-dithian-2-yl)stannane (**8**), 2.4 eq. of 2-phenyl-1,3-dithiane were reacted with 2.4 eq. of n-butyllithium in THF to form the lithium intermediate,

which was afterwards reacted with 1 eq. of dibutyldichlorostannane. Aqueous workup followed by recrystallization of the crude product, gave the target compound as a colorless crystalline solid (86%) in high purity. The structure was confirmed using NMR spectroscopy and the substance was then used without any further purification in the following reaction steps.

2.1.2.2 Synthesis of bisbenzoyldibutylstannane (5)

Since the synthesis of dibutyldi(2-phenyl-1,3-dithian-2-yl)stannane (**8**) could be carried out successfully and this intermediate product could be isolated, it should be used in the next step to prepare bisbenzoyldibutylstannane (**5**). There are several methods known in literature to cleave off a dithiane protection group and simultaneously introduce the carbonyl group.[54, 55] The attempts and investigations in order to obtain the desired compound are described in the following.

2.1.2.2.1 Dithiane deprotection using $I_2/CaCO_3$

In the first attempt to synthesize bisbenzoyldibutylstannane (**5**) from dibutyldi(2-phenyl-1,3-dithian-2-yl)stannane (**8**), a method described by Bouillon and Portella[54] involving iodine and calcium carbonate under aqueous conditions should be tested.

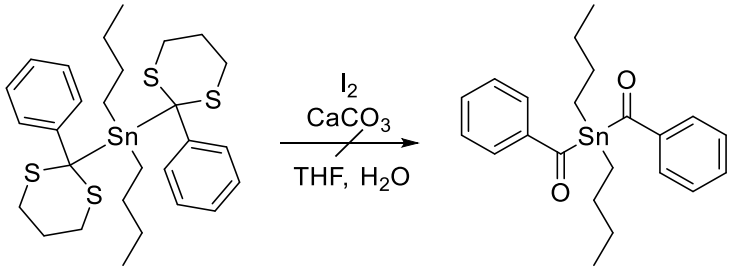

8 **5**

*Scheme 45: Synthesis of bisbenzoyldibutylstannane (**5**) via pathway B using I_2/$CaCO_3$*

For the synthesis of bisbenzoyldibutylstannane (**5**), 1 eq. of previously synthesized dibutyldi(2-phenyl-1,3-dithian-2-yl)stannane (**8**) was weighed into a round bottom flask and dissolved in a 5:1 mixture of THF and water. Then, 12 eq. of calcium carbonate and 12 eq. of iodine were separated into 8 equally large portions where one portion was added to the solution in a 30 min interval. While doing so, the mixture was cooled to 0°C using an ice bath. After complete addition, it was stirred for further 24 h at RT. Afterwards, the mixture was filtrated over silica gel and sat. aqueous sodium dithionite solution was added to the filtrate until a color change to yellow was visible and the excess iodine had been converted. After another filtration step and washing of the filter cake using ethyl acetate, the layers were separated and the aqueous layer was extracted twice with water. The combined organic layers were washed with water and brine and afterwards dried over sodium sulfate. Filtration and evaporation of the solvent in vacuo gave a colorless residue.

A ^{119}Sn-NMR spectrum was measured, from which no tin signal could be detected. Additionally a preliminary photopolymerization experiment in UDMA 1:1 D_3MA was not successful. It was assumed that the synthesis under aqueous conditions or the conditions as a whole had been too harsh for the desired bisacyl compound **5** to form. Product formation either did not occur at all or the target compound **5** decomposed entirely during the work-up procedure. Perhaps residual acid in the ethyl acetate was a problem, so the synthesis was repeated using diethyl ether instead of the ethyl acetate, but no improvement could be obtained here either.

2.1.2.2.2 Dithiane deprotection using diacetoxyiodobenzene/BF_3·$O(Et)_2$

Since the first method did not lead to the expected results, another method to cleave the dithiane groups and restore the carbonyl functionalities should be tested. The method (suggested by Ivoclar Vivadent) using diacetoxyiodobenzene and boron trifluoride diethyl etherate goes without the use of water as the reaction medium. Instead, dry methanol is used. This might be beneficial for a successful isolation of the target compound, since potential hydrolytic degradation processes might be repressed.

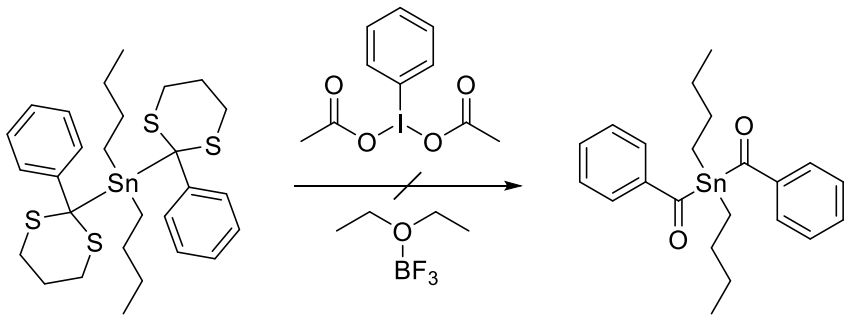

8 **5**

Scheme 46: Synthesis of bisbenzoyldibutylstannane (5) via pathway B using diacetoxyiodobenzene/ BF_3·$O(Et)_2$

For the synthesis of bisbenzoyldibutylstannane (**5**), 1 eq. of previously synthesized dibutyldi(2-phenyl-1,3-dithian-2-yl)stannane (**8**) was weighed into a Schlenk tube and suspended in dry methanol. Subsequently, 4 eq. of diacetoxyiodobenzene and 4 eq. of boron trifluoride diethyl etherate were separated into 4 equally large portions and the first portions were added to the suspension, causing a temperature increase to 40°C. Over intervals of 30 min the other portions were added and the mixture was stirred for 22 h at RT. Afterwards, the mixture was diluted with dry n-pentane and filtrated under inert conditions. The pale yellow filtrate was concentrated to dryness giving a brownish residue, which was then analyzed by NMR spectroscopy.

As in the previous synthesis, both the ^{119}Sn and the ^{1}H NMR spectra did not indicate the formation of the target compound. Obviously, the water as the reaction medium was not the

problem. Since both previously tested methods for restoring the carbonyl groups were unsuccessful, alternatives must still be sought to make bisbenzoyldibutylstannane (**5**) and the compound class of bisacylstannanes as a whole available for a photochemical characterization.

2.1.2.2.3 Dithiane deprotection using $HgCl_2/CdCO_3$

Alternatively, another method for restoring the carbonyl groups from dibutyldi(2-phenyl-1,3-dithian-2-yl)stannane (**8**) should be evaluated. This method, described by Brook et al.[55] was applied for the corresponding silicon and germanium compounds and relies on mercury(II)chloride and cadmium carbonate. Although this method was definitely not the first choice, it may be the only way to successfully synthesize bisbenzoyldibutylstannane (**5**).

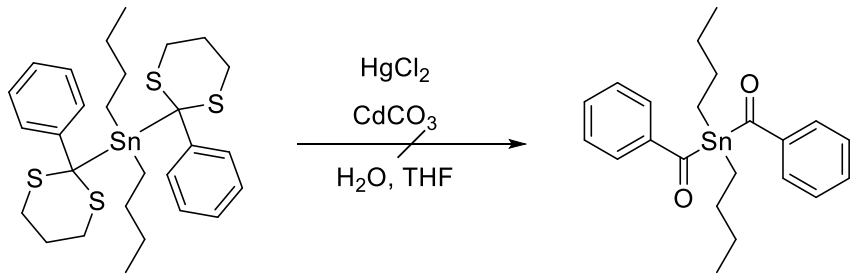

8 **5**

*Scheme 47: Synthesis of bisbenzoyldibutylstannane (**5**) via pathway B using $HgCl_2/CdCO_3$*

For the synthesis of bisbenzoyldibutylstannane (**5**), 1 eq. of previously synthesized dibutyldi(2-phenyl-1,3-dithian-2-yl)stannane (**8**) was weighed in together with 5 eq. of mercury(II)chloride and 5 eq. of cadmium carbonate and dissolved in a 9:1 mixture of THF and water. This mixture was then refluxed for 2 h before measuring a ^{119}Sn-NMR spectrum directly from the reaction mixture via D_2O capillary to ensure inert conditions until the measurement. Two signals were detected (-92.9 ppm and -144.1 ppm), for which it was assumed to belong to the one-fold and the two-fold deprotected stannanes. However, the

solution was hardly colored at this time, so it was further refluxed overnight. Even overnight, the solution did not appear to be yellow, but was completely colorless. Another ^{119}Sn-NMR spectrum after removal of the solvent showed numerous tin signals, which could not be assigned to any known compounds. A separation of those components seemed unreachable at that point.

Since all three attempts to synthesize bisbenzoyldibutylstannane (**5**) from the corresponding dithiane compound via pathway B did not give the desired outcome, it was decided to proceed with pathway C in order to synthesize the first bisacylstannane compound.

2.1.3 Dioxane route (Pathway C)

2.1.3.1 Synthesis of 2-phenyl-1,3-dioxane (9)

In order to test the dioxane route (pathway C) for the synthesis of bisacylstannanes, the starting material 2-phenyl-1,3-dioxane (**9**) needed to be synthesized. Since the analogue dithiane compound was available from previous experiments already, the target compound should initially be synthesized starting from 2-phenyl-1,3-dithiane and 1,3-propanediol using a method described by Karimi et al..[56]

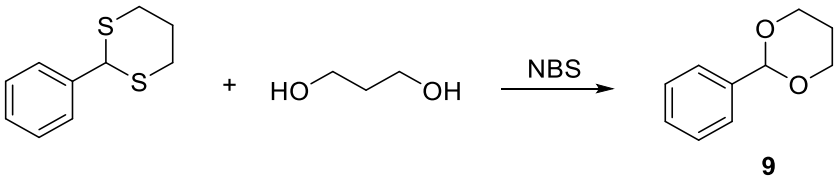

*Scheme 48: Synthesis of 2-phenyl-1,3-dioxane (**9**) from the analogue dithiane*

For the synthesis of 2-phenyl-1,3-dioxane (**9**), 1 eq. of 2-phenyl-1,3-dithiane and 3 eq. of 1,3-propanediol were reacted in dry dichloromethane prior to adding 1 eq. of N-bromosuccinimide in order to form the target compound. After an aqueous workup, the product could be obtained in high purity as colorless, crystalline substance (97%).

When 2-phenyl-1,3-dithiane was not available in the lab anymore, another much more cost-efficient synthesis for 2-phenyl-1,3-dioxane (**9**) was carried out. Firouzabadi et al.[57] described the respective synthesis starting from benzaldehyde. Herein, catalytic amounts of zirconium tetrachloride and triethyl orthoformate are used together with 1,3-propanediol to obtain the target compound.

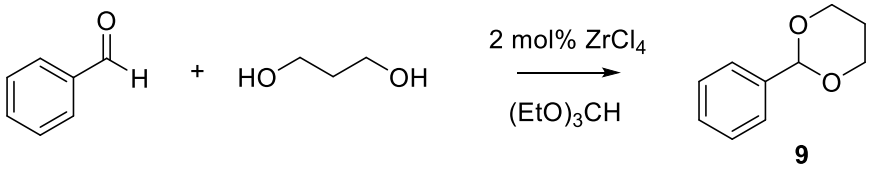

*Scheme 49: Synthesis of 2-phenyl-1,3-dioxane (**9**) from benzaldehyde*

For the synthesis of 2-phenyl-1,3-dioxane (**9**), 1 eq. of benzaldehyde and 1.5 eq. of 1,3-propanediol were reacted in the presence of 1 eq. of triethyl orthoformate and 0.02 eq. of solid zirconium tetrachloride in dry dichloromethane. After quenching with aqueous NaOH and an aqueous workup the product was obtained in high purity as a colorless, crystalline solid (99%).

Both of the evaluated synthesis routes worked really well to synthesize the intermediate 2-phenyl-1,3-dioxane (**9**). Product prepared via both routes was used in the following experiments in order to synthesize the desired bisacylstannanes.

2.1.3.2 Synthesis of dibutylbis(2-phenyl-1,3-dioxane-2-yl)stannane (10)

In order to achieve bisbenzoyldibutylstannane (**5**) via the dioxane route (pathway C), the dioxane-protected compound dibutyldi(2-phenyl-1,3-dioxane-2-yl)stannane (**10**) needed to be synthesized initially. This should be achieved using a similar method as the one described in the chapter above (chapter 2.1.2.1). It is based on the Corey-Seebach reaction,[49] however

a dioxane should be used for the “Umpolung” instead of a dithiane, as described by Kruithof et al..[51]

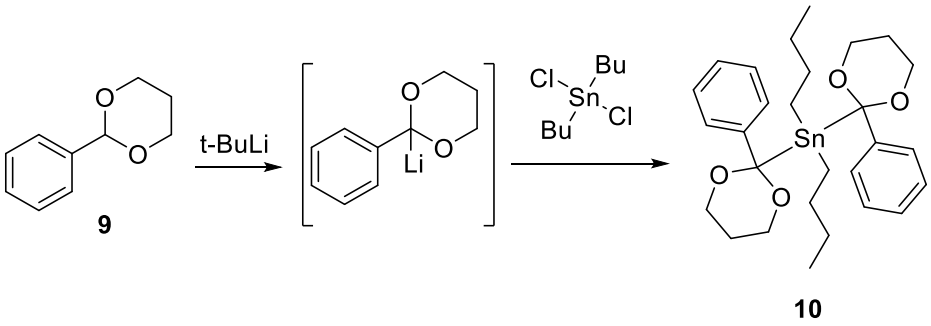

*Scheme 50: Synthesis of dibutylbis(2-phenyl-1,3-dioxane-2-yl)stannane (**10**)*

For the synthesis of dibutyldi(2-phenyl-1,3-dioxane-2-yl)stannane (**10**), a suspension of 2.4 eq. of previously synthesized 2-phenyl-1,3-dioxane (**9**) in a mixture of dry THF and dry n-pentane (5:2) was prepared and cooled to -79°C. Over the period of 15 min, 2.5 eq. of t-butyllithium (1.7 M in pentane) were added at that temperature slowly via syringe and septum giving a turquoise-green solution. The mixture was stirred for 2 h at -79°C before adding a solution of 1 eq. of dibutyldichlorostannane in the same solvent mixture at that temperature. After complete addition, a color change from green to yellow-orange was clearly visible. The mixture was stirred at -79°C for further 3 h and then it was allowed to reach RT overnight. On the next day, the reaction mixture was diluted with diethyl ether and quenched with water. The layers were separated and the aqueous layer was extracted three times with diethyl ether. The combined organic layers were washed with water and dried over sodium sulfate. After filtration and evaporation of the solvent, a highly viscous, light yellow crude product was obtained (81%).

Although the synthesis seemed to be successful, a large amount of the reactant 2-phenyl-1,3-dioxane (**9**) was confirmed to be part of the crude product mixture among other compounds. The purification of dibutyldi(2-phenyl-1,3-dioxane-2-yl)stannane (**10**) was very important, since large amounts of impurities could potentially overcomplicate the successive deprotection step. Therefore, the synthesis should be investigated in greater detail and

optimized. In order to better describe the different attempts to improve the synthesis and the path towards a successful work-up protocol, the reaction should be broken down into its substeps and described one by one.

For the first substep of the reaction (lithiation of 2-phenyl-1,3-dioxane, Scheme 51), a significantly better result could be achieved using tert-butyllithium instead of the n-butyllithium used by Kruithof et al..[51] However, the low solubility of 2-phenyl-1,3-dioxane (**9**) at -79 ° C. (acetone/N_2) in the solvent mixture proposed by Kruithof (THF 5:2 n-pentane) turned out to be problematic. For this reason, the temperature should be raised, but it should be noted that temperature changes can often have considerable influence especially on organometallic reactions (lithiation vs. alkylation). By means of a $CHCl_3/N_2$ bath, the temperature could be raised to -61°C, however this was not enough to achieve complete dissolution of 2-phenyl-1,3-dioxane (**9**) either. Only at a temperature of -42°C (acetonitrile/N_2), the starting material was completely dissolved and t-BuLi could be carefully added dropwise.

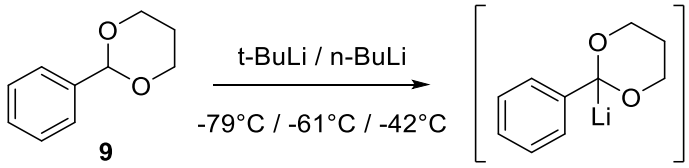

Scheme 51: Synthesis of lithiated 2-phenyl-1,3-dioxane (substep 1)

With continued addition of t-BuLi at -42°C, the solution turned increasingly red. The solution was stirred for a further 45 minutes after the addition had ended. In the second part of the reaction (reaction of the lithiated species with dibutyldichlorostannane), the question of choosing the optimum temperature arose again. This substep (substep 2) was carried out at -42 ° C as well as at -79 ° C, whereby no relevant differences could be observed on the result.

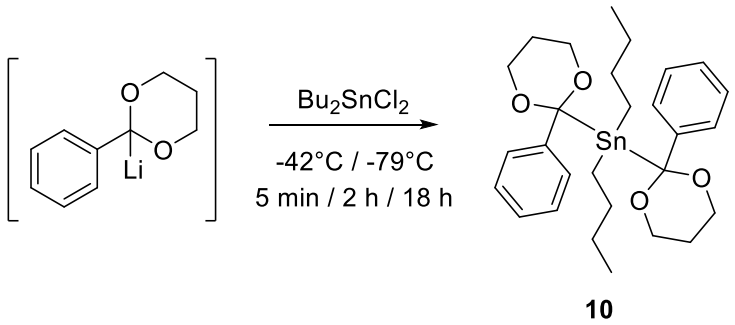

10

Scheme 52: Reaction of the lithiated species with dibutyldichlorostannane (substep 2)

Another possibility for variation was the reaction time of this step. The reaction was stopped once after 5 min already, once after 2 h and once after stirring overnight, with the 2 h reaction time being the most beneficial one of these three. Dibutyldichlorostannane was added in all cases as a solution in THF 5:2 n-pentane, whereby the solution decolorized with continued addition.

Obviously, for this reaction a variety of possible variations (temperature, solvent, reaction time, dropping speed, ...) could be carried out. The molar ratios of the starting materials were varied (2-phenyl-1,3-dioxane (**9**) in excess or equimolar ratios), which did not change the final result either. By being able to vary so many details at each step, it would probably still take a lot of time to find the truly optimal reaction conditions for the synthesis of dibutyldi(2-phenyl-1,3-dioxane-2-yl)stannane (**10**). Nevertheless, the following synthetic protocol describes the method, which led to the best results so far (Scheme 53).

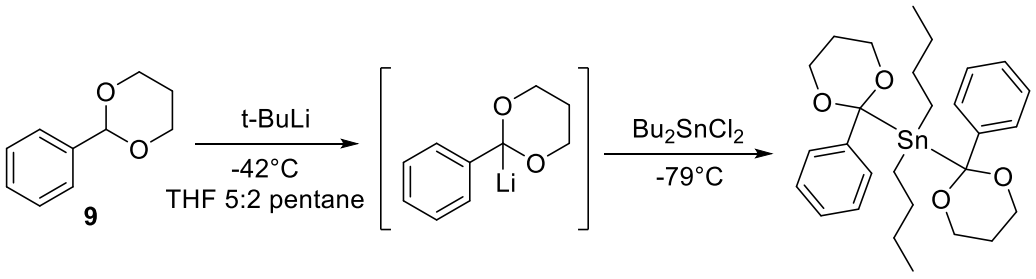

9 **10**

*Scheme 53: Improved synthetic protocol for the synthesis of dibutyldi(2-phenyl-1,3-dioxane-2-yl)stannane (**10**)*

For the synthesis of dibutyldi(2-phenyl-1,3-dioxane-2-yl)stannane (**10**), 2.4 eq. of previously synthesized 2-phenyl-1,3-dioxane (**9**) and 1 eq. of dibutyldichlorostannane were weighed into two separate Schlenk tubes within a Glove box and dissolved in a mixture of THF and n-pentane (5:2) each. Afterwards, the dioxane solution was cooled to -42°C and 2.5 eq. of t-butyllithium (1.7 M in pentane) were added over the period of 15 min at that temperature resulting in a color change to red. The mixture was then stirred for 45 min at -42°C before being cooled to -79°C. At that temperature, the dibutyldichlorostannane solution was added over 15 min (decoloration). The reaction mixture was stirred for 1 h at that temperature before removing the cooling bath and stirring for another hour. Subsequently, the mixture was diluted with diethyl ether and quenched with 5% aqueous $NaHCO_3$ solution. The layers were separated, the aqueous layer was extracted three times with diethyl ether and the combined organic layers were washed with water. After drying over sodium sulfate and filtration the solvent was evaporated in vacuo.

The residue contained the target compound as well as a considerable amount of 2-phenyl-1,3-dioxane (**9**) still and another unidentified compound. To separate the unknown compound from the mixture, a flash column (aluminum oxide, PE 3:1 Et_2O) was used successfully. However, 2-phenyl-1,3-dioxane (**9**) could not be removed entirely in this step. Various precipitation steps in different solvents did not change that. Basically, only aluminum oxide can be used for the purification of the target compound, since the acidic groups on silica gel lead to uncontrolled cleavage of the dioxane protection groups already. When working with dibutyldi(2-phenyl-1,3-dioxane-2-yl)stannane (**10**), it is important to ensure, that the pH is more in the basic range, which is why the quenching step in the synthesis described above was also carried out with a $NaHCO_3$ solution (slightly basic). After purification by means of an aluminum oxide flash column, the product **10** could be isolated as a colorless oil (25%), however the contamination in form of 2-phenyl-1,3-dioxane (**9**) could not be removed entirely after various attempts.

2.1.3.3 Synthesis of bisbenzoyldibutylstannane (5)

The advantages of cleaving the dioxane groups over that of the dithiane groups have already been discussed in detail above. By acid hydrolysis of the cyclic acetal groups, the carbonyl groups should be restored. To realize this, there is a variety of known methods.[58] Since dibutylbis(2-phenyl-1,3-dioxan-2-yl)stannane (**10**) could only be obtained as a mixture with 2-phenyl-1,3-dioxane (**9**), it had to be assumed that the acetal group in 2-phenyl-1,3-dioxane (**9**) would also deprotected during the synthesis of bisbenzoyldibutylstannane (**5**), which should lead to the formation of benzaldehyde. In addition, with each cleavage reaction of the dioxane groups, the corresponding diol is formed (Scheme 54).

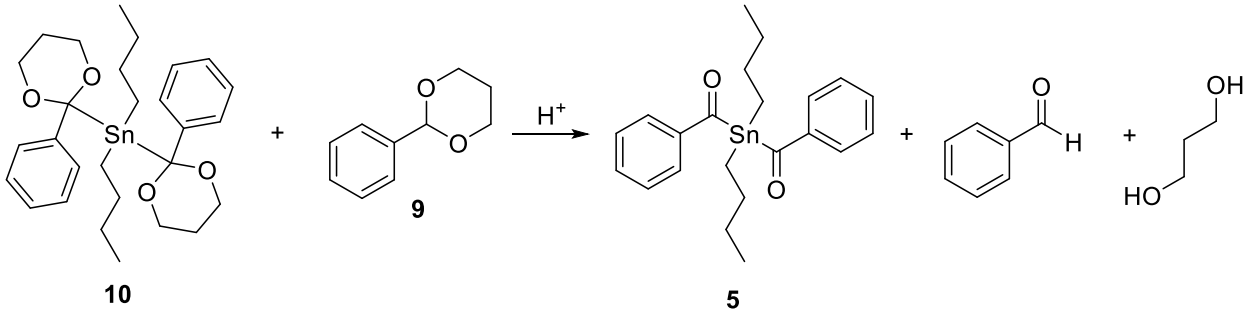

Scheme 54: Parallel deprotection reactions

2.1.3.3.1 Dioxane deprotection using HCl

One way to cleave the dioxane protecting groups is described by Grieco et al..[59] Herein, the protected compound is treated with 5% HCl. Of course, the reaction time and temperature are highly dependent on the starting material used. The detailed procedure for the conversion of dibutylbis(2-phenyl-1,3-dioxan-2-yl)stannane (**10**) to the desired product dibenzoyldibutylstannane (**5**) using HCl is described below.

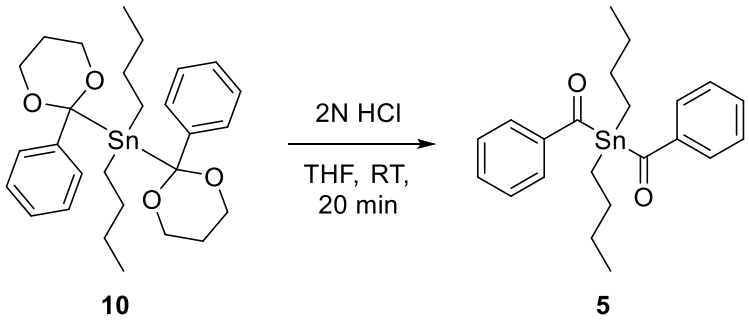

10 **5**

*Scheme 55: Synthesis of bisbenzoyldibutylstannane (**5**) using HCl*

For the synthesis of bisbenzoyldibutylstannane (**5**), 1 eq. of previously synthesized dibutylbis(2-phenyl-1,3-dioxan-2-yl)stannane (**10**, contaminated with 2-phenyl-1,3-dioxane **9**) was dissolved in THF before adding a 2 N aqueous HCl solution. The color change to yellow could be observed instantly. The mixture was stirred for 20 min at RT and then diluted with diethyl ether. The layers were separated and the organic layer was washed three times with water. After drying over sodium sulfate, filtration and evaporation of the solvent in vacuo, the crude product could be obtained as intense yellow, sticky substance.

In order to estimate the necessary reaction time, the reaction was additionally carried out on a small scale in a quartz glass cuvette while UV-Vis kinetics spectra (fixed wavelength: 400 nm) were recorded. The result of these measurements was that the reaction with 2 N HCl was completed within a few seconds already. Interestingly, the same experiments with conc. acetic acid did not lead to conversion of dibutylbis(2-phenyl-1,3-dioxan-2-yl)stannane (**10**).

Thin-layer chromatograms of the crude product indicated 4 different spots in total. In addition to the product spot, one spot could be assigned to benzaldehyde resulting from the deprotection of 2-phenyl-1,3-dioxane (**9**). The other two spots could not be assigned. An attempt to isolate the target compound using a silica gel column resulted in the complete decomposition of the product on the column. Although the deprotection reaction with HCl seemed to work in principle, the applied reaction conditions are obviously too harsh for the target compound. Further experiments with a more diluted HCl solution did not lead to an improvement.

2.1.3.3.2 Dioxane deprotection using a cation exchanger

As a second possibility to synthesize bisbenzoyldibutylstannane (**5**) starting from dibutylbis(2-phenyl-1,3-dioxan-2-yl)stannane (**10**), a deprotection method involving a commercially available cation exchanger (Amberlite IR120, H-form from Fluka) should be envisaged. Since in this route, the cation exchange resin should be easy separable by filtration after the reaction, this method sounds promising especially in terms of purification.

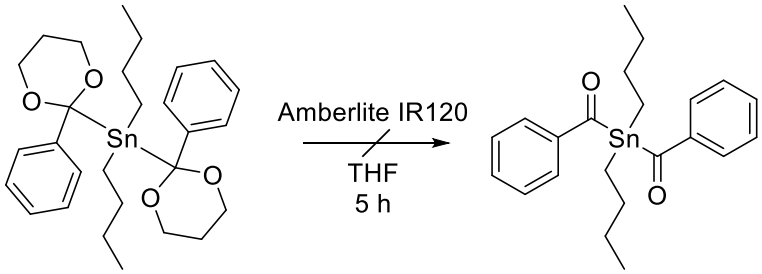

10 **5**

*Scheme 56: Synthesis of bisbenzoyldibutylstannane (**5**) using a cation exchanger*

For the synthesis of bisbenzoyldibutylstannane (**5**), 1 eq. of previously synthesized dibutylbis(2-phenyl-1,3-dioxan-2-yl)stannane (**10**, contaminated with 2-phenyl-1,3-dioxane **9**) was dissolved in THF and an amount equivalent to the tip of a spatula of Amberlite IR120 was added to the solution. The mixture was then stirred for 5 h at RT, however no color change could be observed leading to the assumption, that the reaction was not successful and no product formation occurred. Probably, the acidity of the cation exchanger was not sufficient to cause cleavage of the acetal moieties.

2.1.3.3.3 Dioxane deprotection using PPTS

Another potential method for the synthesis of bisbenzoyldibutylstannane (**5**) from dibutylbis(2-phenyl-1,3-dioxan-2-yl)stannane (**10**) is described by Hagiwara et al..[60]

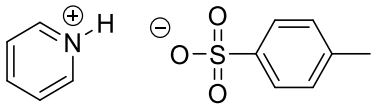

Scheme 57: Pyridinium p-toluenesulfonate (PPTS)

Herein, pyridinium p-toluenesulfonate (PPTS) is used as a deprotection reagent (Scheme 57) under aqueous conditions.

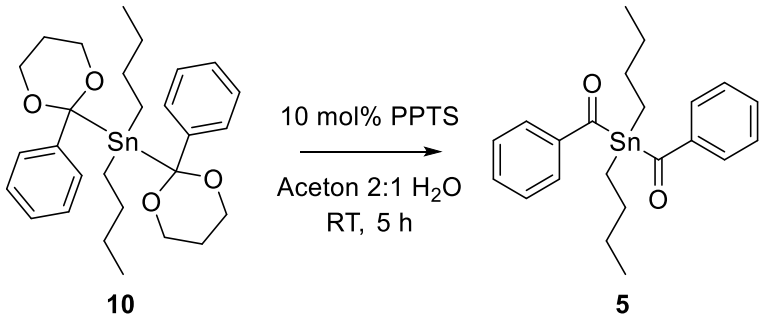

*Scheme 58: Synthesis of bisbenzoyldibutylstannane (**9**) using PPTS*

For the synthesis of bisbenzoyldibutylstannane (**5**), 1 eq. of previously synthesized dibutylbis(2-phenyl-1,3-dioxan-2-yl)stannane (**10**, contaminated with 2-phenyl-1,3-dioxane **9**) was dissolved in acetone. In another reaction vessel, 0.1 eq. of pyridinium p-toluenesulfonate was dissolved in water and this solution was then added to the stannane solution. The mixture was stirred for 5 h at RT, whereby a color change to yellow could be observed after 1 h already. Check for completion using TLC showed, that both dibutylbis(2-phenyl-1,3-dioxan-2-yl)stannane (**10**) and 2-phenyl-1,3-dioxane (**9**) had been deprotected entirely after 5 h. The formation of benzaldehyde from 2-phenyl-1,3-dioxane (**9**) could be confirmed as well. The mixture was diluted with diethyl ether, the layers were separated and the organic layer was washed with water. Since sodium sulfate is slightly alkaline and therefore poses a potential threat to the target compound, drying over sodium sulfate was spared. The solvent was evaporated in vacuo giving an intense yellow, sticky substance.

A thin-layer chromatogram showed, that the crude product mixture contained only one contaminant other than the product (in contrast to deprotection using HCL, chapter

2.1.3.3.1). The only impurity could further be confirmed as benzaldehyde, resulting from the involuntary deprotection of 2-phenyl-1,3-dioxane (**9**). Since a chromatographic purification was not considered due to previous experiences, a distillative method for purification should be tested first. For this purpose, the crude product was transferred to a drying gun. Even at a pressure of 0.03 mbar and 50°C over a period of 5 h benzaldehyde could not be evaporated, using this setup. As a second possibility, precipitation tests in a wide variety of solvents and solvent mixtures were carried out. Since both bisbenzoyldibutylstannane (**5**, due to its butyl chains) and benzaldehyde have high solubility in any organic solvent, this was difficult. Water is the only medium tested in which neither of the two compounds was soluble. In addition to attempts to recrystallize the product, an attempt was carried out to precipitate the product **5** by adding water to an ethanolic solution. Doing so, no purification could be achieved either. Another idea was the concentration of one of the two components via a two-phase system of two organic solvents (MeCN:PE or EtOH:PE). However, also this attempt failed, since both compounds showed very similar solubility in both layers.

Both the deprotection method with HCl and the method with PPTS enabled a successful synthesis of the target compound bisbenzoyldibutylstannane (**5**). Although only one impurity was obtained by the PPTS method (in contrast to the HCl method), it has not been possible to successfully separate it from the product. This is particularly a pity since the side product benzaldehyde occurs only due to inadequate purification of the starting compound dibutylbis(2-phenyl-1,3-dioxan-2-yl)stannane (**10**) and the parallel deprotection of of 2-phenyl-1,3-dioxane (**9**).

2.1.3.4 Synthesis of diphenylbis(2-phenyl-1,3-dioxane-2-yl)stannane (11)

Since the solubility of the dibutyl compounds in all organic solvents is very high and the purification thereby became extremely difficult, the analogous diphenyl compounds diphenylbis(2-phenyl-1,3-dioxane-2-yl)stannane (**11**) and bisbenzoyldiphenylstannane (**6**)

should be synthesized. Since there were already experiences from the synthesis experiments of dibutylbis(2-phenyl-1,3-dioxane-2-yl)stannane (**10**), the best conditions from this synthesis were also used for the synthesis of diphenylbis(2-phenyl-1,3-dioxane-2-yl)stannane (**11**), but were slightly adapted to the significantly different solubility properties (exp. section).

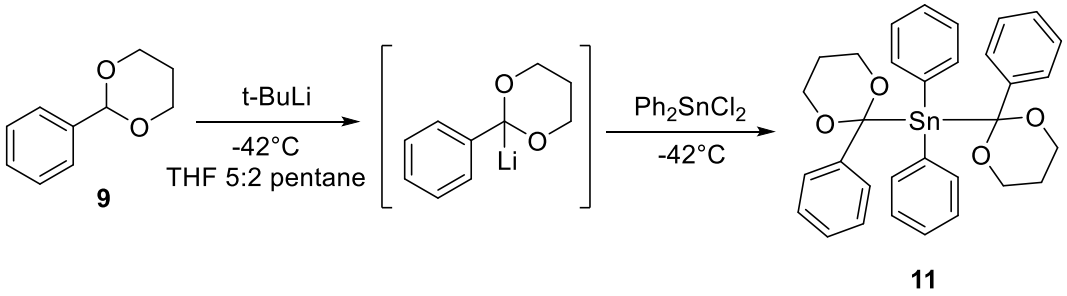

*Scheme 59: Synthesis of diphenylbis(2-phenyl-1,3-dioxan-2-yl)stannane (**11**)*

For the synthesis of diphenyldi(2-phenyl-1,3-dioxane-2-yl)stannane (**11**), 2.4 eq. of previously synthesized 2-phenyl-1,3-dioxane (**9**) were reacted with 2.5 eq. of t-butyllithium to form the lithium intermediate, which was then reacted with 1 eq. of diphenyldichlorostannane to form the desired product. After stirring overnight, a fluffy, colorless precipitate had formed, which was separated from the reaction mixture using filtration under inert conditions. Evaporation of the solvent gave another colorless solid, which could be confirmed as the target compound (40%).

The obtained solid immediately turned to intense yellow after treatment with conc. HCl, so it can be assumed that diphenyldi(2-phenyl-1,3-dioxane-2-yl)stannane (**11**) was present. In order to separate the impurities, the target compound should be purified using an alumina column (silica gel was not possible due to the acidic groups and uncontrolled deprotection reactions). However, since diphenyldi(2-phenyl-1,3-dioxane-2-yl)stannane (**11**) showed a significantly lower solubility in organic solvents and thus was not soluble in mixtures of PE and diethyl ether, a mixture of PE and THF in a ratio of 2:1 was chosen as the eluent. Only one spot was visible on the TLC plate after the column, however a ^{1}H spectrum confirmed the presence of 2-phenyl-1,3-dioxane (**9**) as well as polytetrahydrofuran as impurities once more.

2.1.3.5 Synthesis of bisbenzoyldiphenylstannane (6) using PPTS

As already mentioned above, dibenzoyldiphenylstannane (**6**) appears to be particularly interesting, because it should have a significantly lower solubility in organic solvents compared to dibenzoyldibutylstannane (**5**) and thus possibly a much simpler work-up, for example by precipitation could be possible. Since the deprotection method using pyridinium p-toluenesulfonate[60] gave the best results for bisbenzoyldibutylstannane (**5**), this method should also be applied for the synthesis of the phenyl derivative **6**.

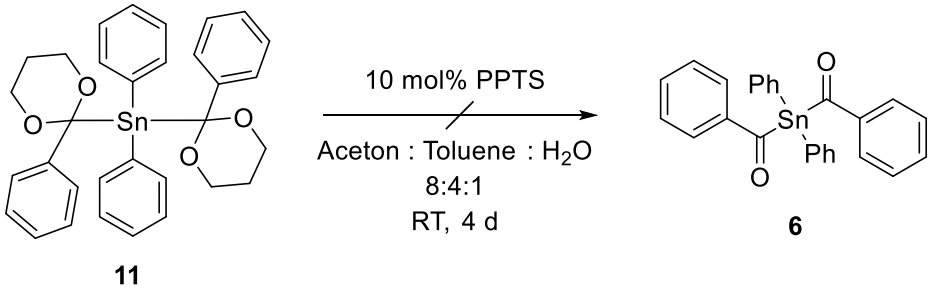

*Scheme 60: Synthesis of bisbenzoyldiphenylstannane (**6**) using PPTS*

For the synthesis of bisbenzoyldiphenylstannane (**6**), 0.1 eq. of pyridinium p-toluenesulfonate was dissolved in water and 1 eq. of previously synthesized diphenylbis(2-phenyl-1,3-dioxan-2-yl)stannane (**11**, contaminated with 2-phenyl-1,3-dioxane (**9**) and poly-THF) was suspended in acetone and added to the aqueous solution at RT and stirred overnight at that temperature. Since the starting material had not been dissolved entirely on the next day, toluene was added. Only a very slight yellowing of the solution was observed. It was assumed, that the reaction proceeded much more slowly than with the analogous dibutyl compound **5** due to the sterically demanding phenyl substituents. For this reason, the mixture was stirred continuously over the weekend. Visually, the solution was not significantly yellow in color even after this long reaction time. The reaction solution was diluted with diethyl ether and the organic phase was washed three times with water. Drying with sodium sulfate was skipped as before and the solvent was evaporated in vacuo giving a slightly yellow mixture which, according to the thin-layer chromatogram, contained mainly diphenylbis(2-phenyl-

1,3-dioxan-2-yl)stannane (**11**), but also a certain amount of benzaldehyde (formed by the parallel deprotection of 2-phenyl-1,3-dioxane **9**).

Presumably, the steric hindrance caused by the phenyl substituents on the tin atom ensures that the deprotection method using pyridinium p-toluoylsulfonate proceeds much worse than with the analogous butyl compound. In the case of the phenyl derivative **6**, the target compound could not be confirmed as being part of the product mixture.

2.1.3.6 Synthesis of 2-mesityl-1,3-dioxane (12)

Due to the rather low stability of the benzoyl derivatives within the class of the bisacylstannanes **5** and **6**, the analogue mesitoyl derivatives shoud be envisaged. To be able to evaluate the dioxane route for the synthesis of bismesitoylstannanes, the starting material 2-mesityl-1,3-dioxane (**12**) needed to be synthesized in the first place. Regarding that, the route described by Firouzabadi et al.[57] was used. This route led to success for the synthesis of 2-phenyl-1,3-dioxane (**9**) already as described in chapter 2.1.3.1.

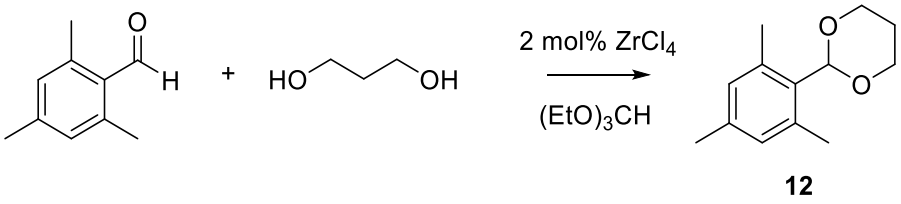

12

*Scheme 61: Synthesis of 2-mesityl-1,3-dioxane (**12**)*

For the synthesis of 2-mesityl-1,3-dioxane (**12**), 1 eq. of 2,4,6-trimethylbenzaldehyde and 1.5 eq. of 1,3-propanediol were reacted in the presence of 1 eq. of triethyl orthoformate and 0.02 eq. of solid zirconium tetrachloride in dry dichloromethane. After quenching with aqueous NaOH and an aqueous workup the product was obtained in high purity as a colorless, crystalline solid after recrystallization from n-pentane (85%).

The preparation method, which worked quite well for 2-phenyl-1,3-dioxane (**9**) already, could also be used to synthesize 2-mesityl-1,3-dioxane (**12**) in high yields after making little adjustments to the work up procedure. The compound **12** was used in the following attempt to synthesize a bisacylstannane compound.

2.1.3.7 Synthesis of dibutylbis(2-mesityl-1,3-dioxane-2-yl)stannane (13)

The successfully synthesized compound 2-mesityl-1,3-dioxane (**12**) should in further consequence be used to prepare the first bismesitoyl compound **13**. Past experience from the attempts to synthesize the corresponding benzoyl derivatives should of course be implemented in doing so. In the first step, the dioxane-protected mesityl compound **13** should be synthesized.

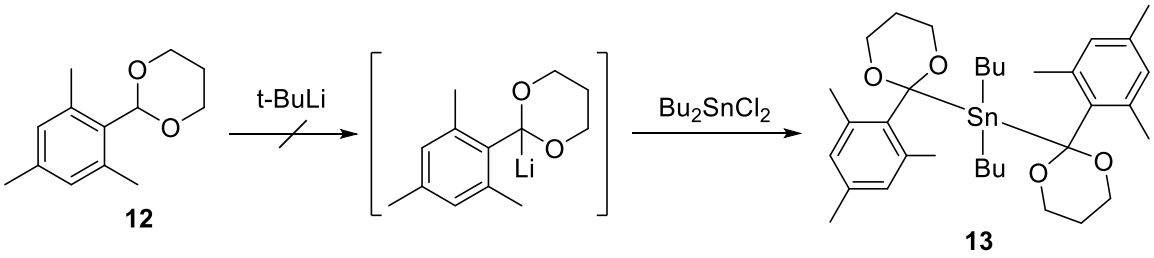

*Scheme 62: Synthesis of dibutylbis(2-mesityl-1,3-dioxane-2-yl)stannane (**13**)*

For the synthesis of dibutylbis(2-mesityl-1,3-dioxane-2-yl)stannane (**13**), a suspension of 2 eq. of previously synthesized 2-mesityl-1,3-dioxane (**12**) in a mixture of dry THF and dry n-pentane (5:2) was prepared and cooled to -42°C. Over the period of 20 min, 2.05 eq. of t-butyllithium (1.7 M in pentane) were added at that temperature slowly via syringe and septum. The mixture was stirred for 2 h at -42°C before adding a solution of 1 eq. of dibutyldichlorostannane in the same solvent mixture at that temperature. After complete addition, the mixture was stirred at -79°C for another hour and then it was allowed to reach RT overnight. On the next day, the reaction mixture was diluted with diethyl ether and

quenched with a 5% aqueous $NaHCO_3$ solution. The layers were separated and the aqueous layer was extracted three times with diethyl ether. The combined organic layers were washed with water and brine and dried over sodium sulfate. After filtration and evaporation of the solvent, a colorless solid was obtained.

This solid was then analyzed by NMR spectroscopy (^{1}H, ^{119}Sn). When looking at the spectra, it quickly becomes clear that the reaction did not proceed as expected. The signals indicate that the lithiation reaction did not take place as desired since the major component of the mixture appeared to be the starting material, 2-mesityl-1,3-dioxane (**12**). It can be assumed, that the steric hindrance, caused by the o-methyl groups prevents the lithiation, as it was the case already with the analogous dithiane compound. Since dibutylbis(2-mesityl-1,3-dioxane-2-yl)stannane (**13**) could not be synthesized using the described dioxane route, the actual target compound bismesitoyldibutylstannane (**7**) could not be prepared as well.

With the described dioxane route, it was for the first time possible to synthesize the target compound bisbenzoyldibutylstannane (**5**). Although the synthesis was quite successful, a complete purification method has yet to be developed. In order to achieve progress in that specific regard, it was decided to proceed with pathway D and test another potential synthetic approach.

2.1.4 Diazo route (Pathway D)

Since all previous attempts to isolate bisacylstannanes have not been entirely successful so far (Pathways A-C), a completely different route to their synthesis should be evaluated. One possibility might be a route, which was quite recently used to synthesize germanium ketoesters (Scheme 63).[52, 61-63]

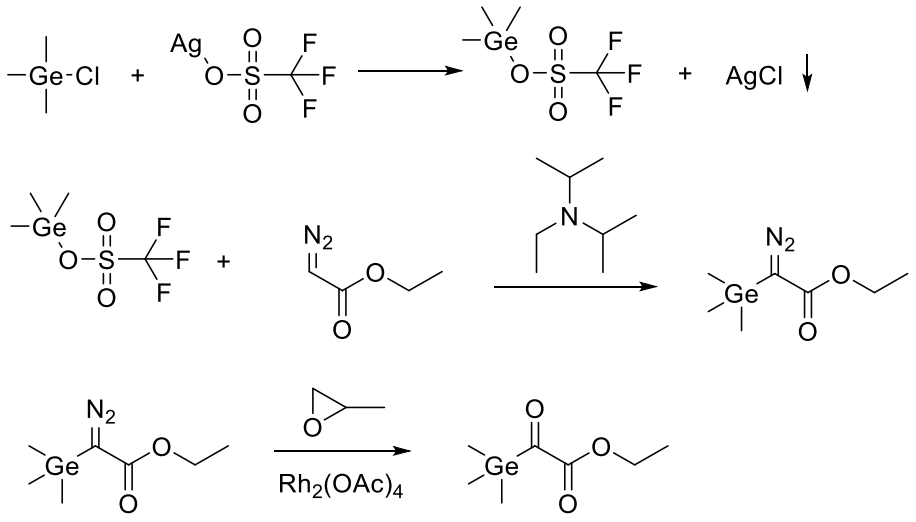

Scheme 63: Preparation of heteroatom-containing α-ketoesters[52]

Instead of ethyldiazo acetate, phenyldiazomethane may possibly be used to form acyl compounds instead of the corresponding α-ketoesters (Scheme 64).

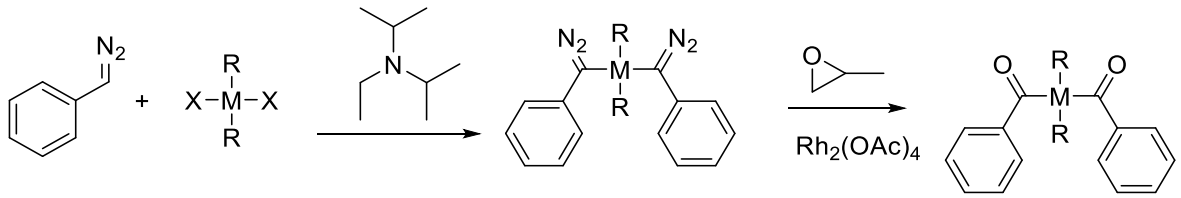

Scheme 64: Proposed route involving phenyldiazomethane for the synthesis of bisacylstannanes

As an electrophilic component, either a bistriflate or the dichloride could be used.[52] With regard to the nucleophilic component, Wheeler[43] showed in his work that the diazo lithium species can also be prepared, but only starting from trimethylstannylphenyldiazomethane. For the synthesis of this compound, he used neither the chlorostannane, nor the stannyl triflate, but a stannanediamine (Scheme 65).

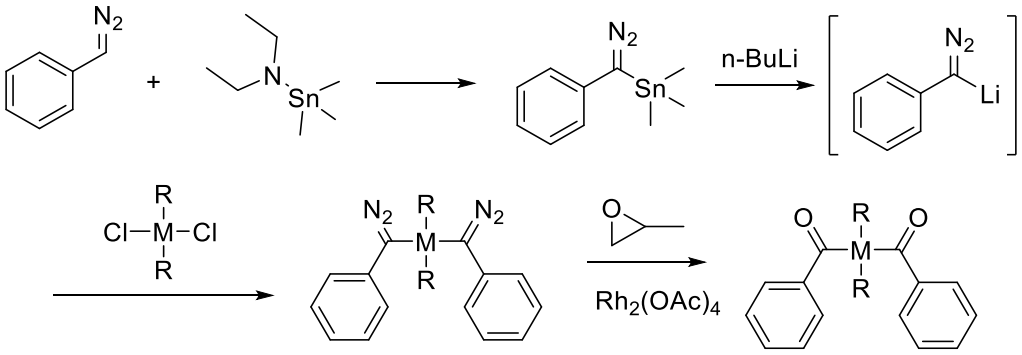

Scheme 65: Proposed route involving a diazo lithium species for the synthesis of bisacylstannanes

If the synthesis of trimethylstannylphenyldiazomethane using a stannanediamine is possible, the synthesis of a corresponding bifunctional compound by means of a stannanediamine could potentially be successful as well (Scheme 66).

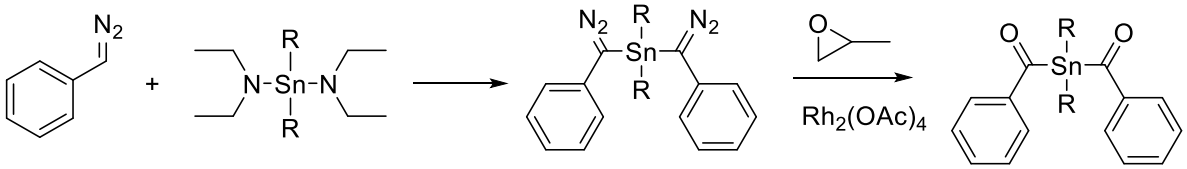

Scheme 66: Proposed route involving a stannanediamine for the synthesis of bisacylstannanes

2.1.4.1 Synthesis of benzaldehyde tosylhydrazone (14)

In order to carry out the further steps of the proposed diazo route with the goal of synthesizing bisacylstannanes, the reactant benzaldehyde tosylhydrazone (**14**) should be prepared initially. This was envisaged as described by Dudman an Reese, starting from benzaldehyde and tosyl hydrazide.[64]

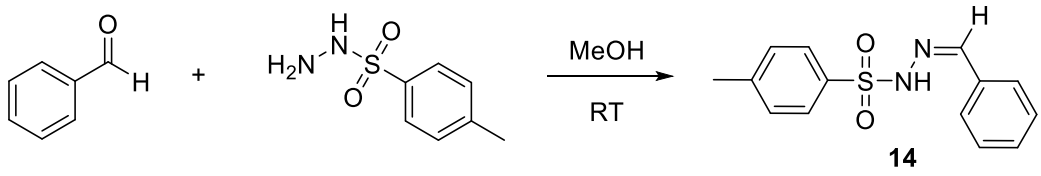

*Scheme 67: Synthesis of benzaldehyde tosylhydrazone (**14**)*

For the synthesis of benzaldehyde tosylhydrazone (**14**), 1.1 eq. of tosyl hydrazide were reacted with 1 eq. of benzaldehyde in dry methanol. The desired product in the form of colorless crystals precipitated directly from the reaction mixture and could be obtained in high purity after washing with cold methanol (78%). The structure of the target compound **14** could be confirmed using NMR spectroscopy and the substance was used in the next steps without any further purification.

2.1.4.2 Synthesis of phenyldiazomethane (15)

In the next step, the previously synthesized benzaldehyde tosylhyrazone (**14**) was used in order to prepare phenyldiazomethane (**15**) as described by Dudman and Reese.[64]

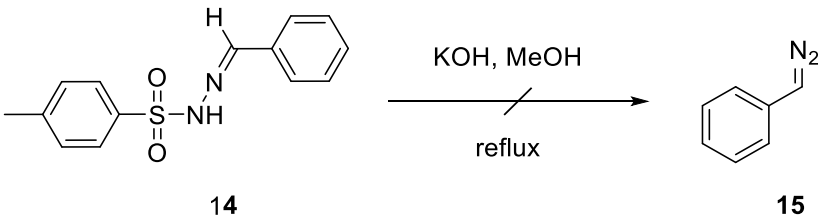

*Scheme 68: Synthesis of phenyldiazomethane (**15**) using potassium hydroxide*

For the synthesis of phenyldiazomethane (**15**), 1 eq. of previously synthesized benzaldehyde tosylhydrazone (**14**) was weighed into a Schlenk tube together with 2 eq. of potassium hydroxide and dry methanol and refluxed for 20 min. Afterwards, the mixture was poured over ice water and the layers were separated. The aqueous layer was extracted 4 times with

dichloromethane and the combined organic layers were washed with a sat. aqueous solution of sodium hydrocarbonate. After drying over magnesium sulfate and filtration, the solvent was evaporated in vacuo giving a very small amount of a colorless solid, which could not be confirmed as the desired product. Probably the given reaction time in literature was not long enough to achieve a considerable amount of product. Instead of adapting the described route, another method for the synthesis of phenyldiazomethane (**15**) was envisaged as described in the following.

Since the first attempt to synthesize phenyldiazomethane (**15**) did not lead to success, another method using sodium hydroxide and benzyltriethylammonium chloride as described by Wulfman et al.[65] and Su et al.[66] should be tested.

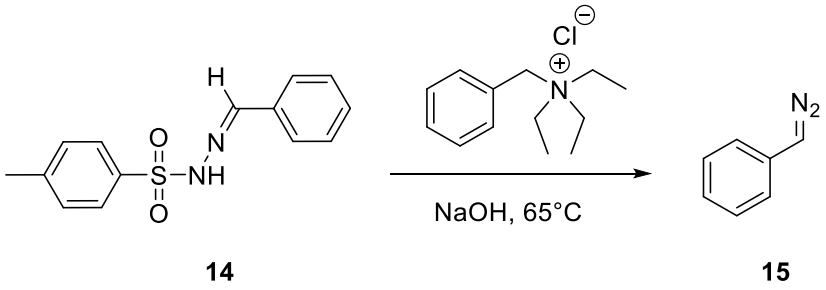

*Scheme 69: Synthesis of phenyldiazomethane (**15**) using sodium hydroxide and benzyltriethylammonium chloride*

For the synthesis of phenyldiazomethane (**15**), 1 eq. of previously synthesized benzaldehyde tosylhydrazone (**14**) was dissolved in dry toluene and then treated with an aqueous solution of sodium hydroxide in the presence of 0.2 eq. of benzyltriethylammonium chloride. After separating the layers, the target compound could be confirmed using ATR-IR (C=N_2: 2060 cm^{-1}) and was subsequently used as a solution in toluene in the synthesis pathway without any further purification.

2.1.4.3 Synthesis of dibutyltetraethylstannanediamine (16)

Wheeler[43] described the use of an stannaneamine as the electrophilic species for the conversion of phenyldiazomethane (**15**). The synthesis of a corresponding diamine **16** was furthermore described by Yoder[67] and Harrypersad[68] and was carried out as described in the following.

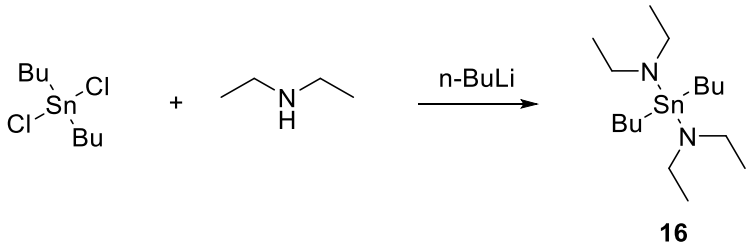

*Scheme 70: Synthesis of dibutyltetraethylstannanediamine (**16**)*

For the synthesis of dibutyltetraethylstannanediamine (**16**), 1 eq. of dibutyldichlorostannane was reacted with 2 eq. of n-butyllithium and 2 eq. of diethylamine in dry diethyl ether. After stirring overnight, the resulting mixture was filtrated under inert conditions and the target compound could be obtained as a yellow liquid (45%) after evaporation of the solvent from the filtrate. The structure was confirmed using NMR spectroscopy and the compound was used in subsequent synthetic steps without any further purification.

2.1.4.4 Synthesis of bis(diazo(phenyl)methyl)dibutylstannane (17)

Since the synthesis of phenyldiazomethane (**15**) and dibutyltetraethylstannanediamine (**16**) could be carried out successfully, these two compounds should now be used in order to synthesize bis(diazo(phenyl)methyl)dibutylstannane (**17**). A similar course of action has been described by Wheeler.[43]

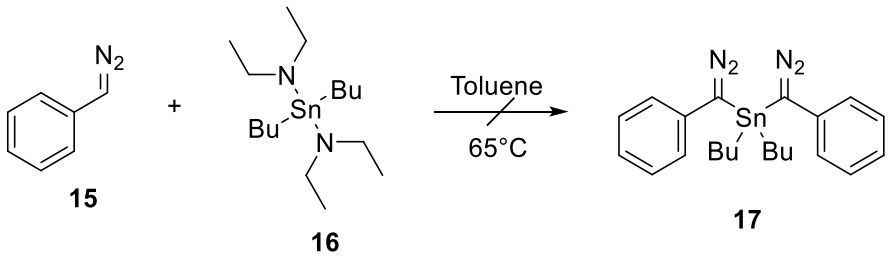

*Scheme 71: Synthesis of bis(diazo(phenyl)methyl)dibutylstannane (**17**)*

For the synthesis of bis(diazo(phenyl)methyl)dibutylstannane (**17**), 1 eq. of previously synthesized dibutyltetraethylstannanediamine (**16**) was weighed into a Schlenk tube and a toluene solution of previously synthesized phenyldiazomethane (**15**, 2 eq.) was added at RT. The resulting mixture was stirred overnight at 65°C and on the next day, a colorless precipitate was filtrated off using a Teflon filter. The precipitate as well as the filtrate was then analyzed by IR and NMR spectroscopy. In the IR spectrum, only one diazo band was visible, namely the one resulting from unreacted phenyldiazomethane (**15**) at 2060 cm^{-1}. The NMR spectra did not prove the formation of even small amounts of the target compound either.

It was assumed, that phenyldiazomethane (**15**) did not provide the necessary reactivity and therefore the lithiated diazo compound might be needed for the preparation of the desired product **17**. According to Wheeler,[43] the synthesis of this compound can only be achieved via the diazo(phenyl)methyltrimethylstannane (**18**, Scheme 72), which is described in the following chapters.

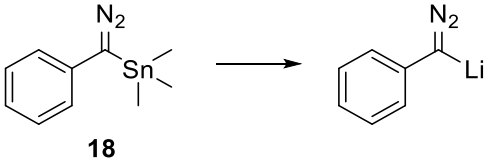

*Scheme 72: Synthesis of the lithiated phenyldiazomethane from diazo(phenyl)methyltrimethylstannane (**18**)*

2.1.4.5 Synthesis of trimethylstannanediethylamine (19)

In order to test the synthesis of diazo(phenyl)methyltrimethylstannane (**18**) and diazophenylmethyl lithium, the monofunctional stannaneamine **19** had to be prepared. For that reason, the method described by Yoder[67] was applied in analogy to the synthesis described above (chapter 2.1.4.3).

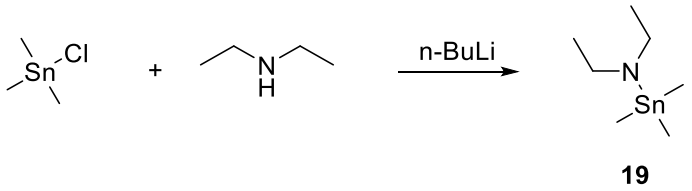

19

*Scheme 73: Synthesis of trimethylstannanediethylamine (**19**)*

For the synthesis of trimethylstannanediethylamine (**19**), 1 eq. of chlorotrimethylstannane was reacted with 1.1 eq. of n-butyllithium and 1 eq. of diethylamine in dry diethyl ether. After stirring overnight, the resulting mixture was filtrated under inert conditions and the target compound could be obtained as a yellow liquid (41%) after evaporation of the solvent from the filtrate. The structure was confirmed using NMR spectroscopy and the compound was used in subsequent synthetic steps without any further purification.

2.1.4.6 Synthesis of diazophenylmethyl lithium

In the next step, the previously synthesized stannaneamine **19** should be reacted with phenyldiazomethane (**15**) to obtain diazo(phenyl)methyltrimethylstannane (**18**), which should subsequently converted to diazophenylmethyl lithium.[43] This species might be needed for a successful synthesis of bis(diazo(phenyl)methyl)dibutylstannane (**17**) and after that bisbenzoyldibutylstannane (**5**).

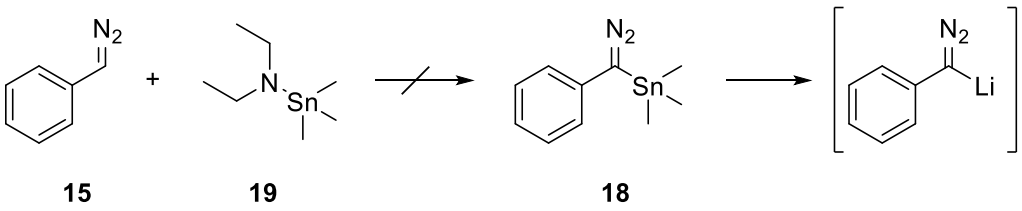

15 **19** **18**

*Scheme 74: Synthesis of diazo(phenyl)methyltrimethylstannane (**18**) and diazophenylmethyl lithium*

For the synthesis of diazophenylmethyl lithium, 1 eq. of previously synthesized trimethylstannanediethylamine (**19**) was dissolved in dry n-pentane and cooled to -78°C. Afterwards, a previously prepared toluene solution of 1 eq. phenyldiazomethane (**15**) was added via syringe at that temperature. The mixture was then warmed to RT and stirred overnight at 50°C. On the next day, an IR spectrum from the reaction mixture showed, that no significant conversion had occurred yet, which is why the temperature was raised to 90°C and stirring was continued for further 24 h. Even after increasing the reaction time, no formation of diazo(phenyl)methyltrimethylstannane (**18**) could be detected. The diazo band of phenyldiazomethane (**15**) at 2060 cm^{-1} did not decrease over time.

Since diazo(phenyl)methyltrimethylstannane (**18**) could not be prepared as expected, diazophenylmethyl lithium could not be synthesized for testing it in the synthesis of bis(diazo(phenyl)methyl)dibutylstannane (**17**). Although the diazo route (pathway D) seems to be a promising route for the synthesis of bisacylstannanes, several attempts failed due to the lacking synthetic accessibility of the necessary bisdiazo precursors as of yet. In order to find an easy and efficient way for the synthesis of the bisacylstannanes, a fifth pathway (pathway E) using bromostannanes should be envisaged and is described in the following chapters.

2.1.5 Bromostannane route (Pathway E)

For the synthesis of bisacylstannanes, several synthetic routes have already been tested, however none of these routes has so far led to the desired results. The synthetic routes failed mostly because the target compounds could not be prepared. Only the route via the dioxane protecting groups (pathway C) led to the desired target compound **5**, however purification was insufficient in this specific case.

Another possibility for the successful isolation of bisacylstannanes could be a route described by Brook and Peddle[53] (Scheme 75). Herein, an tetraorganostannane is prepared initially (potentially via a method described by Marton et al.[69]) and then brominated completely using N-bromosuccinimide. In the final step the carbonyl functionalities are introduced by reaction with silver acetate.

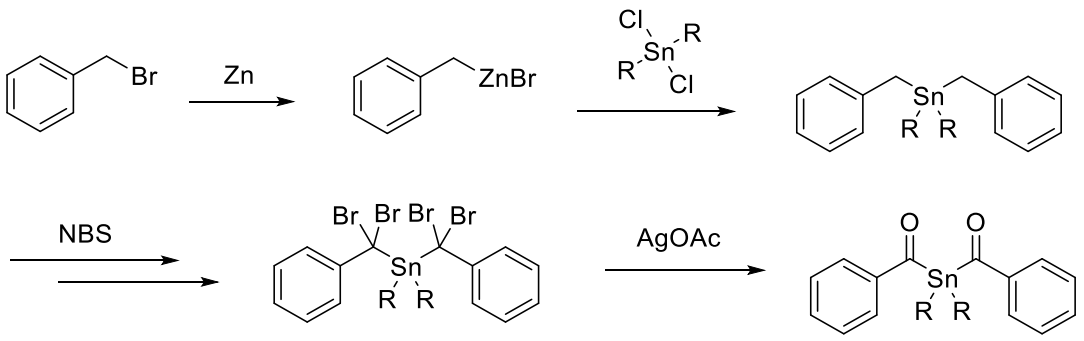

Scheme 75: Proposed bromostannane route (pathway E)

In order to test this bromostannane route (pathway E) for its utility in the synthesis of bisacylstannanes, several synthesis experiments were performed and described below.

2.1.5.1 Synthesis of dibenzyldibutylstannane (20)

To evaluate the bromostannane route for the synthesis of the bisacylstannanes, the first step was to synthesize dibenzyldibutylstannane (**20**). This was realized by referring to a method described by Marton et al.[69] via an organozinc species (Scheme 76).

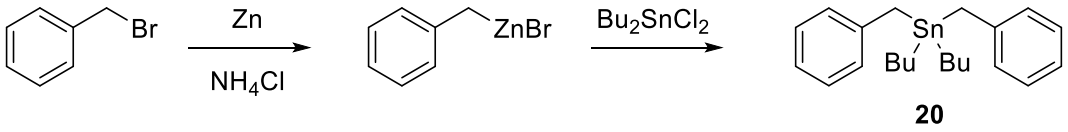

*Scheme 76: Synthesis of dibenzyldibutylstannane (**20**)*

For the synthesis of dibenzyldibutylstannane (**20**), 1 eq. of dibutyldichlorostannane was reacted with 4 eq. of benzyl bromide in the presence of 4 eq. of zinc powder and ammonium chloride in THF. After an aqueous workup, the desired compound could be obtained in high purity as a colorless liquid (82%). The structure was confirmed using NMR spectroscopy and the compound was used without any further purification in the subsequent steps.

2.1.5.2 Bromination and synthesis of bisbenzoyldibutylstannane (5)

In the next step, the successfully synthesized compound dibenzyldibutylstannane (**20**), should be brominated four times using N-bromosuccinimide as described by Brook and Peddle[53] (Scheme 77).

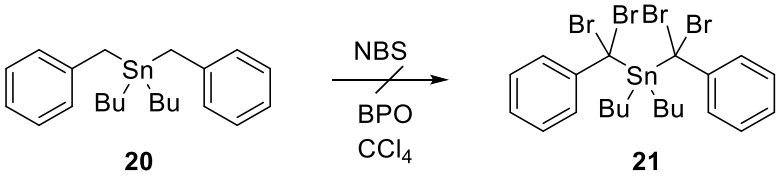

*Scheme 77: Synthesis of tetrabromodibenzyldibutylstannane (**21**) in tetrachlorocarbon*

For the synthesis of tetrabromodibenzyldibutylstannane (**21**), 1 eq. of previously synthesized dibenzyldibutylstannane (**20**) was weighed into a Schlenk tube together with 4 eq. of N-bromosuccinimide (NBS) and a small amount of dibenzoylperoxide (DPO) and dissolved in tetrachlorocarbon. Afterwards, the mixture was refluxed overnight at 77°C. On the next day, a ^{1}H-NMR spectrum was measured directly from the reaction mixture using a D_2O capillary indicating no formation of the tetrabrominated compound **21**. For this reason, the mixture was refluxed for further 2 days over the weekend. Even after this prolonged reaction time the desired compound could not be detected. Obviously, the applied synthetic route gave the three-fold brominated product **22** instead of the fully brominated one (**21**, Scheme 78), which was confirmed using NMR spectroscopy. The reaction mixture was filtrated and the solvent was evaporated from the filtrate in vacuo. The crude product **22** (93%) was then obtained by crystallization from a mixture of ethyl acetate an ethanol at -40°C as a colorless substance (liquid at RT).

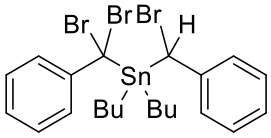

22

*Scheme 78: Tribromodibenzyldibutylstannane (**22**)*

Brook[53] also described for similar silicon compounds, that in some cases the bromination and subsequent oxidation must be realized in two stages (Scheme 79).

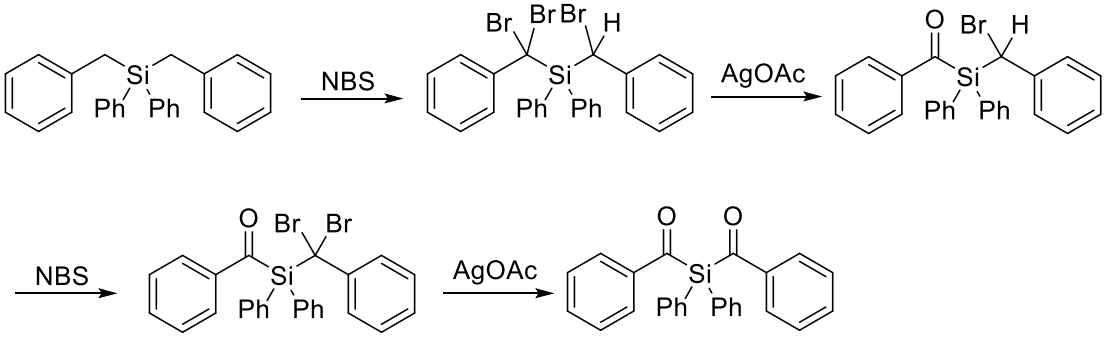

Scheme 79: Synthesis of bisbenzoylsilanes described by Brook[53]

Therefore, in the case of the stannanes, it should also be investigated, whether a two-stage bromination/oxidation is necessary. For this purpose, the unintentionally prepared tribromodibenzyldibutylstannane (**22**) should be converted to ((bromo(phenyl)methyl)dibutylstannyl)(phenyl)methanone (**23**) in the first step (Scheme 80).

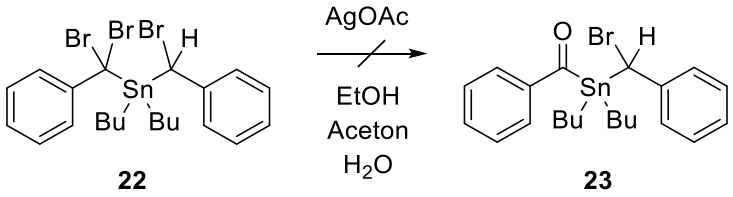

22 **23**

*Scheme 80: Synthesis of ((bromo(phenyl)methyl)dibutylstannyl)(phenyl)methanone (**23**)*

For the synthesis of ((bromo(phenyl)methyl)dibutylstannyl)(phenyl)methanone (**23**), 3.5 eq. of silver acetate and 1 eq. of previously synthesized tribromodibenzyldibutylstannane (**22**) were weighed in and dissolved in a mixture of ethanol, acetone and water. The mixture was stirred at RT overnight and on the next day, a ^{119}Sn spectrum was measured directly from the reaction mixture using a D_2O capillary, however no tin signal could be obtained. The colorless reaction mixture was filtrated, diluted with diethyl ether and the layers were separated. The aqueous layer was extracted twice with diethyl ether and the combined organic layers were washed with water and dried over sodium sulfate. After filtration and evaporation of the solvent in vacuo, a very small amount of a colorless residue was obtained, which was analyzed using NMR spectroscopy. The ^{1}H-NMR spectrum showed, that the mixture contained at least 3 different compounds, however there was still no tin signal visible in the ^{119}Sn-NMR spectrum. Since the mixture additionally did not show any coloration, it could be assumed, that the reaction did not occur as expected. Therefore, the batch was discarded going back to the bromination step.

A second batch, starting again from dibenzyldibutylstannane (**20**), was carried out. In order to obtain a four-fold bromination in only one step and also to reduce the very long reaction time of about 3 days in general, the synthesis described above was carried out in tetrachloroethene instead of tetrachlorocarbon. Tetrachloroethene has a boiling point of

121°C (in contrast to 77 ° C for CCl_4). Therefore, a higher reflux temperature is possible, which should accelerate the reaction significantly.

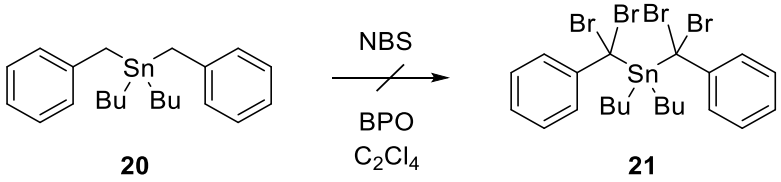

20 **21**

*Scheme 81: Synthesis of tetrabromodibenzyldibutylstannane (**21**) in tetrachloroethene*

The reaction was carried out exactly as described at the beginning of this chapter. The only difference was using tetrachloroethene instead of tetrachlorocarbon. In addition, the excess of N-bromosuccinimide was increased from 4 equivalents to 8 equivalents. However, by making these adjustments, it was still not possible to isolate the desired tetrabrominated product. As before, only tribromodibenzyldibutylstannane (**22**) was formed. Another attempt to oxidize this compound by means of silver acetate also gave the same unsatisfactory results as in the first approach (very small amount, colorless, no ^{119}Sn-NMR signal, mixture of at least 3 compounds).

It is very likely that the conditions for the oxidation with silver acetate are far too harsh in the case of bisacylstannanes. The aqueous medium and the high temperatures in this step are likely to cause immediate decomposition of the product. This assumption also coincides with the experiences already made after the evaluation of other synthetic routes (pathways A-D). The hydrolysis stability of bisacylstannanes seems to be significantly reduced compared to the stability of bisacylgermanes. This finding is also supported by the performed investigations on the corresponding monoacylstannane compounds. Even if a practical route for the isolation of bisacylstannanes could have been found, these compounds would hardly be suitable for industrial use in the dental medicine, due to their rather poor stability against hydrolysis.

2.2 Recap

In order to synthesize bisacylstannanes, five different synthetic routes (pathways A-E) have been tested for these compounds within this work.

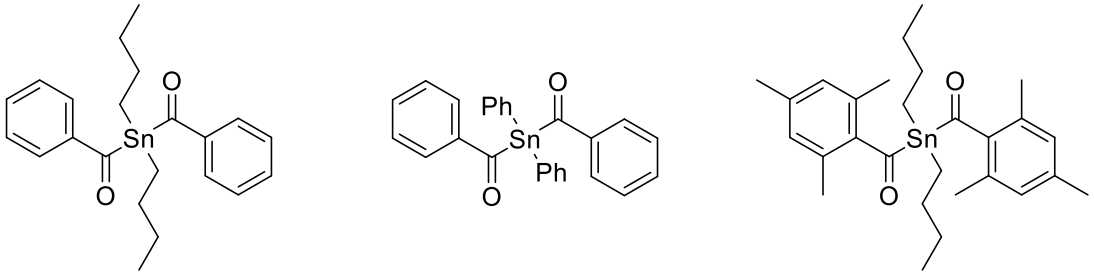

5 **6** **7**

*Scheme 82: Targeted bisacylstannanes **5**-**7***

The stannyl dilithium route (pathway A) probably resulted in the formation of oligo- and polystannanes, preventing a successful isolation of the target compounds **5** and **6** (chapter 2.1.1). The dithiane route (pathway B), which works well for the synthesis of bisacylgermanes,[29] led to the finding that the synthesis of the dithiane-protected stannyl intermediate was in fact possible, however the subsequent cleavage of these groups could not be carried out in the case of the stannanes (chapter 2.1.2) and therefore, the target compound **5** could not be isolated using pathway B either. This issue could be partly solved by using pathway C and the dioxane route. The final step of the synthesis, namely the cleavage of the dioxane groups could be carried out successfully and bisbenzoyldibutylstannane (**5**) could be obtained. However, even after numerous attempts, a viable purification procedure and the isolation of the pure product could not be achieved (chapter 2.1.3). Therefore, additional synthetic routes were envisaged, such as the diazo route (pathway D). The synthesis of bisacylstannanes however failed using this route, since the crucial intermediate bis(diazo(phenyl)methyl)dibutylstannane (**17**) could not be formed (chapter 2.1.4) from previously synthesized phenyldiazomethane (**15**). Similarly, the bromostannane route (pathway E) was unsuccessful due to the failed synthesis attempts of the four-fold brominated intermediate **21** (chapter 2.1.5).

In summary, a viable synthetic protocol and a suitable purification procedure for the synthesis of bisacylstannanes has yet to be found. However, within this work, many different approaches were tested and valuable knowledge could be accumulated, facilitating potential future work on this class of compounds.

3 Tetrakisacylstannanes

Regarding tetrakisacylstannanes, the three target compounds **24**-**26** below were chosen (Scheme 83).

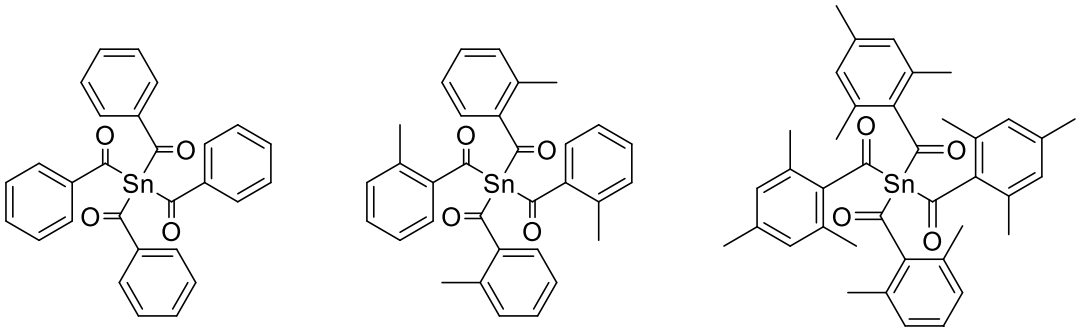

24 **25** **26**

*Scheme 83: Selection of tetrakisacylstannane target compounds **24-26***

As far as a successful isolation of those compounds can be achieved, information about the influence of different substituents on the aromatic ring with regard to stability, absorption properties and photoreactivity should be gathered.

3.1 Synthesis

In order to synthesize the target compounds **24**-**26** successfully, a pathway involving a stannyl potassium species, which is reacted with acid halides in a second step should be envisaged (Scheme 84). This route was applied successfully for the synthesis of tetrafunctional silicon and germanium acyl compounds already.[70, 71] Previous work related to this class of compounds impressively showed the huge potential of those compounds as photoinitiators in radical photopolymerization.[20, 30]

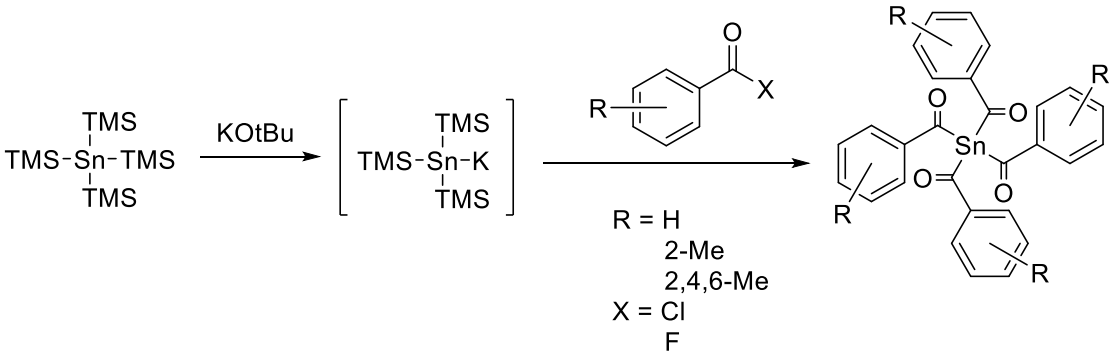

Scheme 84: Potential pathway for the synthesis of tetrakisacylstannanes

Since all reactions involved moisture-sensitive compounds and many of those being light-sensitive in addition to that, all reactions, which demand certain measures concerning these issues were carried out in an orange light lab to exclude light with wavelengths below 520 nm and Schlenk techniques were used to secure complete exclusion of oxygen and moisture. Many reaction mixtures were additionally protected from light using aluminum foil, whenever possible.

3.1.1 Synthesis of tetrakis(trimethylsilyl)stannane (27)

To test the described route for the synthesis of tetrakisacylstannanes, the intermediate tetrakis(trimethylsilyl)stannane (**27**) had to be synthesized initially. For that purpose, a synthesis route described by Buerger and Goetze[72] was targeted. In this route, tetrachlorostannane is reacted with trimethylsilyl chloride using elemental lithium in THF to form the desired product **27**.

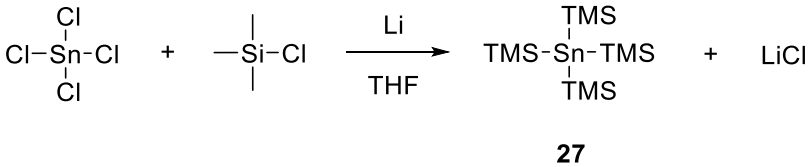

27

*Scheme 85: Synthesis of tetrakis(trimethylsilyl)stannane (**27**)[72]*

For the synthesis of tetrakis(trimethylsilyl)stannane (**27**), 6.25 eq. of chlorotrimethylsilane and 1 eq. of tetrachlorostannane were reacted in the presence of 10 eq. of fine cut Li foil in THF. After stirring overnight the formation of product was confirmed using ^{119}Sn-NMR (-644 ppm). After filtration followed by an aqueous workup, the product **27** could be obtained in very high purity as a crystalline, colorless solid (21%) and was used without any further purification.

The low yield can be explained by a parallel reduction of tetrachlorostannane resulting in the formation of elemental tin, as described by Buerger.[72] This reaction occurs only in the case of germanium and tin, but not in the case of silicon. For tin, the reduction reaction is highly favored compared to the silylation and can make up percentages of up to 80%.

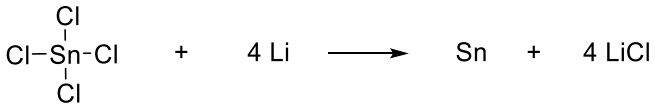

Scheme 86: Parallel reduction of tetrachlorostannane and formation of elemental tin[72]

In general, the chosen route for the synthesis of tetrakis(trimethylsilyl)stannane (**27**) turned out to be very successful, since purification was easy and the product could be used as reactant in the following steps without further treatment. Compound **27** was stored under argon at 7°C in the fridge and did not show any sign of degradation, even after long periods (several months) of storage.

3.1.2 Synthesis of tetrakisbenzoylstannane (24)

Starting from the previously synthesized tetrakis(trimethylsilyl)stannane (**27**) and commercially available benzoyl fluoride, a first attempt to synthesize tetrabenzoylstannane (**24**) should be carried out.

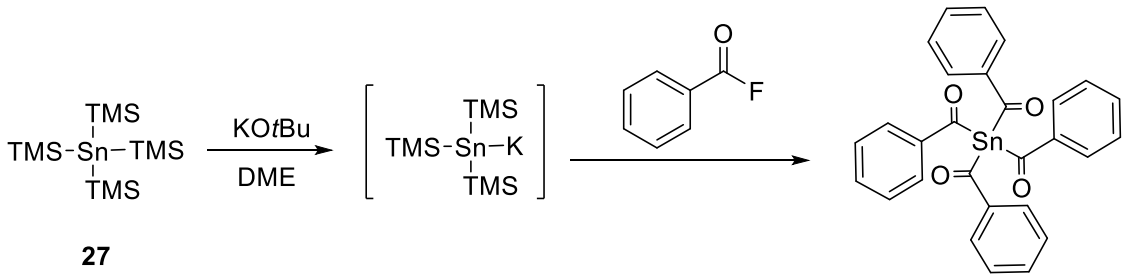

27

24

*Scheme 87: Synthesis of tetrakisbenzoylstannane (**24**)*

For the synthesis of tetrakisbenzoylstannane (**24**), 1 eq. of previously synthesized tetrakis(trimethylsilyl)stannane (**27**) and 1.1 eq. of potassium tert. butoxide were weighed into a dry Schlenk tube and dissolved in dry 1,2-dimethoxyethane. This mixture was stirred for 1 h at RT. In the meantime, a second Schlenk tube was used to dissolve 4.1 eq. of benzoyl fluoride in dry 1,2-dimethoxyethane. Both reaction vessels were cooled to 0°C and then the stannyl potassium solution was added to the acid fluoride solution at that temperature via syringe and septum. Afterwards the resulting mixture was allowed to reach RT overnight during stirring. On the next day, the reaction was diluted with dichloromethane and quenched with cold 3% aqueous H_2SO_4. The layers were separated and the aqueous layer was extracted 3 times with dichloromethane. The combined organic layers were washed twice with water and dried over sodium sulfate. After filtration and concentration of the solution in vacuo, a yellow solution was obtained, from which product **24** should have been crystallized by adding acetonitrile. Even after storing the solution overnight at -18°C, no crystals formed, so the solvents were evaporated entirely, giving a small amount of pale yellow solid.

Although probably a small amount of product **24** was formed during the reaction, it was most likely not sufficiently stable to endure the harsh conditions of an aqueous work-up. Neither a ^{119}Sn-NMR signal could be obtained, nor a successful photopolymerization experiment could be carried out from the crude product mixture. In order to increase the stability of future tetraacylstannanes in aqueous media, other derivatives should be targeted. Methyl

substituents next to the carbonyl moieties could potentially provide sufficient steric hindrance and therefore increase the stability against aqueous hydrolysis.

3.1.3 Synthesis of 2-methylbenzoyl fluoride (28)

In order to synthesize tetrakis(2-methylbenzoyl)stannane (**25**) via acid fluorides the starting material 2-methylbenzoyl fluoride (**28**) should be prepared using a method described by Lee et al.[73] starting from the analogue acid chloride.

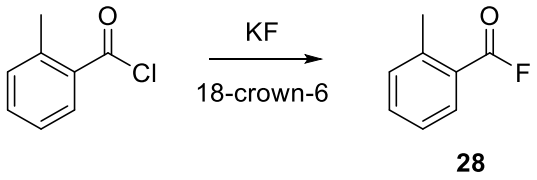

28

*Scheme 88: Synthesis of 2-methylbenzoyl fluoride (**28**)*

For the synthesis of 2-methylbenzoyl fluoride (**28**), 1 eq. of 2-methylbenzoyl chloride was stirred in the presence of 3.6 eq. of potassium fluoride and 0.06 eq. of 18-crown-6-ether in dry 1,2-dimethoxyethane. After refluxing overnight, an aqueous workup led to the isolation of the pure target compound as a colorless liquid (38%). The product was used in the following synthesis steps without any further purification.

3.1.4 Synthesis of tetrakis(2-methylbenzoyl)stannane (25)

Tetrakis(2-methylbenzoyl)stannane (**25**) should be synthesized in analogy to the method used in the synthesis attempt of tetrakisbenzoylstannane (**24**, chapter 3.1.2).

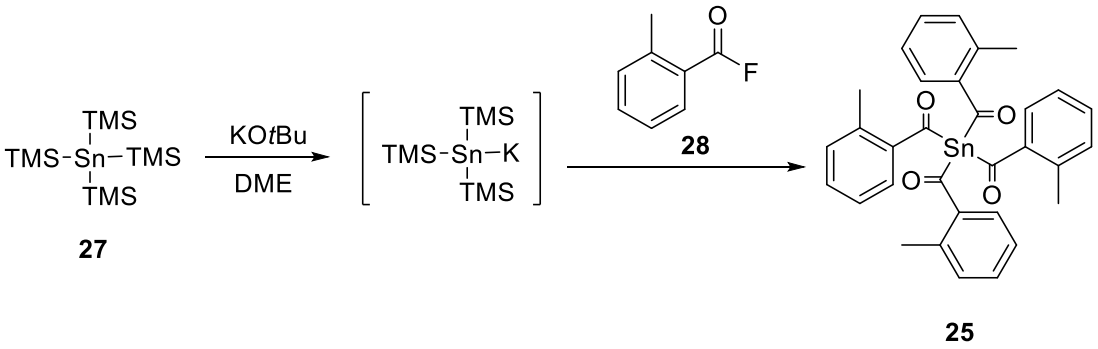

*Scheme 89: Synthesis of tetrakis(2-methylbenzoyl)stannane (**25**)*

For the synthesis of tetrakis(2-methylbenzoyl)stannane (**25**), 1 eq. of previously synthesized tetrakis(trimethylsilyl)stannane (**27**) and 1.1 eq. of potassium tert. butoxide were weighed into a dry Schlenk tube and dissolved in dry 1,2-dimethoxyethane. This mixture was stirred for 1 h at RT. In the meantime, a second Schlenk tube was used to dissolve 4.1 eq. of 2-methylbenzoyl fluoride (**28**) in dry 1,2-dimethoxyethane. Both reaction vessels were cooled to 0°C and then the stannyl potassium solution was added to the acid fluoride solution at that temperature via syringe and septum. Afterwards the resulting mixture was allowed to reach RT overnight during stirring. On the next day, the reaction was diluted with dichloromethane and quenched with cold 3% aqueous HCl. The layers were separated and the aqueous layer was extracted 3 times with dichloromethane. The combined organic layers were washed twice with water and dried over sodium sulfate. After filtration and evaporation of the solvent in vacuo, a small amount of pale yellow solid was obtained.

An initial photopolymerization experiment with the crude product turned out to be negative, so it was tried to crystallize **25** from acetone, which did not lead to success either. In a ^{119}Sn-NMR spectrum, no signal could be detected, as it was the case in the synthesis of tetrabenzoylstannane (**24**) already. Either the target compound **25** did not form in the desired way or it did not endure the harsh conditions of an aqueous work-up.

3.1.5 Synthesis of tetrakis(2,4,6-trimethylbenzoyl)stannane (26) via acid chloride

Tetrakis(2,4,6-trimethylbenzoyl)stannane (**26**) was chosen as target compound, since it should in theory show the highest stability against aqueous hydrolysis due to the steric hindrance provided by the o-methyl groups next to the carbonyl functionalities. In the first attempt, 2,4,6-trimethylbenzoyl chloride should be used for the synthesis, since it is commercially available.

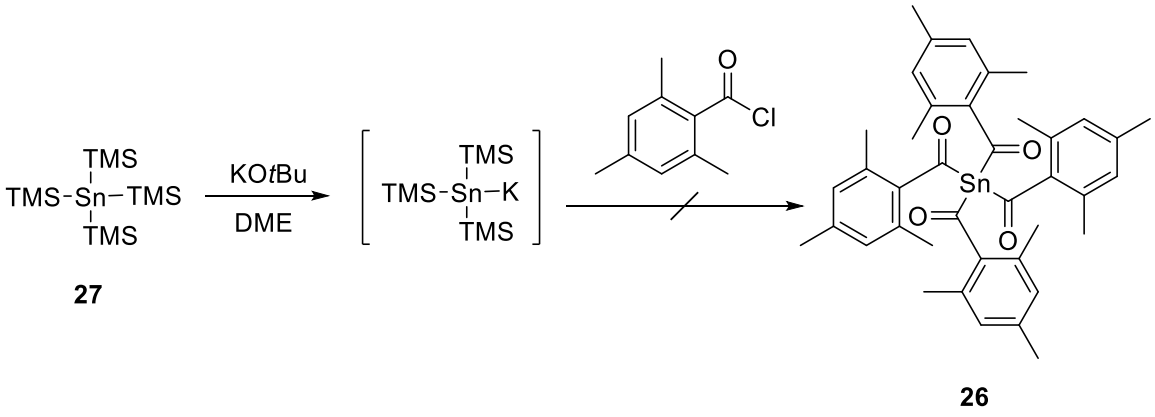

27 **26**

*Scheme 90: Synthesis of tetrakis(2,4,6-trimethylbenzoyl)stannane (**26**) via acid chloride*

For the synthesis of tetrakis(2,4,6-trimethylbenzoyl)stannane (**26**), 1 eq. of previously synthesized tetrakis(trimethylsilyl)stannane (**27**) and 1 eq. of potassium tert. butoxide were weighed into a dry Schlenk tube and dissolved in dry 1,2-dimethoxyethane. This mixture was stirred for 40 min at RT to achieve a clear, yellow solution. In the meantime, a second Schlenk tube was used to dissolve 4 eq. of 2,4,6-trimethylbenzoyl chloride in dry 1,2-dimethoxyethane. Both reaction vessels were cooled to -78°C using an acetone/N_2 bath and then the stannyl potassium solution was added to the acid chloride solution at that temperature via syringe and septum. Afterwards the resulting mixture was allowed to reach RT overnight during stirring. On the next day, the reaction was diluted with diethyl ether and quenched with cold 3% aqueous H_2SO_4. The layers were separated and the aqueous layer was extracted 3 times with diethyl ether. The combined organic layers were washed twice with

water and dried over sodium sulfate. After filtration and evaporation of the solvent in vacuo, a yellow, sticky substance was obtained, which was then analyzed using NMR spectroscopy.

^{1}H- as well as ^{29}Si-NMR spectra showed, that the reaction did not take place as expected. As main components of the obtained mixture, tetrakis(trimethylsilyl)stannane (**27**) as well as a large amounts of 2,4,6-trimethylbenzaldehyde could be identified. Additional signals in the ^{1}H-NMR spectrum might indicate product formation to a very small degree, but attempts to separate the individual components (partial dissolution in various solvents) failed.

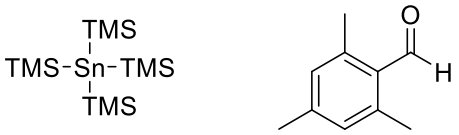

27

*Figure 18: Tetrakis(trimethylsilyl)stannane (**27**) and 2,4,6-trimethylbenzaldehyde*

Overall, either the reaction did not occur in the desired way or the aqueous workup led to a complete degradation of the target compound. Since Radebner et al.[30] showed, that for the synthesis of tetrakisacylgermanes, the usage of the corresponding acid fluorides instead of the acid chlorides led to more satisfying results, this should also be envisaged for the synthesis of target compound **26** (chapter 3.1.7).

3.1.6 Synthesis of 2,4,6-trimethylbenzoyl fluoride (29)

In order to synthesize tetrakis(2,4,6-trimethylbenzoyl)stannane (**26**) via acid fluorides, the starting material 2,4,6-trimethylbenzoyl fluoride (**29**) should be prepared using the method described by Lee et al.,[73] which was already used for the preparation of the o-methyl derivative (**28**) involving excess potassium fluoride and crown ether.

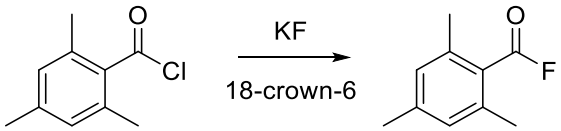

29

*Scheme 91: Synthesis of 2,4,6-trimethylbenzoyl fluoride (**29**)*

For the synthesis of 2,4,6-trimethylbenzoyl fluoride (**29**), 1 eq. of 2,4,6-trimethylbenzoyl chloride was stirred in the presence of 3.6 eq. of potassium fluoride and 0.06 eq. of 18-crown-6-ether in dry 1,2-dimethoxyethane. After refluxing overnight, an aqueous workup led to the isolation of the pure target compound as colorless crystals (96%). The product was used in the following synthesis steps without any further purification.

3.1.7 Synthesis of tetrakis(2,4,6-trimethylbenzoyl)stannane (26) via acid fluoride

As already mentioned above, tetrakis(2,4,6-trimethylbenzoyl)stannane (**26**) should be prepared with a method based on a route, which was already used for the synthesis of tetrakisacylgermanes.[30] Since the attempt of synthesizing the target compound **26** via acid chlorides did not lead to satisfying results, an in situ formation of acid fluoride using an excess of potassium fluoride was envisaged. In the following, the initial synthetic route is described, however a large number of variations was carried out both in the synthesis itself and in the subsequent work-up in order to improve the result. These variations and investigations in terms of optimizing the synthetic method will be described later in this chapter.

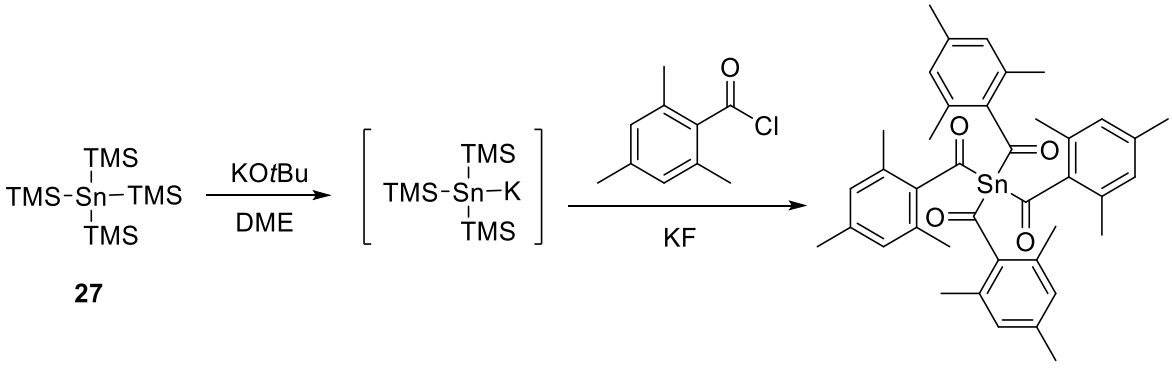

27 **26**

*Scheme 92: Synthesis of tetrakis(2,4,6-trimethylbenzoyl)stannane (**26**, fluoride formation in situ)*

For the synthesis of tetrakis(2,4,6-trimethylbenzoyl)stannane (**26**), 1 eq. of previously synthesized tetrakis(trimethylsilyl)stannane (**27**) and 1.1 eq. of potassium tert. butoxide were weighed into a dry Schlenk tube and dissolved in dry 1,2-dimethoxyethane. This mixture was stirred for 20 min at RT to obtain a clear, yellow solution before measuring a ^{119}Sn-NMR spectrum directly from the solution using a D_2O capillary to check, whether the desired stannyl potassium species could be achieved. Meanwhile, 14.7 eq. of potassium fluoride, 0.24 eq. of 18-crown-6-ether and 4.1 eq. of 2,4,6-trimethylbenzoyl chloride were weighed into another dry Schlenk tube and dissolved in dry 1,2-dimethoxyethane. Both solutions were cooled to 0°C using an ice bath and the stannyl potassium solution was added to the acid chloride solution at that temperature via syringe. After complete addition, the mixture was allowed to reach RT and stirred overnight. On the next day, the solvent was evaporated in vacuo and the residue was taken up in dry n-pentane to precipitate both polar side products as well as most of the target compound **26**. The mixture was filtrated under inert conditions and the obtained solid was washed with dry n-pentane. Parts of the solid mixture were then taken up with dry toluene and insoluble polar components were separated using a centrifuge. n-Pentane was added to the intense yellow solution until no additional precipitate was formed. This precipitate was separated from the solution once more and the solvent was evaporated from the supernatant solution in vacuo giving the crystalline yellow product **26** (13%).

The described purification method has been developed in numerous attempts to successfully isolate **26**. Although the yield was not very high, this method provides a good basis for further optimization. In order to better describe the different attempts to improve the synthesis and the path towards a successful work-up protocol, the reaction should be broken down into its substeps and described one by one.

Regarding the reaction mechanism in greater detail, the formation of tetrakisacylstannanes is expected to occur in analogy to the proposed mechanism for the formation of tetrakisacylgermanes[30] and tetrakisacylsilanes,[20] which was proposed by Radebner et al. (Scheme 93).

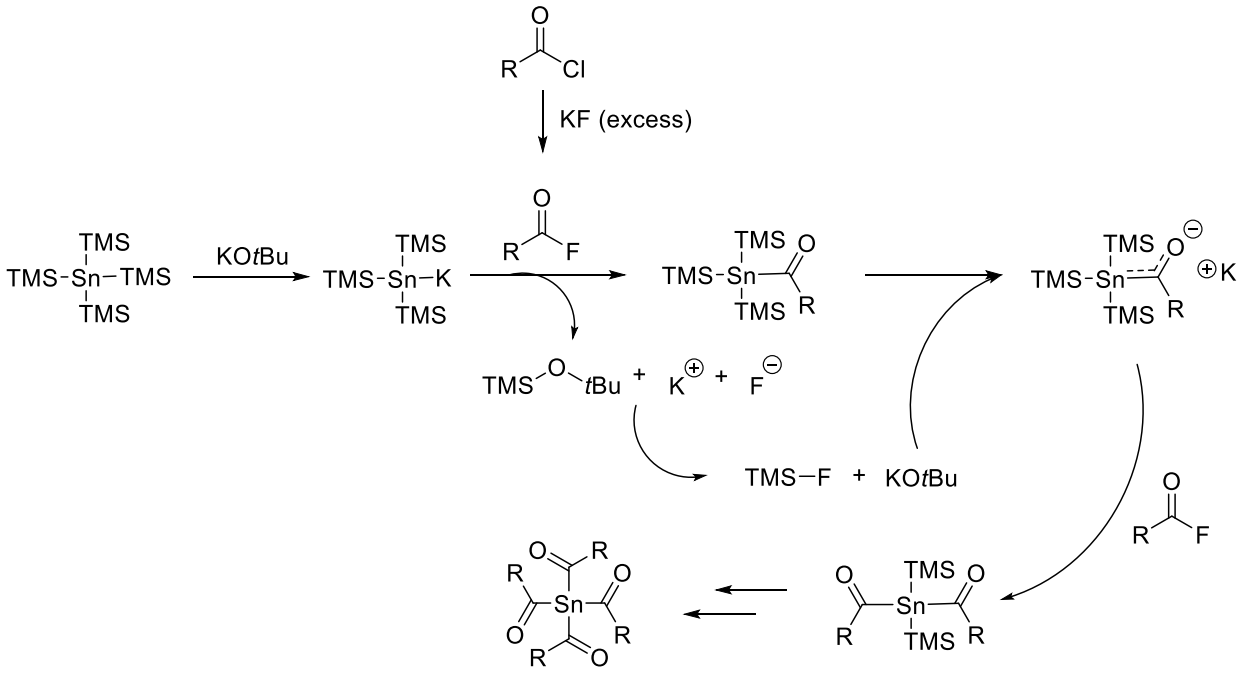

Scheme 93: Proposed mechanism for the synthesis of tetrakisacylstannanes[30]

In the first step, tris(trimethylsilyl)stannyl potassium was prepared by reacting the previously synthesized tetrakis(trimethylsilyl)stannane (**27**) with potassium tert. butoxide (Scheme 94). The two solids were weighed in and then stirred in dry 1,2-dimethoxyethane.

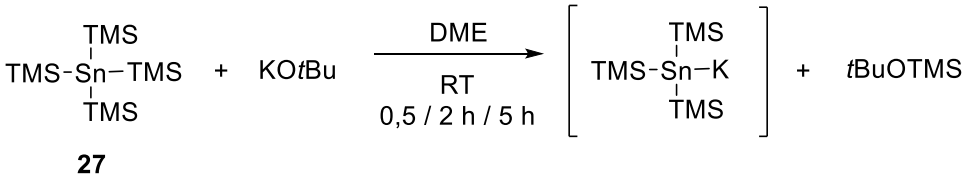

Scheme 94: Synthesis of tris(trimethylsilyl)stannyl potassium (substep 1)

In the course of these investigations, 3 different reaction times were tested: 30 minutes, 2 hours and 5 hours. The result was a similar one in each case. After ^{119}Sn-NMR measurements were carried out directly from the solution using a D_2O capillary, it could be shown that the reaction was complete after 30 min. The signals obtained after 30 minutes remained unchanged even after longer reaction times (Figure 19).

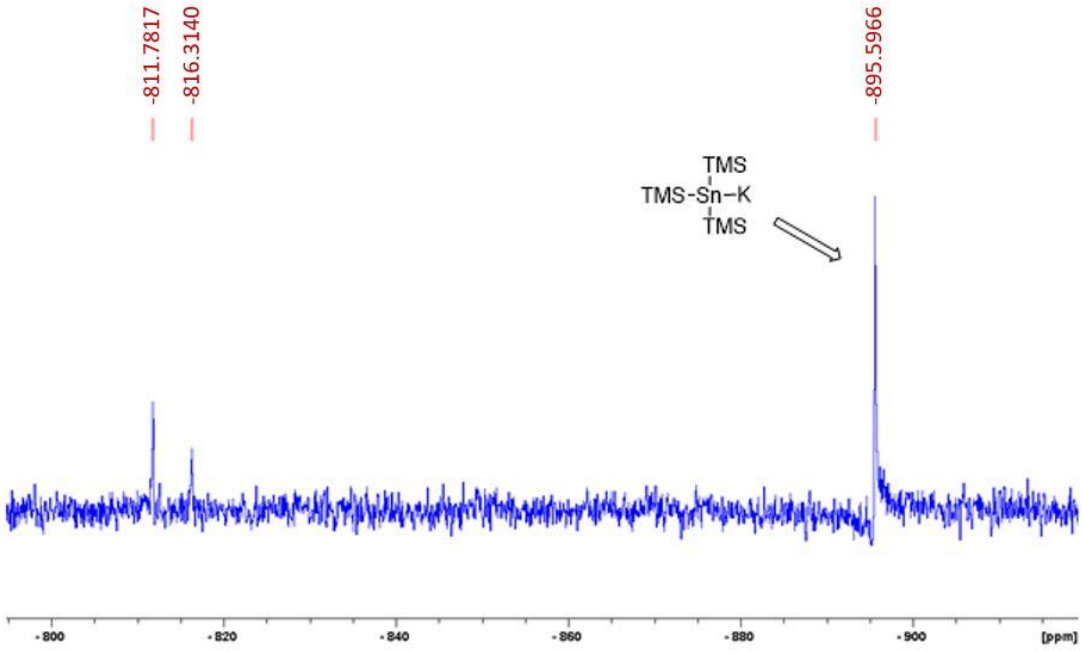

Figure 19: ^{119}Sn-NMR spectrum of the reaction mixture (DME) during the synthesis of tris(trimethylsilyl)stannyl potassium

The NMR signal obtained at -895.6 ppm confirmed the formation of tris(trimethylsilyl)stannyl potassium (Fischer et al.[74]). The other two smaller signals could not be clearly assigned to specific compounds, however it could possibly come from a di- or tripotassium species or from an ether complex formed by solvent molecules. There was no reactant signal (-664.6

ppm) visible, so it could be assumed that full conversion was achieved before moving on to substep 2.

In substep 2, the resulting solution of tris(trimethylsilyl)stannyl potassium was reacted with the acid halide. Assuming the proposed mechanism described above[30] all 4 trimethylsilyl groups should be substituted by mesitoyl groups consecutively. Since the attempt of synthesizing the target compound **26** via acid chlorides did not lead to satisfying results, an in situ formation of acid fluoride using an excess of potassium fluoride was carried out (Scheme 95).

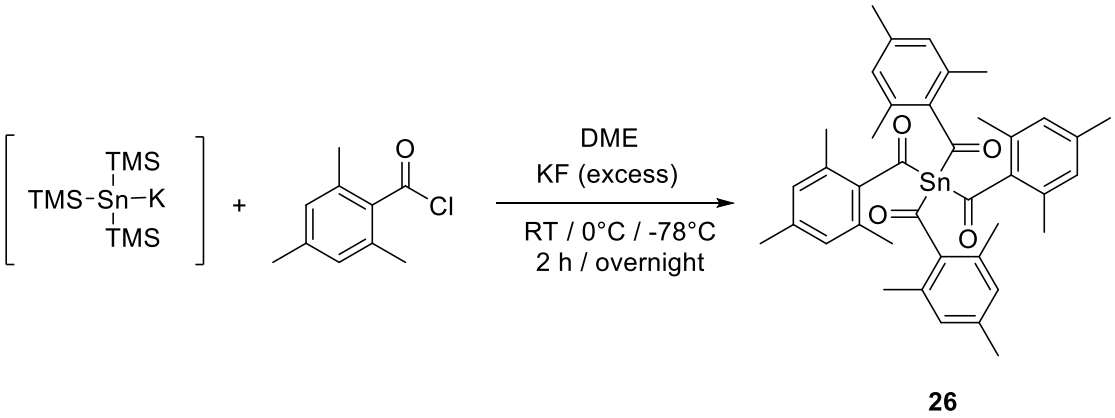

*Scheme 95: Synthesis of tetrakis(2,4,6-trimethylbenzoyl)stannane (**26**) via in situ formed acid fluoride (substep 2)*

Different reaction times (2 h and 18 h) and different temperatures during the addition (RT, 0°C and -78°C) were evaluated for this substep as well. The best results were achieved, when carrying out the reaction overnight and at a temperature of 0°C during the addition of the tris(trimethylsilyl)stannyl potassium solution to the acid halide solution. After stirring overnight, a ^{119}Sn-NMR spectrum was measured directly from the solution using a D_2O capillary (Figure 20).

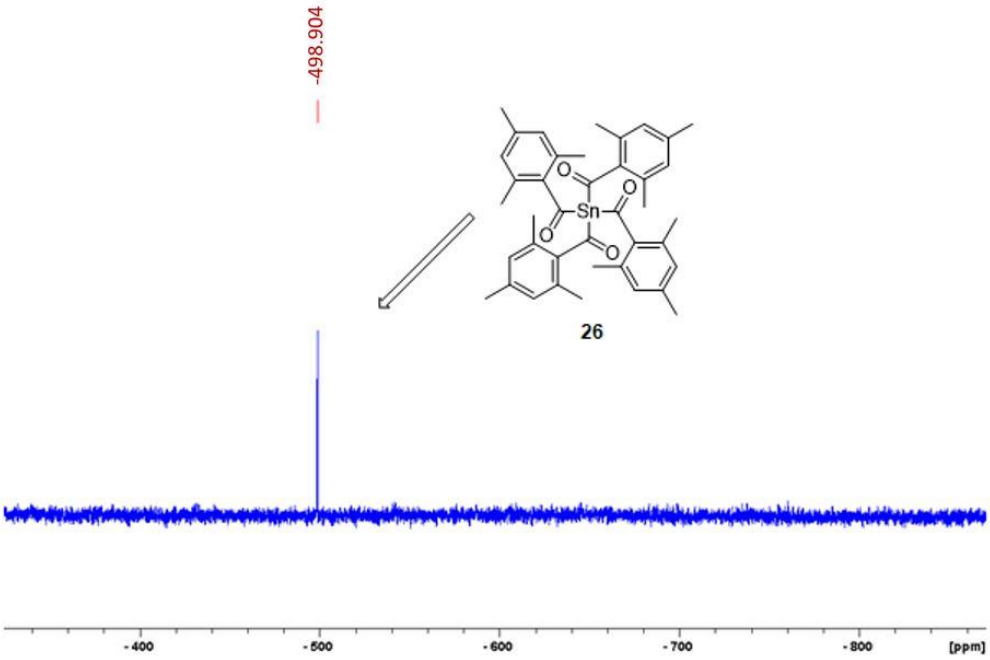

*Figure 20: ^{119}Sn-NMR spectrum of the reaction solution (DME) during the synthesis of tetrakis(2,4,6-trimethylbenzoyl)stannane (2**6**)*

A signal was obtained at -498.9 ppm, which was likely to be the product signal. From this point on, a variety of work-up procedures was tested. The experiments concerning those procedures are described in the following.

In the first attempt, the reaction solution was diluted with diethyl ether and then quenched with cold 3% H_2SO_4. The layers were separated and the aqueous layer was extracted twice with diethyl ether. The combined organic layers were then washed three times with water and dried over sodium sulfate and filtered. The solvent was then evaporated in vacuo to give an intense yellow, sticky solid. This solid contained the product **26**, however the amount of impurities was relatively large. It was recrystallized once from acetone, whereby no increase in purity could be achieved. In addition, since the impurities were assumed to be polar compounds (e.g. 2,4,6-trimethylbenzaldehyde, 2,4,6-trimethylbenzoic acid, etc.), an additional attempt was made to extract the product from the crude product with n-pentane. By carrying out this procedure, no cleaning effect could be achieved, though. In another batch, an attempt was carried out to achieve the purification by chromatographic methods.

For that, a silica gel flash column (PE 5:1 Et_2O) was used. Although all polar components could be separated by doing so, some impurities (probably the anhydride of 2,4,6-trimethylbenzoic acid according to TLC-MS) could not be removed. In addition, the amount of product decreased significantly, which is why it can be assumed that product **26** partly decomposed due to the column. Nevertheless, for another batch a longer silica gel column (PE 15:1 Et_2O) was packed and an attempt to remove this specific impurity was carried out, which was did not lead to satisfying results either. Additionally, the chromatographic separation attempts were performed in the red light laboratory instead of the usual orange light laboratory, since it was assumed that the present light intensity was already sufficient to cause photocleavage of tetrakis(2,4,6-trimethylbenzoyl)stannane (**26**). Even that did not change the result in the end.

Since it was assumed, that the above-described aqueous work-up (quenching + extraction) was causing the problems in the subsequent steps, it was ruled out in further batches. Avoiding an aqueous work-up, 1,2-dimethoxyethane was evaporated in vacuo directly from the reaction mixture. The residue was then taken up in dry n-pentane. Filtration was performed under inert conditions. The ultimate goal of this method was the separation of polar compounds, however, the solubility of product **26** in n-pentane was not very good, which is why only a small amount of product dissolved. Most of the product remained in the filter cake. This procedure and the subsequent steps (taking up in toluene, precipitation of impurities by adding n-pentane) correspond to those in the above-mentioned synthetic protocol and finally led to a successful purification of the target compound.

In another approach, 1,2-dimethoxyethane was removed first and the residue was then taken up with toluene directly. As a result, 5 consecutive precipitation steps were carried out using n-pentane, but no pure product could be obtained. In contrast to the procedure described in the previous paragraph, this approach lacked only the "washing step" with n-pentane, which seems to be essential for the successful isolation of product **26**. In summary, it may be argued that it is best to separate apolar impurities first using a washing step with n-pentane and then

separate the remaining polar contaminants by dissolving in toluene and precipitating with n-pentane as described.

After some optimization of the reaction conditions and after developing a suitable purification method for tetrakis(2,4,6-trimethylbenzoyl)stannane (**26**), larger batches should be synthesized. Since a product yield of 13% is rather low when applying the in situ formation of acid fluoride, another batch should be prepared, for which previously isolated 2,4,6-trimethylbenzoyl fluoride (**29**, chapter 3.1.6) should be used to synthesize the tetrakisacylstannane **26** (Scheme 96). The procedure used for this approach is described below.

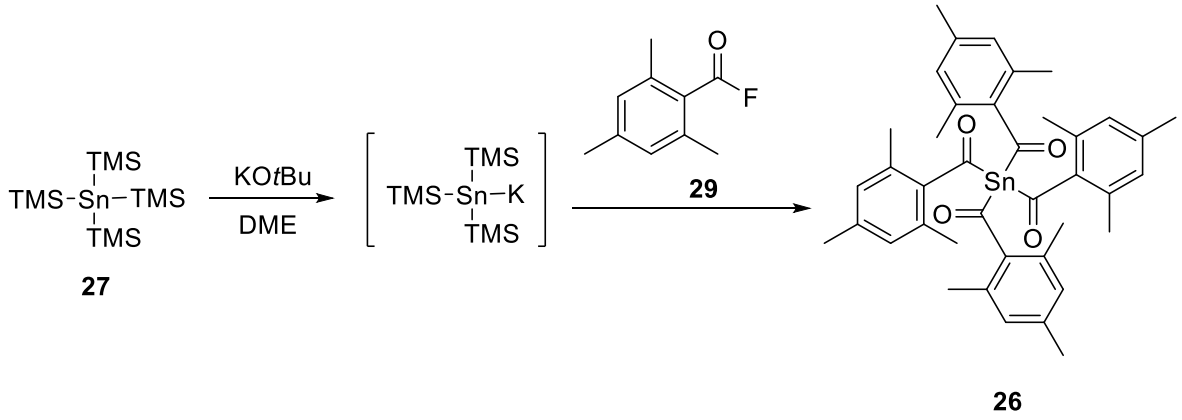

*Scheme 96: Synthesis of tetrakis(2,4,6-trimethylbenzoyl)stannane (**26**) using the previously isolated acid fluoride 29*

For the synthesis of tetrakis(2,4,6-trimethylbenzoyl)stannane (**26**), 1 eq. of previously synthesized tetrakis(trimethylsilyl)stannane (**27**) and 1 eq. of potassium tert. butoxide were weighed into a dry Schlenk tube and dissolved in dry 1,2-dimethoxyethane. This mixture was stirred for 20 min at RT to obtain a clear, yellow solution. In the meantime, 4 eq. of freshly synthesized 2,4,6-trimethylbenzoyl fluoride (**29**) were weighed into another dry Schlenk tube and dissolved in dry 1,2-dimethoxyethane. Both solutions were cooled to 40°C using an acetonitrile/N_2 cooling bath and the stannyl potassium solution was added to the acid fluoride solution slowly at that temperature via syringe, which resulted in a color change to dark red. After complete addition, the mixture was allowed to reach RT and stirred overnight.

On the next day, the solvent was evaporated in vacuo and the residue was taken up in dry n-pentane to precipitate both polar side products as well as most of the target compound. The mixture was filtrated under inert conditions and the obtained solid was washed with dry n-pentane. Parts of the solid mixture were then taken up with dry toluene and insoluble polar components were separated using a centrifuge. n-Pentane was added to the intense yellow solution until no additional precipitate was formed. This precipitate was separated from the solution once more and the solvent was evaporated from the supernatant solution in vacuo giving the crystalline yellow product **26** in a significantly higher yield (58%) compared to the yield achieved when using the method described at the beginning of this chapter. Product **26** was stored under exclusion of light under Argon at 4°C.

It turned out that the synthesis of tetrakis(2,4,6-trimethylbenzoyl)stannane (**26**) works much better with direct use of the isolated acid fluoride **29**. It was possible to develop a practicable route for the synthesis and isolation of the first tetrakisacylstannane compound, which in addition provides reasonable yields. For target compound **26**, a broad photochemical characterization could be carried out (chapter 3.2) to estimate its potential as a novel Type I photoinitiator in dental composites.

3.2 Characterization

To investigate the potential of tetrakis(2,4,6-trimethylbenzoyl)stannane (**26**) as photoinitiator in visible light free radical polymerization, it was compared to 3 well-known compounds in numerous experiments (Scheme 97). Bis(4-methoxybenzoyl)diethylgermane, known by the name of Ivocerin® is an extremely potent state-of-the-art photoinitiator, providing all properties needed for efficient photopolymerization in visible light and is used mainly in dental composites.[47] The new tetrakisacylstannane **26** should be compared to Ivoverin® particularly in terms of photoreactivity at the typical dental LED range, which lies at around 460 nm. Tetrakis(2-methylbenzoyl)germane[30] (K174) provides high structural similarity to the acylstannane and is therefore another interesting reference compound. Bis(2,4-cylcopentadien-1-yl)-bis(2,6-difluoro-3-(1H-pyrrol-1-yl)-phenyl) titanium,[15] commercially available by the name of Irgacure® 784 is particularly designed to work at wavelengths above 500 nm (however is known to show limited photobleaching behavior) and should therefore serve as a reference, when investigating the ability of the acylstannane **26** to initiate polymerizations at longer wavelength ranges.

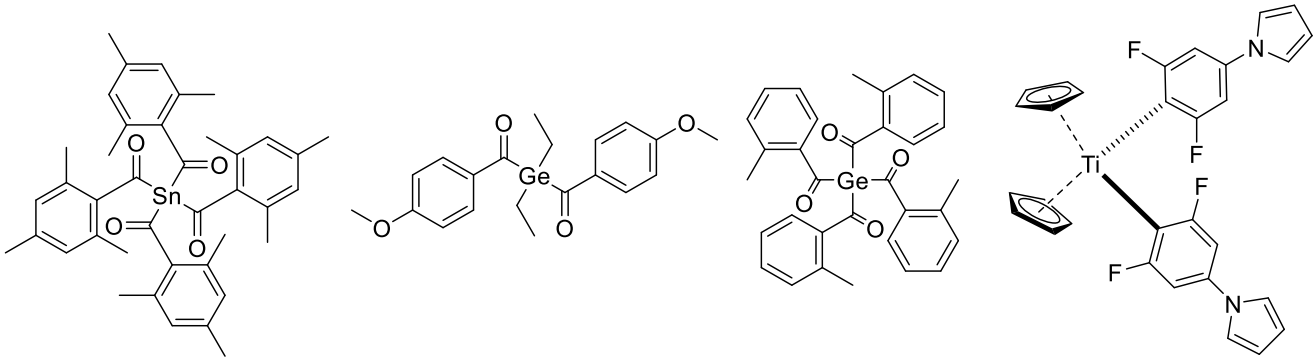

26 Ivocerin® K174 Irgacure® 784

*Scheme 97: Tetrakis(2,4,6-trimethylbenzoyl)stannane (**26**) and reference photoinitiators*

3.2.1 UV/Vis spectroscopy

In order to investigate the absorbance properties of tetrakis(2,4,6-trimethylbenzoyl)stannane (**26**), Ivocerin®, K174 and Irgacure® 784 were each dissolved in dry acetonitrile (c = 1 x 10^{-3} mol L^{-1}) under light protection. Directly afterwards, the samples were placed into quartz cuvettes and the UV/Vis spectra were acquired (Figure 21).

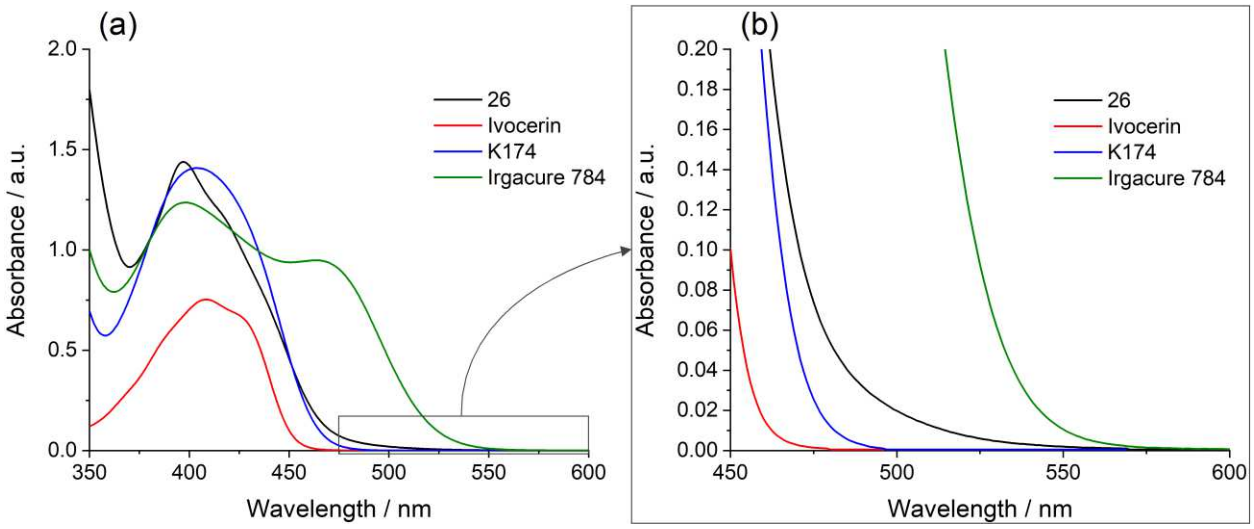

*Figure 21: a) UV/Vis spectra for tetrakis(2,4,6-trimethylbenzoyl)stannane (**26**), Ivocerin®, K174 and Irgacure® 784 as well as b) the expanded tails of nπ* transition bands*

The recorded spectra above show that all 4 photoinitiators show absorption in the visible region of the light. When comparing the 3 acyl compounds it is also clear that the nπ* absorption band of tetrakis(2,4,6-trimethylbenzoyl)stannane (**26**) expires at particularly high wavelengths. It extends to ≈ 550 nm, which corresponds to a bathochromic shift of approximately 50 nm compared to that of Ivocerin® (≈ 480 nm) and K174 (≈ 500 nm), probably caused by the orbital interaction of the tin d orbitals with the π* orbitals of the carbonyl group.[16] The absorption tailout at such high wavelengths is unique among classical type I initiators.

To determine the relevant absorption maxima of all four photoinitiators, mathematical peak deconvolution was carried out (Table 2). For the determination of the molar extinction coefficients ε [L mol^{-1} cm^{-1}] at the absorption maxima, Lambert-Beer law was applied.

$$A = \varepsilon \cdot c \cdot d$$

$A \ldots absorbance$

$c \ldots concentration\ [mol\ L^{-1}]$

$d \ldots path\ length\ [cm]$

Table 2: Collected values for the absorption maxima after peak deconvolution and extinction coefficients

26	Ivocerin	K174	Irgacure 784
λ_1 = 397 nm (ε = 1439 L mol^{-1} cm^{-1})	λ_1 = 393 nm (ε = 626 L mol^{-1} cm^{-1})	λ_1 = 404 nm (ε = 1408 L mol^{-1} cm^{-1})	λ_1 = 398 nm (ε = 1236 L mol^{-1} cm^{-1})
λ_2 = 430 nm (ε = 924 L mol^{-1} cm^{-1})	λ_2 = 408 nm (ε = 753 L mol^{-1} cm^{-1})	λ_2 = 430 nm (ε = 1117 L mol^{-1} cm^{-1})	λ_2 = 463 nm (ε = 948 L mol^{-1} cm^{-1})
	λ_3 = 422 nm (ε = 690 L mol^{-1} cm^{-1})		

3.2.2 Computational studies

In addition, calculations on the electronic states were performed and UV/Vis spectra were calculated (Figure 22). These studies were carried out in cooperation with Dr. Sergej Naumov at the Leibniz Institute of Surface Modification at Leipzig.[48]

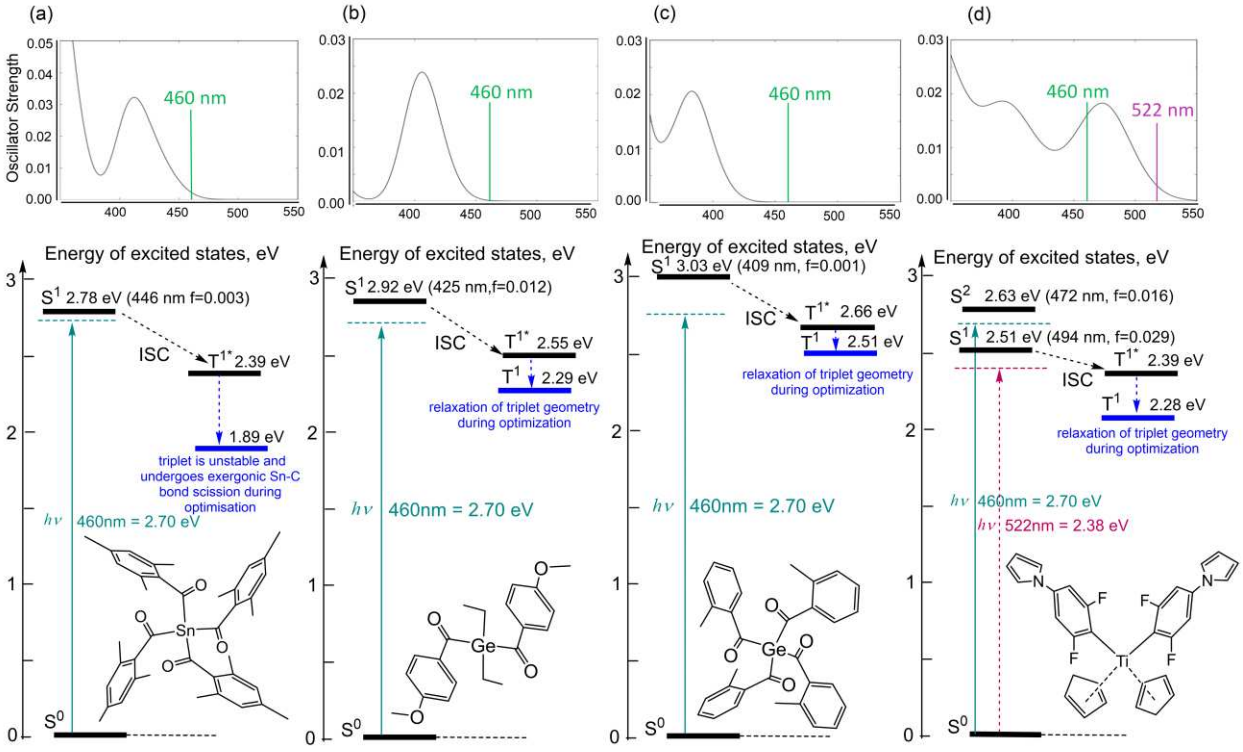

*Figure 22: Calculated UV-VIS spectra and Jablonski energy scheme of the population of the reactive triplet by excitation with 460 nm and 522 nm of acylstannane **26** (a), Ivocerin® (b), K174 (c) and Irgacure® 784 (d) by two-photon excitation of studied TPA PIs (calculated in acetonitrile at the TDM06-D3/LACVP(d,p)/PBE level of theory); f-oscillator strength*

The study of the formation of the reactive triple state T^1 for all 4 compounds and the calculated UV-VIS spectra are shown in the figure above (Figure 22). The calculated spectra coincided well with the experimentally measured ones (chapter 3.2.1), with the absorption bands for the acyl compounds being slightly shifted to shorter wavelengths. Upon absorption of photons with a wavelength of 460 nm (2.70 eV), the first excited singlet state S^1 is occupied and the population of S^1 should be more efficient for the acylstannane **26** and the titanocene, because the S^0-S^1 transition energies are lower than for the other reference initiators. Since the absorption bands for the titanocene are shifted to distinctly higher wavelengths, it is also possible for this compound to occupy S^1 by excitation at 522 nm (2.38 eV). After intersystem crossing (ISC), the excited triple state T^1* can be occupied. Relaxation from this state can then adapt the molecular structure due to a change in the electron distribution after the excitation. The calculations show that the excited states S^1 and T^1 are formed mainly by the excitation of oxygen n electrons into the carbonyl π* orbital. Since these n- and π*-electrons are oriented

perpendicular to each other, low oscillator strengths of the S^0-S^1 transition result. In the case of the titanocene, where additional π electrons can be excited from the aromatic structure to the titanium d orbital, these energies are even lower. The energy of the relaxation from the excited triplet state T^1* in all 3 reference compounds is sufficient to induce exergonic bond-cleavage reactions. The excited triplet state T^1* of the acylstannane **26** showed Sn-C bond cleavage reactions already during triplet optimization, indicating a very efficient formation of reactive species.

3.2.3 Steady state photolysis

For many photopolymerization applications in the visible region of light, it is important that the resulting material does not show any coloration after the polymerization process. This is especially true for dental materials. The photocleavage of the Sn-CO bonds is expected to cause rapid photobleaching for acylstannanes (as well as for acylgermanes). To investigate this behavior, steady-state photolysis experiments were carried out for tetrakis(2,4,6-trimethylbenzoyl)stannane (**26**) and the results were compared with those of the reference compounds. The photoinitiators were dissolved in acetonitrile (c_0 = 1 × 10^{-3} mol L^{-1}) and irradiated by a 460 nm LED. The obtained data are given in the diagrams below (Figure 23).

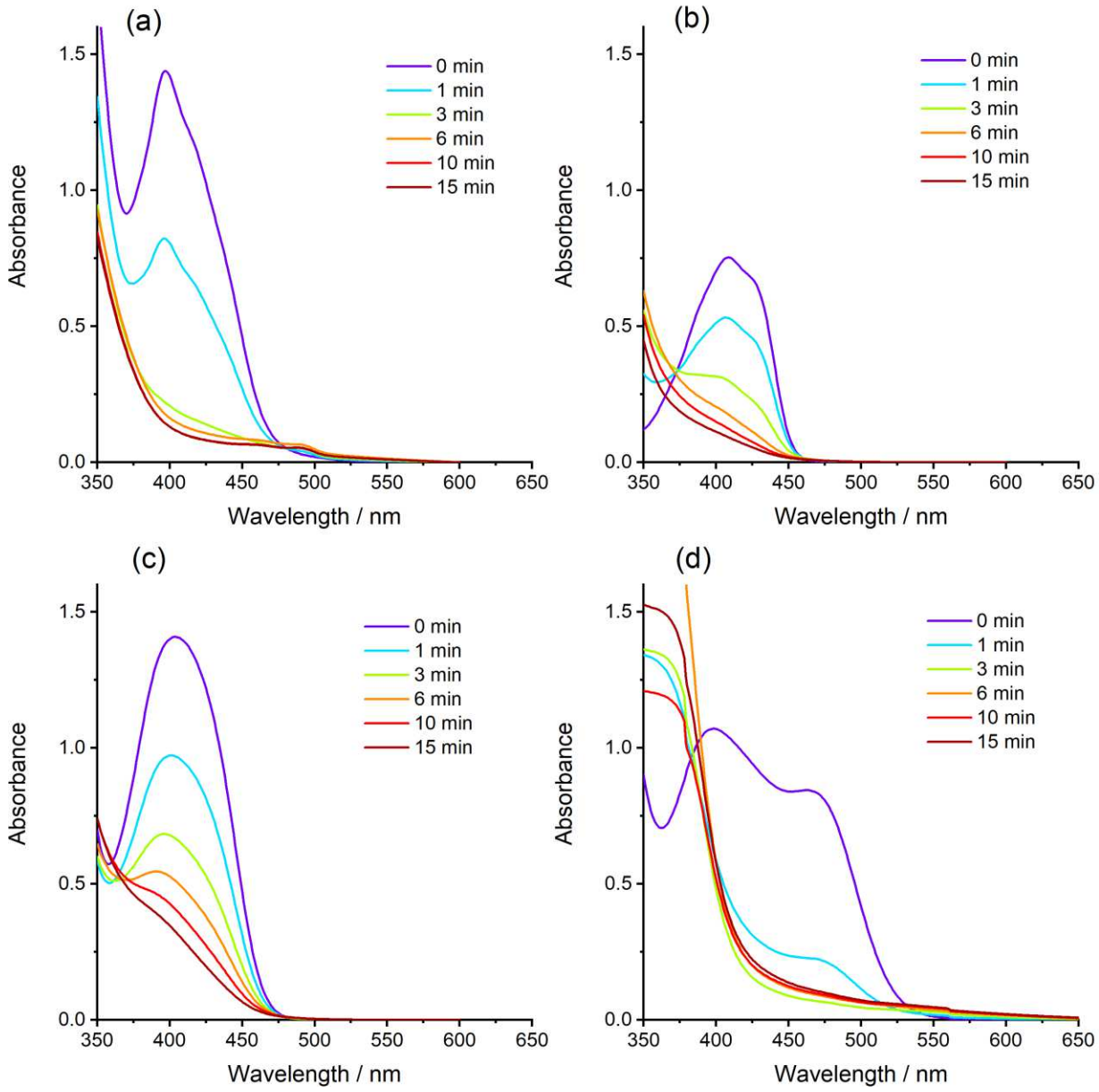

*Figure 23: Steady state photolysis of tetrakis(2,4,6-trimethylbenzoyl)stannane **26** (a), Ivocerin® (b), K174 (c) and Irgacure® 784 (d) under Argon with 460 nm LED in acetonitrile (c_0 = 1x10^{-3} mol L^{-1})*

The achieved data show that the novel acylstannane **26** exhibits very fast photobleaching. Already after 3 min, the absorption in the region of the nπ* band had fallen to a minimum. For the acylgermane compounds, significantly longer irradiation times (15 min) were needed to achieve a similar result. The titanocene also showed a rapid decrease of absorbance in solution, however the photoproducts show absorption up to 650 nm.

Additionally, for all four photoinitiators, the rate of decomposition R_d [mol s^{-1} L^{-1}] as well as the quantum yield of decomposition Φ_d were calculated using the formulas below[75] with the light intensity I_0 (3,00 x 10-6 mol L^{-1} s^{-1}). The values A_0, A_1 and A_2 are absorbances before and after the irradiation times t_1 and t_2.

$$R_d = -\frac{d[PI]}{dt} = \left(\frac{A_1 - A_2}{A_0}\right)\left(\frac{[PI]}{t_1 - t_2}\right)$$

$$\Phi_d = \frac{R_d}{I_0}$$

The achieved values for R_d and Φ_d are given in the table below (Table 3).

Table 3: Calculated values for the rate of photoinitiator decomposition R_d and quantum yield of decomposition Φ_d for all 4 photoinitiators

Photoinitiator	R_d [mol s^{-1} L^{-1}]	Φ_d
26	2.69 x 10^{-6}	0.90
Ivocerin	2.49 x 10^{-6}	0.83
K174	1.84 x 10^{-6}	0.61
Irgacure 784	1.50 x 10^{-6}	0.50

The quantum yield of decomposition Φ_d for tetrakis(2,4,6-trimethylbenzoyl)stannane (**26**) is with a value of 0.90 extraordinarily high. It is much higher than the calculated value of the structurally very similar tetrakis(2-methylbenzoyl)germane (K174, Φ_d = 0.61). It is even higher than the value achieved for the commercially used photoinitiator Ivocerin® (Φ_d = 0.83) indicating an extremely efficient cleavage upon irradiation.

3.2.4 Photo-DSC

To study the ability of tetrakis(2,4,6-trimethylbenzoyl)stannane (**26**) regarding the ability to initiate photopolymerization, photo-DSC experiments were performed in dimethacrylate and

diacrylate formulations. This technique can be used to obtain the maximum time (t_{max}), double bond conversion (DBC) and other parameters like t_{95} and to determine the rate of polymerization (R_p). The curing of the samples was carried out using two different LEDs (460 and 522 nm). The light intensities were 1 W cm^{-2} for the 460 nm LED and 0.42 W cm^{-2} for the 522 nm LED. The measured formulations contained 0.1wt% of tetrakis(2,4,6-trimethylbenzoyl)stannane (**26**) either in a 1:1 mixture of urethanedimethacrylate (UDMA) and decanedioldiacrylate (D_3MA) or in hexanedioldiacrylate (HDDA). An additional 500 ppm of butylhydroxytoluene (BHT) was added as a stabilizer. To ensure good comparability, the concentrations of the other initiators were chosen so that they corresponded to the maximum possible number of cleavable groups (2-fold equimolar amount of Ivocerin®, equimolar amount of K174, 2-fold equimolar amount of Irgacure® 784).

Photo-DSC can be used to determine the double bond conversion (DBC [%]), the time until heat flow maximum is reached (t_{max} [s]), the time until 95 percent of total heat flow is reached (t_{95} [s]) as well as the total heat of polymerization, which is related to the peak area. Additionally, the rate of polymerization R_p can be calculated. These values provide quite good information on photoreactivity of the analyzed compounds.[27]

Double bond conversion can be calculated as shown below:

$$DBC\ [\%] = \frac{\Delta H}{\Delta H_T} \cdot 100$$

ΔH…peak area [kJ mol^{-1}]

ΔH_T…theoretical polymerization heat of the monomer [kJ mol^{-1}]

ΔH_T (UDMA/D_3MA)[48] = 115 kJ mol^{-1}

The rate of polymerization can be determined using:

$$R_p\ [mol\ L^{-1}\ s^{-1}] = \frac{h \cdot \rho_{monomer}}{\Delta H_T}$$

h…peak height [mW mg^{-1}]

$\rho_{monomer}$…density of the monomer

$\rho_{UDMA/D3MA}$[48] = 1030 mg mL^{-1}

The figure below (Figure 24) shows the obtained conversion curves for the formulations containing the selected photoinitiators.

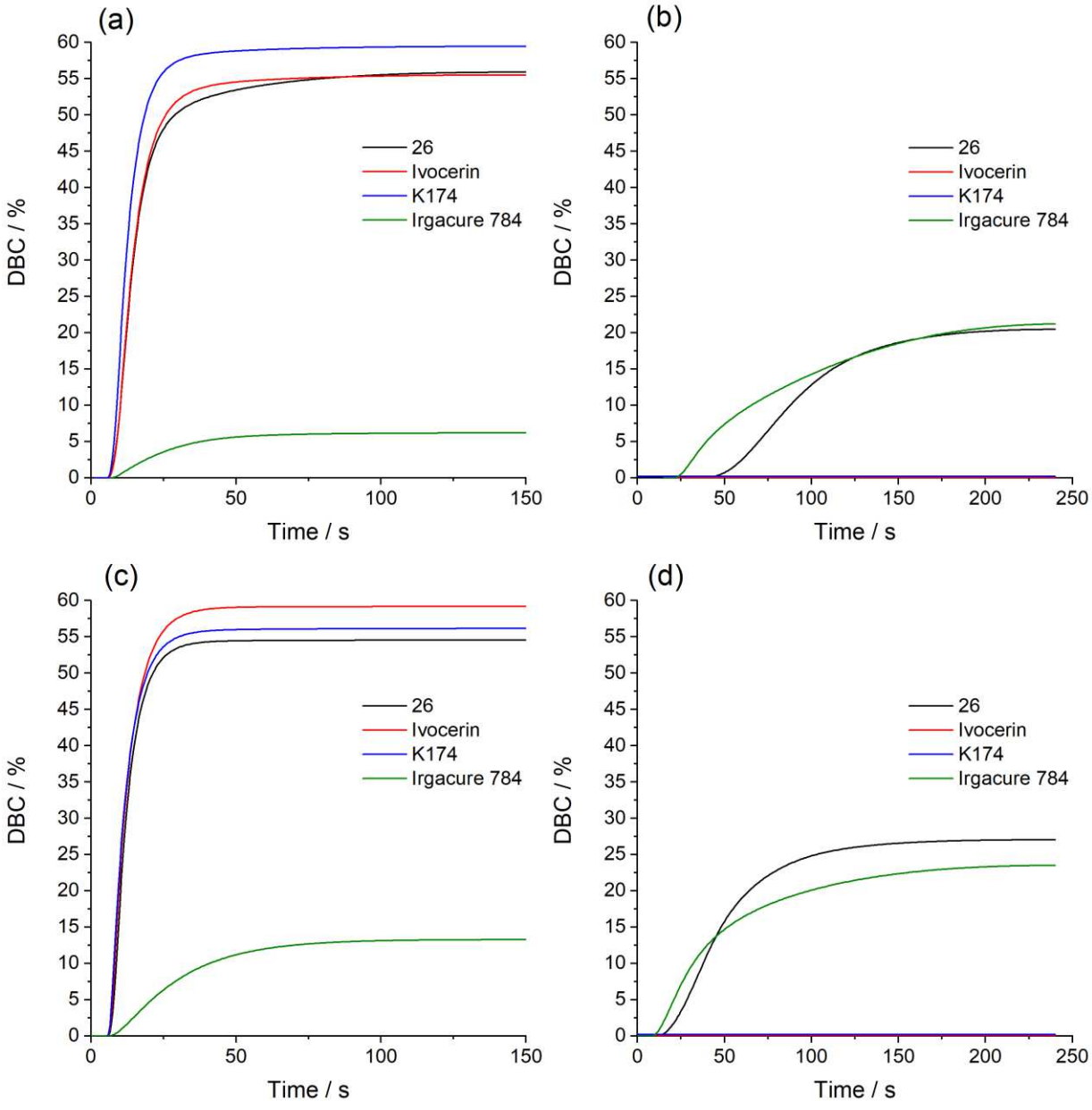

Figure 24: Photo-DSC conversion curves for all 4 photoinitiators in methacrylates using a) a 460 nm LED and b) a 522 nm LED as well as in HDDA using c) a 460 nm LED and d) a 522 nm LED

The obtained conversion curves for the experiments with the 460 nm LED show (Figure 24: a, c) that the photoinitiating activity of tetrakis(2,4,6-trimethylbenzoyl)stannane (**26**) is extremely high in both monomer systems. The values obtained are in the range of those of the reference germanium initiators. As expected, the titanocene shows only low reactivity upon irradiation with the 460 nm LED. Looking at the experiments with the 522 nm LED, the acylstannane **26** was able to initiate the polymerization even at this wavelength, however the two acylgermane compounds Ivocerin® and tetrakis(2-methylbenzoyl)germane (K174) showed no activity (Figure 24: b, d). Comparing the obtained values for the acylstannane **26** and the titanocene, it can be seen that the reactivities of the two initiators are similarly high, however the acylstannane **26** shows a higher final double bond conversion in HDDA. The lower conversions obtained using the 522 nm LED in place of the 460 nm LED for the acylstannane **26** can be explained by the lower light intensity and the lower extinction coefficient of tetrakis(2,4,6-trimethylbenzoyl)stannane (**26**) at 522 nm (chapter 3.2.1). In addition, it can be assumed that upon irradiation with 522 nm only for the tetrakis (and possibly the formed trisacyl species) the absorbance of the nπ * band is sufficiently high to trigger cleavage processes. The remaining bis- and monoacyl species may no longer cleave at this wavelength, as indicated by the slight yellowing of the polymer samples (compared to colorless at 460 nm) immediately after polymerization. The collected values for t_{max}, DBC, t_{95} and R_p are given in the table below.

Table 4: Collected values for t_{max}, DBC, t_{95} and R_p of all photo-DSC experiments

460 nm (UDMA/D_3MA)				
Photoinitiator	**DBC [%]**	**t_{max} [s]**	**t_{95} [s]**	**R_p [mol L^{-1} s^{-1}]**
26	55.9	11.6	45.8	0.23
Ivocerin	55.5	11.1	32.3	0.25
K174	59.4	9.7	26.4	0.31
Irgacure 784	6.2	10.4	60.9	0.11

522 nm (UDMA/D_3MA)				
Photoinitiator	**DBC [%]**	**t_{max} [s]**	**t_{95} [s]**	**R_p [mol L^{-1} s^{-1}]**
26	20.4	74.4	167.7	0.04
Ivocerin	-	-	-	-
K174	-	-	-	-
Irgacure 784	21.3	15.6	169.5	0.04

460 nm (HDDA)				
Photoinitiator	**DBC [%]**	**t_{max} [s]**	**t_{95} [s]**	**R_p [mol L^{-1} s^{-1}]**
26	54.5	9.3	24.2	0.56
Ivocerin	59.2	8.3	25.8	0.56
K174	56.1	8.0	24.3	0.59
Irgacure 784	13.3	15.0	72.5	0.14

522 nm (HDDA)				
Photoinitiator	**DBC [%]**	**t_{max} [s]**	**t_{95} [s]**	**R_p [mol L^{-1} s^{-1}]**
26	27.0	35.5	116.0	0.09
Ivocerin	-	-	-	-
K174	-	-	-	-
Irgacure 784	23.5	19.1	148.5	0.10

3.2.5 Curing depth

Two key parameters govern the polymerization of photosensitive resins: the penetration depth of the light and the energy required for polymerization.[8, 9, 76] The penetration of light follows the Lambert-Beer law as given below, where P_z is the power of light (usually in mW cm^{-2}) at a certain depth z below the surface, P_0 is the power at the surface and D_p is the depth at which the penetrating light intensity falls to 1/e of the surface intensity.[8]

$$P_z = P_0 e^{-z/D_p}$$

For practical reasons the power terms are converted into energy terms and z becomes the curing depth C_d, as long as long as the needed amount of light is present, resulting in the formula below.

$$C_d = D_P \ln\left(\frac{E_0}{E_c}\right)$$

C_d is the depth of the cured resin, E_0 is the energy of light on the surface and E_c is the "critical" energy needed for the initiation of polymerization.[9] The penetration depth and therefore the curing depth is hugely dependent on the absorbance characteristics of the used resin and therefore dependent on the applied irradiation wavelength. Usually, the penetration depth increases with increasing wavelengths as shown in the figure below (Figure 25).

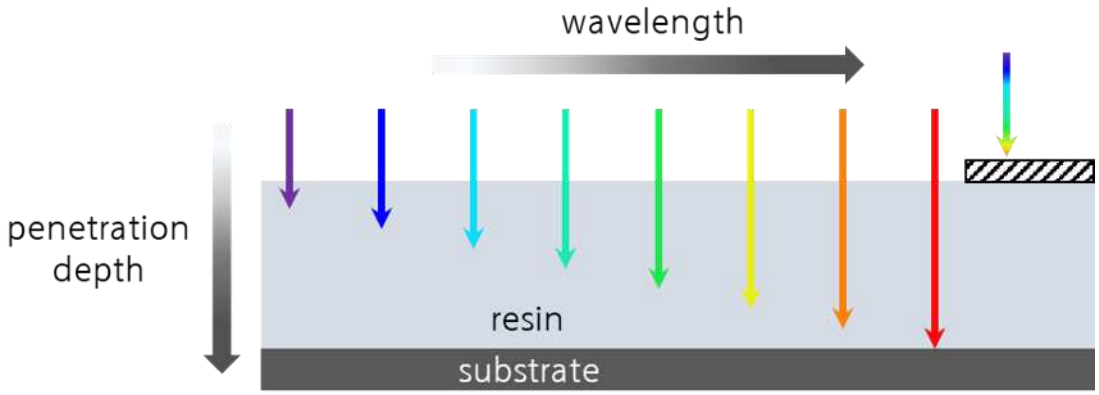

Figure 25: Schematic representation of the wavelength dependency of the penetration depth of light into the material

In order to investigate possible benefits of tetrakis(2,4,6-trimethylbenzoyl)stannane (**26**) in applications such as dental materials and additive manufacturing,[25] experiments on the curing depth in filled systems were performed. The big advantage of light with a higher wavelength is the potentially higher penetration depth of the light into the material, which should lead to higher curing depths. Since the acylstannane compound **26** exhibited absorbance up to ≈550 nm (chapter 3.2.1), a light source with a higher irradiation wavelength might be usable for curing. To investigate this, setups as described below were used (Figure 26). A PTFE cylinder was placed on a glass plate and the light source (460 or 522 nm LED) was

fixed below as shown. The formulations contained HDDA and 50wt% of ZrO_2 as inorganic filler and 0.1wt% of photoinitiator (either acylstannane **26** or Ivocerin®). As a stabilizer, 500 ppm BHT was added additionally. The acylstannane formulation was irradiated using a 522 nm LED and in the case of Ivocerin® a 460 nm LED was utilized. The light intensity for both light sources was set to be 33.5 mW cm^{-2} behind the glass plate and the irradiation time was 240 s for both formulations.

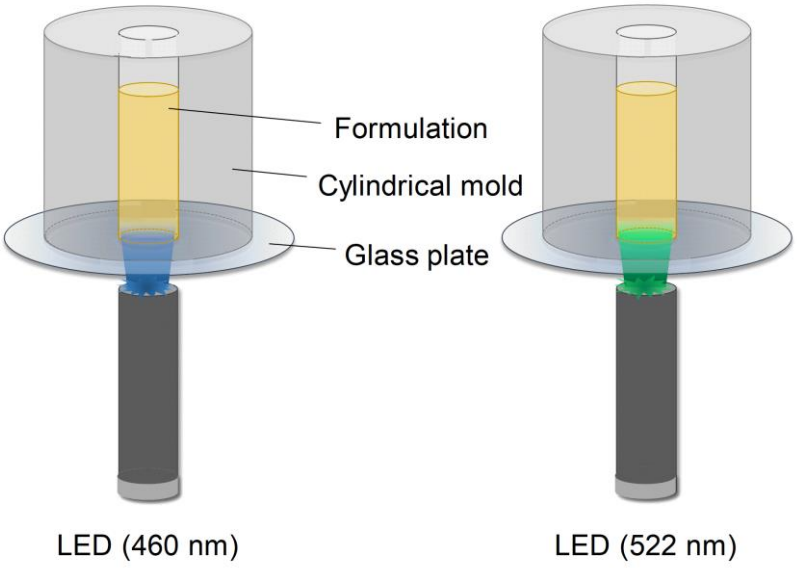

Figure 26: Setups used for the curing depth experiments

After curing, the samples were removed from the mold and unreacted formulation was washed away. The height of the resulting polymeric samples (Figure 27) was then measured at the center.

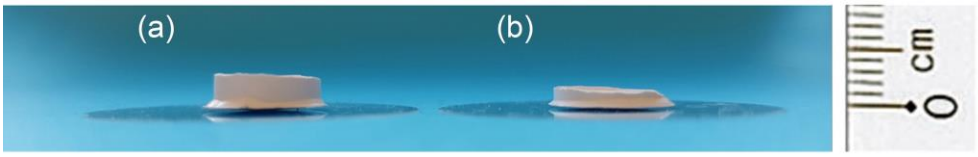

*Figure 27: Curing depth experiments: Resulting polymer after curing of formulation containing 0.1wt% of acylstannane **26** and 50wt% of ZrO_2 in HDDA with a 522 nm LED (a) and a formulation containing 0.1 wt% of Ivocerin® and 50wt% of ZrO_2 in HDDA with a 460 nm LED (b) at the same light intensity*

The sample that contained tetrakis(2,4,6-trimethylbenzoyl)stannane (**26**) and was polymerized using the 522 nm LED showed a much higher curing depth (more than double), proving the higher penetration depth and demonstrating the potential advantages of the acylstannane **26** in applications, in which filled systems are in use.

3.2.6 Green laser curing

In order to further investigate the potential of tetrakis(2,4,6-trimethylbenzoyl)stannane (**26**) as a photoinitiator in polymerizations at wavelengths above 500 nm, additional experiments were performed with a green laser (532 nm). A setup similar to the one described in the previous chapter was used (Figure 28). Instead of the LEDs, a commercially available green laser pointer was placed below the glass plate. A large number of samples were polymerized, with the PI concentration, the filler content (Schott® dental glass) and the irradiation time being varied. For comparison, formulations containing Irgacure® 784 were prepared and tested. Regarding the used resin, a 1:1 mixture of UDMA and D_3MA was used.

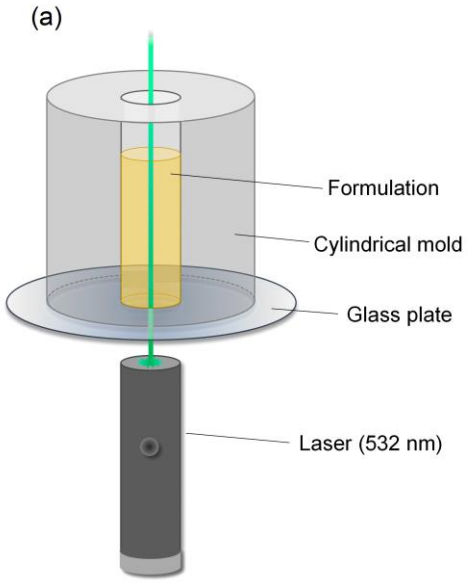

Figure 28: Setup used for green laser curing experiments

The laser was characterized beforehand by measuring an emission spectrum as well as a beam profile (Figure 29, Figure 30).

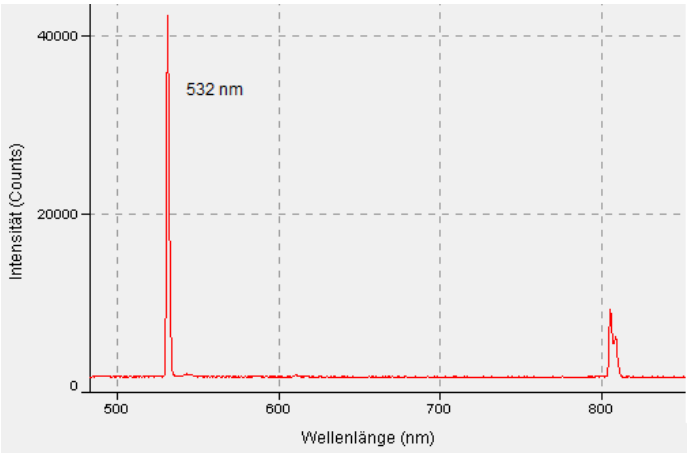

Figure 29: Emission spectrum of the green laser pointer

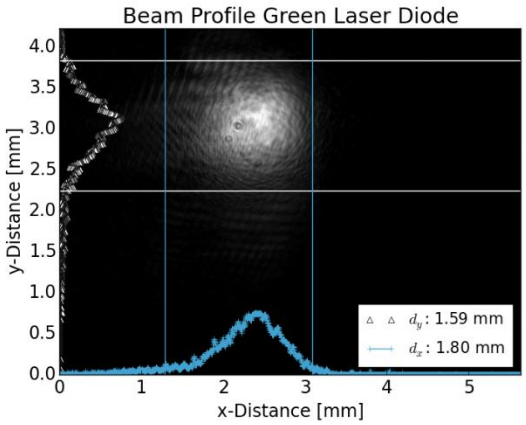

Figure 30: Beam profile of the green laser pointer

The polymer samples obtained from the various test series are given below.

*Figure 31: Cured (300 s) samples containing 0.010, 0.025, 0.050, 0.075, 0.100wt% of acylstannane **26** and 10wt% of filler*

*Figure 32: Cured (300 s) samples containing 0, 10, 30, 50, 70wt% of filler and 0.1wt% of acylstannane **26***

*Figure 33: Samples containing 0.1wt% of acylstannane **26** and 10wt% filler, cured for 60, 120, 200, 300, 500 s*

*Figure 34: Samples containing 0.1wt% of acylstannane **26** and 50wt% filler, cured for 60, 120, 200, 300, 500 s*

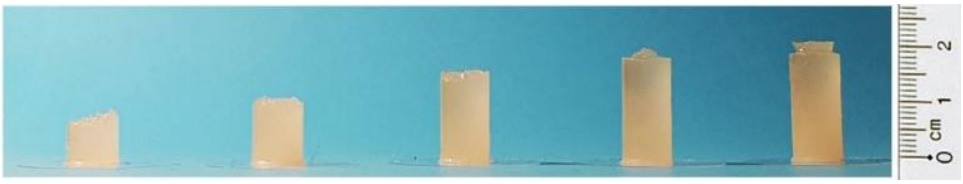

Figure 35: Samples containing 0.1wt% of Irgacure® 784 and 10wt% filler, cured for 60, 120, 200, 300, 500 s

Figure 36: Samples containing 0.1wt% of Irgacure® 784 and 50wt% filler, cured for 60, 120, 200, 300, 500 s

Surprisingly, the absorption of tetrakis(2,4,6-trimethylbenzoyl)stannane (**26**) at 532 nm is still high enough (chapter 3.2.1) to form radicals upon irradiation with light of this wavelength and initiate the polymerization. Even formulations with extremely high filler contents (up to 70% by weight) could be polymerized with the described setup. In addition, the photoinitiator concentration could be lowered extremely and still achieve satisfactory results. With Irgacure® 784, although slightly higher curing depths could be achieved, the polymer samples obtained were still strongly yellow in color even weeks after the experiments were carried out. In contrast, the samples cured with the acylstannane **26** showed rapid photobleaching within the polymer matrix. Additionally, the achieved curing depth values are summarized in the diagram below.

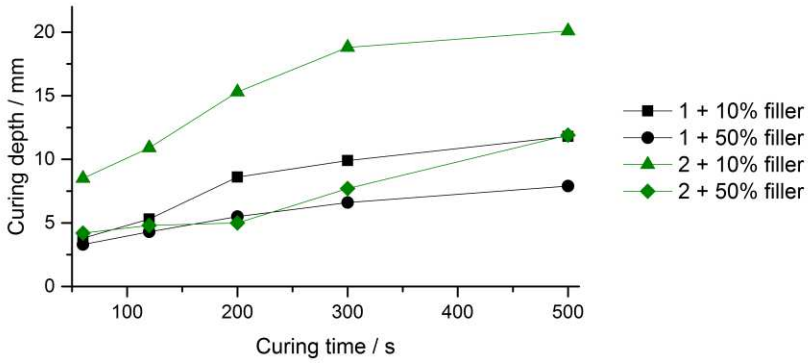

Figure 37: Green laser curing experiments in UDMA:D_3MA (1:1): Compared values for the achieved curing depths with 0.1wt% of PI and different amounts of inorganic filler

3.2.7 Cytocompatibility

Since many tin organyls show considerable cytotoxicity, an additional study was carried out to evaluate the cytocompatibility of tetrakis(2,4,6-trimethylbenzoyl)stannane (**26**) in comparison to the reference initiators. These investigations were carried out in cooperation with Dr. Marica Markovic at the Institute of Materials Science and Technology at TU Wien.[77] For this purpose, L929-mCherry cells were incubated with various concentrations of the photoinitiators in DMSO (Figure 38, 0.1, 0.05, 0.025, 0.0125, 0.00625, 0.003125 mM).[78]

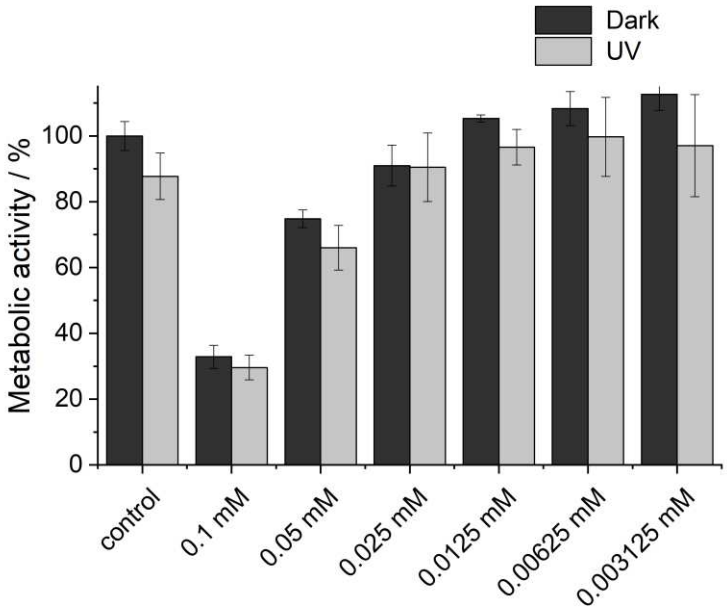

Figure 38: Influence of DMSO on the cells

In addition to investigating the photoinitiators themselves, the photoproducts were also examined after irradiation with UV (Figure 39, 365 nm, 10 min). For photoinitiator concentrations of 0.1 mM, the corresponding amount of DMSO (1%) alone is high enough already to cause cell death (Figure 38). However, the survival rate of the cells at a higher dilution (0.05 mM) rises to about 80%. At this concentration, the metabolic activity of the cells (irradiated and not irradiated) decreased below 60% for all four photoinitiators, with the cells exposed to the acylstannane **26** showing the highest survival rate. At concentrations of 0.025 mM, only the cells exposed to the acylstannane **26** and the titanocene showed a high

metabolic activity of approximately 80%. In contrast, the cells exposed to tetrakis(2-methylbenzoyl)german (K174) showed only 36% metabolic activity (without any UV irradiation). For the irradiated cells at the same concentration, a metabolic activity of over 65% was found for all initiators (70% for the acylstannane **26**). At lower concentrations, metabolic activity was almost always above 80% for all initiators, only for the cells exposed to 0.0125 mM of tetrakis(2-methylbenzoyl)germane (K174) the metabolic activity decreased to 70% (no irradiation).

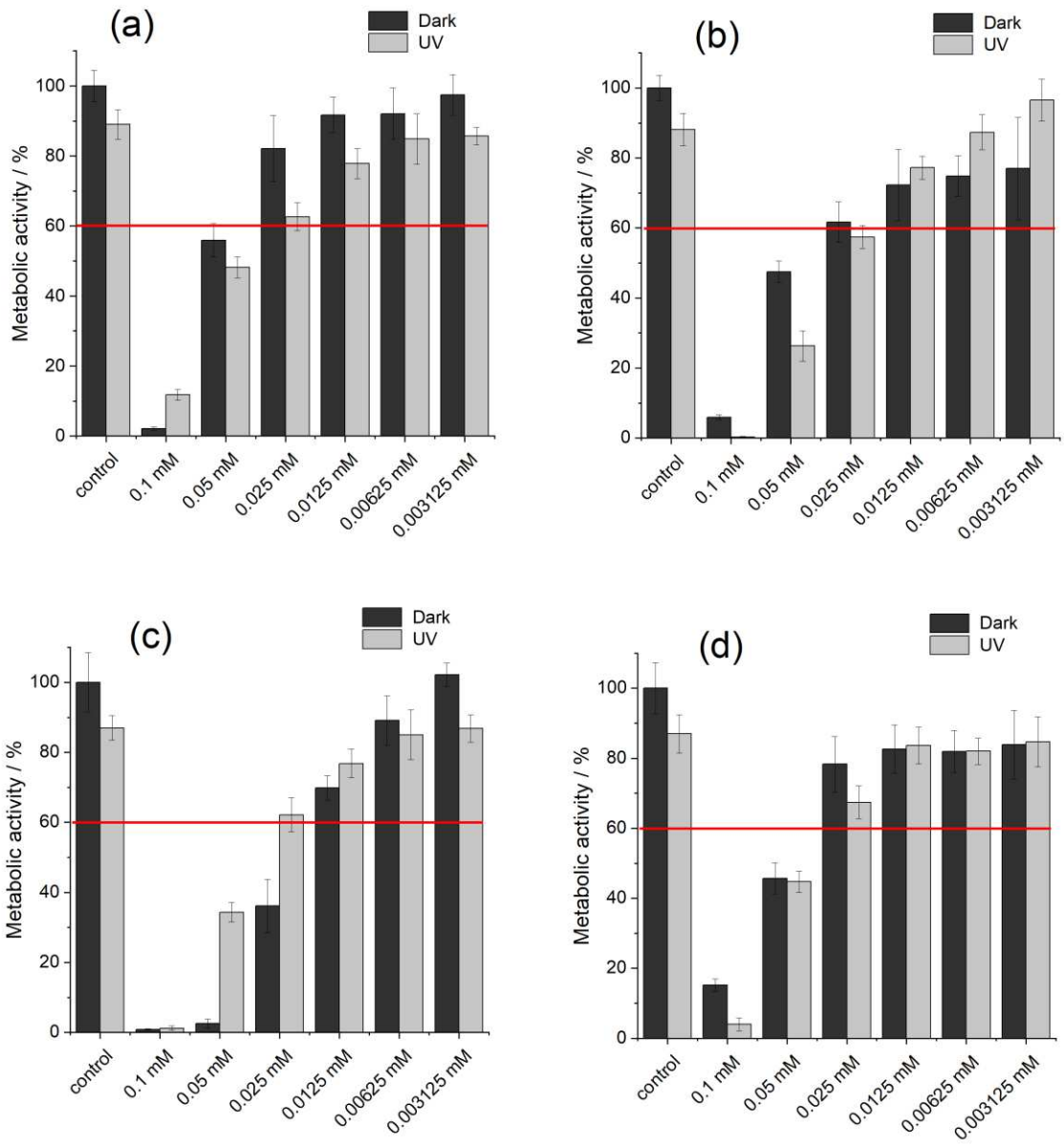

*Figure 39: Evaluation of the biocompatibility of tetrakis(2,4,6-trimethylbenzoyl)stannane **26** (a), Ivocerin® (b), K174 (c) and Irgacure® 784 (d)*

In summary, it can be said that tetrakis(2,4,6-trimethylbenzoyl)stannane (**26**) showed surprisingly high cytocompatibility, especially when compared to the structurally similar tetrakis(2-methylbenzoyl)germane (K174). The values obtained for the acylstannane **26** are consistently in the range of the values obtained for the acylgermane compounds. It was also

astonishing that the photoproducts of the Sn-based photoinitiator **26** did not show particularly high cytotoxicity.

The following figures additionally show the images recorded using a cell microscope (Figure 40, Figure 41). When exposed to a concentration of 0.1 mM of acylstannane **26**, cells had round shape and died to a severe extend. Cell death was caused not only due to the exposure to the photoinitiator, but also due to the high DMSO concentration present within the sample. With a photoinitiator concentration of 0.05 mM survival was much higher and cell morphology was typical for L929 fibriblasts, while with 0.025 mM no difference compared to the control sample could be observed.

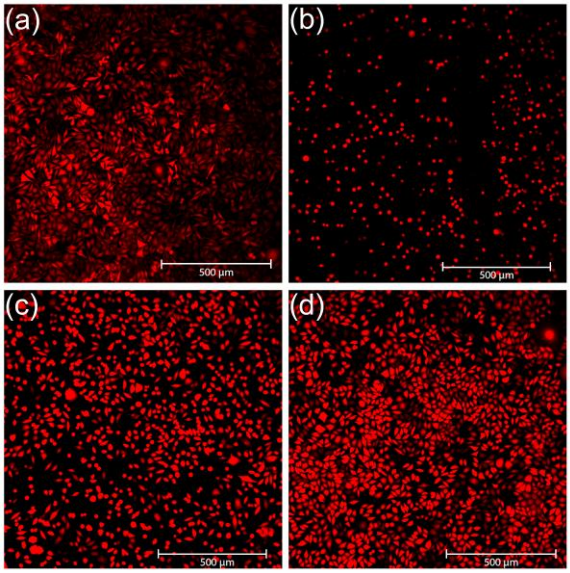

*Figure 40: Cells exposed to the acylstannane **26** in concentrations of a) 0 mM, b) 0.1 mM, c) 0.05 mM and d) 0.025 mM*

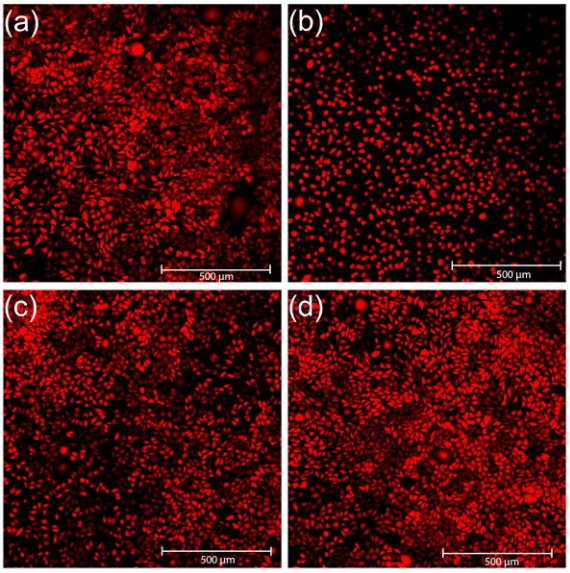

*Figure 41: UV cured cells exposed to the acylstannane **26** in concentrations of a) 0 mM, b) 0.1 mM, c) 0.05 mM and d) 0.025 mM*

3.2.8 Stability in aqueous media

All monomer mixtures in dental composites contain a certain amount of water. This is the reason for the importance of novel photoinitiators to provide sufficient stability in aqueous media (Scheme 98). Therefore, an evaluation of the stability of tetrakis(2,4,6-trimethylbenzoyl)stannane (**26**) in an aqueous environment was carried out using HPLC. For this purpose, 5 different solutions of **26** (A-E) were prepared initially.

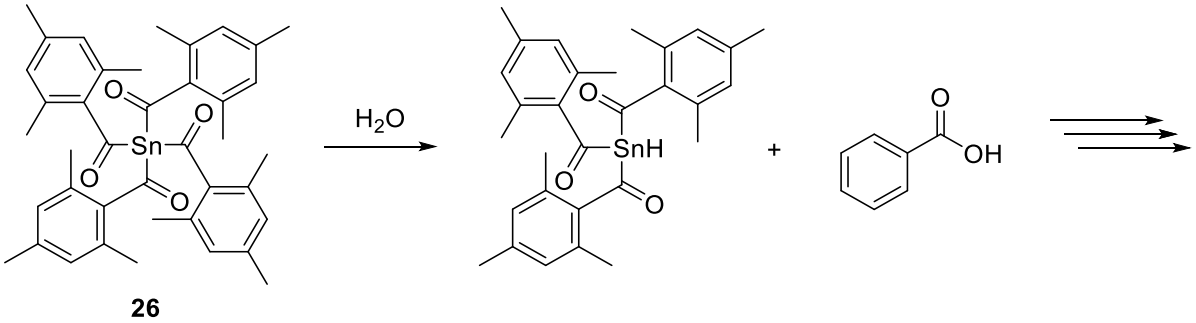

26

Scheme 98: Potential aqueous hydrolysis of tetrakis(2,4,6-trimethylbenzoyl)stannane

Solution A and B each contained 1wt% of photoinitiator **26** in dry acetonitrile, where solution A was purged with Argon and solution B was not. Solutions C-E each contained 0.5wt% of photoinitiator **26** and 10wt% of water. For solution D, a drop of conc. H_3PO_4 was added to simulate the acidic environment of aqueous primer formulations. To solution E, a drop of aqueous 1M NaOH was added to study the hydrolytic stability in basic conditions. For comparative purposes, the analogue solutions were prepared with the reference compounds Ivocerin®, tetrakis(2-methylbenzoyl)germane (K174) and Irgacure® 784.

The solutions E (basic) of all 3 initiators immediately formed a clearly visible precipitate, which is why these samples were not further used in the investigations. Regarding the solutions D (acidic), it was found that tetrakis(2,4,6-trimethylbenzoyl)stannane (**26**) and tetrakis(2-methylbenzoyl)germane (K174) also formed a precipitate upon dissolution of the initiators, which is why these were not further investigated. Thus, only solutions A-C were used for the HPLC experiments (Figure 42, Figure 43, Figure 44). The eluent was a mixture of 90% acetonitrile and 10% water, using a Reversed Phase C18 column (AppliChrom® OTU LipoMare) including a precolumn. Between the measurements, the samples were stored under exclusion of light and at RT.

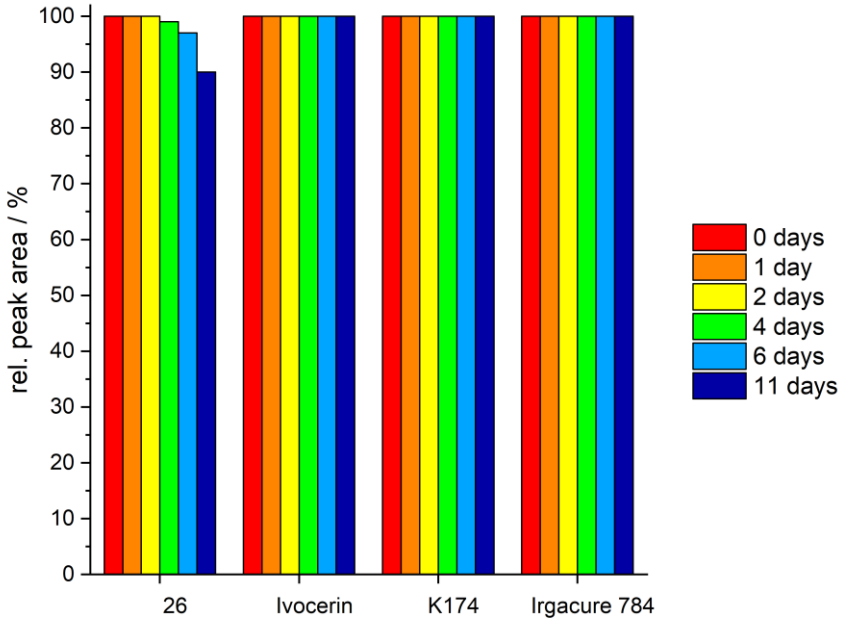

Figure 42: Stability evaluation in acetonitrile under air (solution A)

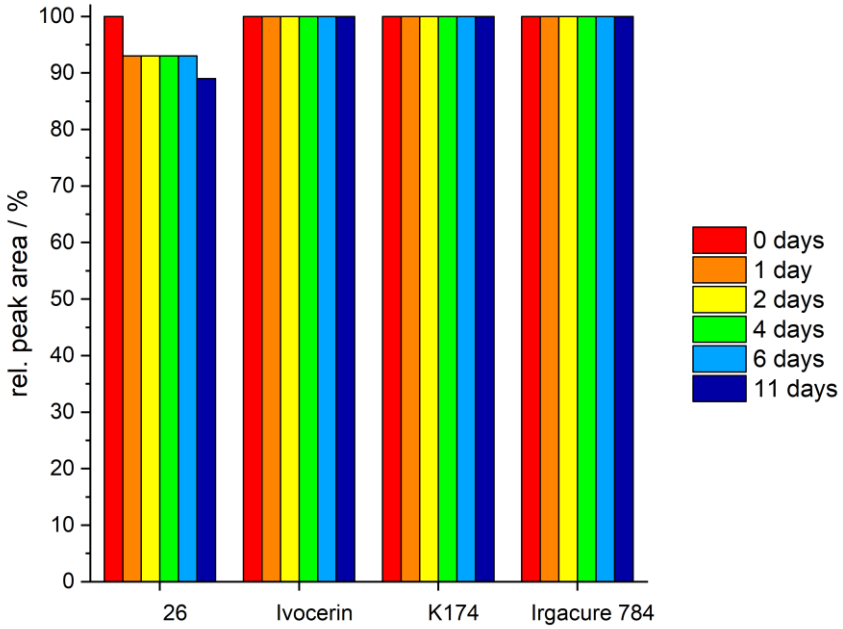

Figure 43: Stability evaluation in acetonitrile under argon (solution B)

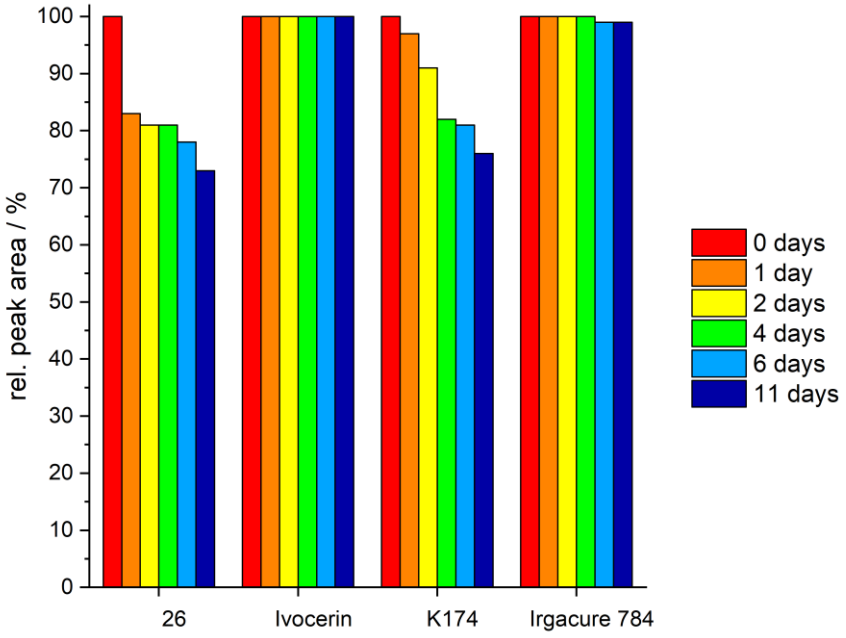

Figure 44: Stability evaluation in acetonitrile and water under air (solution C)

As the tests in pure acetonitrile (solution A and B) show, tetrakis(2,4,6-trimethylbenzoyl)stannane (**26**) provides a high stability in that environment. Especially under an inert gas atmosphere (solution A) almost no degradation of the product took place (97% residual concentration after 6 days). When stored under air (solution B), a residual concentration of 93% was obtained after 6 days. Solutions A and B of the reference initiators showed very high stability (100%). The results obtained for the solutions C (containing 10% of water) are different. Herein, the acylstannane **26** and tetrakis(2-methylbenzoyl)stannane (K174) clearly show rather fast decomposition, with Ivocerin® and Irgacure® 784 remaining stable. For both tetrakisacyl compounds (stannane **26** and germane K174), the residual concentration decreases to about 80% after 6 days. The question arises to what extent this hydrolytic cleavage can be prevented by storage at lower temperatures. Furthermore it has to be mentioned that a water content of 10% is already relatively high compared to the conditions in real formulations.

3.2.9 Storage stability

Since storage stability is a very important factor for the application of photoinitiators in dental composites, a corresponding evaluation should be carried out for tetrakis(2,4,6-trimethylbenzoyl)stannane (**26**) in addition to the evaluation on the hydrolytic stability (chapter 3.2.8). Photo-DSC was chosen in order to compare the heat of reaction of the same formulation resulting from the polymerization after defined intervals of storage time. Therefore, 14 different formulations in UDMA:D_3MA (1:1) were prepared and the type and the concentration of the stabilizer (BHT, TEMPO and MEHQ) as well as the storage temperature were varied (Table 5). Stabilizer-free formulations containing Ivocerin® were prepared for comparison.

*Table 5: Prepared formulations for storage stability evaluations of tetrakis(2,4,6-trimethylbenzoyl)stannane **26***

	Storage temperature °C	26 wt%	Ivocerin wt%	BHT ppm	TEMPO ppm	MEHQ ppm
1	RT	0.10	-	500	-	-
2	RT	0.10	-	1000	-	-
3	RT	0.10	-	-	50	-
4	RT	0.10	-	-	200	-
5	RT	0.10	-	-	-	-
6	50	0.10	-	500	-	-
7	50	0.10	-	1000	-	-
8	50	0.10	-	-	50	-
9	50	0.10	-	-	200	-
10	50	0.10	-	-	-	-
11	RT	-	0.06	-	-	-
12	50	-	0.06	-	-	-
13	RT	0.10	-	-	-	500
14	50	0.10	-	-	-	1000

The heat released in the polymerization of the formulations was measured using the Photo-DSC device at defined time intervals (0, 2, 7, 21, 120 days). The storage of the formulations between the measurements was carried out at room temperature and at 50°C under argon. As a radiation source, a 460 nm LED was used, for which the light intensity was 1 W cm^{-2} directly after the lens of the LED. After carrying out the experiments, the heat flow curve was integrated and the values obtained (in J g^{-1}) were compared to those of the initial measurement (t0).

When mixing the formulations containing MEHQ, it quickly became clear that MEHQ is not suitable as a stabilizer in this case. Both formulations (13 and 14) polymerized spontaneously upon dissolution of the components in the ultrasonic bath. This is most likely due to the much lower steric hindrance in close proximity to the hydroxy group in MEHQ compared to that of BHT (Scheme 99). Formulations 13 and 14 were therefore discarded and not used in the studies on storage stability.

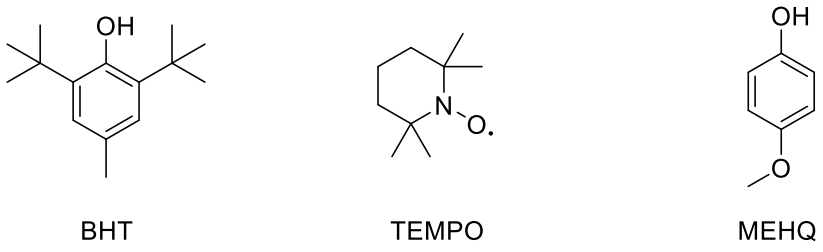

Scheme 99: Used stabilizers in the investigations on storage stability

The diagram below (Figure 45) shows the combined results for the storage stability evaluation of tetrakis(2,4,6-trimethylbenzoyl)stannane (**26**) in a methacrylate mixture of UDMA 1:1 D_3MA when stored at room temperature.

As can be seen from the figure below (Figure 45), the heat of reaction values obtained for the formulation containing the acylstannane **26** without any stabilizer drop to below 80% after 21 days of storage at RT. When BHT (butylhydroxytoluene) is added, however, values above 90% could be achieved. By using TEMPO improvements could be achieved as well. However,

after 120 days of storage polymerization was no longer initiated for the formulation with the acylstannane **26** without any stabilizer. The measured heat of polymerization of the stabilized formulations was significantly lower after 120 days than after 21 days. It was only about 50-70% of the initial value for the formulations containing BHT or TEMPO. The highest stability after 120 days could be obtained with 200 ppm of TEMPO (70% of the initial value).

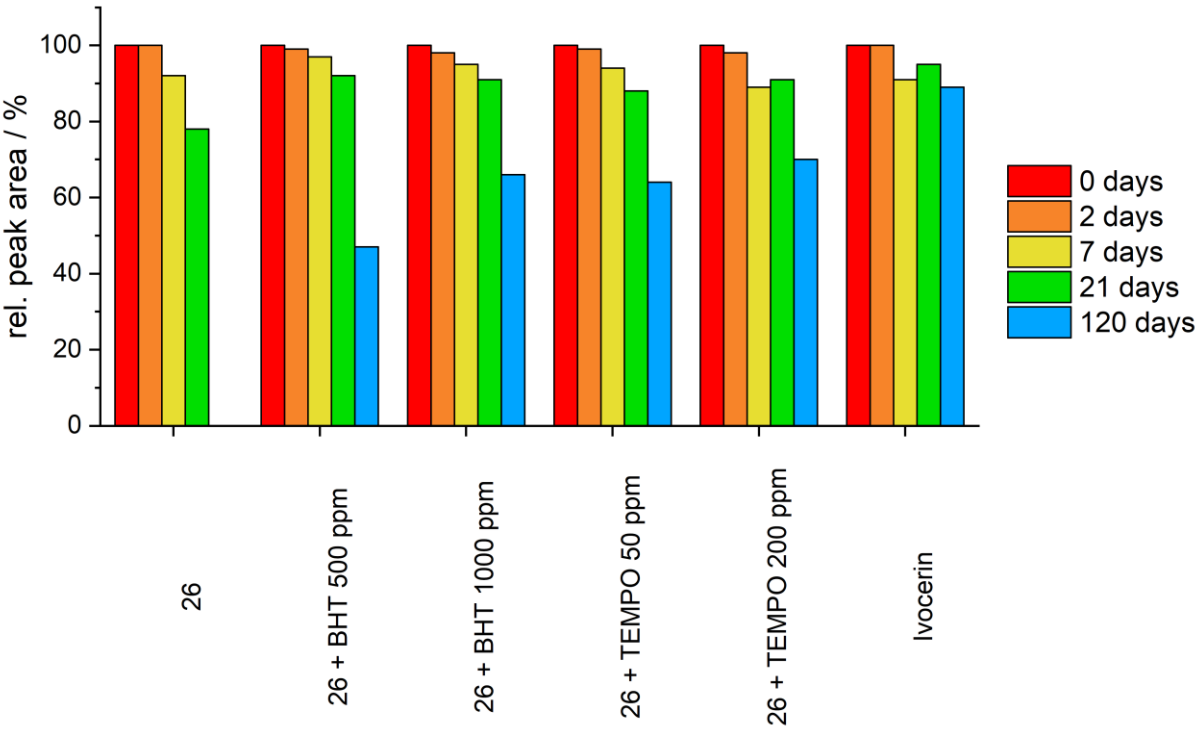

Figure 45: Obtained values for the formulations when stored at RT

When storing the formulation of the acylstannane **26** without stabilizer at 50°C (Figure 46**Fehler! Verweisquelle konnte nicht gefunden werden.**), the heat of polymerization after 21 days even dropped to about 60% of the initial value. Stabilization with BHT also led to significant improvements (values still > 90% after 21 days), with TEMPO bringing only a slight improvement at this storage temperature. When the formulations were stored at 50°C, the mixtures containing tetrakis(2,4,6-trimethylbenzoyl)stannane (**26**, whether stabilized or not) failed to undergo photopolymerization after 120 days of storage. Only the reference mixture containing Ivocerin® gave a similar exotherm as achieved in the beginning.

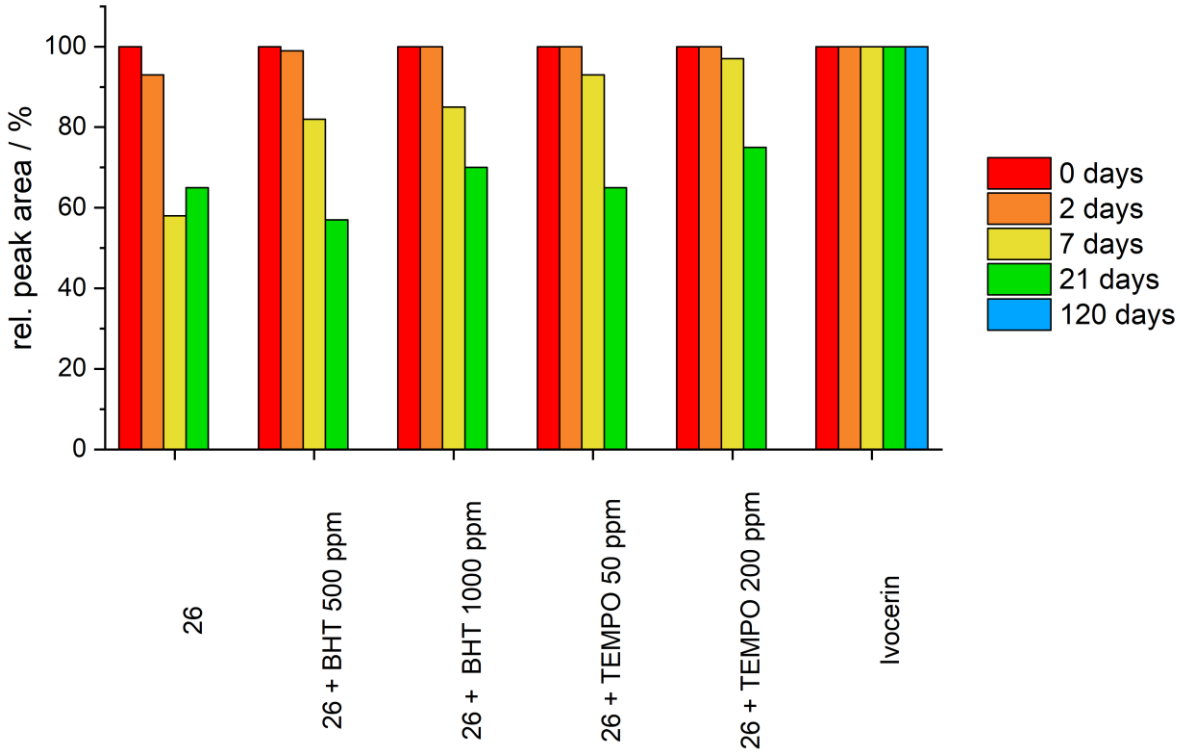

Figure 46: Obtained values for the formulations when stored at 50°C

In summary, when using tetrakis(2,4,6-trimethylbenzoyl)stannane (**26**) as a photoinitiator, a stabilizer such as BHT should be used, especially for longer storage times of the formulations. The storage temperature should be kept as low as possible in order to slow down decomposition reactions. For storage times of the formulations of over 4 months, acylstannane **26** is probably not suitable even at low temperatures, since the addition of stabilizer is not sufficient to completely avoid decomposition processes.

3.3 Recap

As described above, the synthesis of various tetrakisacylstannanes was attempted. In contrast to other derivatives, a viable synthetic route was developed only for tetrakis(2,4,6-trimethylbenzoyl)stannane (**26**), based on the methods described for the germanium analogues.[30] Furthermore, a feasible purification procedure could be established for this compound (chapter 3.1.7).[48]

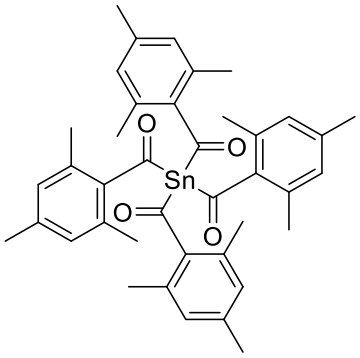

26

*Scheme 100: Tetrakis(2,4,6-trimethylbenzoyl)stannane (**26**)*

Subsequently, numerous experiments were carried out in order to investigate the potential of tetrakis(2,4,6-trimethylbenzoyl)stannane (**26**) as a Type I photoinitiator in dental composites. Extensive studies with the novel compound **26** were carried out in comparison to state of the art systems.[48] The tailout of the nπ* absorption band reached up to extraordinarily long wavelengths (up to 550 nm), which makes it unique within this type of compounds (chapter 3.2.1). These findings were also in line with computational calculations (chapter 3.2.2), carried out in cooperation with the Leibniz Institute of Surface Modification at Leipzig. Tetrakis(2,4,6-trimethylbenzoyl)stannane (**26**) showed very fast photobleaching in solution (chapter 3.2.3) as well as within the polymer network, similar to the monofunctional benzoyltriphenylstannane (**1**) (chapter 1.2.4). It showed very high reactivity compared to current state of the art PIs in methacrylate- and acrylate formulations (chapter 3.2.4). Unlike known acylgermanes, tetrakis(2,4,6-trimethylbenzoyl)stannane (**26**) was able to initiate

polymerization upon green light radiation (522 nm LED, 532 nm laser) leading to higher curing depths in filled systems (chapters 3.2.5 and 3.2.6), which is desirable for many industrial applications. Unlike many organotin compounds, the novel tetrakisacylstannane **26** as well as its photoproducts showed surprisingly low cytotoxicity, especially when compared to similar germanium compounds (chapter 3.2.7), as an evaluation in cooperation with the Institute of Materials Science and Technology at TU Wien showed. A weak point of tetrakis(2,4,6-trimethylbenzoyl)stannane (**26**) seems to be its storage stability, as shown in two different studies (chapters 3.2.8 and 3.2.9), however, improvements could be achieved by adding stabilizers.

All in all, tetrakis(2,4,6-trimethylbenzoyl)stannane (**26**) outperformed current state of the art systems in many ways. It offers great potential for applications, where long irradiation wavelengths are beneficial, such as the curing of highly filled systems in dental medicine.

4 Acylstannanones

Besides the studies concerning mono-, bis- and tetrakisacylstannanes, which are, in terms of their structure the exact analogues to the respective Si- and Ge-compounds, another path should be taken for the unheard-of compound class of acylstannanones (Scheme 101). In contrast to acylstannanes, these compounds contain an oxygen-atom, which is directly bound to the tin atom. This is expected to have an influence on the absorption properties as well as a potential cleavage process and the initiation itself.

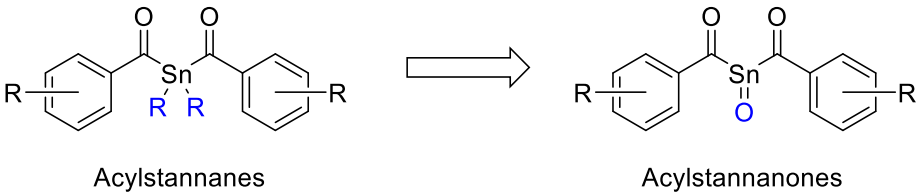

Scheme 101: Acylstannanones as a potential new class of Type I photoinitiators

4.1 Synthesis

A potential way to achieve the first acylstannanone compound could be the synthesis path described below (Scheme 102). The key compound in this route is dichlorotin oxide (**31**), which should be synthesized via bis(trimethylsilyl)peroxide (**30**). Similarly to the dithiane route (evaluated for the synthesis of bisacylstannanes already), dichlorotin oxide (**31**) could potentially be reacted with a lithiated dithiane to form the dithiane-protected stannanone **32**. In the last step, those protecting groups should be cleaved to restore the carbonyl functionalities and therefore obtain bisbenzoylstannanone (**33**).

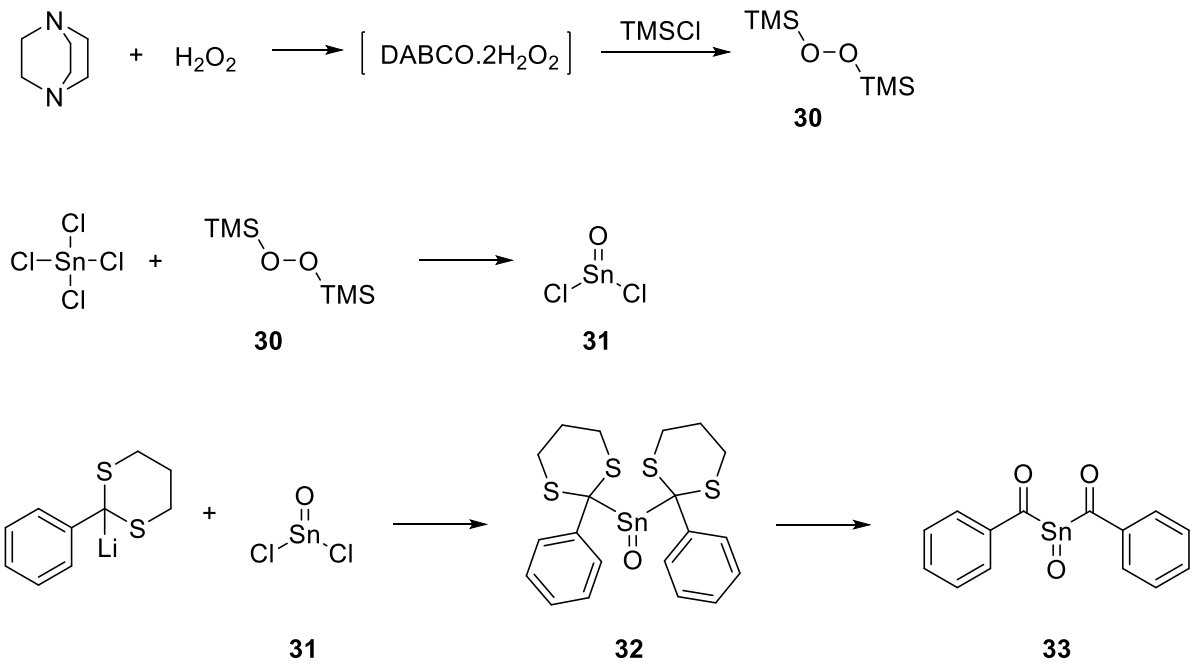

Scheme 102: Proposed synthetic path towards acylstannanones

If this synthesis route leads to a successful isolation of bisbenzoylstannanone (**33**), this compound should be the target of profound photochemical investigations regarding absorption properties, initiation activity as well as storage stability evaluation and solubility tests. In a second phase, biocompatibility should be examined as well.

Since all reactions involved moisture-sensitive compounds and some of those being probably light-sensitive in addition to that, all reactions, which demand certain measures concerning these issues were carried out in an orange light lab to exclude light with wavelengths below 520 nm and Schlenk techniques were used to secure complete exclusion of oxygen and moisture.

4.1.1 Synthesis of bis(trimethylsilyl)peroxide (30)

In the first step bis(trimethylsilyl) peroxide (**30**) should be prepared as this compound was needed for the synthesis of dichlorotin oxide (**31**). This was envisaged referring to a synthesis route published by Taddei and Ricci.[79] Starting from 1,4-diazabicyclo(2.2.2)octane (DABCO), a complex is formed with hydrogen peroxide, with which the desired peroxide **30** compound can subsequently be prepared.

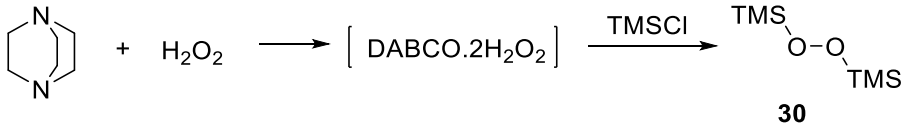

*Scheme 103: Synthesis of bis(trimethylsilyl)peroxide (**30**)*

For the synthesis of bis(trimethylsilyl)peroxide (**30**), 0.5 eq. of 1,4-diazabicyclo(2.2.2)octane (DABCO) were reacted with 1 eq. of hydrogen peroxide to form the DABCO.$2H_2O_2$ complex initially. The colorless solid was separated from the mixture via filtration and after drying in vacuo another 0.5 eq. of DABCO were added before dissolving the solids in dry dichloromethane and reacting them with 1.2 eq. of chlorotrimethylsilane. The byproduct DABCO hydrochloride was separated using filtration and the target compound **30** could be isolated as a colorless liquid after evaporation of the solvent in vacuo (93%). The structure was confirmed using NMR spectroscopy and used without any further purification in the following reaction steps.

4.1.2 Synthesis of dichlorotin oxide (31)

After successful synthesis of bis (trimethylsilyl) peroxide (**30**), this compound should subsequently be used for the synthesis of dichlorotin oxide (**31**). Very little literature on this compound is known, however a publication by Sakurada et al.[80] should be used to carry out the next step and synthesize dichlorotin oxide (**31**).

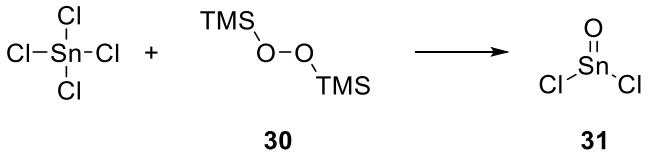

30 **31**

*Scheme 104: Synthesis of dichlorotin oxide (**31**)*

For the synthesis of dichlorotin oxide (**31**), 2.8 eq. of readily prepared bis(trimethylsilyl)peroxide (**30**) were reacted with 1 eq. of tetrachlorostannane. Gas formation was clearly visible before evaporating volatile components within the reaction mixture (solvent, excess peroxide, chlorine, hexamethyldisiloxane) directly through the Schlenk line giving product **31** as colorless crystalline solid (94%). The structure was confirmed using GC-MS an the substance was used without any further purification in the following reaction steps.

4.1.3 Synthesis of 2-phenyl-1,3-dithiane (34)

In order to synthesize the acylstannanone **33**, 2-phenyl-1,3-dithiane (**34**) needed to be synthesized as well to be reacted with the previously prepared dichlorotin oxide (**31**), subsequently. For that purpose, a synthesis route based on the described method by Kazahaya et al.[81] was envisaged.

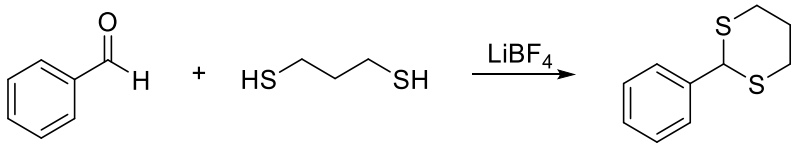

34

*Scheme 105: Synthesis of 2-phenyl-1,3-dithiane (**34**)*

For the synthesis of 2-phenyl-1,3-dithiane (**34**), 1.1. eq. of benzaldehyde and 1 eq. of 1,3-dimercaptopropane were reacted in the presence of 0.1 eq. of lithium tetrafluoroborate.

Aqueous workup and recrystallization from ethyl acetate gave the pure target compound **34** as colorless crystals (20). The structure was confirmed using NMR spectroscopy and used in the further steps without further purification.

4.1.4 Synthesis of bis(2-phenyl-1,3-dithian-2-yl)stannanone (32)

After all the required reactants could be synthesized successfully, the dithiane-protected compound bis(2-phenyl-1,3-dithian-2-yl)stannanone (**32**) should be prepared subsequently. This should be realized analogously to the synthesis route used for the synthesis of the bisacylgermanes (Corey-Seebach reaction) with dichlorotin oxide (**31**) instead of the corresponding diorganodichlorometal compounds (chapter 2.1.2).

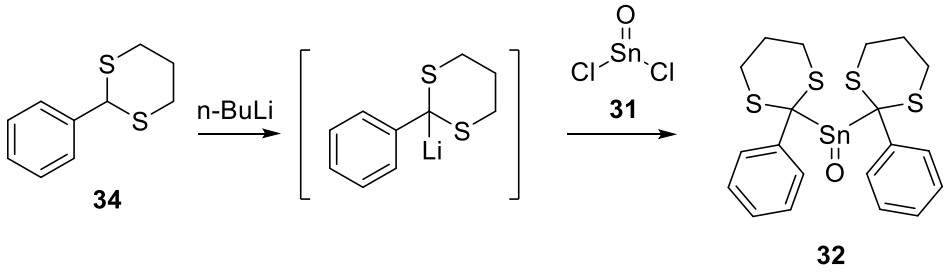

*Scheme 106: Synthesis of bis(2-phenyl-1,3-dithian-2-yl)stannanone (**32**)*

For the synthesis of bis(2-phenyl-1,3-dithian-2-yl)stannanone (**32**), 2.4 eq. of previously synthesized 2-phenyl-1,3-dithiane (**34**) were reacted with 2.6 eq. of n-butyllithium in dry THF to form the lithium intermediate, which was subsequently reacted with 1 eq. of previously synthesized dichlorotin oxide (**31**). Quenching of the reaction mixture with water led to the precipitation of the target compound **32** as colorless solid (34%). The structure was confirmed using NMR spectroscopy, LC-MS and HPLC.

4.1.5 Synthesis of bisbenzoylstannanone (33)

4.1.5.1 Dithiane deprotection using diacetoxyiodobenzene/$BF_3 \cdot OEt_2$

In the next step, analogous to the synthesis of the bisacylgermanes, the dithiane groups in bis(2-phenyl-1,3-dithian-2-yl)stannanone (**32**) should be cleaved off and thus the carbonyl functionalities should be introduced to obtain bisbenzoylstannanone (**33**). To carry out this step, several methods are known.[54, 55] In order to make the reaction conditions as gentle as possible, a method provided by Ivoclar Vivadent involving diacetoxyiodobenzene should be tested in the first place, since this route requires no water in the reaction medium and relatively low reaction temperatures can be applied.

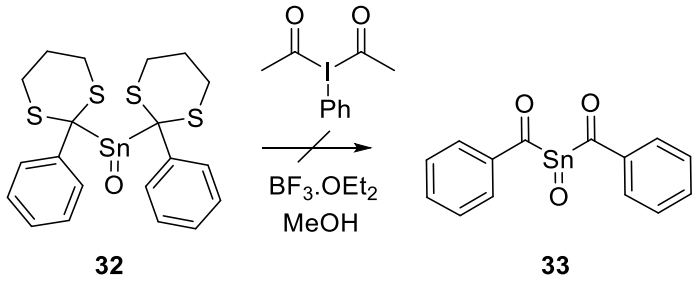

Scheme 107: Dithiane deprotection using diacetoxyiodobenzene/$BF_3 \cdot OEt_2$

For the synthesis of bisbenzoylstannanone (**33**), 4 eq. of diacetoxyiodobenzene and 4 eq. of boron trifluoride diethyl etherate were separated into 4 equally large portions. Then, 1 eq. of previously synthesized bis(2-phenyl-1,3-dithian-2-yl)stannanone (**32**) was weighed into a dry Schlenk tube and suspended in dry methanol. The first portions of diacetoxyiodobenzene and boron trifluoride diethyl etherate were added at RT and the mixture was stirred at that temperature. At intervals of 30 minutes, the remaining portions were added subsequently. The reaction mixture was protected from light using an aluminum foil and stirred overnight at RT. On the next day, the mixture was diluted with diethyl ether and filtrated through silica gel to get rid of the boron trifluoride complex and afterwards concentrated in vacuo. While doing so, an oily yellow phase was formed, which was then separated from the mixture and analyzed using NMR spectrocopy.

No ^{119}Sn-NMR signal could be obtained, but this was also the case for all other compounds containing an Sn=O bond (even after a significant increase in the relaxation time and the number of scans no signal was detectable). With the ^{1}H-NMR spectrum, iodobenzene could be identified as the major component in the mixture, but there were also other signals in the aromatic region that could come from a small amount of the target compound bisbenzoylstannanone (**33**). The supernatant methanolic solution was further concentrated and two more fractions of the yellow, oily phase could be obtained. By washing with various solvents such as n-pentane, ethanol and cyclohexane a separation of the components was attempted, however, further NMR studies after these steps showed that firstly no separation of iodobenzene could be achieved and secondly signals appeared over time, which suggested an increasing concentration of benzil. Attempts to separate the mixture using chromatography failed due to the large number of unknown components. Analysis by HPLC did not yield products with absorbance above 400 nm.

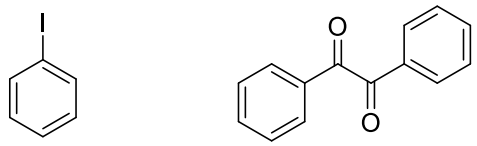

Scheme 108: Iodobenzene and benzil as main components in the reaction mixture

The presence of benzil might indicate that the product was formed (nevertheless in a very low yield), but decomposes rapidly.

4.1.5.2 Dithiane deprotection using $HgCl_2/CdCO_3$

Since the first method for cleaving off the dithiane protective groups did not lead to the desired result, another method, namely the one with mercuric chloride and cadmium carbonate should be tested.[55] To obtain more detailed information about the processes

occurring during the reaction, the reaction should be monitored by taking samples from the mixture and subsequent HPLC measurements (including UV-VIS detection).

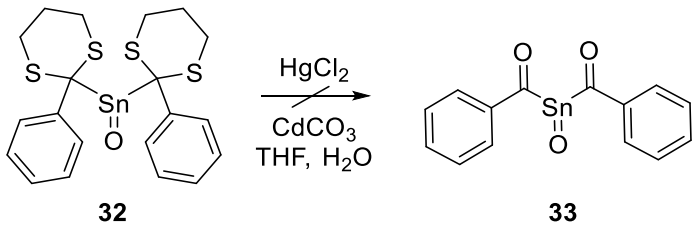

32 **33**

Scheme 109: Dithiane deprotection using $I_2/CaCO_3$

For the synthesis of bisbenzoylstannanone (**33**), 1 eq. of previously synthesized bis(2-phenyl-1,3-dithian-2-yl)stannanone (**32**) was weighed into a Schlenk tube together with 7 eq. of mercury chloride and 7 eq. of cadmium carbonate, suspended in a 8:1 mixture of THF and water and stirred at RT. Regarding the HPLC measurements, a first sample was taken at 0 h. The next sampling took place after 1 h and 3 h while stirring at RT. Since no significant decrease in the reactant peak was observed after this time, the reaction mixture was refluxed after 4 h of stirring at RT. Even after another hour at now elevated temperature hardly any change in the chromatogram could be detected, which is why the mixture was refluxed overnight. On the next day, the reactant peak had almost disappeared and instead, at least 2 other peaks appeared (reaction products A and B). The UV-VIS spectra of those peaks (retention times: 2.25 min and 2.55 min, rev. phase C_{18} – silica, MeCN 95:5 H_2O) are given below (Figure 47, Figure 48, Figure 49).

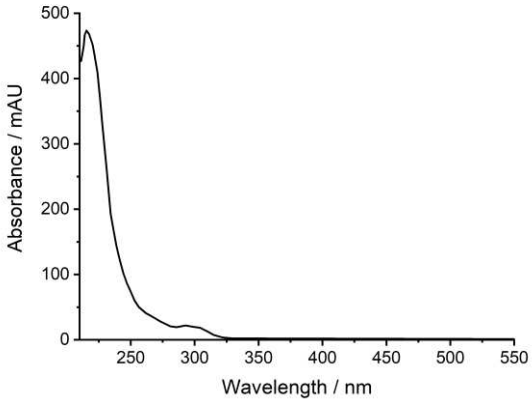

*Figure 47: UV-VIS spectrum (HPLC) of bis(2-phenyl-1,3-dithian-2-yl)stannanone (**32**)*

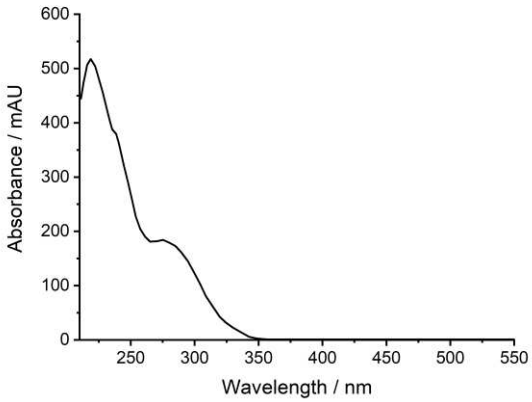

Figure 48: Spectrum (HPLC) of reaction product A

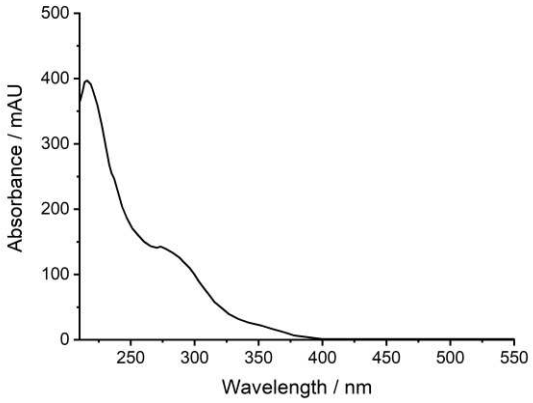

Figure 49: Spectrum (HPLC) of reaction product B

It can be assumed, that reaction products A and B are in fact the "onefold" and the "twofold" deprotected stannanone compounds (Scheme 110).

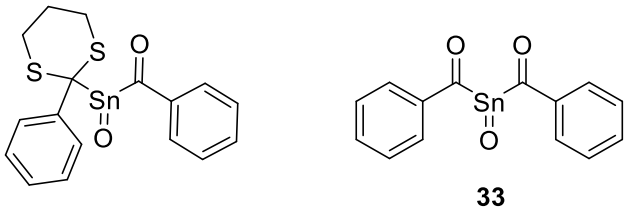

33

*Scheme 110: "Onefold" and "twofold" deprotected compound **33***

If this is the case, this means that an Sn=O bond in addition to the benzoyl chromophore by no means leads to a further bathochromic shift. Rather, the opposite is the case. The two detected compounds show absorption only to barely below 400 nm.

4.1.5.3 Dithiane deprotection using $I_2/CaCO_3$

In order to complete the evaluation of possible synthetic routes for acylstannanones, the third common cleavage method using iodine and calcium carbonate[54] should also be tested, although hardly any results other than those obtained by the other two methods are to be

expected. Monitoring the reaction by taking samples and HPLC measurements was carried out in a similar fashion as in the previous synthesis attempt.

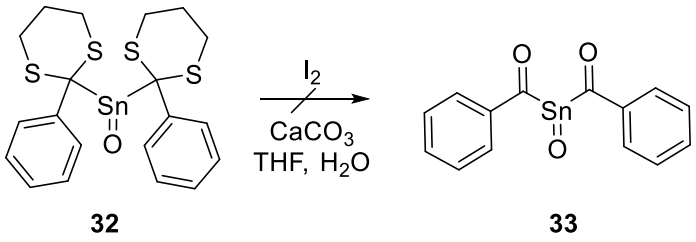

32 **33**

Scheme 111: Dithiane deprotection using I_2/$CaCO_3$

For the synthesis of bisbenzoylstannanone (**33**), 1 eq. of previously synthesized bis(2-phenyl-1,3-dithian-2-yl)stannanone (**32**) was weighed into a Schlenk tube together with 12 eq. of iodine and 12 eq. of calcium carbonate, suspended in a 8:1 mixture of THF and water and stirred at RT. Regarding the HPLC measurements, a first sample was taken at 0 h. The next sampling took place after 1 h and 3 h while stirring at RT. Since the peak height of the reactant bis(2-phenyl-1,3-dithian-2-yl)stannanone (**32**) had decreased a lot over time, but was still clearly visible, the reaction mixture was stirred overnight at RT for completion. The HPLC monitoring, which was continued on the next day did not lead to different findings than the ones acquired from the previous synthesis attempt. Nevertheless, the reaction mixture was worked up starting with a filtration over silica gel. Then, a saturated aqueous sodium dithionite solution was added until the solution changed its color from brown to slightly yellow. After diluting with diethyl ether and addition of water, the layers were separated. The aqueous layer was extracted twice with diethyl ether and the combined organic layers were evaporated to dryness in vacuo, giving a very small amount of a pale yellow solid, which showed the same HPLC peaks as the mixture obtained using the method involving mercury chloride. Benzil could be detected as well, confirming the potentially low stability, which was observed in the attempt involving diacetoxyiodobenzene already. In conclusion, either bisbenzoylstannanone (**33**) cannot be isolated from the synthetic routes tested or the compound has no satisfactory properties (absorption, stability) for the target application.

4.2 Recap

One goal of this work was the first-time synthesis of an acylstannanone compound and the comparison of its photochemical properties with the corresponding acylstannanes and -germanes. The first steps of the disposed synthetic route via dichlorotin oxide (**31**) was successful and the last intermediate bis(2-phenyl-1,3-dithian-2-yl)stannanone (**32**) could be prepared (chapter 4.1.4) rather easily. However, the final step (dithiane deprotection) turned out to be more complicated than expected. Several attempts were carried out to isolate the compound bisbenzoylstannanone (**33**, Scheme 112), but failed most probably due to stability issues. To investigate this reaction step in greater detail, reaction control via HPLC and UV/Vis detection was carried out. This strategy led to the conclusion, that the target compound **33** might be formed to some extent during the reaction of the reactant with mercury chloride, but the oxygen bound directly to the tin atom does not lead to a bathochromic shift of the nπ* transition band (chapter 4.1.5.2). Regarding this, the rather low stability and the potentially very difficult development of a viable purification procedure, no further effort was made towards a successful isolation of an acylstannanone.

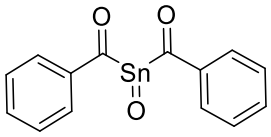

33

*Scheme 112: Targeted acylstannanone **33***

Summary

Recently, the scope of visible light-induced photopolymerization was largely expanded by the development of advanced applications like curing of dental composites or lithography-based ceramic manufacturing. To achieve sufficient curing depths in such highly filled systems, very reactive photoinitiators, which show absorption in the visible range are of great interest. The longer the wavelength of the light used for the curing of these systems, the higher curing depths can be achieved. Type II photoinitiators offer great potential regarding absorption around 500 nm, but suffer from lower photoinitiating activity due to the slower bimolecular mechanisms of radical formation and often reveal poor photobleaching properties. Current state of the art Type I initiators (e.g. acylgermanes) circumvent these problems, however usually show very low photoinitiating activity upon exposure with light of wavelengths close to and above 500 nm.

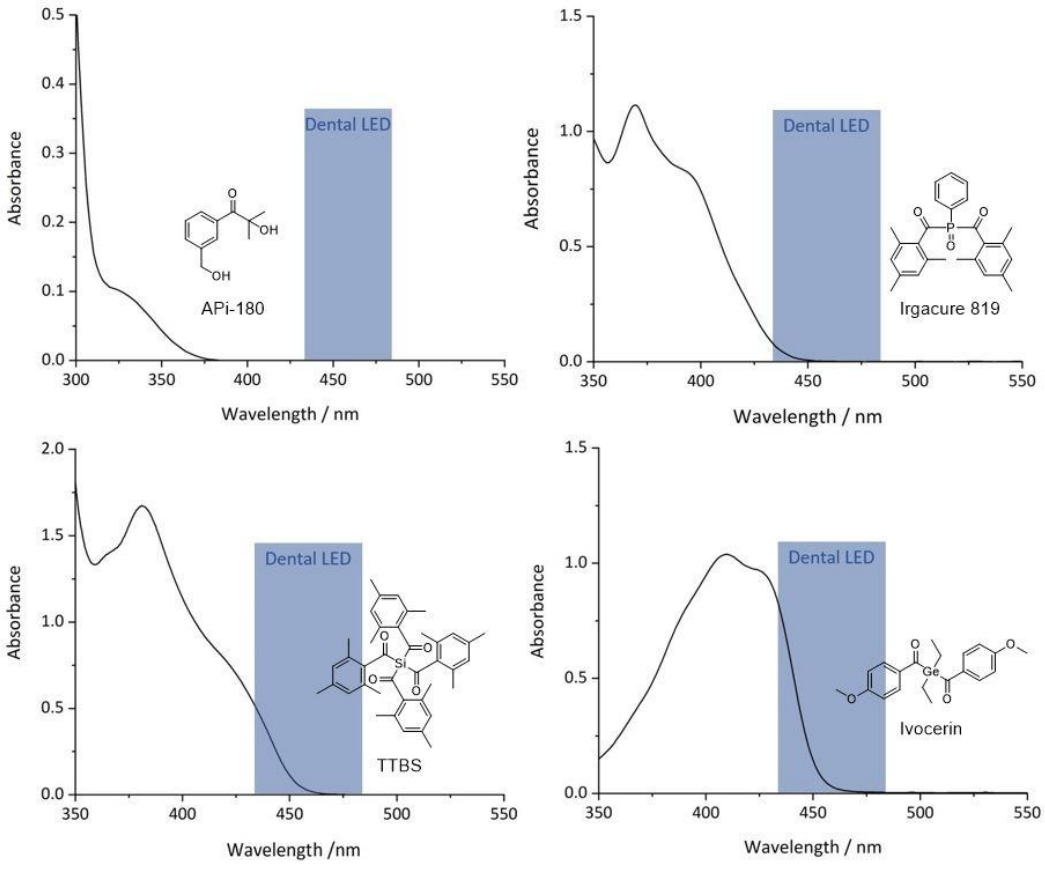

The goal of this work was the development of a novel Type I photoinitiator leading to improvements of the current state of the art in dental composites. To achieve this, the compound class of the acylstannanes was chosen to be targeted within this work. The potential bathochromic shift, caused by an overlap of the π and π* orbitals of the carbonyl group with the empty d orbitals of the tin atom led to the expectation, that the nπ*- transition in acylstannanes occurs above 450 nm. Thus, the scope of this dissertation was the synthesis and the photochemical characterization of mono-, bis- and tetrakisacylstannanes.

In order to synthesize monoacylstannanes **1**-**4** as potential visible light photoinitiators, two different synthetic pathways were tested (stannyl lithium route and hexaorganodistannane route). The stannyl lithium route (chapter 1.1.1) led to the successful preparation of benzoyltriphenylstannane (**1**), for which a suitable purification protocol could be developed. For mesitoyltriphenylstannane (**2**), a lower product yield was obtained using pathway A and the compound was not isolated in high purity. Using pathway B (chapter 1.1.2), the trimethyl derivatives benzoyltrimethylstannane (**3**) and mesitoyltrimethylstannane (**4**) could be prepared, however these compounds showed rather low stability and were therefore not isolated in high purity. Furthermore, pathway B was tested for the synthesis of benzoyltriphenylstannane (**1**), unsuccessfully though.

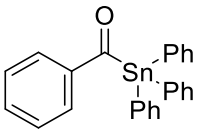

1

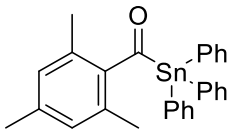

2

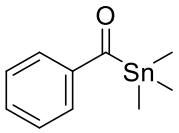

3

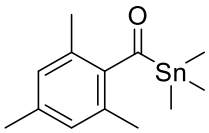

4

The synthesized monoacylstannanes **1**-**3** were then characterized regarding their photochemical properties. The nπ* absorption band of the benzoylstannanes **1** and **3** was clearly red-shifted compared to the germanium reference (chapter 1.2.1) and particularly benzoyltriphenylstannane (**1**) showed very high initiation activity in methacrylates (chapter 1.2.2). Investigations regarding the stability of the monoacylstannanes in aqueous media showed, that the introduction of a bulkier mesitoyl group instead of the benzoyl chromophore leads to increased stabilities (chapter 1.2.3). Additionally, steady state

photolysis experiments in solution were carried out to evaluate the photobleaching behavior of benzoyltriphenylstannane (**1**) in comparison to a monoacylgermane, in which the acylstannane **1** showed extraordinarily fast photobleaching (chapter 1.2.4). Overall, benzoyltriphenylstannane (**1**) was found to be superior to similar germanium compounds in many ways. Benefits like the easy and rather cheap synthesis as well as the red-shifted absorbance, the high reactivity and the very fast photobleaching make benzoyltriphenylstannane (**1**) a potential alternative in applications like the curing of dental fillings. Solely in terms of hydrolytic stability, improvements could be necessary to realize its usage in dental composites.

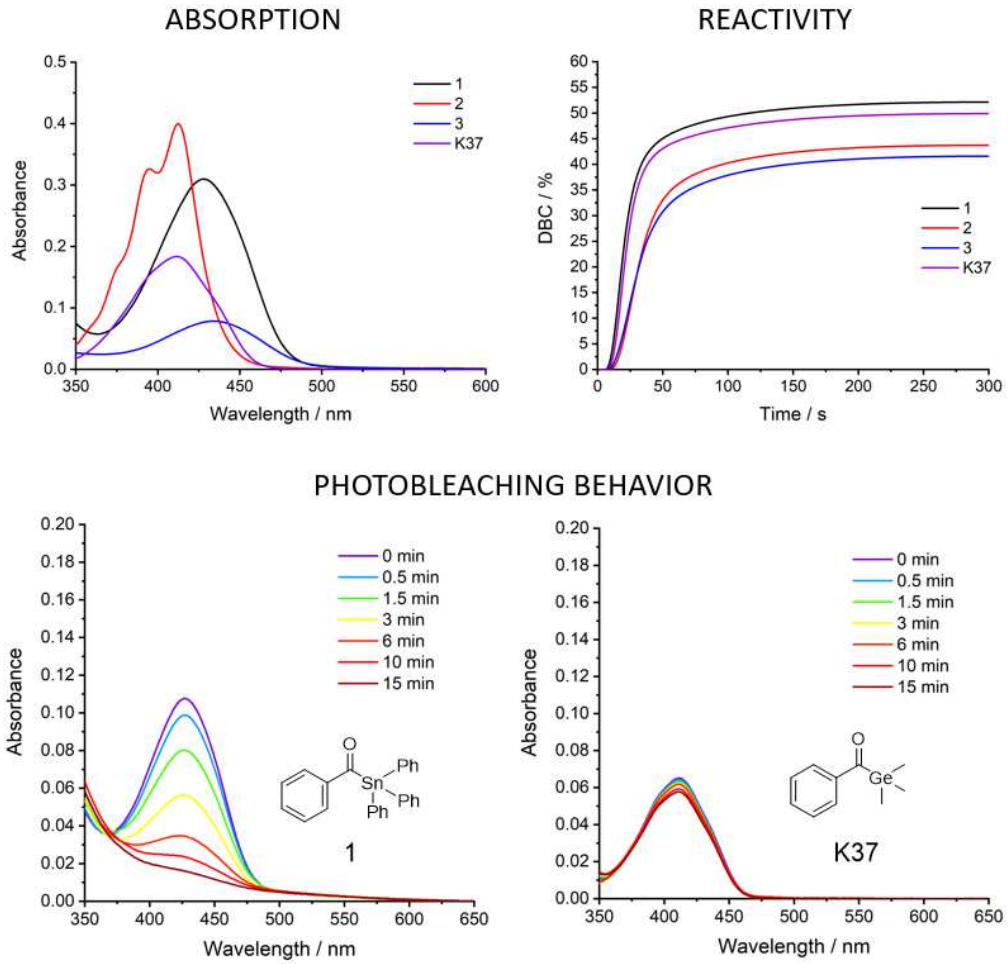

In order to synthesize bisacylstannanes, five different synthetic routes (pathways A-E) have been envisaged for these compounds within this work.

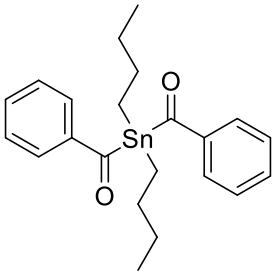

5

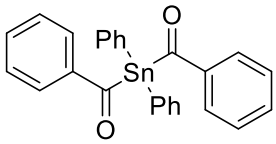

6

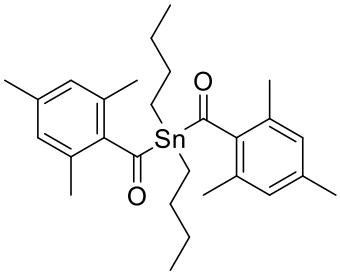

7

The stannyl dilithium route (pathway A) probably resulted in the formation of oligo- and polystannanes, preventing a successful isolation of the target compounds **5** and **6** (chapter 2.1.1). The dithiane route (pathway B) led to the finding, that the synthesis of the dithiane-protected stannyl intermediate was in fact possible, however the subsequent cleavage of these groups could not be carried out in the case of the stannanes (chapter 2.1.2) and therefore, the target compound **5** could not be isolated using pathway B either. This issue could be partly solved by using pathway C and the dioxane route. The final step of the synthesis, namely the cleavage of the dioxane groups could be carried out successfully and bisbenzoyldibutylstannane (**5**) could be obtained. However, even after numerous attempts, a viable purification procedure and the isolation of the pure product could not be achieved (chapter 2.1.3). Therefore, additional synthetic routes were envisaged, such as the diazo route (pathway D). The synthesis of bisacylstannanes however failed using this route, since the crucial intermediate bis(diazo(phenyl)methyl)dibutylstannane (**17**) could not be formed (chapter 2.1.4) from previously synthesized phenyldiazomethane (**15**). Similarly, the bromostannane route (pathway E) was unsuccessful due to the failed synthesis attempts of the four-fold brominated intermediate **21** (chapter 2.1.5). In summary, a viable synthetic protocol and a suitable purification procedure for the synthesis of bisacylstannanes has yet to be found. However, within this work, many different approaches were tested and valuable knowledge could be accumulated, facilitating potential future work on this class of compounds.

Subsequently, the synthesis of various tetrakisacylstannanes was attempted. In contrast to the other derivatives, a viable synthetic route was only developed for tetrakis(2,4,6-

trimethylbenzoyl)stannane (**26**). Furthermore, a feasible purification procedure could be established for this compound (chapter 3.1.7).

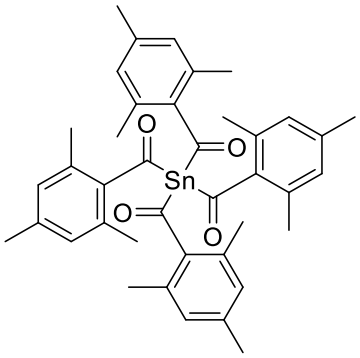

26

Thus, numerous experiments were carried out in order to investigate the potential of tetrakis(2,4,6-trimethylbenzoyl)stannane (**26**) as a Type I photoinitiator in dental composites.

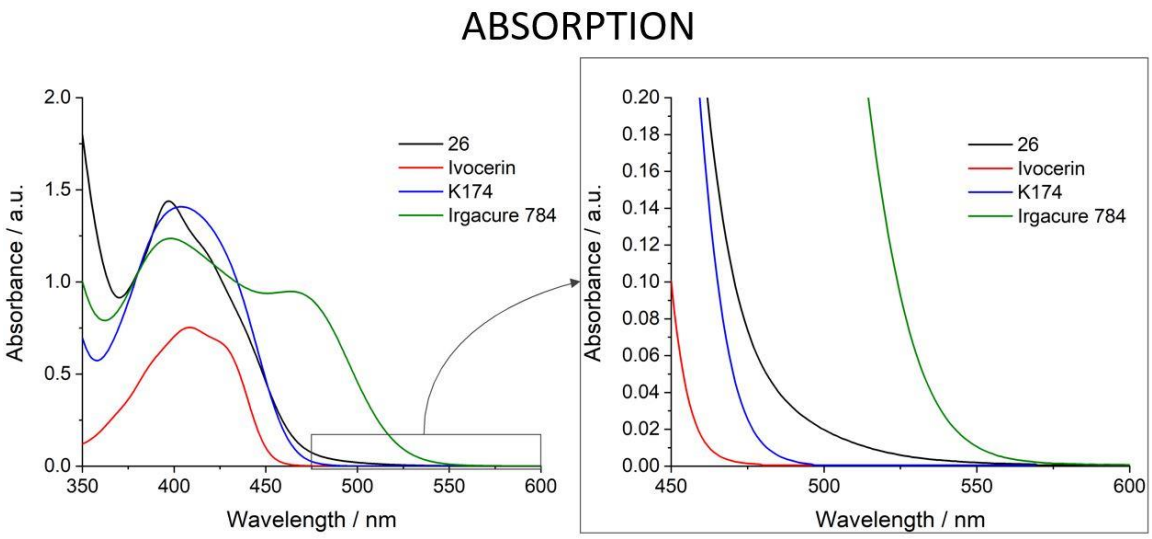

Extensive studies with compound **26** were carried out in comparison to state of the art systems. The tailout of the nπ* absorption band reached up to extraordinarily long wavelengths (up to 550 nm), which makes it unique within this type of compounds (chapter 3.2.1). These findings were also in line with computational calculations (chapter 3.2.2), carried out in cooperation with the Leibniz Institute of Surface Modification at Leipzig.

Tetrakis(2,4,6-trimethylbenzoyl)stannane (**26**) showed very fast photobleaching in solution (chapter 3.2.3) as well as within the polymer network, similar to the monofunctional benzoyltriphenylstannane (**1**) (chapter 1.2.4).

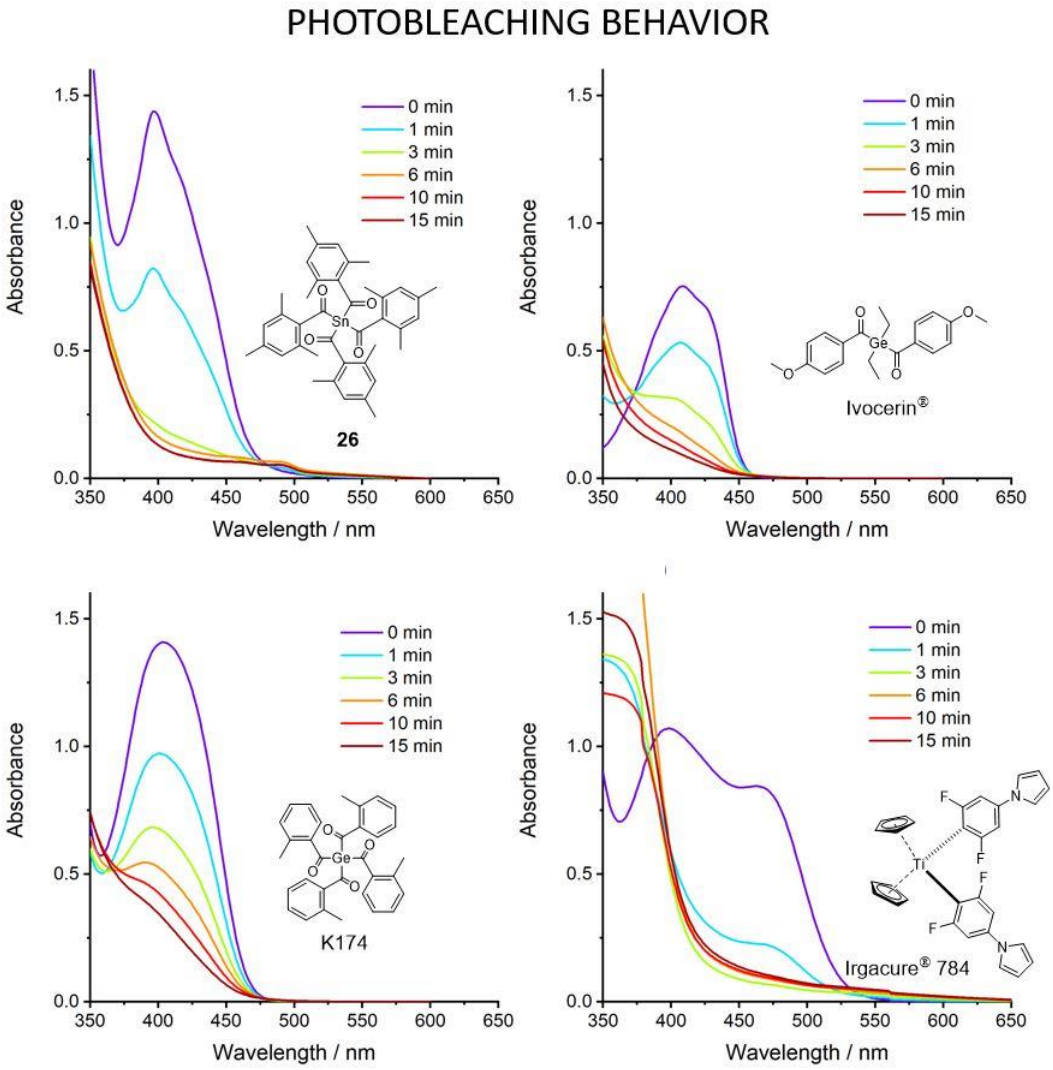

It showed very high reactivity compared to current state of the art PIs in methacrylate- and acrylate formulations (chapter 3.2.4). Unlike known acylgermanes, tetrakis(2,4,6-trimethylbenzoyl)stannane (**26**) was able to initiate polymerization upon green light radiation (522 nm LED, 532 nm laser) leading to higher curing depths in filled systems (chapters 3.2.5 and 3.2.6), which is desirable for many industrial applications. Unlike many organotin compounds, the novel tetrakisacylstannane **26** as well as its photoproducts showed

surprisingly low cytotoxicity, especially when compared to similar germanium compounds (chapter 3.2.7), as an evaluation in cooperation with the Institute of Materials Science and Technology at TU Wien showed.

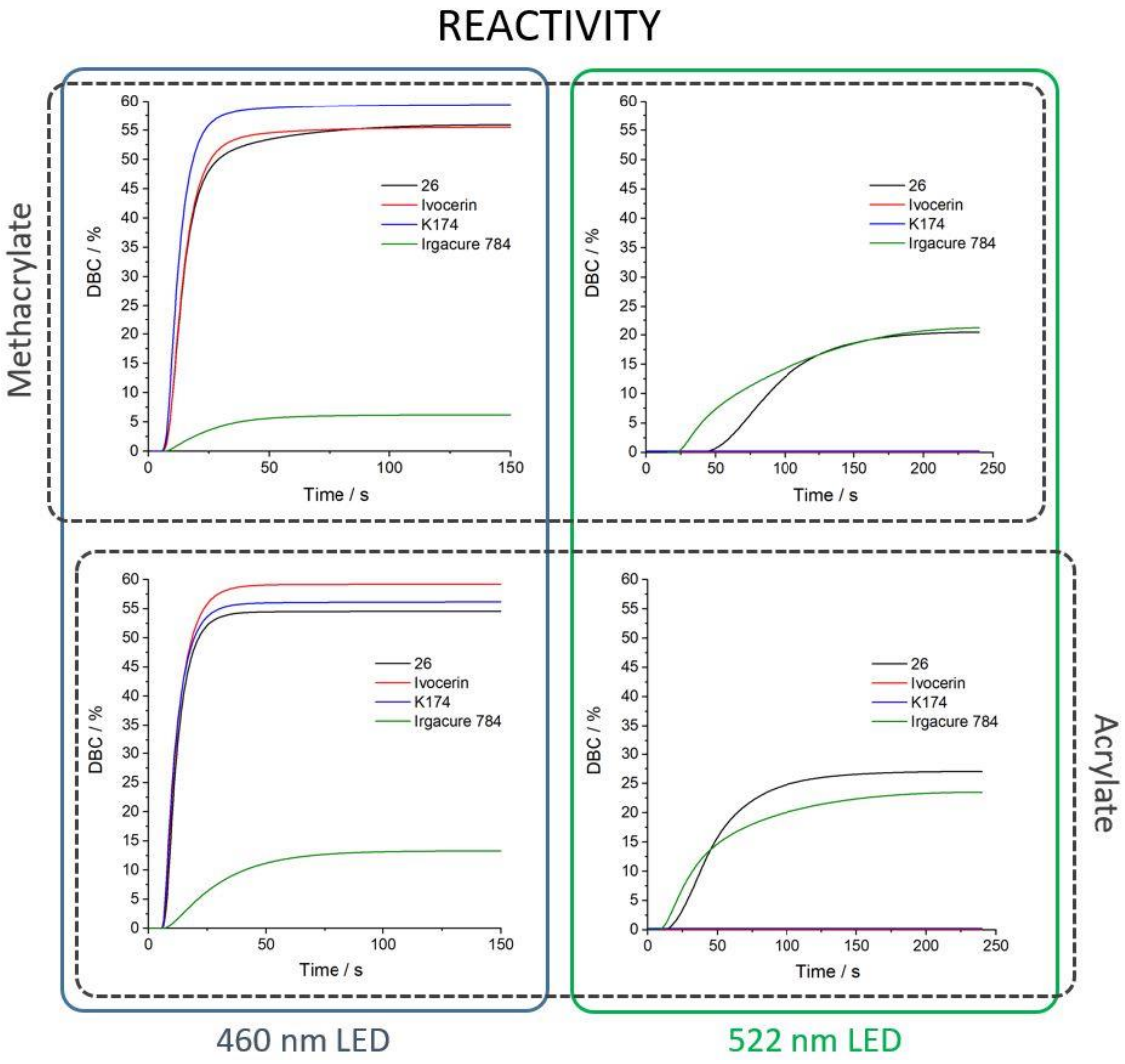

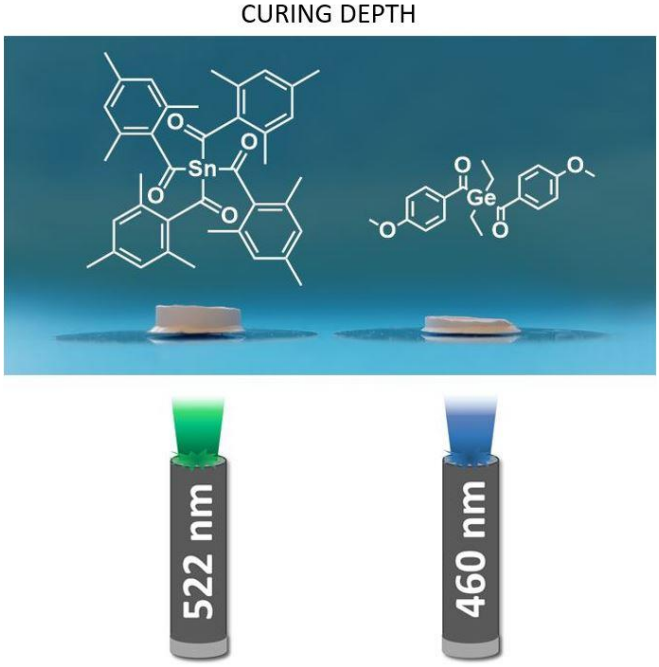

A weak point of tetrakis(2,4,6-trimethylbenzoyl)stannane (**26**) seems to be its storage stability, as shown in two different studies (chapters 3.2.8 and 3.2.9), however, improvements could be achieved by adding stabilizers. All in all, tetrakis(2,4,6-trimethylbenzoyl)stannane (**26**) outperformed current state of the art systems in many ways. It offers great potential for applications, where long irradiation wavelengths are beneficial, such as the curing of highly filled systems in dental medicine.

Besides the studies concerning mono-, bis- and tetrakisacylstannanes, another path should be taken for the unheard-of compound class of acylstannanones. In contrast to acylstannanes, these compounds contain an oxygen-atom, which is directly bound to the tin atom. This was expected to influence the absorption properties as well as the potential cleavage process and the initiation itself.

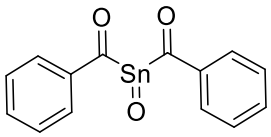

33

The first 3 synthesis steps towards an isolation of bisbenzoylstannanone (**33**) could be carried out successfully. The preparation of dichlorotin oxide (**31**) was successful and the last intermediate bis(2-phenyl-1,3-dithian-2-yl)stannanone (**32**) could be prepared (chapter 4.1.4) rather easily. However, the final step (dithiane deprotection) turned out to be more complicated than expected. Several attempts were carried out to isolate the compound bisbenzoylstannanone (**33**), but failed most probably due to stability issues. To investigate this reaction step in greater detail, reaction control via HPLC and UV/Vis detection was carried out. This strategy led to the conclusion, that the target compound **33** might be formed to some extent during the reaction of the reactant with mercury chloride, but the oxygen bound directly to the tin atom does not lead to a bathochromic shift of the nπ* transition band (chapter 4.1.5.2). Regarding this, the rather low stability and the potentially very difficult development of a viable purification procedure, no further effort was made towards a successful isolation of an acylstannanone.

Experimental section

1 Monoacylstannanes

1.1 Synthesis

1.1.1 Stannyl lithium route (Pathway A)

1.1.1.1 Synthesis of benzoyltriphenylstannane (1)

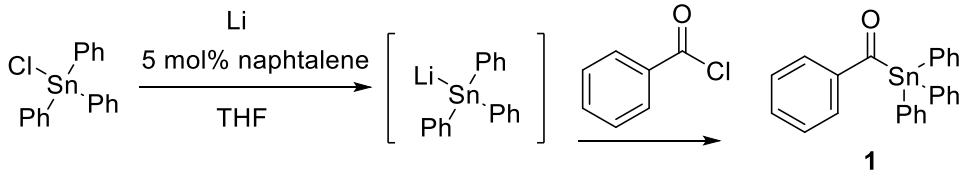

1

Compound	Equivalents	n [mmol]	m [g]	V [mL]
Chlorotriphenylstannane	1.00	4.39	1.69	
Lithium foil	3.00	13.18	0.09	
Benzoyl chloride	1.06	4.66		0.54
Naphtalene	0.05	0.22	0.03	

The reaction was carried out in an orange light lab to exclude light with wavelengths below 520 nm and Schlenk techniques were used to secure complete exclusion of oxygen and moisture. For the synthesis of benzoyltriphenylstannane (**1**), 1 eq. of chlorotriphenylstannane (1.69 g, 4.39 mmol) and 3 eq. of fine cut lithium foil (0.09 g, 13.18 mmol) were weighed into separate Schlenk tubes inside a glove box and 10 mL of dry THF was added to each of the reaction vessels. The Schlenk tubes were connected to a Schlenk line and 0.05 eq. of naphthalene (0.03g, 0.22 mmol) were added to the lithium suspension as a catalyst. The suspension was placed in an ultrasonic bath for 20 min at 20°C and then for another 30 min intensively stirred (RT), whereupon the suspension quickly turned dark. The solution of chlorotriphenylstannane was then added to the lithium suspension at RT over 20 min via syringe and the color of the mixture changed back to colorless. After stirring at RT for 4 h, another Schlenk tube was prepared, containing a solution of 1.06 eq. of benzoyl chloride (0.54 mL, 4.66 mmol) in 10 mL dry THF. Both mixtures were then cooled to -78°C and the stannyl lithium solution was then added to the acid chloride solution at that temperature over 20

min. After complete addition, the cooling bath was removed and the reaction mixture was allowed to reach RT under complete light exclusion. After stirring for 17 h at RT, the solvent was evaporated directly using the Schlenk line and a cooling trap. The residue was then taken up in 20 mL of dry n-pentane and filtrated under inert conditions. Afterwards, the solvent was evaporated from the filtrate and the product could be obtained as intensively yellow powder in high purity (1.25 g, 63% yield). The substance was stored under argon and light exclusion at 4°C.

mp.:	58°C
GC-MS (CH_2Cl_2):	m/z (rel.): 455 (M, 4%) ; 379 (6%) ; 351 (100%) ; 197 (44%) ; 120 (10%) ; 77 (10%)
^{1}H-NMR: δ_H (ppm, 400 MHz, $CDCl_3$):	7.82 – 7.28 (20H, m, Ar-**H**)
^{13}C-NMR: δ_C (ppm, 100 MHz, $CDCl_3$):	161.35 (C=O) ; 141.56 ; 137.24 ; 136.14 ; 135.11 ; 132.64 ; 128.31 ; 128.04 ; 127.82 ; 127.73 (C_{arom})
^{119}Sn-NMR: δ_{Sn} (ppm, 149 MHz, $CDCl_3$):	-217.74

1.1.1.2 Synthesis of mesitoyltriphenylstannane (2)

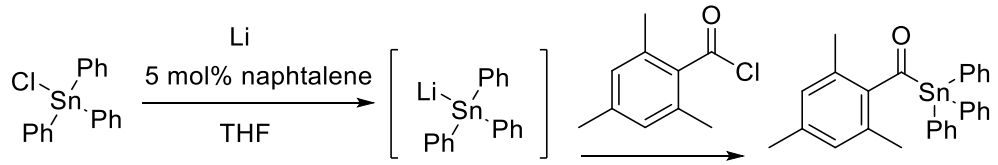

2

Compound	Equivalents	n [mmol]	m [g]	V [mL]
Chlorotriphenylstannane	1.00	2.01	0.78	
Lithium foil	3.00	6.03	0.04	
2,4,6-Trimethylbenzoyl chloride	1.06	2.13		0.36
Naphtalene	0.05	0.10	0.01	

The reaction was carried out in an orange light lab to exclude light with wavelengths below 520 nm and Schlenk techniques were used to secure complete exclusion of oxygen and moisture. For the synthesis of mesitoyltriphenylstannane (**2**), 1 eq. of chlorotriphenylstannane (0.78 g, 2.01 mmol) and 3 eq. of fine cut lithium foil (0.04 g, 6.03 mmol) were weighed into separate Schlenk tubes inside a glove box and 10 mL of dry THF was added to each of the reaction vessels. The Schlenk tubes were connected to a Schlenk line and 0.05 eq. of naphthalene (0.01 g, 0.10 mmol) were added to the lithium suspension as a catalyst. The suspension was placed in an ultrasonic bath for 20 min at 20°C and then for another 30 min intensively stirred (RT), whereupon the suspension quickly turned dark. The solution of chlorotriphenylstannane was then added to the lithium suspension at RT over 20 min via syringe and the color of the mixture changed back to colorless. After stirring at RT for 4 h, another Schlenk tube was prepared, containing a solution of 1.06 eq. of 2,4,6-trimethylbenzoyl chloride (0.36 mL, 2.13 mmol) in 10 mL dry THF. Both mixtures were then cooled to -78°C and the stannyl lithium solution was then added to the acid chloride solution at that temperature over 20 min. After complete addition, the cooling bath was removed and the reaction mixture was allowed to reach RT under complete light exclusion. After stirring for 17 h at RT, the solvent was evaporated directly using the Schlenk line and a cooling trap. The residue was then taken up in dry n-pentane and filtrated under inert conditions. Afterwards, the solvent was evaporated from the filtrate and the crude product could be obtained as intensively yellow sticky substance (0.68 g, 68% yield). The substance was stored under argon and light exclusion at 4°C.

^{1}H-NMR: δ_H (ppm, 400 MHz, C_6D_6): 7.69 – 7.53 (6H, m, Ar-**H**) ; 7.14 – 7.08 (9H, m, Ar-**H**) ; 6.48 (2H, s, Ar-**H**) ; 2.35 (6H, s, C**H**$_3$) ; 1.99 (3H, s, C**H**$_3$)

^{119}Sn-NMR: δ_{Sn} (ppm, 149 MHz, C_6D_6): -239.10

1.1.2 Hexaorganodistannane route (Pathway B)

1.1.2.1 Synthesis of benzoyltrimethylstannane (3)

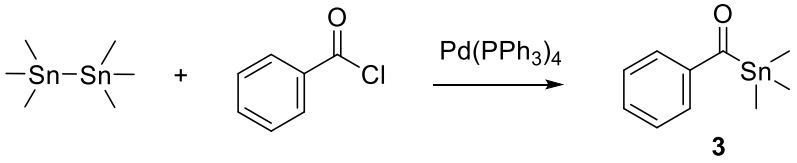

3

Compound	Equivalents	n [mmol]	m [g]	V [mL]
Hexamethyldistannane	1.00	3.72		0.78
Benzoyl chloride	1.00	3.72		0.43
Tetra(triphenylphosphine)palladium	0.05	0.19	0.22	

The reaction was carried out in an orange light lab to exclude light with wavelengths below 520 nm and Schlenk techniques were used to secure complete exclusion of oxygen and moisture. For the synthesis of benzoyltrimethylstannane (**3**), 1 eq. of hexamethyldistannane (0.78 mL, 3.72 mmol) as well as 0.05 eq. of palladium catalyst (0.22 g, 0.19 mmol) were weighed into a dry Schlenk tube within a Glove box and dissolved in 10 mL of dry THF. The Schlenk tube was then transferred to a Schlenk line and 1 eq. of benzoyl chloride (0.43 mL, 3.72 mmol) was added via syringe. The clear yellow solution was then heated to reflux and stirred for 16 h. On the next day, a dark brown solution was obtained, which was then filtrated through Al_2O_3. After washing with 25 mL of diethylether, the solvents were removed in vacuo. The yellow-orange oil (0.83 g, 83% yield) was confirmed to be the desired product using GC-MS and NMR spectroscopy, still showing small impurities. The compound was stored under argon in the freezer (-18°C) under complete exclusion of light.

GC-MS (CH_2Cl_2): m/z (rel.): 269 (M, 10%) ; 226 (14%), 165 (61%) ; 105 (100%)

^{1}H-NMR: δ_H (ppm, 400 MHz, C_6D_6): 7.14 – 6.89 (5H, m, Ar-**H**) ; 0.23 (9H, s, C**H**$_3$)

^{119}Sn-NMR: δ_{Sn} (ppm, 149 MHz, C_6D_6): -85.61

1.2 Characterization

1.2.1 UV/Vis spectroscopy

Benzoyltriphenylstannane (**1**), mesitoyltriphenylstannane (**2**), benzoyltrimethylstannane (**3**), mesitoyltrimethylstannane (**4**) and benzoyltrimethylgermane (K37) were dissolved in dry acetonitrile (c = 1 x 10-3 mol L^{-1}, 10 mL solutions each) under light protection (orange-light lab, excluding light with wavelengths below 520 nm). Directly afterwards, the samples were placed into quartz cuvettes (optical path length d = 10 mm) and the spectra were recorded, applying an acetonitrile background measurement. UV/Vis measurements were carried out using a Lambda 950 device from Perkin Elmer equipped with a PMT detector.

1.2.2 Photo-DSC

Photo-DSC experiments were carried out using a NETZSCH DSC 204 F1 setup with autosampler. As light sources either an Exfo OmniCure LX400 UV LED spot curing system (460 nm) was used. The intensity was adjusted to be 1 W cm^{-2} directly after the lens of the LED. The used monomer was a mixture of urethanedimethacrylate (UDMA) and decanedioldiacrylate (D_3MA) in a ratio of 1:1. A formulation containing 0.5wt% of the acylgermane K37 was prepared first and then equimolar solutions of the monoacylstannanes **1**-**3** were prepared. The photoinitiators were dissolved in the monomer using an ultrasonic bath with thermostat (30°C). During the preparation of the mixtures, light with wavelengths below 520 nm was excluded (orange light lab). For each experiment, two DSC pans were prepared from the same solution (double test). As a reference, a DSC pan filled with pure monomer solution was placed into the device. The double bond conversion (DBC) can be calculated from the peak area (ΔH [J mol^{-1}]) and the theoretical heat of polymerization of the monomer system ($\Delta H_{T,UDMA/D3MA}$ = 115 kJ mol^{-1}).[82] The maximum rate of polymerization R_p [mol L^{-1} s^{-1}] can be determined using the following equation containing h [mW mg^{-1}] (height

of the exothermic signal) and the densities of the used monomers ρ ($\rho_{UDMA/D3MA}$ = 1030 mg mL^{-1}).

1.2.3 Stability in aqueous media

Solutions of benzoyltriphenylstannane (**1**), mesitoyltriphenylstannane (**2**), benzoyltrimethylstannane (**3**) and benzoyltrimethylgermane (K37) were prepared in a 9:1 mixture of acetonitrile and water (c = 1 x 10^{-5} mol L^{-1}). Afterwards, HPLC measurements with UV/Vis detection were carried out after 0, 4, 7 and 11 days. In between. The samples were stored at room temperature under light exclusion. The obtained peak areas where referred to the peak area measured directly after dissolving (internal standard: acetylnaphtalene). HPLC measurements were carried out on a JASCO PU-2089 Plus quarternary gradient pump, a JASCO LC-Net II /ADC hardware interface and a JASCO AS-2057 Plus autosampler. The samples were run on a reversed phase fused silica column with a flow of 1 mL min^{-1} and a runtime of 30 min with 70% acetonitrile and 30% as eluent (gradient to 100% acetonitrile after 15 min). Detection was carried out with a PDA detector. The samples were dissolved in acetonitrile and filtered before analysis.

1.2.4 Steady state photolysis

Solutions of c_0 = 5 x 10^{-4} mol L^{-1} of benzoyltriphenylstannane (**1**) and benzoyltrimethylgermane (K37) in acetonitrile (40 mL) were transferred into a two-necked photoreactor. The solutions were degassed using argon for 20 minutes and then irradiated from below using a dental LED (Bluephase C 8, 430-490 nm). For irradiation, the mode "High Power" was selected, which corresponds to an intensity of 800 mW cm^{-2}. Within the flask directly behind the flask wall an "effective" intensity of 300 mW cm^{-2} was measured. The distance between dental LED and photoreactor was 4 mm. The reaction solution was then

irradiated while stirring at 500 rpm and samples (each 1.5 mL) were taken in a certain interval (0 min, 0.5 min, 1.5 min, 3 min, 6 min, 10 min, 15 min). For each sample, an UV/Vis spectrum was acquired using a Lambda 950 device from Perkin Elmer equipped with a PMT detector. Due to the experimental setup used, it is ensured, that almost all light is absorbed by the solution inside the photoreactor. Therefore, the different extinction coefficients should not have a significant influence on the photobleaching behavior.

2 Bisacylstannanes

2.1 Synthesis

2.1.2 Dithiane route (Pathway B)

2.1.2.1 Synthesis of dibutyldi(2-phenyl-1,3-dithian-2-yl)stannane (8)

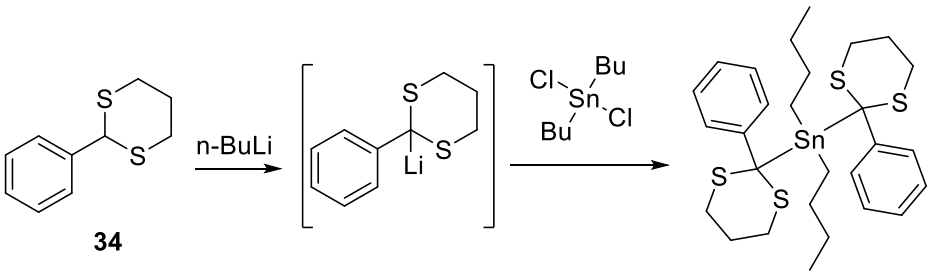

34 8

Compound	Equivalents	n [mmol]	m [g]	V [mL]
2-Phenyl-1,3-dithiane (**34**)	2.40	30.79	6.05	
n-Butyllithium (2.5 M solution in hexanes)	2.40	30.79		12.32
Dibutyldichlorostannane	1.00	12.83	3.90	

The reaction was carried out in an orange light lab to exclude light with wavelengths below 520 nm and Schlenk techniques were used to secure complete exclusion of oxygen and moisture. For the synthesis of dibutyldi(2-phenyl-1,3-dithian-2-yl)stannane (**8**), 2.4 eq. of 2-phenyl-1,3-dithiane (**34**, 6.05 g, 30.79 mmol) were weighed into a dry Schlenk tube and dissolved in 40 mL of dry THF. The solution was cooled to 0°C and 2.4 eq. of n-butyllithium (2.5 M in hexanes, 12.32 mL, 30.79 mmol) were added slowly via syringe and septum while stirring. The mixture was then stirred at that temperature for 2 h. In the meantime, 1 eq. of dibutyldichlorostannane (3.90 g, 12.83 mmol) was weighed into another Schlenk tube within a Glove box and dissolved in 20 mL of dry THF. This solution was then added to the organolithium solution at 0°C and the resulting mixture was stirred for further 3 h at that temperature. To complete the reaction, the mixture was put into the fridge overnight at 7°C. On the next day the reaction was quenched with water (100 mL) and diluted with ethyl acetate (40 mL). The layers were separated and the aqueous layer was extracted twice with ethyl acetate (30 mL each). The combined organic layers were washed twice with water (30

mL each) and with brine (30 mL), before being dried over sodium sulfate. Filtration and evaporation of the solvent in vacuo gave a colorless, viscous liquid, which was further dried in vacuo and dissolved in 10 mL of diethylether. After storing the recrystallization solution at - 18°C for 4 days, the target compound was obtained as colorless crystals (6.88 g, 86% yield). The product was stored in the fridge at 7°C under Argon and the structure was confirmed using NMR spectroscopy.

^{1}H-NMR: δ_H (ppm, 400 MHz, $CDCl_3$): 7.85 – 7.78 (4H, m, Ar-**H**) ; 7.25 – 7.17 (4H, m, Ar-**H**) ; 7.07 – 6.99 (2H, m, Ar-**H**) ; 2.75 (4H, m) ; 2.17 (4H, m) ; 2.09 (2H, m) ; 1.76 (2H, m) ; 1.35 (4H, m) ; 1.17 (4H, m) ; 1.07 (4H, m) ; 0.77 (6H, t, C**H**$_3$)

^{119}Sn-NMR: δ_{Sn} (ppm, 149 MHz, $CDCl_3$): -61.12

2.1.3 Dioxane route (Pathway C)

2.1.3.1 Synthesis of 2-phenyl-1,3-dioxane (9)

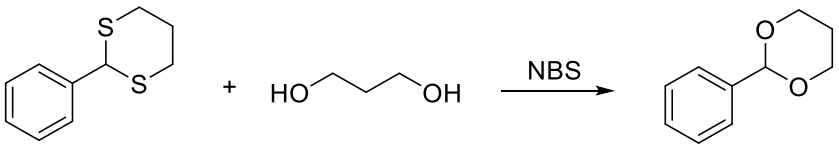

34 **9**

Compound	Equivalents	n [mmol]	m [g]	V [mL]
2-Phenyl-1,3-dithiane (**34**)	1.00	29.00	5.69	
1,3-Propanediol	3.00	86.97		6.30
N-Bromosuccinimide	1.00	29.00	5.16	

For the synthesis of 2-phenyl-1,3-dioxane (**9**), 1 eq. of 2-phenyl-1,3-dithiane (**34**, 5.69 g, 29.00 mmol) and 3 eq. of 1,3-propanediol (6.30 mL, 86.97 mmol) were dissolved in 60 mL of dry dichloromethane prior to adding 1 eq. of N-bromosuccinimide (5.16 g, 29.00 mmol) and

stirring for 15 min at RT. Completion of the reaction was checked using TLC. The mixture was then diluted with a 10% aqueous solution of NaOH (40 mL) and the layers were separated. The aqueous layer was extracted 3 times with dichloromethane (40 mL each) and the organic layers were washed with 10% aqueous NaOH (20 mL) and water (twice with 40 mL each). Afterwards the combined organic layers were dried over sodium sulfate, filtrated and the solvent was evaporated in vacuo. During the evaporation of the solvent, a small amount of colorless solid precipitated, which was removed in an additional filtration step. After doing so, the product could be obtained in high purity as colorless, crystalline substance (4.60 g, 97% yield).

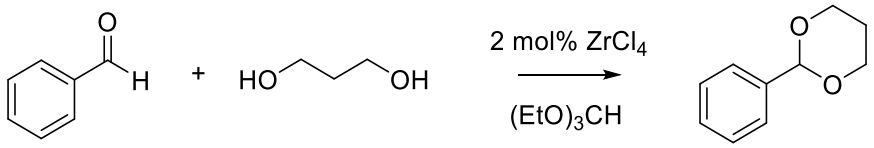

9

Compound	Equivalents	n [mmol]	m [g]	V [mL]
Benzaldehyde	1.00	60.90		6.16
1,3-Propanediol	1.50	91.35		6.56
Triethyl orthoformate	1.00	60.90		10.08
Zirconium tetrachloride	0.02	1.22	0.28	

For the synthesis of 2-phenyl-1,3-dioxane (**9**), 1 eq. of benzaldehyde (6.16 mL, 60.90 mmol), 1.5 eq. of 1,3-propanediol (6.56 mL, 91.35 mmol) and 1 eq. of triethyl orthoformate (10.08 mL, 60.90 mmol) were weighed in and dissolved in 100 mL of dry dichloromethane. Then, 0.02 eq. of solid zirconium tetrachloride (0.28 g, 1.22 mmol) were added at RT carefully and the mixture was stirred for 35 min at RT. Completion was checked via GC-MS and the mixture was quenched using cold 10% aqueous NaOH (150 mL). The layers were separated and the aqueous layer was extracted 3 times with dichloromethane (40 mL each). The combined organic layers were then washed with water (3 times with 40 mL each) and dried over sodium sulfate. After filtration and removal of the solvent in vacuo, excess benzaldehyde was

removed using high vacuum (50°C, 0.04 mbar). The product was obtained in high purity as a colorless, crystalline solid (9.9 g, 99% yield).

GC-MS (CH_2Cl_2): m/z (rel.): 163 (M, 82%) ; 105 (100%) ; 77 (52%)

^{1}H-NMR: δ_H (ppm, 400 MHz, C_6D_6): 7.71 – 7.66 (2H, m, Ar-**H**) ; 7.22 – 7.06 (3H, m, Ar-**H**) ; 5.34 (1H, s, RSC**H**SR) ; 3.92 – 3.85 (2H, m, propyl-**H**) ; 3.50 – 3.40 (2H, m, propyl-**H**) ; 2.58 – 2.39 (1H, m, propyl-**H**) ; 2.01 – 1.75 (1H, m, propyl-**H**)

IR (ATR, cm^{-1}): 2956, 2870, 1469, 1456, 1398, 1239, 1096, 988, 949, 909, 758, 699

2.1.3.2 Synthesis of dibutylbis(2-phenyl-1,3-dioxane-2-yl)stannane (10)

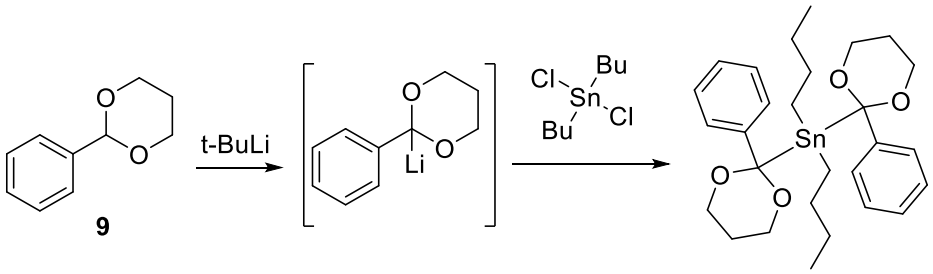

9 **10**

Compound	Equivalents	n [mmol]	m [g]	V [mL]
2-Phenyl-1,3-dioxane (**9**)	2.40	8.58	1.41	
Dibutyldichlorostannane	1.00	3.58	1.09	
t-Butyllithium (1.7 M in n-pentane)	2.50	8.94		5.26

The reaction was carried out in an orange light lab to exclude light with wavelengths below 520 nm and Schlenk techniques were used to secure complete exclusion of oxygen and moisture. For the synthesis of dibutyldi(2-phenyl-1,3-dioxane-2-yl)stannane (**10**), 2.4 eq. of previously synthesized 2-phenyl-1,3-dioxane (**9**, 1.41 g, 8.58 mmol) and 1 eq. of dibutyldichlorostannane (1.09 g, 3.58 mmol) were weighed into two separate Schlenk tubes within a Glove box and each compound was dissolved in 20 mL of a mixture of THF and n-pentane (5:2) each. Afterwards, the dioxane solution was cooled to -42°C and 2.5 eq. of t-butyllithium (1.7 M in pentane, 5.26 mL, 8.94 mmol) were added over the period of 15 min at that temperature resulting in a color change to red. The mixture was then stirred for 45 min at -42°C before being cooled to -79°C. At that temperature, the dibutyldichlorostannane solution was added over 15 min (decoloration). The reaction mixture was stirred for 1 h at that temperature before removing the cooling bath and stirring for another hour. Subsequently, the mixture was diluted with 50 mL of diethyl ether and quenched with 5% aqueous $NaHCO_3$ solution (50 mL). The layers were separated, the aqueous layer was extracted three times with diethyl ether (25 mL each) and the combined organic layers were washed with water (3 times with 25 mL each). After drying over sodium sulfate and filtration, the solvent was evaporated in vacuo. To remove a large part of excess 2-phenyl-1,3-dioxane, a flash column (Al_2O_3, PE 3:1 Et_2O) was used. By doing so, the product could be isolated as a colorless oil (0.51 g, 25% yield), however the contamination in form of 2-phenyl-1,3-dioxane could not be removed entirely after various attempts.

R_f (Al_2O_3, PE 3:1 Et_2O): 0.6

^{1}H-NMR: δ_H (ppm, 400 MHz, C_6D_6): 7.68 – 7.62 (4H, m, Ar-**H**) ; 7.36 – 7.29 (4H, m, Ar-**H**) ; 7.15 – 7.09 (2H, m, Ar-**H**) ; 3.92 – 3.84 (4H, m) ; 1.80 – 1.71 (2H, m) ; 1.60 – 1.50 (4H, m) ; 1.42 – 1.31 (6H, m) ; 1.28 – 1.20 (2H, m) ; 1.15 – 1.01 (6H, m) ; 0.97 (6H, t, C**H**$_3$)

^{119}Sn-NMR: δ_{Sn} (ppm, 149 MHz, C_6D_6): -75.09

2.1.3.4 Synthesis of diphenylbis(2-phenyl-1,3-dioxane-2-yl)stannane (11)

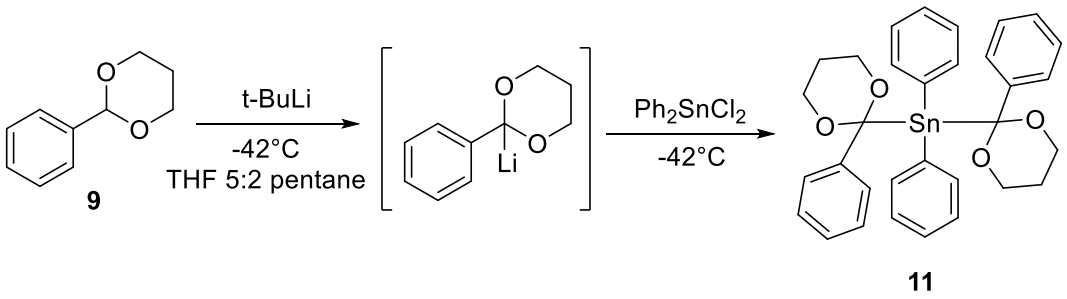

Compound	Equivalents	n [mmol]	m [g]	V [mL]
2-Phenyl-1,3-dioxane (**9**)	2.40	8.01	1.32	
Diphenyldichlorostannane	1.00	3.34	1.15	
t-Butyllithium (1.7 M in n-pentane)	2.50	8.34		4.91

The reaction was carried out in an orange light lab to exclude light with wavelengths below 520 nm and Schlenk techniques were used to secure complete exclusion of oxygen and moisture. For the synthesis of diphenyldi(2-phenyl-1,3-dioxane-2-yl)stannane (**11**), 2.4 eq. of previously synthesized 2-phenyl-1,3-dioxane (**9**, 1.32 g, 8.01 mmol) and 1 eq. of diphenyldichlorostannane (1.15 g, 3.34 mmol) were weighed into two separate Schlenk tubes within a Glove box and dissolved in 20 mL of a mixture of THF and n-pentane (5:2) each. Afterwards, the dioxane solution was cooled to - 42°C and 2.5 eq. of t-butyllithium (1.7 M in pentane, 4.91 mL, 8.34 mmol) were added over the period of 15 min at that temperature resulting in a color change to red. The mixture was then stirred for 45 min at -42°C. At that temperature, the diphenyldichlorostannane solution was added over 15 min (decoloration). The reaction mixture was stirred for 2 h at that temperature before removing the cooling bath and stirring overnight. On the next day, a fluffy, colorless precipitate had formed, which was separated from the reaction mixture using filtration under inert conditions. Evaporation of the solvent from the filtrate gave the crude product as a colorless solid. To remove a large part of excess 2-phenyl-1,3-dioxane as well as lithium chloride, a flash column (Al_2O_3, PE 2:1 THF) was used. By doing so, the product could be isolated as a colorless solid (0.80 g, 40% yield), however the contamination in form of 2-phenyl-1,3-dioxane could not be removed entirely after various attempts.

R_f (Al_2O_3, PE 2:1 THF): 0.9

^{1}H-NMR: δ_H (ppm, 400 MHz, THF-d_8): 7.17 – 6.93 (20H, m, Ar-**H**) ; 4.21 – 4.07 (8H, m) ; 2.06 – 1.95 (2H, m) ; 1.68 – 1.62 (2H, m)

^{119}Sn-NMR: δ_{Sn} (ppm, 149 MHz, THF-d_8): -170.52

2.1.3.6 Synthesis of 2-mesityl-1,3-dioxane (12)

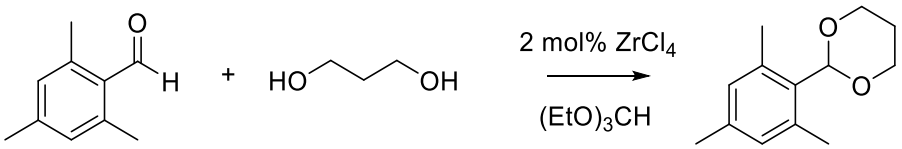

12

Compound	Equivalents	n [mmol]	m [g]	V [mL]
2,4,6-Trimethylbenzaldehyde	1.00	24.24		3.42
1,3-Propanediol	1.50	36.36		2.61
Triethyl orthoformate	1.00	24.24		4.01
Zirconium tetrachloride	0.02	0.49	0.11	

For the synthesis of 2-mesityl-1,3-dioxane, 1 eq. of 2,4,6-trimethylbenzaldehyde (3.42 mL, 24.24 mmol), 1.5 eq. of 1,3-propanediol (2.61 mL, 36.36 mmol) and 1 eq. of triethyl orthoformate (4.01 mL, 24.24 mmol) were weighed in and dissolved in 35 mL of dry dichloromethane. Then, 0.02 eq. of solid zirconium tetrachloride (0.11 g, 0.49 mmol) were added at RT carefully and the mixture was stirred overnight at RT. On the next day, completion was checked via GC-MS and the mixture was quenched using cold 10% aqueous NaOH (70 mL). The layers were separated and the aqueous layer was extracted 3 times with dichloromethane (40 mL each). The combined organic layers were then washed with water (3 times with 40 mL each) and dried over sodium sulfate. Filtration and evaporation of the

solvent led to the crude product in form of a colorless solid, which was then purified via recrystallization from n-pentane (4.25 g, 85% yield).

GC-MS (CH_2Cl_2): m/z (rel.): 206 (M, 61%) ; 191 (23%) ; 148 (100%) ; 119 (17%)

^{1}H-NMR: δ_H (ppm, 400 MHz, C_6D_6): 6.75 (2H, s, Ar-**H**) ; 5.80 (1H, s, C**H**) ; 3.92 (2H, m, C**H**2) ; 3.48 (2H, m, C**H**$_2$) ; 2.57 (6H, s, Ar-C**H**$_3$) ; 2.10 (3H, s, Ar-C**H**$_3$) ; 1.90 (1H, m, C**H**$_2$) ; 0.72 (1H, m, C**H**$_2$)

2.1.4 Diazo route (Pathway D)

2.1.4.1 Synthesis of benzaldehyde tosylhydrazone (14)

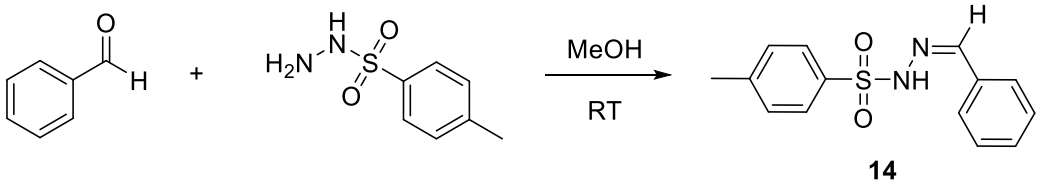

14

Compound	Equivalents	n [mmol]	m [g]	V [mL]
Benzaldehyde	1.00	16.93		1.73
Tosyl hydrazide	1.10	18.62	3.47	

Schlenk techniques were used to secure complete exclusion of oxygen and moisture. For the synthesis of benzaldehyde tosylhydrazone (**14**), 1.1 eq. of tosyl hydrazide (3.47 g, 18.62 mmol) were weighed into a dry Schlenk tube within a Glove Box and dissolved in 40 mL of dry methanol. The reaction vessel was then transferred to a Schlenk line and 1 eq. of benzaldehyde (1.73 mL, 16.93 mmol) was added at RT over 10 min. Afterwards the mixture was stirred for 2 h at RT and stored overnight in the freezer at -18°C. On the next day, the product in the form of colorless crystals was obtained via filtration and washing with a small

amount of cold methanol. The filtrate solution was then concentrated and another fraction of product could be obtained. The colorless crystals (3.60 g, 78% yield) were dried in vacuo and were then stored at -18°C under Argon.

^{1}H-NMR: δ_H (ppm, 400 MHz, C_6D_6): 2.41 (3H, s, Ar-C**H**$_3$) ; 7.29 – 7.41 (5H, m, Ar-**H**) ; 7.54 – 7.61 (2H, d, Ar-**H**) ; 7.76 (1H, s, C**H**=N) ; 7.84 (1H, br., N**H**) ; 7.85 – 7.90 (2H, d, Ar-**H**)

2.1.4.2 Synthesis of phenyldiazomethane (15)

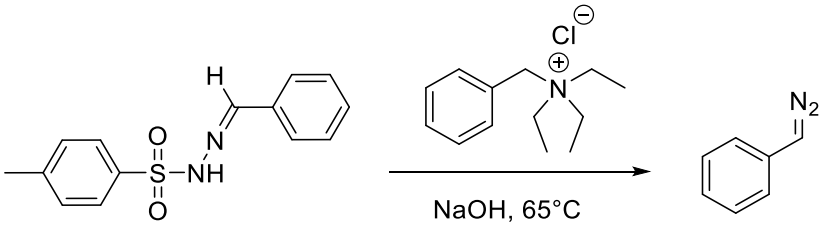

14 **15**

Compound	Equivalents	n [mmol]	m [g]	V [mL]
Benzaldehyde tosylhydrazone (**14**)	1.00	2.55	0.70	
Benzyltriethylammonium chloride	0.20	0.51	0.12	

The reaction was carried out in an orange light lab to exclude light with wavelengths below 520 nm and Schlenk techniques were used to secure complete exclusion of oxygen and moisture. For the synthesis of phenyldiazomethane (**15**), 1 eq. of previously synthesized benzaldehyde tosylhydrazone (**14**, 0.70 g, 2.55 mmol) was dissolved in 40 mL of dry toluene and then added to a 14wt% aqueous solution of sodium hydroxide (40 mL), containing 0.2 eq. of benzyltriethylammonium chloride (0.12 g, 0.51 mmol). The mixture was warmed to 65°C and stirred for 2 h at that temperature. Afterwards, it was cooled to RT and the layers were separated. The organic layer was washed with water (2 times with 30 mL each), dried

over magnesium sulfate and filtrated. The target compound was confirmed in the resulting intense orange solution using ATR-IR and stored at -18°C under Argon and light exclusion.

IR (ATR, cm^{-1}): 2060 ($C{=}N_2$)

2.1.4.3 Synthesis of dibutyltetraethylstannanediamine (16)

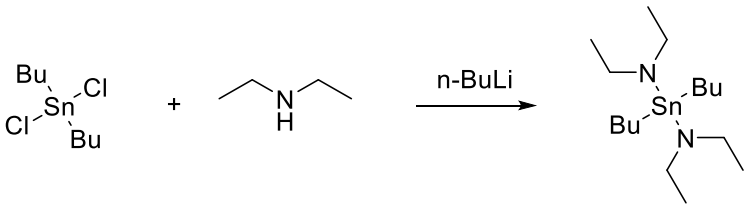

16

Compound	Equivalents	n [mmol]	m [g]	V [mL]
Dibutyldichlorostannane	1.00	5.30	1.61	
Diethylamine	2.00	10.60		1.10
n-Butyllithium (2.5 M in hexanes)	2.10	11.14		4.50

Schlenk techniques were used to secure complete exclusion of oxygen and moisture. For the synthesis of dibutyltetraethylstannanediamine (**16**), 1 eq. of dibutyldichlorostannane (1.61 g, 5.30 mmol) was weighed into a dry Schlenk tube and dissolved in 15 mL of dry diethyl ether. In another Schlenk tube, 2 eq. of diethylamine (1.10 mL, 10.60 mmol) were dissolved in 10 mL of dry diethylether. This solution was then cooled to 0°C before adding 2 eq. of n-butyllithium (2.5 M in hexanes, 4.50 mL, 11.14 mmol) slowly at that temperature. The mixture was then allowed to reach RT over 2 h and cooled to 0°C once more. At this temperature, the dichlorostannane solution was added via syringe over 15 min before removing the cooling bath and stirring the reaction mixture overnight. On the next day, the orange mixture was filtrated using a Teflon filter within a Glove Box and the solvent was evaporated from the highly moisture-sensitive product in vacuo. The product could be obtained as a yellow to orange liquid (0.90 g, 45% yield) and was stored at -18°C under Argon.

^{1}H-NMR: δ_H (ppm, 400 MHz, C_6D_6): 0.82 - 1.11 (10H, m, $SnCH_2CH_2C\mathbf{H}_2C\mathbf{H}_3$) ; 1.12 - 1.20 (6H, t, $NCH_2C\mathbf{H}_3$) ; 1.31 - 1.44 (4H, m, $SnCH_2C\mathbf{H}_2CH_2CH_3$) ; 1.52 - 1.72 (4H, m, $SnC\mathbf{H}_2CH_2CH_2CH_3$) ; 3.00 - 3.19 (4H, m, $NC\mathbf{H}_2CH_3$)

^{119}Sn-NMR: δ_{Sn} (ppm, 149 MHz, C_6D_6): 19.93

2.1.4.5 Synthesis of trimethylstannanediethylamine (19)

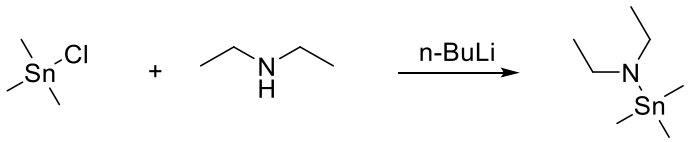

19

Compound	Equivalents	n [mmol]	m [g]	V [mL]
Chlorotrimethylstannane	1.00	8.48	1.69	
Diethylamine	1.00	8.48		0.87
n-Butyllithium (2.5 M in hexanes)	1.10	9.32		3.73

Schlenk techniques were used to secure complete exclusion of oxygen and moisture. For the synthesis of trimethylstannanediethylamine (**19**), 1 eq. of chlorotrimethylstannane (1.69 g, 8.48 mmol) was dissolved in 15 mL of dry diethyl ether. In a separate flask, 1 eq. of diethylamine (0.87 mL, 8.48 mmol) was weighed in and dissolved in 10 mL of dry diethyl ether. This solution was then cooled to -78°C and 1.1 eq. of n-butyllithium (2.5 M in hexanes, 3.73 mL, 9.32 mmol) were added over a period of 15 minutes at that temperature. The mixture was then stirred for 30 min at -78°C before adding the previously prepared solution of chlorotrimethylstannane via syringe resulting in the formation of a colorless precipitate. The mixture was allowed to reach RT and then refluxed overnight. On the next day, the

mixture was cooled to RT and filtrated using a Teflon filter within a Glove box. The solvent was evaporated in vacuo giving the target compound as an orange to red liquid (0.82 g, 41% yield), which was stored at -18°C under Argon.

^{1}H-NMR: δ_H (ppm, 400 MHz, C_6D_6): 0.13 - 0.32 (9H, m, SnC**H**$_3$) ; 0.99 (6H, t, NCH$_2$C**H**$_3$) ; 2.43 - 2.53 (4H, m, NC**H**$_2$CH$_3$)

2.1.5 Bromostannane route (Pathway E)

2.1.5.1 Synthesis of dibenzyldibutylstannane (20)

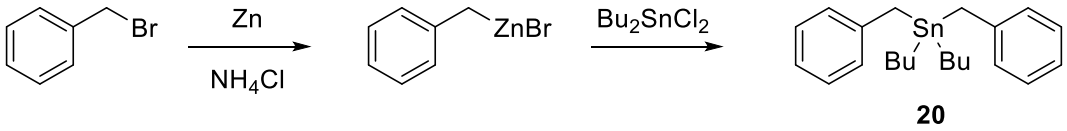

20

Compound	Equivalents	n [mmol]	m [g]	V [mL]
Benzyl bromide	4.00	65.82		7.82
Zinc powder	4.00	65.82	4.30	
Dibutyldichlorostannane	1.00	16.46	5.00	

For the synthesis of dibenzyldibutylstannane (**20**), 4 eq. of zinc powder (4.30 g, 65.82 mmol) were weighed into a Schlenk tube together with a 2.5:1 mixture of sat. aqueous NH_4Cl (50 mL) and THF (20 mL). Then, 1 eq. of dibutyldichlorostannane (5.00 g, 16.46 mmol) was dissolved in 5 mL of THF and then added to the mixture. Subsequently, 4 eq. of benzyl bromide (7.82 mL, 65.82 mmol) were added via syringe over 10 min at RT, causing the mixture to warm up. After complete addition, the two-layered reaction mixture was stirred for 1.5 h at RT before separating the layers. The aqueous layer was extracted 2 times with diethyl ether (30 mL each) and the combined organic layers were washed with sat. aqueous NH_4Cl (2 times

with 30 mL each). Drying over sodium sulfate, filtration and evaporation of the solvents in vacuo yielded the pure product as a colorless liquid (5.59 g, 82% yield).

^{1}H-NMR: δ_H (ppm, 400 MHz, $CDCl_3$): 7.21 - 7.12 (4H, m, Ar-**H**) ; 7.03 – 6.88 (6H, m, Ar-**H**) ; 2.29 (4H, s, Ph-C**H**2-Sn) ; 1.47 – 1.12 (9H, m, Bu-**H**) ; 0.87 – 0.75 (9H, m, Bu-**H**)

^{119}Sn-NMR: δ_{Sn} (ppm, 149 MHz, $CDCl_3$): -15.29

3 Tetrakisacylstannanes

3.1 Synthesis

3.1.1 Synthesis of tetrakis(trimethylsilyl)stannane (27)

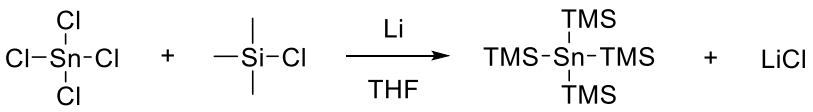

27

Compound	Equivalents	n [mmol]	m [g]	V [mL]
Lithium foil	10.00	486.06	3.37	
Trimethylchlorosilane	6.25	303.79		38.56
Tetrachlorostannane	1.00	48.61		5.68

The reaction was carried out under argon atmosphere, securing the exclusion of moisture and oxygen. For the synthesis of tetrakis(trimethylsilyl)stannane (**27**), 10 eq. of lithium foil (3.37 g, 468.06 mmol) were put into a predried Schlenk tube together with 100 mL of dry tetrahydrofuran. During stirring, a mixture of 6.25 eq. of trimethylchlorosilane (38.56 mL, 303.79 mmol) and 1 eq. of tetrachlorostannane (5.68 mL, 48.61 mmol) was added via dropping funnel slowly over 30 min at -78°C. After the addition, the cooling bath was removed and the mixture was allowed to reach RT overnight. On the next day, the mixture was refluxed for 3 h and after cooling down to RT filtrated over Celite. The mixture was then quenched using cold 1 N H_2SO_4 (100 mL) and the layers were separated. The aqueous layer was extracted 3 times with diethyl ether (3 times with 25 mL each) and the combined organic layers were then washed with water 3 times (20 mL each). The organic layers were dried over sodium sulfate and the solvent was evaporated in vacuo. Drying using high vacuum yielded the pure product as a colorless solid (4.24 g, 21 % yield).

^{1}H-NMR: δ_H (ppm, 400 MHz, C_6D_6): 0.37 (36H, s, C**H**$_3$)

^{29}Si-NMR: δ_{Si} (ppm, 80 MHz, C_6D_6): -9.69 (4Si, s, **Si**$(CH_3)_3$)

^{119}Sn-NMR: δ_{Sn} (ppm, 149 MHz, C_6D_6): -664.10

3.1.3 Synthesis of 2-methylbenzoyl fluoride (28)

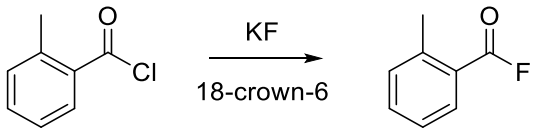

28

Compound	Equivalents	n [mmol]	m [g]	V [mL]
2-Methylbenzoyl chloride	1.00	21.72		2.83
Potassium fluoride	3.60	78.18	4.54	
18-Crown-6-ether	0.06	1.30	0.34	

Schlenk techniques were used to secure complete exclusion of oxygen and moisture. For the synthesis of 2-methylbenzoyl fluoride (**28**), 1 eq. of 2-methylbenzoyl chloride (2.83 mL, 21.72 mmol), 3.6 eq. of potassium fluoride (4.54 g, 78.18 mmol) and 0.06 eq. of 18-crown-6-ether (0.34 g, 1.30 mmol) were suspended in 30 mL of dry 1,2-dimethoxyethane and the mixture was then refluxed overnight. On the next day, the mixture was cooled down to RT and water was added carefully until the aqueous layer turned clear. Afterwards, the layers were separated and the aqueous layer was extracted 2 times with n-pentane (15 mL each). The combined organic layers were then dried over sodium sulfate. After filtration and evaporation of the solvent in vacuo, the product (colorless liquid, 1.12 g, 38% yield) could be obtained, which was carefully stored under Argon at -18°C.

GC-MS (acetone): m/z (rel.): 138 (M, 52%) ; 118 (86%) ; 90 (100%)

3.1.6 Synthesis of 2,4,6-trimethylbenzoyl fluoride (29)

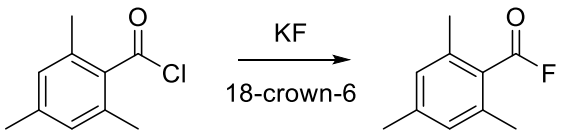

29

Compound	Equivalents	n [mmol]	m [g]	V [mL]
2,4,6-Trimethylbenzoyl chloride	1.00	30.08		5.02
Potassium fluoride	3.60	108.30	6.29	
18-Crown-6-ether	0.06	1.81	0.48	

Schlenk techniques were used to secure complete exclusion of oxygen and moisture. For the synthesis of 2,4,6-trimethylbenzoyl fluoride (**29**), 1 eq. of 2,4,6-trimethylbenzoyl chloride (5.02 mL, 30.08 mmol), 3.6 eq. of potassium fluoride (6.29 g, 108.30 mmol) and 0.06 eq. of 18-crown-6-ether (0.48 g, 1.81 mmol) were suspended in dry 1,2-dimethoxyethane (30 mL) and the mixture was then refluxed overnight. On the next day, the mixture was cooled down to RT and then water was added until the aqueous phase turned clear. Afterwards, the layers were separated and the aqueous phase was extracted 3 times with n-pentane (10 mL each). The combined organic layers were then washed twice with 15 mL of water each and dried over sodium sulfate. After filtration and evaporation of the solvent in vacuo, the target compound (colorless crystals, 4.81 g, 96% yield) could be obtained in high purity, which was then stored under Argon at -18°C.

^{1}H-NMR: δ_H (ppm, 400 MHz, C_6D_6): 6.46 (2H, s, Ar-**H**) ; 2.22 (6H, s, C**H**$_3$) ; 1.90 (3H, s, C**H**$_3$)

^{19}F-NMR: δ_F (ppm, 368 MHz, C_6D_6): 52.69

3.1.7 Synthesis of tetrakis(2,4,6-trimethylbenzoyl)stannane (26)

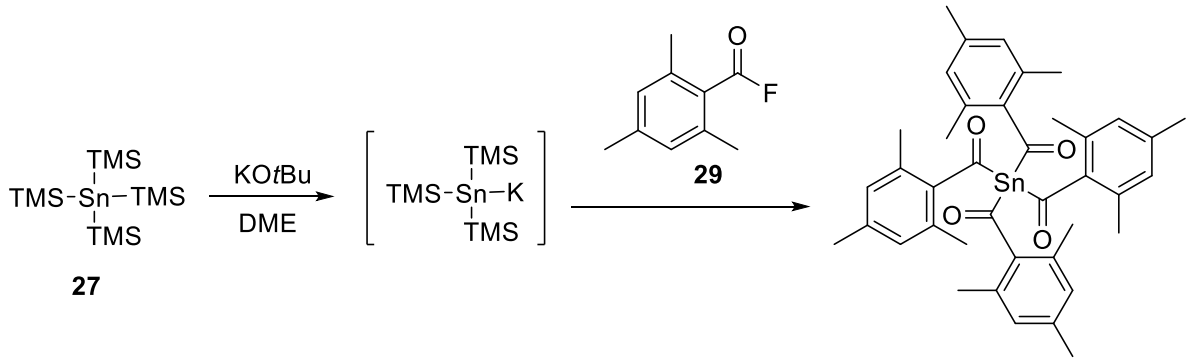

27

26

Compound	Equivalents	n [mmol]	m [g]	V [mL]
Tetrakis(trimethylsilyl)stannane (**27**)	1.00	5.93	2.44	
Potassium tert-butoxide	1.00	5.93	0.67	
2,4,6-Trimethylbenzoyl fluoride (**29**)	4.00	23.71	3.94	

The reaction was carried out in an orange light lab to exclude light with wavelengths below 520 nm and Schlenk techniques were used to secure complete exclusion of oxygen and moisture. For the synthesis of tetrakis(2,4,6-trimethylbenzoyl)stannane (**26**), 1 eq. of previously synthesized tetrakis(trimethylsilyl)stannane (**27**, 2.44 g, 5.93 mmol) and 1 eq. of potassium tert. butoxide (0.67 g, 5.93 mmol) were weighed into a dry Schlenk tube and dissolved in 15 mL of dry 1,2-dimethoxyethane. This mixture was stirred for 20 min at RT to obtain a clear, yellow solution. In the meantime, 4 eq. of freshly synthesized 2,4,6-trimethylbenzoyl fluoride (**29**, 3.94 g, 23.71 mmol) were weighed into another dry Schlenk tube and dissolved in 15 mL of dry 1,2-dimethoxyethane. Both solutions were cooled to -40°C using an acetonitrile/N_2 cooling bath and the stannyl potassium solution was then added to the acid fluoride solution slowly at that temperature via syringe, which resulted in a color change to dark red. After complete addition, the mixture was allowed to reach RT and stirred overnight. On the next day, the solvent was evaporated in vacuo and the residue was taken up in dry n-pentane (15 mL) to precipitate both polar side products as well as most of the target compound. The mixture was filtrated under inert conditions and the obtained solid was washed with dry n-pentane (2 times with 4 mL each). After drying, the target compound

could be extracted from the solid using dry toluene (6 x 10 mL). After evaporation of the toluene, pure tetrakis(2,4,6-trimethylbenzoyl)stannane could be obtained as intense yellow solid (2.44 g, 58% yield) and was stored under Argon and light protection at 4°C.

m.p.: 92 - 94°C

Anal. Calcd. for $C_{40}H_{44}O_4Sn$: C, 67.91 ; H, 6.27. **Found:** C, 66.61 ; H, 6.27.

^{1}H-NMR: δ_H (ppm, 400 MHz, C_6D_6): 6.37 (8H, s, Ar-**H**) ; 2.21 (24H, s, C**H**$_3$) ; 1.99 (12H, s, C**H**$_3$)

^{13}C-NMR: δ_C (ppm, 151 MHz, C_6D_6): 242.68 (C=O) ; 143.30 ; 137.97 ; 130.92 ; 128.00 (C_{arom}) ; 19.94 ($C_{p\text{-}methyl}$) ; 17.83 ($C_{o\text{-}methyl}$)

^{119}Sn-NMR: δ_{Sn} (ppm, 149 MHz, C_6D_6): -499.22

3.2 Characterization

All characterization experiments were carried out under light protection (exclusion of light with wavelengths below 520 nm) in an orange-light or in a red-light (light of wavelengths between 610 and 650 nm) laboratory. Additionally, if possible, darkly tinted glassware as well as aluminum foil was used.

3.2.1 UV/Vis spectroscopy

Tetrakis(2,4,6-trimethylbenzoyl)stannane (**26**), Ivocerin®, tetrakis(2-methylbenzoyl)germane (K174) and Irgacure® 784 were dissolved in dry acetonitrile ($c = 1 \times 10^{-3}$ mol L^{-1}, 10 mL solutions each) under light protection (orange-light lab, excluding light with wavelengths below 520 nm). Directly afterwards, the samples were placed into quartz cuvettes (optical path length d = 10 mm) and the spectra were recorded. UV/Vis measurements were carried out using a Lambda 950 device from Perkin Elmer equipped with a PMT detector. Pure acetonitrile was measured as a background. For mathematical peak deconvolution, PeakFit v4.12 by SigmaPlot was used. The deconvolution procedure was as follows: Datafit via Residuals method with Löss Smoothing algorithm using AI expert for optimal smoothing. Peak type Lorentz area; Amplitude Threshold 2%; correlation coefficient r2 > 0.99.

3.2.2 Computational studies

All computational studies were carried out in cooperation with Dr. Sergej Naumov at the Leibniz Institute of Surface Modification at Leipzig.[48] Density Functional Theory (DFT) calculations were carried out using the M06-D3 density functional. The MO6-D3 functional is parameterized for organometallic and non-covalent interactions.[73] It includes physically and chemically important London dispersion interactions.[83] This computational model was already successfully used for calculations of metal-organic complexes in our previous works.[84-86] The molecular geometries and energies of all the calculated molecules were

calculated at the M06-D3/LACVP** level of theory as implemented in the program Jaguar 9.4.[87] The LACVP** basis set uses the standard 6-31G(d,p) basis set for light elements and the LAC pseudopotential[88] for heavier elements, such as Ti, Sn and Ge in this case. Frequency calculations were carried out at the same level of theory to characterize the stationary points on the potential surface and to obtain total enthalpy (H) and Gibbs free energy (G) at a standard temperature of 298.15 K using unscaled vibrations. The reaction enthalpies (ΔH) and Gibbs free energies of reactions (ΔG) were calculated as the difference of the total enthalpies H and the Gibbs free energies G between the reactants and products, respectively. To take solvent effects (acetonitrile in our case) on the structure and reaction parameters of studied molecules into account (acetonitrile) the calculations were done using Jaguar's dielectric continuum Poisson-Boltzmann solver (PBF),[89] which fits the field produced by the solvent dielectric continuum to another set of point charges. The UV/Vis electronic transition spectra and energies of excited states both singlets (S^1-S^n) and triplet (T^1*) were calculated in acetonitrile with the Time Dependent (TD DFT)[90] method at M06-D3/LACVP**/PBE level of theory at ground state geometry. The energies of lowest triplet state (T^1) were calculated as the difference of the energies between the most stable structures of the ground state singlet (S^0) and optimized triplet state.

3.2.3 Steady state photolysis

A two-necked photoreactor (40 mL) was equipped with a quickfit, which had been closed with a quartz window. One end of an optical waveguide was then placed on this quartz window inside the quickfit, the other end was connected to the light source. For irradiation of the PI solutions, an Exfo OmniCure LX400 UV LED spot curing system (460 nm) was used. The intensity of the LED was in both cases adjusted to be 1 W cm^{-2} right after the quartz window (corresponds to 70% intensity on the display of the control unit). Tetrakis(2,4,6-trimethylbenzoyl)stannane (**26**) as well as the reference initiators were dissolved in acetonitrile (40 mL solution, each c_0 = 1 x 10^{-3} mol L^{-1}). Each solution was then transferred to

the photoreactor and degassed with Argon for 20 min. The reaction solution was then irradiated while stirring at 500 rpm and samples (each 1.5 mL) were taken in a certain interval (0, 1, 3, 6, 10, 15 min). For each sample, an UV/Vis spectrum was acquired using a Lambda 950 device from Perkin Elmer equipped with a PMT detector. Due to the experimental setup used, it is ensured, that almost all light is absorbed by the solution inside the photoreactor. Therefore, the different extinction coefficients should not have a significant influence on the photobleaching behavior.

3.2.4 Photo-DSC

Photo-DSC experiments were carried out using a NETZSCH DSC 204 F1 setup with autosampler. As light sources either an Exfo OmniCure LX400 UV LED spot curing system (460 nm) or an 522 nm LED, provided by Ivoclar Vivadent® was used. The intensity was adjusted to be 1 W cm^{-2} directly after the lens of the 460 nm LED and 0.42 W cm^{-2} directly after the lens of the 522 nm LED. The prepared formulation contained 0.1wt% of acylstannane **26** in either a 1:1 molar mixture of urethanedimethacrylate (UDMA) and decanedioldimethacrylate (D_3MA) or hexanedioldiacrylate (HDDA). For comparison, a formulation of Ivocerin® (2 times the equimolar amount of the used amount of acylstannane **26**), tetrakis(2-methylbenzoyl)germane (K174, equimolar amount of the used amount of acylstannane **26**) and titanocene (2 times the equimolar amount of the used acylstannane **26**) in the same monomer mixture were prepared as well. The amounts of photoinitiator used were those related to the amount of cleavable groups (and therefore formed radicals) present in the structures. The photoinitiators were dissolved in the monomer using an ultrasonic bath with thermostat (30°C). During the preparation of the mixtures, light with wavelengths below 520 nm was excluded (orange light lab). For each experiment, two DSC pans were prepared from the same solution (double test). As a reference, a DSC pan filled with pure monomer solution was placed into the device. The double bond conversion (DBC) can be calculated from the peak area (ΔH [J mol^{-1}]) and the theoretical heat of polymerization of the monomer system

($\Delta H_{T,UDMA/D3MA}$ = 115 kJ mol^{-1};[82] $\Delta H_{T,HDDA}$ = 172 kJ mol^{-1}).[91] The maximum rate of polymerization R_p [mol L^{-1} s^{-1}] can be determined using the following equation containing h [mW mg^{-1}] (height of the exothermic signal) and the densities of the used monomers ρ ($\rho_{UDMA/D3MA}$ = 1030 mg mL^{-1}; ρ_{HDDA} = 1010 mg mL^{-1}).

3.2.5 Curing depth

A cylindrical Teflon mold was placed on a glass plate and the light source was attached directly to the glass plate from below. Two formulations were prepared, one containing 0.1wt% of tetrakis(2,4,6-trimethylbenzoyl)stannane (**26**) and 50 wt% of zirconium oxide (inorganic filler) in hexanediol diacrylate (HDDA) and the other one containing 0.1wt% of Ivocerin® and the same amount of inorganic filler in the same acrylate. As stabilizer 500 ppm of butylated hydroxytoluene (BHT) was added. For dissolution of the PIs, the formulations were put into an ultrasonic bath with thermostat (30°C). The formulations were then put into the cylindrical mold and cured for 240 s. In the case of Ivocerin® a 460 nm LED (Exfo OmniCure LX400 UV LED spot curing system) was used for curing, however, for the sample containing tetrakis(2,4,6-trimethylbenzoyl)stannane (**26**) a 522 nm LED provided by Ivoclar Vivadent® was utilized. The intensities of both light sources were adjusted to be 33.5 mW cm^{-2} directly behind the glass plate. After curing, residual uncured formulation was discarded and the obtained polymeric samples were washed with acetone. The height of the polymeric samples was then measured in the center and compared to give a relation between the achieved curing depths.

3.2.6 Green laser curing

Green laser curing experiments were carried out using a low-price commercial green laser pointer by Hightech XPoint (model LP-890). It emits at 532 nm with an intensity of 5.34 mW

mm^{-2}. The laser was characterized beforehand by measuring an emission spectrum as well as a beam profile (general section: chapter 3.2.6).

A cylindrical mold was placed on a glass plate and the laser pointer was attached directly to the glass plate from below (general section: chapter 3.2.6). The mold was then filled with formulations containing a 1:1 mixture of urethanedimethacrylate (UDMA) and decanedioldiacrylate (D_3MA), different amounts of Schott® Dental Glass (GM27884) as an inorganic filler (0, 10, 30, 50, 70wt%) as well as different amounts of tetrakis(2,4,6-trimethylbenzoyl)stannane **26** (0.010, 0.025, 0.050, 0.075, 0.100wt%) or Irgacure® 784. The formulations were then cured for a certain period of time (60, 120, 200, 300, 500 s), residual uncured formulation was discarded and the resulting polymeric samples were washed with acetone. The curing depths of the samples were then measured and further the coloration of the samples was checked visually to obtain information about the photobleaching behavior of the PIs within the methacrylate network.

3.2.7 Cytocompatibility

All studies were carried out in cooperation with Dr. Marica Markovic at the Institute of Materials Science and Technology at TU Wien.[48] For cytocompatibility testing, L929-mCherry cells were cultivated in an incubator in humid atmosphere with 5% of carbon dioxide at 37°C. The medium was refreshed every second day. For testing, 96-well plates (in total 10) were seeded with 5000 cells per well and left in the incubator overnight for the cells to attach. On the next day the cells were exposed to different concentrations of tetrakis(2,4,6-trimethylbenzoyl)stannane (**26**), Ivocerin®, tetrakis(2-methylbenzoyl)germane (K174) and Irgacure® 784 and therefore incubated with 100 µL of different dilutions of the photointiators in DMSO (0.10, 0.05, 0.025, 0.0125, 0.00625 and 0.003125 mM). Each in two plates, the first one for evaluation of the cytotoxicity of the photoinitiator itself, and the second one to investigate cytocompatibility after exposure to UV light. In parallel two plates were used to

evaluate background cytotoxicity of the DMSO solution in the medium (same exact concentrations used for the dilution of photoinitiators). All plates had wells with non-treated cells as control samples, every concentration had at least 6 repetitions. The plates were exposed to the UV light source at 365 nm for 10 min, all plates (treated and untreated with UV light) were reaped in aluminum foil to ensure that they are protected from light exposure and left in cell culture incubator for 24 h. The cell culture experiments were conducted under red light in order to prevent unintended cleavage of the photoinitiators. After 24 h of incubation period with photoinitiators/DMSO, the culture medium was exchanged twice to remove residues of photoinitiator and cell viability was evaluated. The resazurin-based assay PrestoBlue Cell Viability Reagent was diluted 1:10 with medium and 100 µL per well were applied and incubated for 1 h. Because of the reducing environment of viable cells, this reagent is transformed and turns red, becoming highly fluorescent. The fluorescence was then measured with a plate reader (excitation 560 nm, emission 590 nm). After correction for background fluorescence, the results of the cells exposed to different concentrations of photoinitiators were compared to each other and to the controls using One Way Anova Dunnett's Multiple Comparisons Test. It was assumed, that metabolic activity of the 24 h control not exposed to photoinitiators is 100 %. Statistical evaluation of the data was performed using a software package IBM SPSS Statistic 25.0 and Excel 2016 (Microsoft Office). 5000 cells per well (96-well plates) were seeded directly into the wells of cell culture plates (at least 6 repetitions). Metabolic activity was then measured 24 h after cell seeding. For cell microscopy a LSM 700 by Zeiss was used. L929-mCherry survival was compromised with various concentrations of the acylstannane **26**.

3.2.8 Stability in aqueous media

Five different solutions of acylstannane **26** (A-E) were prepared. Solution A and B each contained 1wt% of photoinitiator **26** in dry acetonitrile, where solution A was purged with Argon and solution B was not. Solutions C-E each contained 0.5wt% of photoinitiator **26** and

10wt% of water. For solution D, a drop of conc. H_3PO_4 was added to simulate the acidic environment of aqueous primer formulations. To solution E, a drop of aqueous 1 M NaOH was added to study the hydrolytic stability in basic conditions. For comparative purposes, the analogue solutions were prepared with the reference compounds Ivocerin®, tetrakis(2-methylbenzoyl)germane (K174) and Irgacure® 784. Then, HPLC runs were conducted, the eluent being a mixture of 90% acetonitrile and 10% water. A reversed phase C18 column (AppliChrom® OTU LipoMare) including a precolumn was used. Between the measurements, the samples were stored under exclusion of light and at RT. The obtained peak areas where referred to the peak area measured directly after dissolving (internal standard: acetylnaphtalene).

3.2.9 Storage stability

Photo-DSC was carried out in order to compare the heat of reaction of the same formulation resulting from the polymerization after defined intervals of storage time. Therefore, 2 different formulations of **26** in UDMA:D_3MA (1:1) were prepared and the type and the concentration of the stabilizer (BHT, TEMPO and MEHQ) as well as the storage temperature were varied (Table 5). Stabilizer-free formulations containing Ivocerin® were prepared for comparison. The heat released in the polymerization of the formulations was measured using a NETZSCH DSC 204 F1 setup with autosampler at defined time intervals (0, 2, 7, 21, 120 days). The storage of the formulations between the measurements was carried out at room temperature and at 50°C under argon. As a radiation source, Exfo OmniCure LX400 UV LED spot curing system (460 nm) was used, for which the light intensity was adjusted to be 1 W cm^{-2} directly after the lens of the LED. After carrying out the experiments, the heat flow curve was integrated and the values obtained (in J g^{-1}) were compared to those of the initial measurement

4 Acylstannanones

4.1 Synthesis

4.1.1 Synthesis of bis(trimethylsilyl)peroxide (30)

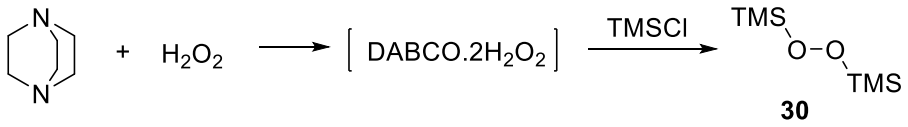

30

Compound	Equivalents	n [mmol]	m [g]	V [mL]
1,4-Diazabicyclo(2.2.2)octane	1.00	180.00	19.96	
Hydrogen peroxide (30% solution)	1.00	180.00		22.66
Chlorotrimethylsilane	1.20	220.00		27.99

Schlenk techniques were used to secure complete exclusion of oxygen and moisture. For the synthesis of bis(trimethylsilyl)peroxide (**30**), 0.5 eq. of 1,4-diazabicyclo(2.2.2)octane (9.98 g, 89.00 mmol) were weighed into a dry Schlenk tube and dissolved in 150 mL of dry THF. The solution was then cooled to 0°C using an ice bath and 1 eq. of hydrogen peroxide (30% solution, 22.66, 180 mmol) was added slowly via syringe and septum. The instantly formed $DABCO.2H_2O_2$ complex precipitated as a colorless solid, which was filtrated and dried in vacuo for 2 h. Afterwards, another 0.5 eq. of 1,4-diazabicyclo(2.2.2)octane (9.98 g, 89.00 mmol) was added to the solid complex and the powder mixture was dried for further 4 h in vacuo to remove potential traces of moisture. On the next day, the mixture was dissolved in 300 mL of dry dichloromethane and cooled to 0°C. At this temperature, 1.2 eq. of chlorotrimethylsilane (27.99 mL, 220 mmol) were added via syringe and septum and after stirring at that temperature for 3 h, a large amount of colorless precipitate (DABCO hydrochloride) had formed. The hydrochloride was separated using filtration and the filtrate was concentrated in vacuo. Afterwards, 200 mL of dry n-pentane were then added to ensure complete precipitation of the undesired hydrochloride. After another filtration step and evaporation of the solvent, the target compound could be obtained as a colorless liquid (8.40 g, 93% yield), which was stored at 7°C under Argon.

Yield: 8.40 g (93%)

^{1}H-NMR: δ_H (ppm, 400 MHz, C_6D_6): 0.21 (18H, s, SiC**H**$_3$)

^{29}Si-NMR: δ_{Si} (ppm, 80 MHz, C_6D_6): 26.60 (2Si, s, **Si**$(CH_3)_3$)

4.1.2 Synthesis of dichlorotin oxide (31)

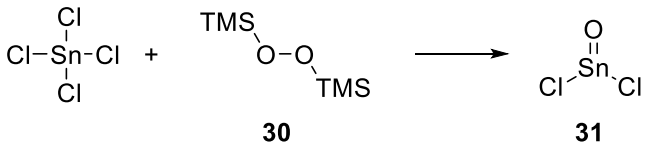

30 **31**

Compound	Equivalents	n [mmol]	m [g]	V [mL]
Bis(trimethylsilyl)peroxide (**30**)	2.80	47.09	8.40	
Tetrachlorostannane	1.00	16.83		1.97

Schlenk techniques were used to secure complete exclusion of oxygen and moisture. For the synthesis of dichlorotin oxide (**31**), 2.8 eq. of readily prepared bis(trimethylsilyl)peroxide (**30**, 8.40 g, 47.09 mmol) was weighed into a dry Schlenk tube and dissolved in 50 mL of dry dichloromethane. Then, the solution was cooled to 0°C and 1 eq. of tetrachlorostannane (1.97 mL, 16.83 mmol) was added carefully using a syringe and a septum. After complete addition, the cooling bath was removed and the mixture was stirred at RT for 2 h. Gas formation was clearly visible at that point. Then, volatile components within the reaction mixture (solvent, excess peroxide, chlorine, hexamethyldisiloxane) were evaporated directly through the Schlenk line and a cooling trap giving the product as colorless crystalline solid (3.25 g, 94% yield). The product was stored in the fridge at 7°C under Argon.

Yield: 3.25 g (94%)

GC-MS (CH_2Cl_2): m/z (rel.): 206 (M, 100%) ; 190 (10%) ; 135 (3%) ; 119 (1%)

4.1.3 Synthesis of 2-phenyl-1,3-dithiane (34)

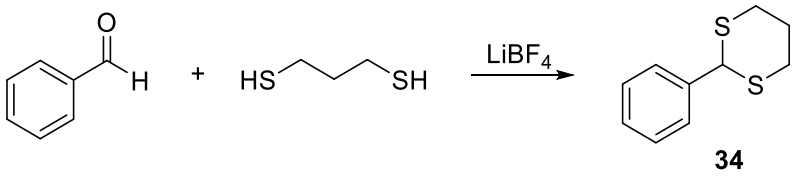

34

Compound	Equivalents	n [mmol]	m [g]	V [mL]
Benzaldehyde	1.10	56.03		5.70
1,3-Dimercaptopropane	1.00	50.93		5.10
Lithium tetrafluoroborate	0.10	5.09	0.48	

For the synthesis of 2-phenyl-1,3-dithiane (**34**), 1.1. eq. of benzaldehyde (5.70 mL, 56.03 mmol) and 0.1 eq. of lithium tetrafluoroborate (0.48 g, 5.09 mmol) were weighed into a Schlenk tube and while stirring, 1 eq. of 1,3-dimercaptopropane (5.10 g, 50.93 mmol) was added slowly at RT via syringe and septum. After complete addition, the mixture was stirred for 1.5 h at RT and was then dissolved in 50 mL of ethyl acetate. This solution was transferred to a separating funnel and washed 3 times with water (30 mL each) to remove the borate salt. The organic layer was then dried over sodium sulfate, filtrated and the solvent was removed in vacuo afterwards. The crude product was recrystallized from ethyl acetate giving the pure target compound as colorless crystals (1.96 g, 20% yield).

Yield: 1.96 g (20%)

^{1}H-NMR: δ_H (ppm, 400 MHz, $CDCl_3$): 7.51 - 7.43 (2H, m, Ar-**H**) ; 7.40 - 7.27 (3H, m, Ar-**H**) ; 5.17 (1H, s, Ar-C**H**) ; 3.07 (2H, t, C**H$_2$**) ; 2.91

(2H, d, C**H**$_2$) ; 2.24 – 2.11 (1H, m, C**H**$_2$) ; 2.01 – 1.86 (1H, m, C**H**$_2$)

4.1.4 Synthesis of bis(2-phenyl-1,3-dithian-2-yl)stannanone (32)

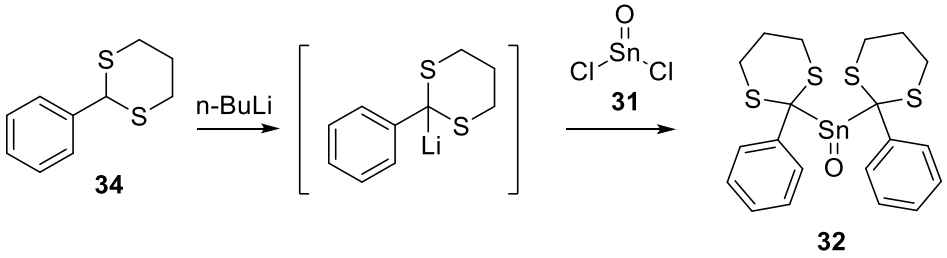

Compound	Equivalents	n [mmol]	m [g]	V [mL]
2-Phenyl-1,3-dithiane (**34**)	2.40	9.96	1.96	
Dichlorotin oxide (**31**)	1.00	4.15	0.85	
n-Butyllithium (2.5 M in hexanes)	2.64	10.96		4.38

The reaction was carried out in an orange light lab to exclude light with wavelengths below 520 nm and Schlenk techniques were used to secure complete exclusion of oxygen and moisture. For the synthesis of bis(2-phenyl-1,3-dithian-2-yl)stannanone (**32**), 2.4 eq. of 2-phenyl-1,3-dithiane (**34**, 1.96 g, 9.96 mmol) were weighed into a dry Schlenk tube and dissolved in 35 mL of dry THF. The solution was cooled to 0°C and 2.6 eq. of n-BuLi (2.5 M in hexanes, 4.38 mL, 10.96 mmol) were added at that temperature via syringe and septum. The color of the mixture changed to dark and was stirred for 2 h at 0°C. In the meantime, 1 eq. of dichlorotin oxide (**31**, 0.85 g, 4.15 mmol) was weighed into another Schlenk tube within a Glove Box and dissolved in 15 mL of dry diethyl ether. This solution was then added to the lithiated dithiane solution slowly at 0°C. The mixture was stirred for 3 h at 0°C and then stored overnight in the fridge at 4°C. On the next day, it was quenched with 100 mL of water leading to the precipitation of the target compound as a colorless solid, which was filtrated off and dried in vacuo (1.72 g, 34% yield).

Yield:	1.72 g (34%)
^{1}H-NMR: δ_H (ppm, 400 MHz, C_6D_6):	7.59 - 7.44 (4H, m, Ar-**H**) ; 7.23 - 7.12 (6H, m, Ar-**H**) ; 2.67 (4H, d, C**H**$_2$) ; 2.55 (4H, d, C**H**$_2$) ; 2.01 – 1.88 (2H, m, C**H**$_2$) ; 1.82 – 1.73 (2H, m, C**H**$_2$)
LC-MS:	m/z (rel.): 525 ; 331 ; 255

HPLC (rev. phase C_{18} silica, MeCN 95:5 H_2O): 2.71 min

Materials and equipment

Chemicals and solvents: All chemicals were either purchased from Sigma Aldrich®, TCI® and abcr GmbH® or provided by Ivoclar Vivadent®. The compounds were stored as suggested by the manufacturer and, if not stated otherwise, used as received. The used solvents were either received in anhydrous quality or further dried using standard procedures and were stored under inert conditions.

TLC: Aluminum plates by Merck coated with either silica gel 60 F_{254} or aluminum oxide 60 F_{254} were used.

NMR spectroscopy: The NMR signals (^{1}H, ^{13}C, ^{19}F, ^{29}Si, ^{119}Sn) were measured on a BRUKER Avance DRX-400 FT-NMR spectrometer. C_6D_6, $CDCl_3$, THF-d_8 and D_2O with a degree of deuteration of ≥ 99,50% were used as solvents. For the ^{29}Si signals, the INEPT pulse sequence (insensitive nuclei enhanced by polarization transfer) was applied.

GC-MS: The measurements were carried out on a Thermo Fisher Scientific ITQ 1100 employing a Fused Silica capillary column (30m x 0.25mm).

HPLC: The measurements were carried out on a modular HP Agilent 1100 device, equipped with a HP photodiode array detector and quarternary gradient pump. For the separation, an OUT LipoMare C18 reversed phase column (105 Å; 5 µm, 150 x 4 mm) was used. The device was equipped with an auto sampler and the ChemStation software for LC 3D systems form Ailent Technologies (vB03.02-SR2 [341]) was used.

LC-MS: The measurements were carried out on a Shimadzu LCMS-2020 MS detector with DUISI ionization.

IR: All spectra were measured on a Perkin Elmer Spectrum 65 FT-IR Spectrometer with a Specac MKII Golden Gate ATR system.

Elemental analysis: Elemental analysis was carried out at the microanalysis laboratory at the University of Vienna.

Melting point: Melting points were obtained from an Optimelt MPA100 automated melting point apparatus.

UV/Vis spectroscopy: The measurements were carried out using a Lambda 950 device from Perkin Elmer equipped with a PMT detector and quartz cuvettes (d = 10 mm). For mathematical peak deconvolution, PeakFit v4.12 by SigmaPlot was used.

Photo-DSC: The experiments were carried out on a NETZSCH DSC 204 F1 with autosampler.

Light sources: Depending on the specific experiment, different light sources were used:

- OmniCure (Lumen Dynamics Series 2000) + 400-500 nm filter
- Exfo OmniCure LX400 UV LED spot curing system (460 nm)
- Bluephase C8 (470 nm) by Ivoclar Vivadent
- Green LED (522 nm) by Ivoclar Vivadent
- Green laser pointer (532 nm, model LP-890) by Hightech X-Point

For light intensity measurements, an Ocean Optics USB 2000+ spectrophotometer device was used.

Abbreviations

ATR	Attenuated total reflection
BHT	2,6-Di-*tert*-butyl-4-methylphenol
bis-GMA	Bisphenol A diglycidylmethacrylate
BPO	Dibenzoylperoxide
CQ	Camphorquinone
D_3MA	Decanediol dimethacrylate
DABCO	Diazabicyclo(2.2.2)octane
DBC	Double bond conversion
DCM	Dichloromethane
DMAB	Dimethylamino benzoic acid ethyl ester
DME	1,2-dimethoxyethane
DSC	Differencial scanning calorimetry
GC	Gas chromatography
HDDA	1,6-Hexanedioldiacrylate
HPLC	High pressure liquid chromatography
IC	Internal conversion
ISC	Intersystem crossing
IR	Infrared
K37	Benzoyltrimethylgermane
LC	Liquid chromatography
LDA	Lithium diisopropylamide
MEHQ	4-Methoxyphenol
MS	Mass spectrometry
NBS	N-bromosuccinimide
NMR	Nuclear magnetic resonance
PI	Photoinitiator
PPTS	Pyridinium p-toluenesulfonate
RT	Room temperature
TEGDMA	Triethylen glycol dimethacrylate
TEMPO	(2,2,6,6-Tetramethylpiperidin-1-yl)oxyl
THF	Tetrahydrofuran
TLC	Thin layer chromatography
UDMA	Urethane dimethacrylate
UV	Ultraviolet

Compound structures

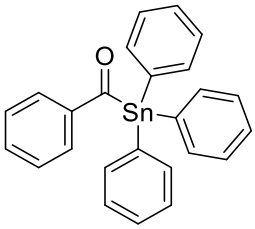

1

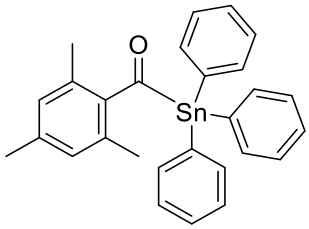

2

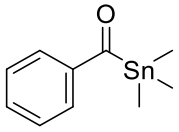

3

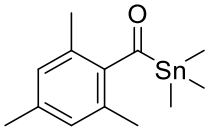

4

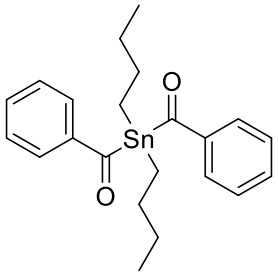

5

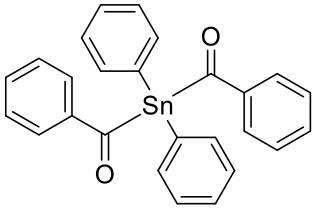

6

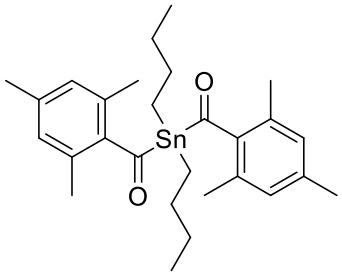

7

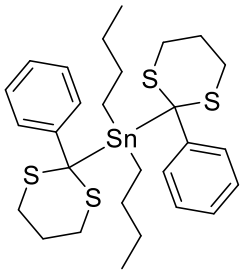

8

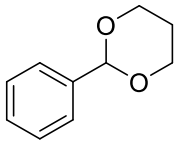

9

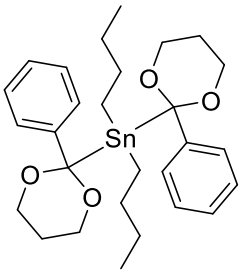

10

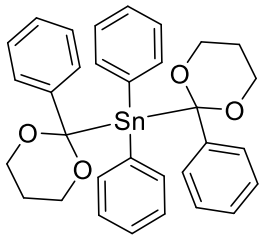

11

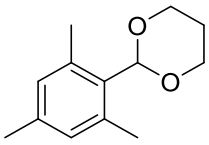

12

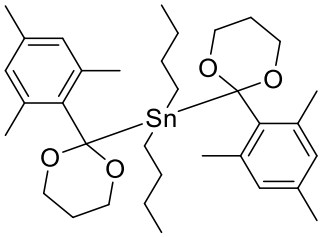

13

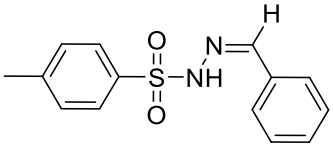

14

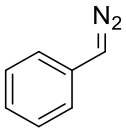

15

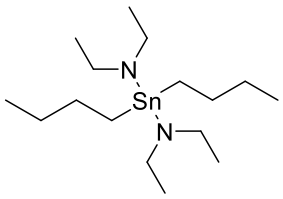

16

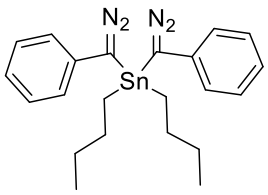

17

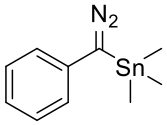

18

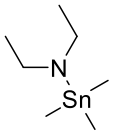

19

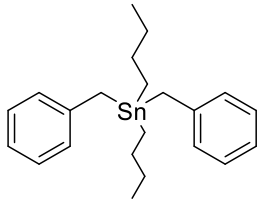

20

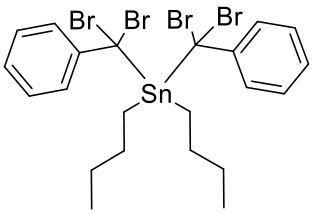

21

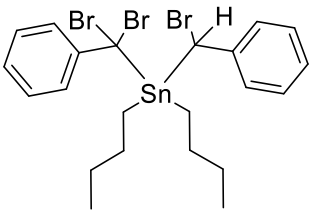

22

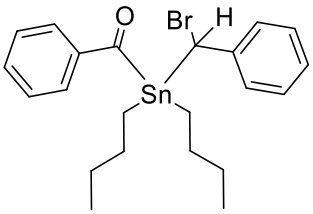

23

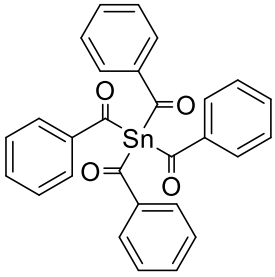

24

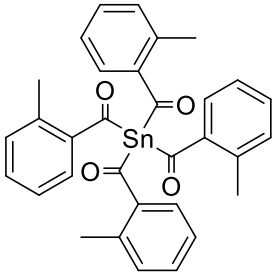

25

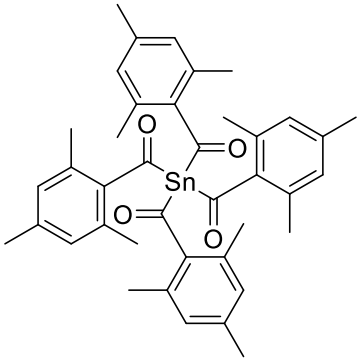

26

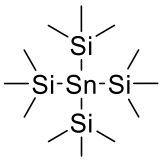

27

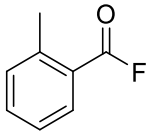

28

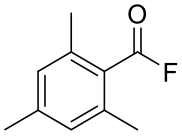

29

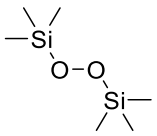

30

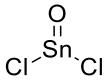

31

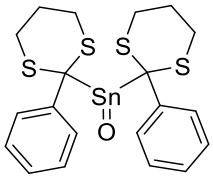

32

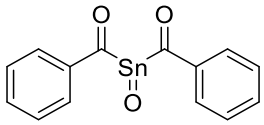

33

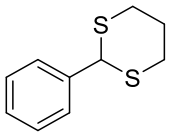

34

Literature

1. Younis, O.; Asgar, K.; Powers, J. M. Initiation of cracks in dental amalgam. *J. Dent. Res.* **1975,** 54 (6), 1133-7 DOI: 10.1177/00220345750540060601.

2. Greener, E. H. Anodic polarization of new dental amalgams. *J. Dent. Res.* **1976,** 55 (6), 1142 DOI: 10.1177/00220345760550063601.

3. Moradzadeh, A. https://crystaldentalcenters.com/blog/amalgam-vs-composite-fillings-whats-the-best-option-for-you **2014,** (24.01.2019),

4. Albert, P.; Dermann, K.; Rentsch, H. Amalgam and its alternatives. *Chem. Unserer Zeit* **2000,** 34 (5), 300-305.

5. Schroeder, K. D., Diagram of a healthy human molar showing the enamel, cementum, pulp, and dentin which make up the structure, as well as the surrounding tissues. In *Wikimedia Commons*, 1280px-Human_tooth_diagram-en.svg, Ed. **2016;** pp Creative Commons Attribution-Share Alike 4.0 International license.

6. Combe, E. C.; Burke, F. T.; Douglas, W. H., *Dental biomaterials*. Kluwer Academic Boston: **1999**.

7. Van Landuyt, K.; Yoshida, Y.; Hirata, I.; Snauwaert, J.; De Munck, J.; Okazaki, M.; Suzuki, K.; Lambrechts, P.; Van Meerbeek, B. Influence of the chemical structure of functional monomers on their adhesive performance. *Journal of dental research* **2008,** 87 (8), 757-761.

8. Bennett, J. Measuring UV curing parameters of commercial photopolymers used in additive manufacturing. *Addit. Manuf.* **2017,** 18, 203-212 DOI: 10.1016/j.addma.2017.10.009.

9. Jacobs, P. F. In *Fundamentals of stereolithography*, 1992 International Solid Freeform Fabrication Symposium, 1992; 1992.

10. Crivello, J. V., Dietliker, K. K., *Chemistry & Technology of UV & EB Formulation for Coatings, Inks & Paints*. 2nd edition ed.; SITA Technology Ltd: **1998;** Vol. 3: Photoinitiators for Free Radical, Cationic & Anionic Photopolymerisation.

11. Gruber, H. F. Photoinitiators for free radical polymerization. *Prog. Polym. Sci.* **1992,** 17 (6), 953-1044 DOI: 10.1016/0079-6700(92)90006-K.

12. Quaranta, M.; Borisov, S. M.; Klimant, I. Indicators for optical oxygen sensors. *Bioanal Rev* **2012,** 4 (2-4), 115-157.

13. Monroe, B. M. Photochemistry of α-dicarbonyl compounds. *Advan. Photochem.* **1971,** 8, 77-108 DOI: 10.1002/9780470133385.ch2.

14. Kayser, R. H.; Young, R. H. The photoreduction of methylene blue by amines. I. A flash photolysis study of the reaction between triplet methylene blue and amines. *Photochem. Photobiol.* **1976,** 24 (5), 395-401 DOI: 10.1111/j.1751-1097.1976.tb06845.x.

15. Fouassier, J. P.; Lalevee, J., *Photoinitiators for Polymer Synthesis: Scope, Reactivity and Efficiency*. Wiley-VCH: **2012**.

16. Terauchi, K.; Sakurai, H. Ultraviolet spectral studies: esters of aroylphosphonic acids. *Bull. Chem. Soc. Jap.* **1969,** 42 (3), 821-3 DOI: 10.1246/bcsj.42.821.

17. Berlin, K. D.; Burpo, D. H. Ultraviolet spectral studies of conjugation in esters of acylphosphonic acids. *J. Org. Chem.* **1966,** 31 (4), 1304-6 DOI: 10.1021/jo01342a520.

18. Gruuetzmacher, H.; Ott, T.; Dietliker, K. Polymer-bound bisacylphosphine oxides. US8883872B2, 2014.

19. Ellrich, K.; Herzig, C. Bisacylphosphine oxide and its use. DE3443221A1, 1986.

20. Mitterbauer, M.; Haas, M.; Stueger, H.; Moszner, N.; Liska, R. Tetrakis(2,4,6-Trimethylbenzoyl)Silane-A Novel Photoinitiator for Visible Light Curing. *Macromol. Mater. Eng.* **2017,** 302 (5), 1600536 DOI: 10.1002/mame.201600536.

21. Ganster, B.; Fischer, U. K.; Moszner, N.; Liska, R. New Photocleavable Structures. Diacylgermane-Based Photoinitiators for Visible Light Curing. *Macromolecules (Washington, DC, U. S.)* **2008,** 41 (7), 2394-2400 DOI: 10.1021/ma702418q.

22. Moszner, N.; Fischer, U. K.; Ganster, B.; Liska, R.; Rheinberger, V. Benzoyl germanium derivatives as novel visible light photoinitiators for dental materials. *Dent. Mater.* **2008,** 24 (7), 901-907 DOI: 10.1016/j.dental.2007.11.004.

23. Moszner, N.; Salz, U.; Fischer, U. K.; Liska, R.; Gruber, H.; Ganster, B. Polymerizable compositions of binder with acylgermane initiators, preparation of moldings and other uses. US20080076847A1, 2008.

24. Moszner, N.; Rheinberger, V. M.; Salz, U.; Gruber, H.; Liska, R.; Ganster, B.; Ullrich, G. Photopolymerizable dental materials with bisacylphosphine oxides as initiators. US20070027229A1, 2007.

25. Schwentenwein, M.; Homa, J. Additive Manufacturing of Dense Alumina Ceramics. *Int. J. Appl. Ceram. Technol.* **2015,** 12 (1), 1-7 DOI: 10.1111/ijac.12319.

26. Benedikt, S.; Wang, J.; Markovic, M.; Moszner, N.; Dietliker, K.; Ovsianikov, A.; Gruetzmacher, H.; Liska, R. Highly efficient water-soluble visible light photoinitiators. *J. Polym. Sci., Part A: Polym. Chem.* **2016,** 54 (4), 473-479 DOI: 10.1002/pola.27903.

27. Mitterbauer, M. Synthesis of novel Si-based long wavelength photoinitiators for dental applications. Diploma thesis, Technische Universität Wien, **2016**.

28. Duff, J. M.; Brook, A. G. Photoisomerization of acylsilanes to siloxycarbenes, and their reactions with polar reagents. *Can. J. Chem.* **1973,** 51 (17), 2869-83 DOI: 10.1139/v73-429.

29. Ganster, B. Bathochrom verschobene Photoinitiatoren für Dentalformulierungen. University of Technology Vienna, **2007**.

30. Radebner, J.; Eibel, A.; Leypold, M.; Gorsche, C.; Schuh, L.; Fischer, R.; Torvisco, A.; Neshchadin, D.; Geier, R.; Moszner, N.; Liska, R.; Gescheidt, G.; Haas, M.; Stueger, H. Tetraacylgermanes: Highly Efficient Photoinitiators for Visible-Light-Induced Free-Radical Polymerization. *Angew. Chem., Int. Ed.* **2017,** 56 (11), 3103-3107 DOI: 10.1002/anie.201611686.

31. Peddle, G. J. D. The preparation and properties of α-tin ketones. *J. Organometal. Chem.* **1968,** 14 (1), 139-47 DOI: 10.1016/S0022-328X(00)92649-4.

32. Wyatt, P. B. Acylstannanes (including S, Se, and Te analogues). *Sci. Synth.* **2003,** 5, 423-432.

33. Tamborski, C.; Ford, F. E.; Soloski, E. J. Preparation and reactions of trialkyltinlithium. *J. Org. Chem.* **1963,** 28, 237-9 DOI: 10.1021/jo01036a516.

34. Corey, L. D.; Singh, S. M.; Oehlschlager, A. C. A novel reaction of α-halo epoxides with trialkylstannates. *Can. J. Chem.* **1987,** 65 (8), 1821-7 DOI: 10.1139/v87-306.

35. Singh, S. M.; Oehlshlager, A. C. Metallometalation of allenes: an exploratory study. *Can. J. Chem.* **1991,** 69 (12), 1872-80 DOI: 10.1139/v91-271.

36. Capperucci, A.; Degl'Innocenti, A.; Faggi, C.; Reginato, G.; Ricci, A.; Dembech, P.; Seconi, G. A general access to acylstannanes. *J. Org. Chem.* **1989,** 54 (12), 2966-8 DOI: 10.1021/jo00273a036.

37. Marshall, J. A.; Garofalo, A. W.; Hinkle, K. W. Synthesis of (S,E)-1-(methoxymethoxy)-1-tributylstannyl-2-butene. *Org. Synth.* **2000,** 77, 98-106 DOI: 10.15227/orgsyn.077.0098.

38. Marshall, J. A.; Gung, W. Y. SE' Addition of homochiral α-alkoxyallylstannanes to aldehydes. *Tetrahedron* **1989,** 45 (4), 1043-52 DOI: 10.1016/0040-4020(89)80015-8.

39. Bolz, P. R.; Kunze, U.; Winter, W. Nucleophilic addition of (triphenylstannyl)lithium to carbon disulfide. *Angew. Chem.* **1980,** 92 (3), 227-8.

40. Kunze, U.; Tischer, R. Nucleophilic addition of triorganotin anions to carbon disulfide. IX. Synthesis and complexation of novel triphenylstannane dithioesters. *Chem. Ber.* **1987,** 120 (7), 1099-104.

41. Quintard, J. P.; Elissondo, B.; Mouko-Mpegna, D. Some aspects on the reactivity of α-chloro-α-ethoxymethyltributyltin: reductive etherification of aromatic aldehydes and demonstration of formyltributyltin during the hydrolysis. *J. Organomet. Chem.* **1983,** 251 (2), 175-87.

42. Kosugi, M.; Naka, H.; Sano, H.; Migita, T. Preparation and some properties of acyltin compounds. *Bull. Chem. Soc. Jpn.* **1987,** 60 (9), 3462-4 DOI: 10.1246/bcsj.60.3462.

43. Wheeler, M. T. Synthesis and chemistry of phenyl(trimethylstannyl)diazomethane and lithium phenyldiazomethane. **1990**.

44. Wang, D.-Y.; Wang, C.; Uchiyama, M. Stannyl-Lithium: A Facile and Efficient Synthesis Facilitating Further Applications. *J. Am. Chem. Soc.* **2015,** 137 (33), 10488-10491 DOI: 10.1021/jacs.5b06587.

45. Mitchell, T. N.; Kwetkat, K. A convenient laboratory-scale preparation of trimethylacyltins. *Synthesis* **1990,** (11), 1001-2 DOI: 10.1055/s-1990-27075.

46. Ye, E.; Tan, H.; Li, S.; Fan, W. Y. Self-organization of spherical, core-shell palladium aggregates by laser-induced and thermal decomposition of [Pd(PPh3)4]. *Angew. Chem., Int. Ed.* **2006,** 45 (7), 1120-1123 DOI: 10.1002/anie.200503408.

47. Moszner, N. Z., F.; Liska, R.; Fischer, U.K.; Burtscher, P.; Salz, U.; Rheinberger, V.; Gruber, H.; Ganster, B. Polymerisable compositions comprising acyl-germanium as initiators. 2007.

48. Mitterbauer, M.; Knaack, P.; Naumov, S.; Markovic, M.; Ovsianikov, A.; Moszner, N.; Liska, R. Acylstannanes: Cleavable and Highly Reactive Photoinitiators for Radical Photopolymerization at Wavelengths above 500 nm with Excellent Photobleaching Behavior. *Angew Chem Int Ed Engl* **2018,** 57 (37), 12146-12150 DOI: 10.1002/anie.201804094.

49. Corey, E. J.; Seebach, D. Carbanions of 1,3-dithianes. Reagents for C-C bond formation by nucleophilic displacement and carbonyl addition. *Angew. Chem., Int. Ed. Engl.* **1965,** 4 (12), 1075-77 DOI: 10.1002/anie.196510752.

50. Beate, G., Dissertation. In *Technische Universität Wien*.

51. Kruithof, K. J. H.; Schmitz, R. F.; Klumpp, G. W. Synthesis of silyl, germyl, and stannyl alk-1-ynyl ketones from 2-lithio-2-(trimethylsilylethynyl)-1,3-dioxane. *J. Chem. Soc., Chem. Commun.* **1983,** (5), 239 DOI: 10.1039/c39830000239.

52. Gauss, P. Advanced additives for radical photopolymerization. Technische Universität Wien, **2019**.

53. Brook, A. G.; Peddle, G. J. D. Dibenzoylsilanes and substituted benzoylsilanes [spectra]. *Can. J. Chem.* **1963,** 41 (9), 2351-6 DOI: 10.1139/v63-341.

54. Bouillon, J.-P.; Portella, C. Synthesis and intramolecular aldol reactions of 1,6- and 1,7-bis(acylsilanes). *Eur. J. Org. Chem.* **1999,** (7), 1571-1580 DOI: 10.1002/(SICI)1099-0690(199907)1999:7<1571::AID-EJOC1571>3.0.CO;2-4.

55. Brook, A. G.; Duff, J. M.; Jones, P. F.; Davis, N. R. Synthesis of silyl and germyl ketones. *J. Am. Chem. Soc.* **1967,** 89 (2), 431-4 DOI: 10.1021/ja00978a047.

56. Karimi, B.; Seradj, H.; Maleki, J. Highly efficient and chemoselective interchange of 1,3-oxathioacetals and dithioacetals to acetals promoted by N-halosuccinimide. *Tetrahedron* **2002,** 58 (22), 4513-4516 DOI: 10.1016/S0040-4020(02)00389-7.

57. Firouzabadi, H.; Iranpoor, N.; Karimi, B. Zirconium tetrachloride (ZrCl4) catalyzed highly chemoselective and efficient acetalization of carbonyl compounds. *Synlett* **1999,** (3), 321-323 DOI: 10.1055/s-1999-2605.

58. Greene, T. W.; Wuts, P. G., *Protective Groups in Organic Synthesis*. Third Edition ed.; John Wiley and Sons, Inc.: **1999**.

59. Grieco, P. A.; Nishizawa, M.; Oguri, T.; Burke, S. D.; Marinovic, N. Sesquiterpene lactones: total synthesis of (±)-vernolepin and (±)-vernomenin. *J. Am. Chem. Soc.* **1977,** 99 (17), 5773-80 DOI: 10.1021/ja00459a039.

60. Hagiwara, H.; Uda, H. A total synthesis of (+)-perrottetianal A. *J. Chem. Soc., Chem. Commun.* **1987,** (18), 1351-3 DOI: 10.1039/c39870001351.

61. Drake, J. E.; Khasrou, L. N.; Majid, A. Trimethylgermyl methane- and trifluoromethanesulfonates. *J. Inorg. Nucl. Chem.* **1981,** 43 (7), 1473-8 DOI: 10.1016/0022-1902(81)80319-3.

62. Ioannou, M.; Porter, M. J.; Saez, F. Conversion of 1,3-oxathiolanes to 1,4-oxathianes using a silylated diazoester. *Tetrahedron* **2005,** 61 (1), 43 - 50 DOI: 10.1016/j.tet.2004.10.063.

63. Bolm, C.; Kasyan, A.; Heider, P.; Saladin, S.; Drauz, K.; Guenther, K.; Wagner, C. Synthesis and Use of α-Silyl-Substituted α-Hydroxyacetic Acids. *Org. Lett.* **2002,** 4 (13), 2265-2267 DOI: 10.1021/ol025911n.

64. Dudman, C. C.; Reese, C. B. Preparation of aryldiazoalkanes from 2,4,6-triisopropylbenzenesulfonyl hydrazones. *Synthesis* **1982,** (5), 419-21 DOI: 10.1055/s-1982-29821.

65. Wulfman, D. S.; Yousefian, S.; White, J. M. Metal salt-catalyzed carbenoids. XIX. The synthesis of aryldiazomethanes. *Synth. Commun.* **1988,** 18 (18), 2349-52 DOI: 10.1080/00397918808082380.

66. Su, G.; Mu, H.; Za, D.; Zeng, L.; Cativiela, C.; Hammer, R. P.; Yu, K. Stereospecific synthesis of trans-2,3-diaryl substituted 1-aminocyclopropanecarboxylic acid derivatives. *Synth. Commun.* **2003,** 33 (16), 2873-2884 DOI: 10.1081/SCC-120022177.

67. Yoder, C. H.; Zuckerman, J. J. Amination and transamination as routes to fourth group diamines. *J. Am. Chem. Soc.* **1966,** 88 (21), 4831-9 DOI: 10.1021/ja00973a015.

68. Harrypersad, S.; Foucher, D. Alternating polystannanes: syntheses and properties. *Chem. Commun. (Cambridge, U. K.)* **2015,** 51 (33), 7120-7123 DOI: 10.1039/C5CC00568J.

69. Marton, D.; Russo, U.; Stivanello, D.; Tagliavini, G.; Ganis, P.; Valle, G. C. Preparation of Benzylstannanes by Zinc-Mediated Coupling of Benzyl Bromides with Organotin Derivatives. Physicochemical Characterization and Crystal Structures. *Organometallics* **1996,** 15 (6), 1645-50 DOI: 10.1021/OM9507742.

70. Ohshita, J.; Tokunaga, Y.; Sakurai, H.; Kunai, A. Reactions of Lithium Silenolates with Acyl Halides. First Synthesis of Di- and Tetraacylsilanes. *J. Am. Chem. Soc.* **1999,** 121 (25), 6080-6081 DOI: 10.1021/JA990889N.

71. Marschner, C. A new and easy route to polysilanylpotassium compounds. *Eur. J. Inorg. Chem.* **1998,** (2), 221-226 DOI: 10.1002/(SICI)1099-0682(199802)1998:2<221::AID-EJIC221>3.0.CO;2-G.

72. Buerger, H.; Goetze, U. Trimethylsilyl derivatives of germanium and tin. Electron-balance bonds of silicon. *Angew. Chem., Int. Ed. Engl.* **1968,** 7 (3), 212-13 DOI: 10.1002/anie.196802122.

73. Lee, I.; Shim, C. S.; Chung, S. Y.; Kim, H. Y.; Lee, H. W. Cross-interaction constants as a measure of transition state structure. Part 1. The degree of bond formation in nucleophilic substitution reactions. *J. Chem. Soc., Perkin Trans. 2* **1988,** (11), 1919-23.

74. Fischer, R.; Baumgartner, J.; Marschner, C.; Uhlig, F. Tris(trimethylsilyl)stannyl alkali derivatives: Syntheses and NMR spectroscopic properties. *Inorg. Chim. Acta* **2005,** 358 (11), 3174-3182 DOI: 10.1016/j.ica.2005.04.006.

75. Rabek, J. F. In *Experimental and analytical methods for the investigation of radiation curing*, 1993; Elsevier: 1993; pp 329-452.

76. dos Santos, G. B.; Alto, R. V. M.; Sampaio Filho, H. R.; da Silva, E. M.; Fellows, C. E. Light transmission on dental resin composites. *Dent. Mater.* **2008,** 24 (5), 571-576 DOI: 10.1016/j.dental.2007.06.015.

77. Mitterbauer, M.; Knaack, P.; Naumov, S.; Markovic, M.; Ovsianikov, A.; Moszner, N.; Liska, R. Acylstannane: Spaltbare und hochreaktive Photoinitiatoren für radikalische Photopolymerisationen bei Wellenlängen über 500 nm mit exzellentem Photobleaching. *Angewandte Chemie* **2018,** 130 (37), 12323-12327 DOI: 10.1002/ange.201804094.

78. Knezevic, L.; Schaupper, M.; Muhleder, S.; Priglinger, E.; Redl, H.; Holnthoner, W.; Knezevic, L.; Schaupper, M.; Muhleder, S.; Priglinger, E.; Redl, H.; Holnthoner, W.; Knezevic, L.; Schimek, K.; Schimek, K.; Hasenberg, T.; Marx, U. Engineering Blood and Lymphatic Microvascular Networks in Fibrin Matrices. *Front Bioeng Biotechnol* **2017,** 5, 25.

79. Taddei, M.; Ricci, A. Electrophilic hydroxylation with bis(trimethylsilyl) peroxide. A synthon for the hydroxyl cation. *Synthesis* **1986,** (8), 633-5 DOI: 10.1055/s-1986-31725.

80. Sakurada, I.; Yamasaki, S.; Kanai, M.; Shibasaki, M. Dichlorotin oxide-catalyzed new direct functionalization of olefins: synthesis of trans β-azidohydrins and 1,2-diols. *Tetrahedron Lett.* **2000,** 41 (14), 2415-2418 DOI: 10.1016/S0040-4039(00)00176-3.

81. Kazahaya, K.; Tsuji, S.; Sato, T. Entirely solvent-free procedure for the synthesis of distillable 1,3-dithianes using lithium tetrafluoroborate as a reusable catalyst. *Synlett* **2004,** (9), 1640-1642 DOI: 10.1055/s-2004-829084.

82. Bauernschmitt, R.; Ahlrichs, R. Treatment of electronic excitations within the adiabatic approximation of time dependent density functional theory. *Chem. Phys. Lett.* **1996,** 256 (4,5), 454-464 DOI: 10.1016/0009-2614(96)00440-X.

83. Zhao, Y.; Truhlar, D. G. The M06 suite of density functionals for main group thermochemistry, thermochemical kinetics, noncovalent interactions, excited states, and transition elements: two new functionals and systematic testing of four M06-class functionals and 12 other functionals. *Theor. Chem. Acc.* **2008,** 120 (1-3), 215-241 DOI: 10.1007/s00214-007-0310-x.

84. Grimme, S.; Antony, J.; Ehrlich, S.; Krieg, H. A consistent and accurate ab initio parametrization of density functional dispersion correction (DFT-D) for the 94 elements H-Pu. *J. Chem. Phys.* **2010,** 132 (15), 154104/1-154104/19 DOI: 10.1063/1.3382344.

85. Kahnt, A.; Peuntinger, K.; Dammann, C.; Drewello, T.; Hermann, R.; Naumov, S.; Abel, B.; Guldi, D. M. Kinetic Studies of the Reduction of [Co(dmgH)2(py)(Cl)] Revisited: Mechanisms, Products, and Implications. *J. Phys. Chem. A* **2014,** 118 (25), 4382-4391 DOI: 10.1021/jp501947y.

86. Stolz, F.; Appun, J.; Naumov, S.; Schneider, C.; Abel, B. A Complex Catalytic Reaction Caught in the Act: Intermediates and Products Sampling Online by Liquid µ-Beam Mass Spectrometry and Theoretical Modeling. *ChemPlusChem* **2017,** 82 (2), 334 DOI: 10.1002/cplu.201600600.

87. Beyer, N.; Steinfeld, G.; Lozan, V.; Naumov, S.; Flyunt, R.; Abel, B.; Kersting, B. Structure and Bonding in Nickel-Thiolate-Iodine Charge-Transfer Complexes. *Chem. - Eur. J.* **2017,** 23 (10), 2303-2314 DOI: 10.1002/chem.201604460.

88. *Jaguar*, Version 9.4; Schrodinger, Inc.: 2016.

89. Wadt, W. R.; Hay, P. J. Ab initio effective core potentials for molecular calculations. Potentials for main group elements sodium to bismuth. *J. Chem. Phys.* **1985,** 82 (1), 284-98 DOI: 10.1063/1.448800.

90. Tannor, D. J.; Marten, B.; Murphy, R.; Friesner, R. A.; Sitkoff, D.; Nicholls, A.; Honig, B.; Ringnalda, M.; Goddard, W. A., III. Accurate First Principles Calculation of Molecular Charge Distributions and Solvation Energies from Ab Initio Quantum Mechanics and Continuum Dielectric Theory. *J. Am. Chem. Soc.* **1994,** 116 (26), 11875-82 DOI: 10.1021/ja00105a030.

91. Gorsche, C.; Koch, T.; Moszner, N.; Liska, R. Exploring the benefits of β-allyl sulfones for more homogeneous dimethacrylate photopolymer networks. *Polym. Chem.* **2015,** 6 (11), 2038-2047 DOI: 10.1039/C4PY01582G.